

Том 4 № 3 (2018)

ISSN 2413-9203

# ТРАНСПОРТНЫЕ СИСТЕМЫ И ТЕХНОЛОГИИ

рецензируемый научный журнал

**TRANSPORTATION  
SYSTEMS AND  
TECHNOLOGY**  
peer-review journal

**VOL. 4 ISSUE 3 (2018)**

[transst.ru](http://transst.ru)

**УЧРЕДИТЕЛЬ И ИЗДАТЕЛЬ**

Федеральное государственное бюджетное образовательное учреждение высшего образования «Петербургский государственный университет путей сообщения Императора Александра I» (ФГБОУ ВО ПГУПС)

**«ТРАНСПОРТНЫЕ СИСТЕМЫ И ТЕХНОЛОГИИ»**

Электронный рецензируемый научный журнал  
Выходит ежеквартально – 4 раза в год  
Основан в 2013 году

**ИНДЕКСАЦИЯ**

РИНЦ (Российский индекс научного цитирования)  
Google Scholar  
WorldCat  
Ulrich's Periodical Directory

**КОНТАКТЫ**

**Адрес:** 190031, Санкт-Петербург, наб. реки Фонтанки, 115, ауд. 9/11-5  
**E-mail:** info@trassyst.ru  
**WEB:** www.trassyst.ru  
**Телефон:** +7 (812) 6198152; +7 (911) 2384445

Научный редактор Ю. Ф. Антонов, доктор технических наук, профессор  
Перевод на английский язык А. Ю. Гнатенко  
Выпускающий редактор Т. С. Антонова  
Редактор сайта А. В. Дитрих  
Литературный редактор Е. В. Васильева  
Верстка А. А. Стуканова

**СВИДЕТЕЛЬСТВО о регистрации средства массовой информации**

Эл№ФС77-53673 от 17.04.2013 г. выдано Федеральной службой по надзору в сфере связи, информационных технологий и массовых коммуникаций

**ОПИСАНИЕ ЖУРНАЛА**

Сетевой электронный журнал "Транспортные системы и технологии" публикует статьи фундаментального характера и прикладного направления, а также обзорные статьи, относящиеся ко всем видам транспортной технологии

**ПУБЛИКАЦИЯ В ЖУРНАЛЕ**

Журнал отбирает материал для публикации из числа присланных для рассмотрения рукописей. В ходе отбора проводится независимое двойное слепое рецензирование членами редакционной коллегии и внешними экспертами. Для публикации рукопись, а также все сопроводительные и дополнительные файлы следует направить в редакцию через личный кабинет на сайте журнала по URL: <http://trassyst.ru/>  
Рукопись и дополнительные материалы следует оформить в соответствии с правилами редакции, см. подробно по URL: <https://trassyst.ru/trassyst/about/submissions>

**ПОДПИСКА**

Журнал распространяется через Интернет без ограничений и по адресно-целевой подписке через редакцию

**ТРАНСПОРТНЫЕ СИСТЕМЫ  
И ТЕХНОЛОГИИ****Том 4, № 3****2018****ЭЛЕКТРОННЫЙ РЕЦЕНЗИРУЕМЫЙ  
НАУЧНЫЙ ЖУРНАЛ****ГЛАВНЫЙ РЕДАКТОР****Зайцев Анатолий Александрович,**

доктор экономических наук, профессор, Санкт-Петербург, Россия

**ЗАМЕСТИТЕЛЬ ГЛАВНОГО РЕДАКТОРА, НАУЧНЫЙ РЕДАКТОР****Антонов Юрий Федорович,** доктор технических наук, профессор, Санкт-Петербург, Россия**МЕЖДУНАРОДНАЯ РЕДАКЦИОННАЯ КОЛЛЕГИЯ**

**Ганиев Ривнер Фазылович,** академик Российской академии наук, Директор Института машиноведения им. А. А. Благонравова Российской академии наук, Москва, Россия

**Глухих Василий Андреевич,** академик Российской академии наук, Научный руководитель НИИЭФА им. Д.В. Ефремова, доктор технических наук, профессор, Санкт-Петербург, Россия

**Колесников Владимир Иванович,** академик Российской академии наук, президент Ростовского государственного университета путей сообщения, доктор технических наук, профессор, Ростов, Россия

**Ли Вэйли,** PhD, профессор, Пекинский транспортный университет, Пекин, КНР

**Клюшпис Йоханнес,** доктор наук 2-й степени, полный профессор Дегендорфской высшей технической школы, Мюнхен, Германия

**Хан Хьён-Сук,** PhD, начальник Департамента Маглев и линейных двигателей, старший научный сотрудник Корейского института машиностроения и материаловедения (KIMM), Тэджон, Республика Корея

**Мыльников Сергей Владимирович,** кандидат биологических наук, доцент, ученый секретарь ООО «Эко-Вектор», Санкт-Петербург, Россия

**Богданов Александр Владимирович,** Доктор физико-математических наук, профессор, Санкт-Петербургский Государственный университет, Санкт-Петербург, Россия

**Подсорин Виктор Александрович,** доктор экономических наук, профессор Российского университета транспорта, Москва, Россия

**Соколова Яна Викторовна,** кандидат экономических наук, MBA, Заместитель руководителя Научно-образовательного центра инновационных пассажирских перевозок ПГУПС, Санкт-Петербург, Россия

**Ма Чжисюнь,** PhD, сотрудник Национального транспортно-инженерного центра Маглев, доцент Университета Тунцзи, Шанхай, КНР

**Фэй Ни,** PhD, Эйндховенский технологический университет, Эйндховен, Северный Брабант, Нидерланды

**Линь Гобинь,** PhD, профессор, директор Национального транспортно-инженерного центра Маглев, доцент Университета Тунцзи, Шанхай, КНР

**FOUNDER AND PUBLISHER**

Emperor Alexander I St. Petersburg State Transport University  
St. Petersburg, Russia

**“TRANSPORTATION SYSTEMS AND TECHNOLOGY”**

Electronic peer-reviewed journal  
Issued 4 times a year (quarterly)  
Established in 2013

**INDEXING**

eLibrary (Russian Science Citation Index)  
Google Scholar  
WorldCat  
Ulrich's Periodical Directory

**CONTACTS**

**Address:** 190031, St. Petersburg, 115 Moskovskiy Ave., room 9/11-5  
**E-mail:** info@trassyst.ru  
**Website:** www.trassyst.ru  
**Phone:** +7 (812) 6198152; +7 (911) 2384445

Science Editor Yu. F. Antonov, Doctor of Technical Science, Professor  
Translation into English A. Yu. Gnatenko  
The Executive Editor T. S. Antonova  
WEB- Editor A. V. Dietrichs  
Literary Editor E. V. Vasileva  
Layout Editor A. A. Stukanova

**AIMS & SCOPE**

Network electronic journal “Transportation Systems and Technology” publishes articles of a fundamental nature and application areas, as well as review articles pertaining to all types of transport technology

**JOURNAL CONTENT SELECTION**

The journal selects based on the double-blind peer-review conducted by members of the editorial board and external experts.

To be published, the manuscript and all accompanying files should be sent to the editorial team through a personal account on the journal's website at: <http://trassyst.ru/>

The manuscript and additional materials should be prepared and arranged in accordance with the author guidelines (see in detail at: <https://trassyst.ru/trassyst/about/submissions>)

**SUBSCRIPTION**

The Journal is distributed via Internet for free and by subscription via Editorial office

# TRANSPORTATION SYSTEMS AND TECHNOLOGY

**Vol. 4, Issue 3**

**2018**

## ELECTRONIC PEER-REVIEWED RESEARCH JOURNAL

**EDITOR-IN-CHIEF**

Anatoly Zaitsev, Doctor of Economics, Professor, St. Petersburg, Russia

**DEPUTY EDITOR-IN-CHIEF, THE SCIENTIFIC EDITOR**

Yuri Antonov, Dr. Sc., Professor, St. Petersburg, Russia

**INTERNATIONAL EDITORIAL BOARD**

Rivner Ganiev, Academician of the Russian Academy of Sciences, Director  
Mechanical Engineering Research Institute of the Russian Academy of Sciences,  
Moscow, Russia

Vasily Glukhikh, Academician of the Russian Academy of Sciences, Scientific  
Adviser at JSC «D.V. Efremov Institute of Electrophysical Apparatus», Doctor of  
Technical Science, Professor, St. Petersburg, Russia

Vladimir Kolesnikov, Academician of the Russian Academy of Sciences, The  
president Rostov State Transport University, Doctor of Technical Science,  
Professor, Rostov, Russia

Weili Li, Ph.D., Professor, Beijing Jiaotong University, Beijing, China

Kluehspies Johannes, 2nd Dr.'s Degree, Full Professor at Deggendorf Institute of  
Technology, Munich, Germany

Han Hyung-Suk, PhD, Head of the Department of Maglev and Linear Drives,  
Principle Researcher, Korea Institute of Machinery & Material (KIMM), Daejeon,  
the Republic of Korea

Sergey Mylnikov, PhD, Associate professor, Scientific secretary LCC “Eco-Vector”,  
St. Petersburg, Russia

Aleksandr V. Bogdanov, Dr Pphys.-mat. of Science, professor, St. Petersburg State  
University, Russian Federation, St. Petersburg, Russia

Viktor Podsorin, Doctor of Economics Science, Professor Russian Transport  
University, Moscow, Russia

Yana Sokolova, PhD, MBA, Deputy Head Scientific-Educational Center for  
Innovative Passenger Transport Emperor Alexander I St. Petersburg State  
Transport University, St. Petersburg, Russia

Ma Zhixun, PhD, National Maglev Transportation Engineering Technology R&D  
Center (NMTC), Associate Professor, Tongji University, Shanghai, China

Fei Ni, PhD, Technische Universiteit Eindhoven: Eindhoven, Noord-Brabant,  
Netherlands

Lin Guobin, PhD, National Maglev Transportation Engineering Technology  
R&D Center (NMTC), Director, Professor, Tongji University, Shanghai,  
China

СОДЕРЖАНИЕ		TABLE OF CONTENTS
ОБЗОРЫ		REVIEWS
<b>Дитц Д., Биндер А.</b> Синхронная машина на основе постоянных магнитов с активным магнитным подшипником с нулевой последовательностью, соединенным с шестерней	5	<b>Dietz D., Binder A.</b> PM Synchronous Machine with Zero-Sequence Current Driven Star Point-Connected Active Magnetic Thrust Bearing
<b>Лapidус Б.М.</b> Магнитная левитация – фундаментальная основа для сверхскоростных вакуумно-левитационных транспортных технологий	26	<b>Lapidus B.M.</b> Magnetic Levitation as the Fundamental Basis for Superfast Vacuum Levitation Transport Technologies
<b>Линь Г., Шэн Х.</b> Применение и дальнейшее развитие транспорта Маглев в Китае	36	<b>Lin G., Sheng X.</b> Application and Further Development of Maglev Transportation in China
<b>Большаник П.В.</b> Эволюция, прогноз и преобладающие тренды развития транспорта Югры	44	<b>Bolshanik P.V.</b> Forecast of Yugra Transport Development
<b>Рампельманн Р., Кёлер Р.</b> Опыт обслуживания скоростного подвижного состава Маглев в Шанхае	65	<b>Rampelmann R., Köhler R.</b> Service Experiences Maglev Vehicles Shanghai
ОРИГИНАЛЬНЫЕ СТАТЬИ		ORIGINAL STUDIES
<b>Сундуков Е.Ю., Селиванов Л.Ф., Сундуков В.Е.</b> Маглев-системы на основе эстакады арочного типа	72	<b>Sundukov E.Y., Selivanov L.F., Sundukova V.E.</b> The maglev-systems on the basis of trestle of arch type
<b>Аппунн Р., Франтцхельд Й., Йеттер М., Лёзер Ф.</b> MULTI® - опытная модель бесканатного лифта в испытательной башне в городе Ротвайль	80	<b>Appunn R., Frantzheld J., Jetter M., Löser F.</b> MULTI® – Rope-less Elevator Demonstrator at Test Tower Rottweil
<b>Като М., Хирата К.</b> Управление резонансным приводом с тремя степенями свободы при помощи нового векторного управления	90	<b>Kato M., Hirata K.</b> Control of Three-Degree-of-Freedom Resonant Actuator Driven by Novel Vector Control

<p><b>Ван Х.Х., Ю.Й., Линь И., Лу Д.Ц., Цинь Ф.</b>          Схема увеличения скорости с использованием источника питания 3000 В постоянного тока для низкоскоростного маглев</p>	<p><b>102</b></p>	<p><b>Wang X.H., Yu. J., Lin Y., Lu D.Q., Qin F.</b>          Speed Increasing Scheme by Using 3000 V DC Power Supply for Low-Speed Maglev</p>
<p><b>Волек А.Л.</b>          Грузовой Маглев - перспективный путь развития в США</p>	<p><b>117</b></p>	<p><b>Wolek A.L.</b>          MagLev Freight - One Possible Path Forward in the USA</p>
<p><b>Кирхнер М.</b>          Эмпирическое исследование потенциальных проблем, связанных с использованием лифтов на основе магнитной левитации</p>	<p><b>134</b></p>	<p><b>Kirchner M.</b>          Empirical investigation of possible concerns regarding the use of magnetic levitation elevators</p>
<p><b>Поляков В.А., Хачапуридзе Н.М.</b>          Продольное движение магнитолевитирующего поезда (результаты моделирования)</p>	<p><b>143</b></p>	<p><b>Polyakov V.A, Khachapuridze N.M.</b>          Magnetically levitated train's longitudinal motion (simulation results)</p>
<p><b>Сунь П., Ге К., Ли И., Ван Х.</b>          Исследования бессенсорного управления скоростью движения Маглев с двойным источником питания</p>	<p><b>154</b></p>	<p><b>Sun P., Ge Q., Li Y., Wang X.</b>          Research on Speed Sensorless Control of Maglev Train with Double-End Power Supply</p>

DOI 10.17816/transsyst2018435-25

© D. Dietz, A. Binder

Institute of Electrical Energy Conversion – Darmstadt, Technical University  
(Darmstadt, Germany)

## BEARINGLESS PM SYNCHRONOUS MACHINE WITH ZERO-SEQUENCE CURRENT DRIVEN STAR POINT-CONNECTED ACTIVE MAGNETIC THRUST BEARING

**Abstract:** Common cylindrical bearingless drives require a separate thrust bearing, which is fed by a DC supply. Here, a technique is presented, which enables the feeding of the thrust bearing by an artificially generated zero-sequence current between the two star points of the two parallel windings in the bearingless PM synchronous machine. This way, no additional DC supply for an axial active magnetic bearing is needed. It is replaced by two three-phase inverters as stator winding supply, which are needed in any case to generate torque and lateral rotor force in the motor. This examination explains the technique of adapting the electric potential of the star points in two three-phase windings of the motor. The focus is on the determination of the operating area (maximum zero-sequence current and band width). It is constrained by the bearingless motor due to torque and lateral force ripple as well as additional eddy current losses. On the other hand, the DC link voltage and the modulation degree of the inverter for simultaneous motor operation as well as the bearing inductance limit the system dynamic. It is shown that the proposed technique is applicable for a modulation degree  $< 0.866$ , taking into account that other constraints by the bearingless machine and the inverter are mainly noncritical.

**Keywords:** Bearingless drive, combined winding, zero-sequence current, star point-connected thrust bearing, active magnetic bearing

### INTRODUCTION

Active magnetic self-bearing motors, often referred to as bearingless motors (BM), combine two functions in a single device: the torque generation by an electric machine and the suspension force generation by an active magnetic bearing (AMB) [1, 2, 3]. BMs can be categorized mainly into two groups: First and most prominent, into motors, which generate lateral rotor forces but require a separate axial AMB [4–7]. Second, into motors which do not require an additional axial AMB. Among these, there are BMs which do not need an axial position control due to a disk-like and thereby self-stabilizing rotor [8–12]. Other topologies can actively generate



axial rotor force by a conical rotor [13, 14] or a chessboard structure on the rotor surface [15]. However, the complexity in terms of manufacturing effort and control disable these interesting solutions from industrial use. For lower power classes ( $< 500$  W) also topologies are available, which passively stabilize the axial rotor position by means of several permanent magnet (PM) layers [16].

The predominant field of application for AMB-suspended drives is the use as high-speed drive because AMBs inherently mitigate the friction losses and enable the rotor rotation around its inertia axis to suppress vibration forces [1, 2, 17]. As such, small rotor diameters are necessary to keep the mechanical stress in the rotor at a suitable level. However, for these rotors, commonly cylindrical, a separate AMB for axial position control, a so-called thrust AMB, is required. Often the thrust bearing is realized parallel to a radial AMB as combined AMB [5] on the non-drive end (NDE) of the shaft, whereas the BM is mounted on the drive end (DE) in order to achieve a short axial length. But even if two BMs as two half-motors are used [18], an additional axial AMB is required. In any case, this axial AMB is usually fed by a DC chopper, which is costly.

Here, a technique is presented to avoid the additional DC supply. Therefore, it is made use of the fact that BMs typically are equipped with two star-connected winding systems. That means all the six motor terminals are used to generate torque, radial and axial force at the same time. In [19] it is shown that the electric scalar potential between the two star points  $Z_A$  and  $Z_B$  can be artificially adapted in order to generate a controllable current between  $Z_A$  and  $Z_B$ . Altogether, the

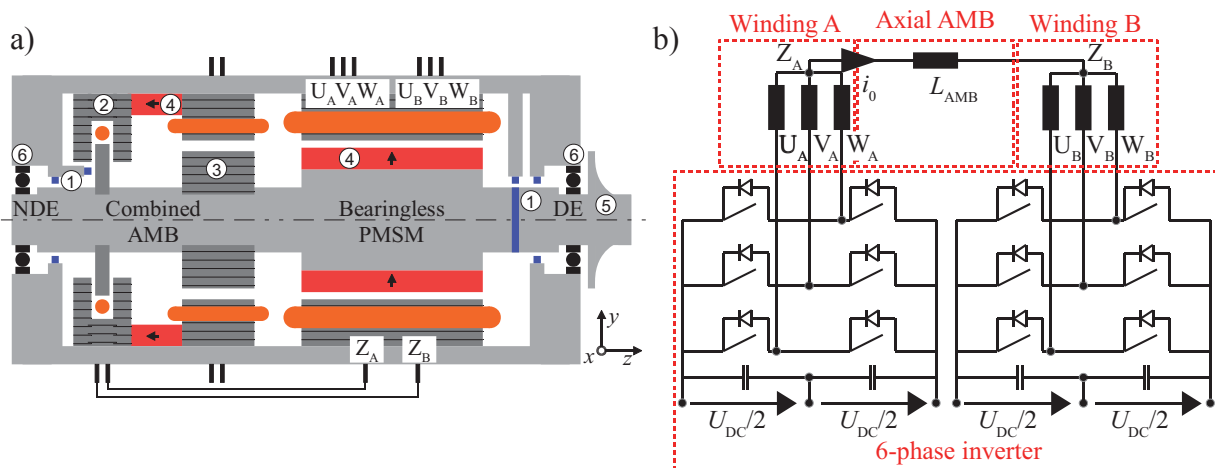


Fig. 1. Drive components (schematic) (1) Position and rotor angle sensors, (2) Axial part of combined AMB, (3) Radial part of combined AMB, (4) PM with magnetization direction, (5) Turbo-compressor wheel, (6) Safety bearings at drive and non-drive end (DE / NDE) a; simplified electric circuit of the bearingless machine and the axial AMB b

proposed technique is beneficial for high-speed bearingless motors with cylindrical rotors. A schematic overview of the drive system is given in Fig. 1a.

In the section “The bearingless PM synchronous machine” the bearingless machine is presented which the novel technique will be applied to. This is followed by the explanation of generating artificially a zero-sequence current system. The focus of the article is on the last two sections where the constraints inherently given by the motor and by the inverter are explained.

## THE BEARINGLESS PM SYNCHRONOUS MACHINE

A prototype machine with a double three-phase winding was built which is similar to that in Fig. 1. In this prototype the thrust bearing is conventionally fed by a DC supply. It is not possible to apply the presented technique since the star points are insulated and not accessible. The function of this machine is, however, introduced shortly because the demonstrated principle refers to this machine topology. In [4, 20, 21] the winding topology as well as measuring results are presented in detail. Its main parameters are listed in Table 1. It is important to note that the technique is applicable for every bearingless machine which exhibits two three-phase windings fed by the same inverter.

Table 1. Motor specifications

Rated speed / $\text{min}^{-1}$	$n_N$	60 000
Rated torque / mNm	$M_N$	105
Rated lateral force / N	$F_N$	8.2
Rated phase voltage / V	$U_{s,N}$	42
Rated phase current for torque / A	$I_{cw,N}$	3.18
Rated phase current for lateral force / A	$I_{ccw,N}$	2.26
Rated total phase current / A	$I_{s,N}$	3.90
Rated current for axial force / A	$I_{0,N}$	0.9
Stator bore outer/inner diameter / mm	$d_{s,o}/d_{s,i}$	70/35
Stator stack length / mm	$l_{Fe}$	40
Bandage thickness / mm	$h_b$	1.5
Magnet height / mm	$h_{PM}$	2.75
Mechanical air gap $(d_{s,i} - d_{r,o})/2$ / mm	$\delta$	1.0
Rotor mass / g	$m_r$	800
Number of turns per phase (6 phases)	$N_{s,6}$	22
Number of pole pairs (torque/suspension winding)	$p/p_{sus}$	1/2



In this machine a combined two-layer winding replaces the common drive and suspension windings. When accordingly fed it is possible to generate a field wave of pole count  $2p = 2$ , equal to the rotor field pole count, and a field wave of pole count  $2p_{\text{sus}} = 2p + 2 = 4$  simultaneously. In interaction with the rotor field, the  $2p$ -pole field wave generates tangential force, whereas the  $2p_{\text{sus}}$ -pole field wave generates lateral force for rotor suspension. Starting from a conventional four-pole three-phase winding, this is possible if the winding per phase (e.g. phase U) is separated into two spatially opposed coil groups (e.g.  $U_A$  and  $U_B$ ). Each of these coil groups is now fed by a separate phase yielding six phases consisting of the phase belt sequence  $+U_A, +W_B, +V_A, +U_B, +W_A, +V_B$ . The phase belts indexed by A (B) are referred to as three-phase system A (B). They are both star-connected, yielding the two star-points  $Z_A$  and  $Z_B$ . If the two systems are fed in phase a counter-clockwise rotating  $2p_{\text{sus}}$ -pole field wave occurs so that the phase sequence is reversed ( $i_{\text{ccw}}$ ) for clockwise field wave rotation. If they are fed in phase opposition a clockwise rotating  $2p$ -pole field wave occurs by  $i_{\text{cw}}$ . In practice, both field waves are needed with clockwise rotation. So a superposition yields an elliptical current space vector orbit per three-phase system A and B consisting theoretically of two symmetrical three-phase current space vectors with reversed rotation [4, 20, 21]. This principle is used to realize the supply of the separate thrust bearing (inductance  $L_{\text{AMB}}$ ) by an artificially generated current  $i_0$  between the star points  $Z_A$  and  $Z_B$ . This is shown in Fig. 1b where  $U_{\text{DC}}$  is the DC link voltage of the inverter.

## GENERATION OF THE REQUIRED ZERO-SEQUENCE VOLTAGE

The proposed technique relies on a conventional space vector pulse width modulation (SVPWM) [3]. That means, that for each of the elliptical three-phase current systems  $I_A$  and  $I_B$  a current controller determines a certain voltage space vector in the stator-fixed coordinate systems ( $\alpha_A$ - $\beta_A$  and  $\alpha_B$ - $\beta_B$ ). This voltage requirement depends solely on the torque and radial suspension force requirement, whereas the axial force requirement is introduced at a later state. The amplitude of the applied phase voltages  $\hat{u}_{A,s}$  and  $\hat{u}_{B,s}$  which in the case of a symmetrical voltage system is equal to the length of the voltage space vectors  $\underline{u}_A$  and  $\underline{u}_B$  is limited by the hexagon in Fig. 2a. In this case, due to the superposition of the clockwise and counter-clockwise voltage system, the main axes of the ellipses determine the inverter voltage rating. These main axes are determined by the algebraic sum of the required clockwise and counter-clockwise rotating voltage space vectors for torque and lateral force generation. However, since the  $2p$ -pole rotor field does not induce into the imaginary  $2p_{\text{sus}}$ -pole suspension winding, the voltage trajectory is

only slightly elliptical, so that mainly the back-EMF of the  $2p$ -pole rotor field determines the voltage requirement as in common rotating field machines.

According to Fig. 2a the inverter states 0, ..., 7 are related to the phase terminal electric potentials  $\varphi_U$ ,  $\varphi_V$  and  $\varphi_W$ . They can take the discrete values  $U_{DC}/2$  ( $-U_{DC}/2$ ) when the related high-side switches are turned on (off). As the voltage space vector moves through the sectors I, ..., VI (Fig. 2a) the adjoining inverter states are realized for a calculated time  $t_0, \dots, t_7$ . For the traditional symmetrical SVPWM the calculation of  $t_0, \dots, t_7$  is well explained in literature [3, 22]. This technique is commonly used for three-phase inverters when operated in field-oriented control. It is important to note that only the time spans  $t_1$ ,  $t_2$  and  $t_{passive}$  are mandatory for the torque and lateral force generation. The position of the time spans as well as the composition of  $t_{passive}$  within one switching period, however, can be arbitrarily chosen. This is made use of for the here presented technique. The independent control of the zero-sequence voltage and the phase voltages by means of extended *Park* and *Clarke* transformations is discussed in detail in [19]. The equivalent circuit of the current loop including the motor windings A and B and the axial AMB and defining the orientation of  $i_0$  and  $u_0$  is depicted in Fig. 2b. According to that the *Ohmic*-inductive voltage drop  $u_0$  over the thrust AMB is dependent on the difference in electric potential between phase terminals  $\varphi_{U,A}$ ,  $\varphi_{V,A}$ ,  $\varphi_{W,A}$  and  $\varphi_{U,B}$ ,  $\varphi_{V,B}$ ,  $\varphi_{W,B}$ . That is, every time a difference in potential between the star points occurs, a current is flowing if the star points are connected. This is inherently the case if the active voltage vectors in the two systems A and B are different ( $t_{1,A} \neq t_{1,B}$  and  $t_{2,A} \neq t_{2,B}$ ).

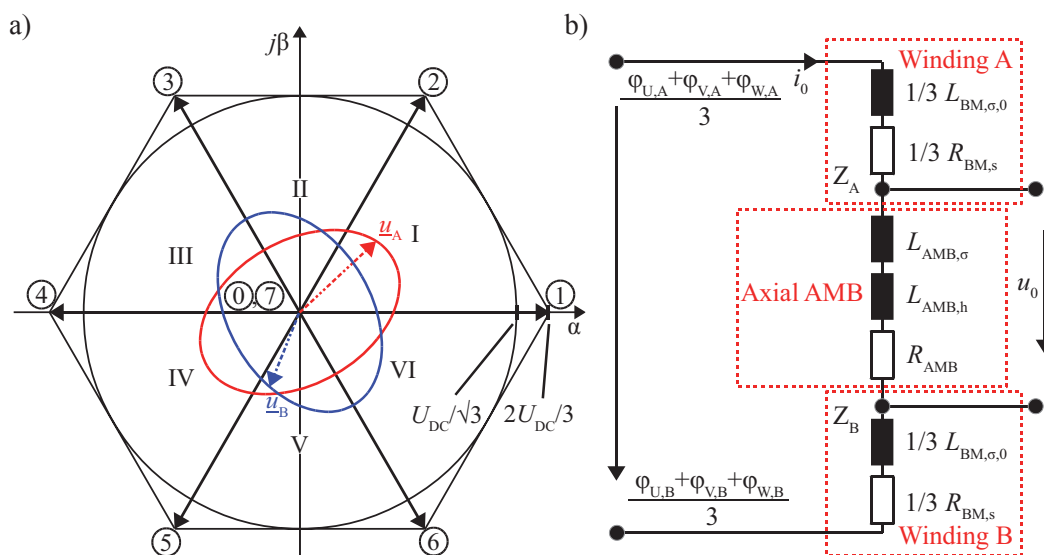


Fig. 2. Switching states (circled) and voltage space vector trajectories in the stator-fixed  $\alpha$ - $\beta$ -reference frame related to the voltage limit a; and equivalent circuit for the zero-sequence current component  $i_0$  b

However, the overlapping time spans where a difference in potential is present can be influenced by variation of the time spans  $t_{0,A}$ ,  $t_{7,A}$ ,  $t_{0,B}$  and  $t_{7,B}$ . Aside from the dependency of the difference in the star point potential also the relation between motor and AMB impedance as voltage divider  $k_{eq}$  (1) affects the maximum voltage over the terminals of the thrust AMB. Obviously the AMB impedance should be high in relation to the motor zero-sequence impedance for a dynamic current response. On the other hand, the overall impedance should be small for the same reason. The voltage at the AMB can be calculated according to (2) and can be written as (3), where  $\bar{u}_0|_{T_{sw}}$  is the average voltage over one switching period  $T_{sw}$ .

$$u_0 \sim k_{eq} = \frac{3 \cdot (\omega L_{AMB,h} + \omega L_{AMB,\sigma} + R_{AMB})}{3 \cdot (\omega L_{AMB,h} + \omega L_{AMB,\sigma} + R_{AMB}) + 2 \cdot (\omega L_{BM,\sigma,0} + R_{BM,s})} \quad (1)$$

$$\bar{u}_0|_{T_{sw}} = \frac{k_{eq}}{T_{sw}} \int_0^{T_{sw}} \left( \frac{\varphi_{U,A}(t) + \varphi_{V,A}(t) + \varphi_{W,A}(t)}{3} - \frac{\varphi_{U,B}(t) + \varphi_{V,B}(t) + \varphi_{W,B}(t)}{3} \right) dt \quad (2)$$

$$\bar{u}_0|_{T_{sw}} = \frac{U_{DC} \cdot k_{eq}}{2 \cdot T_{sw}} \cdot \left( \underbrace{\frac{t_{2,A} - t_{1,A}}{3} + \frac{t_{1,B} - t_{2,B}}{3}}_{\text{Fixed time spans by different active voltage vectors in system A and B}} + \underbrace{\frac{t_{7,A} - t_{0,A} + t_{0,B} - t_{7,B}}{3}}_{\substack{\text{Controllable time spans for artificial} \\ \text{zero-sequence voltage generation} \\ t_{z,AMB}}} \right) \quad (3)$$

$$t_{\text{passive},A} = t_{0,A} + t_{7,A} = T_{sw} - t_{\text{active},A}; \quad t_{\text{passive},B} = t_{0,B} + t_{7,B} = T_{sw} - t_{\text{active},B} \quad (4)$$

The time spans  $t_{1,A}$ ,  $t_{2,A}$ ,  $t_{1,B}$  and  $t_{2,B}$  are known since they are previously calculated. Therefore, up to now the parameters  $\{t_{z,AMB}, t_{\text{passive},A}, t_{\text{passive},B}\} \in \mathbb{R}_3$  are known (3, 4) whereas the unknown parameters are  $\{t_{0,A}, t_{7,A}, t_{0,B}, t_{7,B}\}$ . To solve this under-determined system another condition has to be introduced. It is selected in a way that the overlapping time span  $t_7 - t_0$  is proportional ( $t_0 \rightarrow t_{0,lin}$ ,  $t_7 \rightarrow t_{7,lin}$ ) to the relation between the time span for the passive voltage vectors of one system and the total time span for passive voltage vectors. From that system (5) results, which can be solved by applying *Cramer's* rule. However, (5) yields solutions which can be both positive and negative. Therefore, the solution space must be limited to (6), resulting in a nonlinear switching behavior.

$$\begin{pmatrix} 1 & 1 & 0 & 0 \\ 0 & 0 & 1 & 1 \\ -1 & 1 & 1 & -1 \\ t_{\text{passive},B} & -t_{\text{passive},B} & t_{\text{passive},A} & -t_{\text{passive},A} \end{pmatrix} \cdot \begin{pmatrix} t_{0,A,lin} \\ t_{7,A,lin} \\ t_{0,B,lin} \\ t_{7,B,lin} \end{pmatrix} = \begin{pmatrix} t_{\text{passive},A} \\ t_{\text{passive},B} \\ t_{z,AMB} \\ 0 \end{pmatrix} \quad (5)$$

$$\begin{cases} t_{0,A} = \frac{1}{2} \cdot \left( t_{\text{passive},A} - \frac{t_{\text{passive},B}}{t_{\text{passive},A} + t_{\text{passive},B}} \cdot t_{z,AMB} \right) & \forall t_{0,A,\text{lin}} > 0 \\ t_{0,A} = 0 \wedge t_{7,A} = t_{\text{passive},A} & \forall t_{0,A,\text{lin}} < 0 \end{cases} \quad (6a)$$

$$\begin{cases} t_{7,A} = \frac{1}{2} \cdot \left( t_{\text{passive},A} + \frac{t_{\text{passive},B}}{t_{\text{passive},A} + t_{\text{passive},B}} \cdot t_{z,AMB} \right) & \forall t_{7,A,\text{lin}} > 0 \\ t_{7,A} = 0 \wedge t_{0,A} = t_{\text{passive},A} & \forall t_{7,A,\text{lin}} < 0 \end{cases} \quad (6b)$$

$$\begin{cases} t_{0,B} = \frac{1}{2} \cdot \left( t_{\text{passive},B} + \frac{t_{\text{passive},A}}{t_{\text{passive},A} + t_{\text{passive},B}} \cdot t_{z,AMB} \right) & \forall t_{0,B,\text{lin}} > 0 \\ t_{0,B} = 0 \wedge t_{7,B} = t_{\text{passive},B} & \forall t_{0,B,\text{lin}} < 0 \end{cases} \quad (6c)$$

$$\begin{cases} t_{7,B} = \frac{1}{2} \cdot \left( t_{\text{passive},B} - \frac{t_{\text{passive},A}}{t_{\text{passive},A} + t_{\text{passive},B}} \cdot t_{z,AMB} \right) & \forall t_{7,B,\text{lin}} > 0 \\ t_{7,B} = 0 \wedge t_{0,B} = t_{\text{passive},B} & \forall t_{7,B,\text{lin}} < 0 \end{cases} \quad (6d)$$

Altogether, the active inverter switching instants can be calculated according to [3], whereas the passive inverter states are given by (6). However, the time spans of the two systems are coupled by (6) so that a common module for a three-phase inverter must be replaced by a novel six-phase module.

## CONSTRAINTS BY THE BEARINGLESS MOTOR

If the two windings A and B are fed by a DC current as described above the M.M.F. distribution  $V(\gamma, t)$  normal to the stator surface for the considered PM synchronous machine results as to see in Fig. 3. It is important to note that the current through the axial AMB is only one third in each phase, following *Kirchhoff's* law (see Fig. 2 b)). From that it can be concluded that, aside from the symmetrical three-phase systems  $i_{\text{cw}}$  and  $i_{\text{ccw}}$ , the zero-sequence component  $i_0(t)$  introduces field harmonics of order  $\nu = 3, 9, 15, \dots$  according to (9). This field distribution does not move but is constant if  $i_0$  is constant and pulsates with  $f_{\text{ax}}$  if  $i_0$  is sinusoidal and  $f_{\text{ax}}$ -frequent.

$$V_\nu(\gamma, t) = \sum_{\nu=3,9,15,\dots}^{\infty} \frac{4}{\pi} \cdot \frac{1}{\nu} \cdot m \cdot N_c \cdot \frac{i_0(t)}{3(9)} \cdot \cos(\nu \cdot \gamma); \quad N_c: \text{number of coil turns}$$

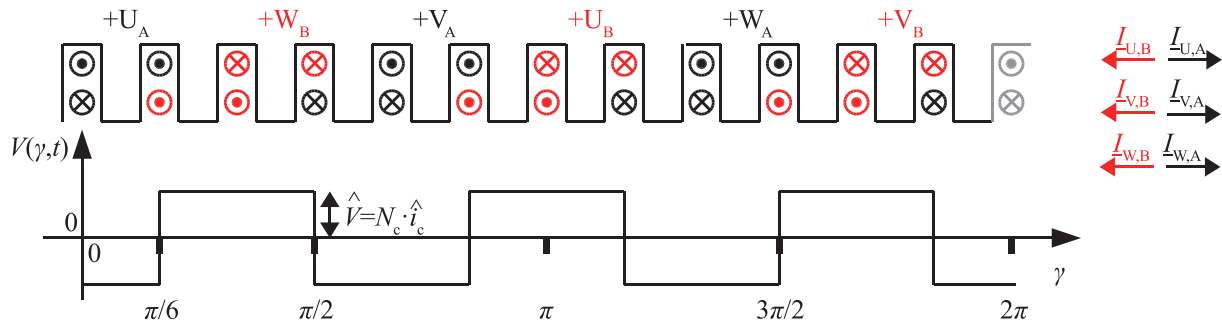


Fig. 3. M.M.F.-distribution  $V(\gamma,t)$  normal to the stator surface at the stator inner bore (circumferential angle  $\gamma$ ) for a pure zero-sequence current feeding  $i_0(t)$ , where coil current  $i_c(t) = i_0(t)/3$  and coil turn count is  $N_c$

Especially the third harmonic ( $\nu = 3$ ) is harmful since higher harmonics only account for 2 % of the total field normal to the stator surface. The resulting field has to be taken care of for two reasons. First, like in a transformer, it induces a voltage in the phase winding due to a certain zero-sequence inductance  $L_{\text{BM},\sigma,0}$ . This inductance together with the phase resistance forms a voltage divider according to (Fig. 2b). Therefore, it is desirable to keep the motor zero-sequence impedance low. However, for the given system the zero-sequence motor inductance  $L_{\text{BM},\sigma,0} = 57 \mu\text{H}$  is negligible compared to the AMB inductance  $L_{\text{AMB}} = 15 \text{ mH}$  (both from 2D finite element (FE) simulation by means of the software *JMAG*, winding overhang inductance analytically calculated). The second harmful influence of the six-pole field distribution is on the motor operation and treated hereafter. It yields torque ripple, force ripple and eddy current losses in the PM.

For all these fields of interest the worst case is active for a pure DC current feeding as shown in Fig. 4, 5. That means, the field distribution in Fig. 3 does not pulsate but is constant. The influence of the zero-sequence current on the *Ohmic* losses in the conductors is negligible and, thus, not considered here.

## Torque ripple

The impact of the zero-sequence current on the torque ripple  $w_M$  is estimated analytically and via 2D FE simulation (Fig. 4). First, the analytical calculation process is shown in order to explain the origin of the torque ripple. It relies on the 2D *Maxwell* stress tensor  $(f_r, f_t)^T$  (r: radial, t: tangential) in cylindrical coordinates and uses the assumptions of infinite iron permeability as well as neglectation of the slotting, curvature and end effect.

The field wave of the  $\nu$ th stator and the  $\mu$ th rotor harmonic with respect to the circumferential angle  $\gamma$  of the stator field  $B_{s,\nu}(\gamma,t)$  as well as of the rotor  $B_{r,\mu}(\gamma,t)$  are superimposed at each time and are integrated over a closed surface in the air gap

(stack length  $l_{Fe}$ ). This yields the time depending torque  $M(t)$  (10, 11);  $N_s$ : Number of turns per phase,  $k_{w,v}$ : winding factor of  $v$ th harmonic,  $m$ : phase count,  $r_{s,i}$ : bore radius,  $i$ : torque harmonic order.

$$M(t) = \int_0^{l_{Fe}} \int_0^{2\pi} (f_t(\gamma, t) \cdot r_{s,i}) d\gamma dz = \quad (10)$$

$$= M_1 \cdot \sin(\varphi_{r,1} - \varphi_{s,1}) + \sum_{i=3,9,15,\dots}^{\infty} \hat{M}_i \cdot \sin(i \cdot \omega_s t + i \cdot \varphi_{r,i} - \varphi_{s,i})$$

From that, it can be concluded that apart from the well-known constant term an additional time-depending component is present. This component is of sinusoidal character, oscillating with frequencies  $i \cdot \omega_s$  ( $i = v = \mu$ ) according to the product of synchronous frequency  $\omega_s$  and order of magnetic field space harmonics of equal pole count  $v = \mu = 3, 9, 15, \dots$  excited by the zero-sequence current  $i_0$ . Here, most crucially the harmonic  $v = \mu = 3$  produces a non-constant torque, oscillating with frequency  $3 \cdot f_s$ . One option to get rid of any torque ripple of this nature is to improve the magnetization pattern so that the PM excites a field distribution which is purely sinusoidal ( $\hat{B}_{r,\mu} = 0 \forall i \neq \mu$ ).

From (10) the torque coefficients  $M_i$  can be calculated according to (11). From that, the low influence of a zero-sequence feeding can be seen. Equation (11) is valid for  $m = 3$  phases. The analytical result (*Analyt. DC-current*) for the third harmonic current ripple is proved at rated operation by the FE simulation (*FE DC-current*) results from Fig. 4b.

$$M_1 = \hat{i}_{cw} \cdot k_{w,1} \cdot 2 \cdot m \cdot N_s \cdot \hat{B}_{r,1} \cdot l_{Fe} \cdot r_{s,i} ; M_{1,N} = 124.956 \text{ mNm}$$

$$\hat{M}_i = \frac{i_0}{3} \cdot k_{w,i} \cdot 2 \cdot m \cdot N_s \cdot \hat{B}_{r,\mu=i} \cdot l_{Fe} \cdot r_{s,i} ; \hat{M}_{3,N} = 0.096 \frac{\text{mNm}}{\text{A}} \cdot i_0 \quad (11)$$

$$\Rightarrow w_M = 0.077 \frac{\%}{\text{A}} ; w_M = \left| \frac{M_{\max} - M_{\min}}{M_{\max} + M_{\min}} \right|$$

So far the zero-sequence current was assumed to be constant. However, sometimes due to mechanical imbalance and external force disturbances the axial force requirement as well as the linked current  $i_0(t)$  is not constant. The calculation is not shown here, but it can be concluded that a time variant zero-sequence current introduces new frequencies in the torque harmonic spectrum. This can be harmful if certain resonances are excited by these frequencies. However, the force ripple (*FE AC-current*, Fig. 4b) is smaller in any case compared to the DC feeding. Fig. 4b shows the torque ripple amplitude for different zero-sequence current feedings ( $\hat{i}_0 = 0 \dots 10.5 \text{ A}$ ) at rated operation. For usual operation no more than  $i_0 = 1 \text{ A}$

( $i_0/3 < 0.33$  A) is needed. From Fig. 4b it can be concluded that a zero-sequence feeding to this extent has no crucial influence on the torque ripple, staying below 0.2 %.

## Force ripple

The origin of the ripple  $w_F$  in the lateral force is explained equivalent to the torque ripple calculation. To do so the *Maxwell* stress tensor ( $f_r, f_t$ )<sup>T</sup> has to be evaluated, taking into account that the force in the  $x$ - $y$  coordinate system is needed for control purpose. In the calculation, stator and rotor field harmonics of order  $\nu, \mu > 3$  are neglected for clarity since their influence is very small. The composition of the active lateral force is depicted in (12).

$$\begin{aligned} F_x(t) &= F_{op} \cdot \cos(\varphi_{r,1} - \varphi_{s,2}) + F_{dis} \cdot \cos(\varphi_{s,1} - \varphi_{s,2}) + \\ &\quad + \hat{F}_{var,1} \cdot \cos(\omega_s t + \varphi_{s,2} - \varphi_{s,3}) + \hat{F}_{var,2} \cdot \cos(2 \cdot \omega_s t - \varphi_{s,2} + 3 \cdot \varphi_{r,3}) \\ F_y(t) &= F_{op} \cdot \sin(\varphi_{r,1} - \varphi_{s,2}) + F_{dis} \cdot \sin(\varphi_{s,1} - \varphi_{s,2}) - \\ &\quad - \hat{F}_{var,1} \cdot \sin(\omega_s t + \varphi_{s,2} - \varphi_{s,3}) + \hat{F}_{var,2} \cdot \sin(2 \cdot \omega_s t - \varphi_{s,2} + 3 \cdot \varphi_{r,3}) \end{aligned} \quad (12)$$

From (12) it can be seen that the lateral force in one distinct direction consists of four components whereof two are constant. The force coefficients can be calculated according to (13). Equation (13) is valid for  $m = 3$  phases. The result is proved by FE simulations (see Fig. 4a). The two constant components cover the force component  $F_{op}$ , necessary for operation, and the component  $F_{dis}$ , representing the disturbing influence of the stator drive field by  $i_{cw}$  on the stator suspension field by  $i_{ccw}$ . The latter is not further discussed here.

$$\begin{aligned} F_{op} &= -\frac{1}{2} \cdot \hat{i}_{ccw} \cdot k_{w,2} \cdot 2 \cdot m \cdot N_s \cdot \hat{B}_{r,1} \cdot l_{Fe} \left( \frac{r_{s,i}}{p_{s,2} \cdot \delta} + 1 \right); \quad |F_{op,N}| = 8.584 \text{ N} \\ \hat{F}_{var,1} &= \hat{i}_{ccw} \cdot \frac{i_0}{3} \cdot k_{w,2} \cdot k_{w,3} \cdot m^2 \cdot N_s^2 \cdot \mu_0 \cdot l_{Fe} \left( \frac{r_{s,i}}{9 \cdot \delta^2 \cdot \pi} - \frac{2}{3 \cdot r_{s,i} \cdot \pi} + \frac{1}{9 \cdot \delta \cdot \pi} \right); \\ \left| \hat{F}_{var,1,N} \right| &= 0,0073 \frac{\text{N}}{\text{A}} \cdot i_0 \rightarrow w_{F,1,N} = 0,085 \frac{\%}{\text{A}}; \quad w_F = \left| \frac{F_{max} - F_{min}}{F_{max} + F_{min}} \right| \\ \hat{F}_{var,2} &= -\hat{i}_{ccw} \cdot k_{w,2} \cdot m \cdot N_s \cdot \hat{B}_{r,3} \cdot l_{Fe} \left( \frac{r_{s,i}}{p_{s,2} \cdot \delta} - 1 \right); \\ \left| \hat{F}_{var,2,N} \right| &= 0,021 \text{ N} \rightarrow w_{F,2,N} = 0,25 \text{ \%} \end{aligned} \quad (13)$$

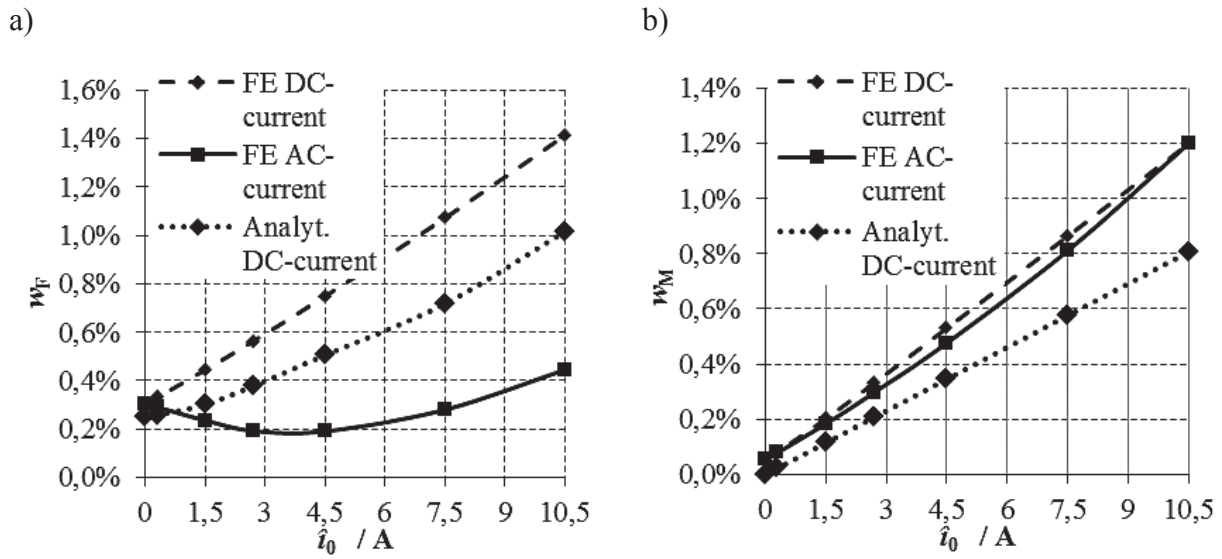


Fig. 4. Calculated force ripple  $w_F$  a; calculated torque ripple  $w_M$  b for different zero-sequence current feedings at  $n_N = 60000 \text{ min}^{-1}$ ,  $M_N = 105 \text{ mNm}$ , FE: results from FE simulation (*JMAG*), AC feeding at  $\omega_{ax} = \omega_s$ ; Other operating points behave similarly

Of importance are the two time variant components  $F_{\text{var},1}$  and  $F_{\text{var},2}$ .  $F_{\text{var},1}$  is excited by the interaction between the constant six-pole field wave by  $i_0$  and the rotating four-pole field wave by  $i_{\text{ccw}}(t)$ . The force generation results from the difference in pole count by  $\pm 2$ . However, one field wave is caused by a  $f_s$ -frequent current  $i_{\text{ccw}}(t)$ , whereas the other results from a DC current  $i_0$ . From this difference the force ripple frequency is  $f_{F,\text{var},1} = f_s - 0 = f_s$ . The amplitude is proportional to the zero-sequence current  $i_0$  (13). For rated operation this force ripple is  $w_{F,1,N} < 0.1 \%$  (13) and not crucial compared to other disturbing influences. The second time variant component  $F_{\text{var},2}$  results from the third rotor field harmonic, rotating with synchronous velocity  $v_{\text{syn}} = f_{r,\mu} / \mu$  and, therefore,  $f_{r,3} = 3 \cdot f_s$  in case of a not purely sinusoidal magnetization in interaction with the four pole stator field wave, excited by the  $f_s$ -frequent current  $i_{\text{ccw}}(t)$ . From this difference the force ripple frequency is  $f_{F,\text{var},2} = 3 \cdot f_s - f_s = 2 \cdot f_s$ . This force ripple is in effect even if no zero-sequence current is fed. It dominates the ripple of  $F_{\text{var},1}$  for values of  $i_0 < 3 \text{ A}$  (13). The calculation with a time variant zero-sequence current is not shown here. It can introduce new frequencies in the lateral force spectrum that may be harmful. However, for the often considered case ( $n \propto f_s \propto \omega_{ax}$ ) it can be seen that no force ripple harmonic is introduced.

From Fig. 4a it can be concluded that a zero-sequence feeding to this extent has no crucial influence on the force ripple, staying below 0.5 %. That means, the force ripple is mostly dominated by the  $2 \cdot \omega_s$ -frequent part  $F_{\text{var},2}$ , which is caused by the 3<sup>rd</sup> rotor field harmonic ( $\mu = 3$ ).



## Eddy current losses in the PM

Generally, every stator-excited magnetic field wave differing from the operating wave induces voltages in eddy current loops formed by the conductive permanent magnet material due to the difference in rotational speed. Keeping the losses caused by these eddy currents low yields low rotor losses. This is a well-known design goal for many reasons [26]. Therefore, the following section shows the criticality of the zero-sequence current with respect to its induced eddy current losses in the PM. To understand the process a 2D analytical eddy current calculation in the form of a multilayer travelling-wave problem was carried out first. For simplicity it was made for a planar geometry. The analytical calculation of eddy current losses in the form of multilayer travelling-wave problems has been extensively discussed in literature [26–28]. The calculation process is elaborate and not shown here. The results from this calculation are shown in Table 2 and compared with the 2D FE simulation results under the same assumptions.

Table 2. Calculated eddy current losses in the rotor for the simplified 2D planar geometry ( $\kappa_{PM} = 1.25 \text{ Ms}\cdot\text{m}^{-1}$ ,  $\kappa_{shaft} = 1.92 \text{ Ms}\cdot\text{m}^{-1}$ ,  $\mu_{r,PM} = 1$ ,  $\mu_{r,shaft} = 100$ )

Harmonic $\nu$	Machine part	Analytical	FE
2 ( $\hat{i}_{ccw} = 3,2 \text{ A}$ )	PM	2.61 W	2.55 W
	shaft	0.79 W	0.58 W
3 ( $i_0/3 = 1 \text{ A}$ )	PM	0.52 W	0.51 W
	shaft	0.08 W	0.11 W
3 ( $i_0/3 = 3,5 \text{ A}$ )	PM	6.33 W	6.32 W
	shaft	1.04 W	1.08 W

The results from the simplified 2D Cartesian geometry show the same tendency as the results from the 2D cylindrical geometry (Fig. 5). If less than 1 A zero-sequence current per phase ( $i_0 < 3 \text{ A}$ ) is injected, there are no relevant additional losses in the rotor of the machine. However, from 1 A the losses increase quickly according to  $I^2 \cdot R$ . Consequently a bearing current of  $i_0 < 3 \text{ A}$  is not crucial and is seen to be the upper limit for the operating current, i.e.  $i_{0,\max} = 3 \text{ A}$  (see Fig. 15).

## CONSTRAINTS BY THE INVERTER

This section focuses on the dependency between the bearing performance and the operation point of the PWM-operated MOSFET inverter. Generally, one important design goal of the magnetic suspension control to ensure stability is

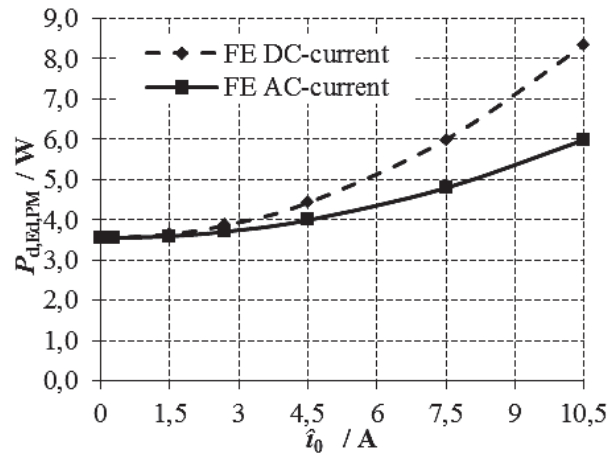


Fig. 5. Calculated eddy current losses  $P_{d,FE,PM}$  in the permanent magnets for different zero-sequence current feedings at rated operation ( $n_N = 60000 \text{ min}^{-1}$ ,  $M_N = 105 \text{ mNm}$ ) from 2D FE simulations (*JMAG*); other operating points show similar characteristics

the sufficiently fast change rate of the bearing current which is influenced by the required current amplitude, the frequency and voltage rating of the inverter as well as of the bearing inductance. In this case the amplitude of the current is limited by the motor tolerance for a zero-sequence current ( $i_{0,max} = 3 \text{ A}$ ). The frequency range and voltage amplitude of the current is limited by the inverter ( $U_{DC,max} = 150 \text{ V}$ ,  $f_{sw,max} = 60 \text{ kHz}$ ). Apart from these given parameters, the system design-related time constant of the plant ( $\tau_{plant} = 10.64 \text{ ms}$ , see Fig. 2b) plays an important role. The choice of the desired parameters for a stiff control is limited in reality. Given the time constant of the plant and staying within the tolerance range of the zero-sequence current for the motor it is mainly dependent of the inverter.

In addition to this general statement, the difficulty has to be treated that the inverter capacity is constrained by the generation of the torque and suspension field in the bearingless motor. As can be seen from the switching instant calculation (section “Generation of the required zero-sequence voltage”), the generation of the two voltage systems is treated with priority. In accordance with that, it can be shown by simulation that neither in steady state nor in transient condition the zero-sequence voltage changes its time harmonic spectrum of the torque and lateral force generating motor currents. On the other hand, the operation point of the motor, determining the inverter operation point, influences the zero-sequence current slope and the axial bearing performance. Different points of operation that show this crucial impact are investigated by means of the software *Simulink* assuming ideal switching behavior in the following order: variable bearing current step response at rated motor operation, fixed bearing current step response at variable motor speed, inherent zero-sequence current with and without control, operating area for variable sinusoidal bearing current.

## Variable bearing current step response at rated motor operation

Fig. 6 gives insight into the transient behavior of the bearing current for rated motor operation. In this and the following time plots  $i_{0,\text{ideal}}$  gives the theoretical current in case of a pure DC voltage feeding  $u_{0,\text{ideal}}$  (ideal inverter behavior, no PWM).  $i_0$  and  $u_0$  are the real current and real voltage, resulting from the pulse width modulated inverter.

In Fig. 6a it can be seen that current follows within 0.3 ms in comparison with the ideal case where the current follows within 0.1 ms. In this scenario the inverter shows the well-known lack element behavior. For a reference step of  $i_{0,\text{ref}} = 3$  A (Fig. 6b) the current follows within 0.9 ms which is again three times the time span of the pure DC voltage feeding. Further, the non-linear behavior which results from the zero-voltage time span calculation can be seen. However, it is already can be shown that the disturbing effect of the inverter on the controller circuit is acceptable for current requirements  $i_0 < 1$  A.

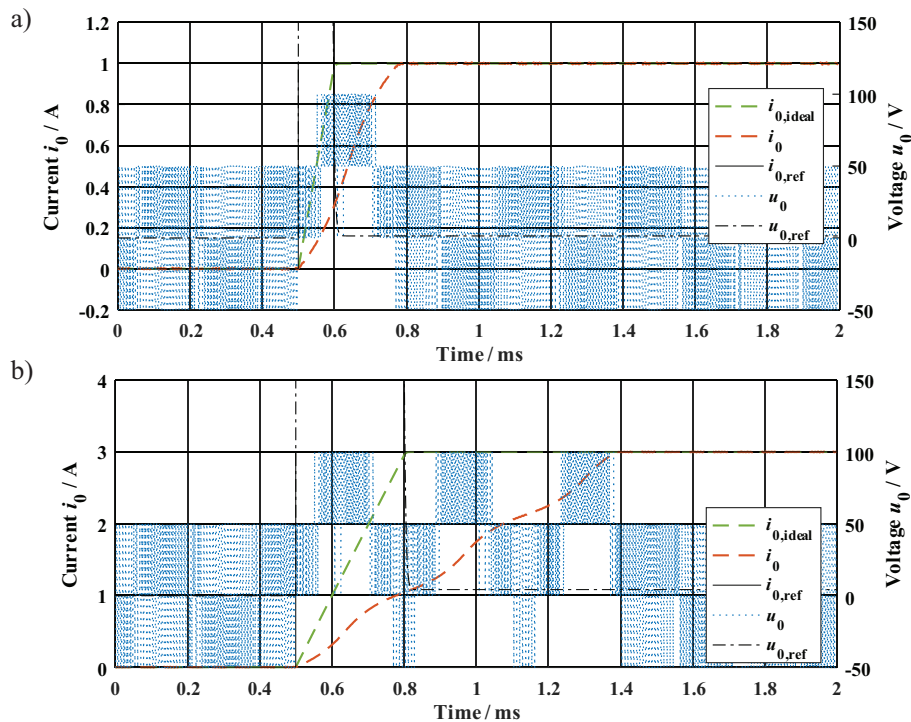


Fig. 6. Simulated step response response for a reference current step of  $i_{0,\text{ref}}=1$  A a; and  $i_{0,\text{ref}}=3$  A b; 0.5 ms at rated motor operation ( $f_{s,N} = 1000$  Hz,  $\hat{U}_{cw} = 60$  V,  $\hat{U}_{ccw} = 3.2$  V,  $f_{sw} = 60$  kHz)

## Fixed bearing current step response at variable motor speed

The influence of the inverter utilization by the motor operation, i.e. the modulation degree given by the back-EMF related motor speed, on the bearing

current slope has to be considered. This question is directly linked to the provided zero-voltage time spans which can be used in order to generate the zero-sequence current artificially. Therefore, Fig. 7 compares the zero-voltage duty states  $d_{0,A}$ ,  $d_{7,A}$ ,  $d_{0,B}$ ,  $d_{7,B}$  for Fig. 6a  $n/n_N = 2/3$  and Fig. 6b  $n/n_N = 4/3$ .

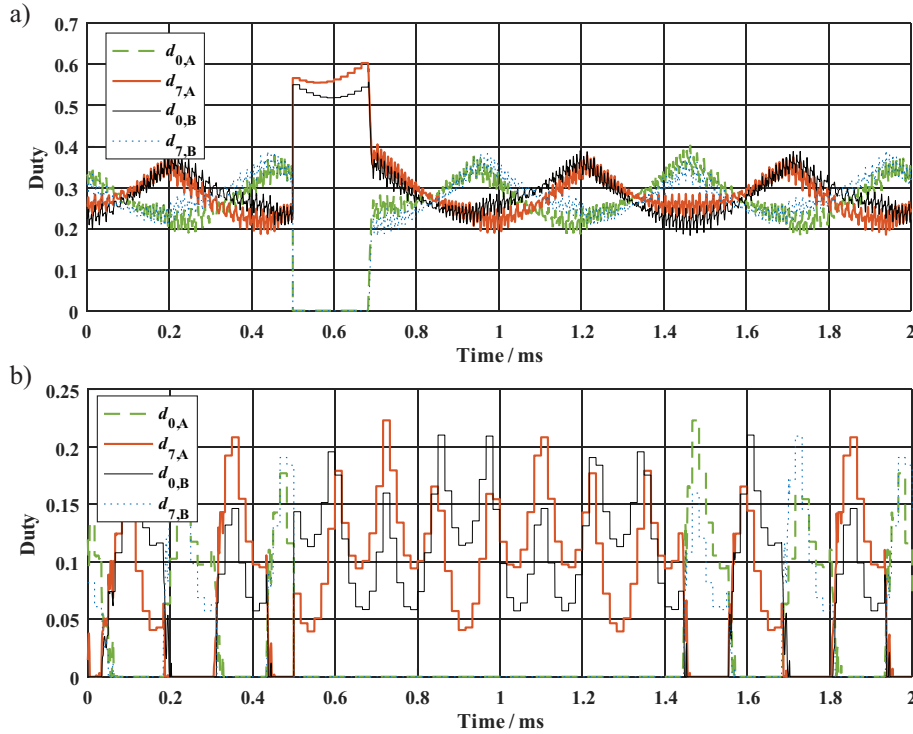


Fig. 7. Simulated zero-voltage duty states  $d_{0,A}$ ,  $d_{7,A}$ ,  $d_{0,B}$ ,  $d_{7,B}$  for a reference current step of  $i_{0,ref} = 1$  A at 0.5 ms at rated suspension operation ( $\hat{u}_{ccw} = 3.2$  V,  $\hat{i}_{ccw} = 3.2$  A) and different modulation degrees: a –  $\hat{u}_{cw} = 40$  V ( $m_a = 0.5$ ,  $n \approx 40\,000$  min<sup>-1</sup>); b –  $\hat{u}_{cw} = 80$  V ( $m_a = 0.96$ ,  $n \approx 80\,000$  min<sup>-1</sup>)

A step-like zero-sequence current requirement occurs at 0.5 ms requiring the maximum zero-sequence voltage (positive). Therefore,  $d_{7,A}$  and  $d_{0,B}$  (all high-side switches of system A on and all low-side switches of system B on) are as big as possible whereas  $d_{0,A}$  and  $d_{7,B}$  are kept zero. This clearly shows that the remaining zero-voltage time span declines from approximately  $T_{sw}/2$  to  $T_{sw}/8$ . Reciprocally to that, these time spans are kept constantly at their maximum level four times longer at  $n/n_N = 4/3$  than at  $n/n_N = 2/3$ . Consequently, the current rise time is longer for higher modulation degrees. It can be shown approximately that twice the modulation degree leads to a four times longer rise time.

### Inherent zero-sequence current with and without control

At high modulation degrees another problem occurs: The zero-sequence current exhibits a 3<sup>rd</sup> harmonic with regards to the synchronous frequency

disturbing the bearing operation which cannot be counteracted by the current controller since the DC link voltage is too small to realize fast current changes within the short passive voltage instant (compare Fig. 9). Therefore, a third harmonic occurs for modulation degrees  $m_a > \sqrt{3}/2$  which is equal to a voltage space vector of length  $U_{DC}/2$ . For comparison the zero-sequence current  $i_{0,\text{non-control}}$  for the case of a symmetrical SVM without zero-sequence current control is given. In order to explain the existence of the third harmonic, Fig. 8 can be consulted. It shows the electric potential of the two star points  $Z_A$ , i.e.  $u_{\gamma,A}$  and  $Z_B$ , i.e.  $u_{\gamma,B}$  for the discrete switching states. For the case of block commutation, i.e.  $t_{\text{active}} = T_{\text{sw}}$  and  $t_{\text{passive}} = 0$ , the potential of one star point pulsates between  $U_{DC}/6$  and  $-U_{DC}/6$  three times per electrical period. The magnitude of the  $u_0$  between the two star points depends on both electric potentials  $u_{\gamma,A}$  and  $u_{\gamma,B}$ . This means, if the two voltage systems are fed in common-mode, no voltage is active between  $Z_A$  and  $Z_B$ . Therefore, the lateral force generating common-mode voltage system does not lead to a ripple in  $u_0$ .

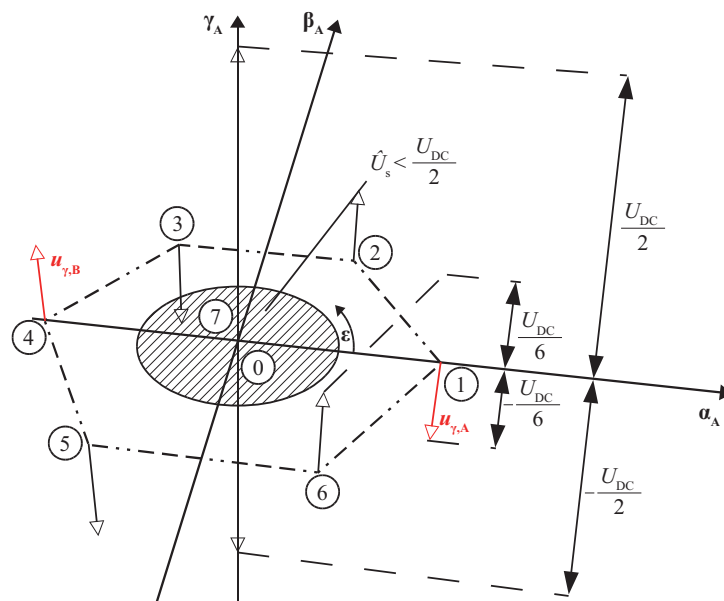


Fig. 8. Switching instants 0, 1, ..., 7 and related electric potentials at the star points  $Z_A$  ( $u_{\gamma,A}$ ) and  $Z_B$  ( $u_{\gamma,B}$ ) in a 3D ( $\alpha$ - $\beta$ - $\gamma$ ) diagram; red: electric potential  $u_{\gamma,A}$  and  $u_{\gamma,B}$  at  $\varepsilon = 0^\circ$  for differential-mode feeding

However, the differential-mode feeding of  $u_{\text{cw}}$  leads to a difference in potential, since the two clockwise systems  $u_{\text{cw},A}$  and  $u_{\text{cw},B}$  are geometrically opposed in the  $\alpha$ - $\beta$ -plane. That is, while system A is e.g. in state 1 ( $u_{\gamma,A} = U_{DC}/6$ ), system B is in instant 4 ( $u_{\gamma,B} = -U_{DC}/6$ ), leading to an amplitude of  $u_0 = U_{DC}/3$ . A sixth of an electric period later system A is in instant 2 ( $u_{\gamma,A} = -U_{DC}/6$ ), system B is in instant 5 ( $u_{\gamma,B} = U_{DC}/6$ ), leading to an amplitude of  $u_0 = -U_{DC}/3$ . This pattern continues, so

that for block commutation the voltage drop of the AMB can be given by (14), neglecting the common-mode feeding. Hence, the zero-crossings of this function are at the switching states when the voltage space vector is between two discrete switching states at odd multiples of  $\varepsilon = \pi/6$ . The maxima of (14) are located at even multiples of  $\varepsilon = \pi/6$  (Fig. 8). In order to explain, from which modulation degree this third harmonic occurs, a condition must be found, so that the amplitude of (14) is zero. As explained, only the instants, when the active voltage vector is composed of only one active switching state, must be considered, e.g.  $t_{\text{active,A}} = t_{1,A}$  and  $t_{\text{active,B}} = t_{4,B}$ . Since  $t_{\text{active,A}} = t_{\text{active,B}}$  due to symmetrical differential-mode feeding, it is obvious that the condition for  $u_0 = 0$  must be fulfilled over one switching period by  $\bar{u}_{\gamma,A}|_{T_{\text{sw}}} = 0$  and  $\bar{u}_{\gamma,B}|_{T_{\text{sw}}} = 0$  yielding (15).

$$u_0(t) = \frac{4}{\pi} \cdot \frac{U_{\text{DC}}}{3} \cdot \cos(3 \cdot (\omega_s \cdot t - \varepsilon)) \quad (14)$$

By applying (3) and (15), it can be shown that the maximum space vector amplitude is  $\hat{U}_s = U_{\text{DC}}/2$ , i.e.  $m_a = \sqrt{3}/2$ , which is in accordance with (15). Consequently, it can be said that the system is applicable for  $n < 1.25 n_N$  which is related to a maximum axial force frequency  $f_{\text{ax,max}}$ . This gives an accurate estimation of the maximum applicable modulation degree regardless the exact system parameters. Moreover, the given system meets the shown behavior despite its slightly elliptical voltage space vector orbit, since  $\hat{u}_{\text{ccw}} \approx 0.05 \cdot \hat{u}_{\text{cw}}$ .

$$\begin{aligned} \bar{u}_{\gamma}|_{T_{\text{sw}}} &= \pm \frac{U_{\text{DC}}}{6} \cdot t_{\text{active}} \mp \frac{U_{\text{DC}}}{2} \cdot t_{\text{passive}} = 0 \\ \Rightarrow t_{\text{active}} &\leq \frac{3}{4} \cdot T_{\text{sw}} \wedge t_{\text{passive}} > \frac{1}{4} \cdot T_{\text{sw}} \Rightarrow \hat{U}_s \leq \frac{U_{\text{DC}}}{2} ; m_a \leq \frac{\sqrt{3}}{2} \end{aligned} \quad (15)$$

## Operating area for variable sinusoidal bearing current

In order to describe the operating area of the axial AMB system it is necessary to point out which requirements the position controller sets for the current controller. The controller design of the thrust magnetic bearing is not in the focus here. However, from the system it is known that an average current of  $i_0 = 0.9$  A is needed in order to levitate the rotor if it is operated vertically so that the thrust bearing carries the rotor. From that it is estimated that the maximum zero-sequence current of  $i_0 = 3$  A is sufficient even for vertical operation.

In the previous section, it was shown that the slew rate of the current is limited by the inverter voltage rating. This results in a limited operating frequency range for the system: At low frequency, e.g.  $i_0 = \text{const.}$ , the tolerance of the zero-

sequence current in the bearingless motor limits the operation in terms of maximum axial force generation (solid lines in Fig. 9). At high frequency, however, the inverter voltage rating (together with the given time constant of the plant) limits the operation (dashed line in Fig. 9). That is, the current cannot follow the reference signal anymore. If the voltage drop over the plant resistance  $R_{\text{plant}}$  is neglected the relation between bearing current and required voltage is given by (16) according to [1]. Here,  $f_{\text{ax}}$  is the bearing current frequency and  $L_{\text{plant}}$  is the bearing and motor inductance of the circuit.

$$\hat{u}_0 = 2\pi \cdot f_{\text{ax}} \cdot L_{\text{plant}} \cdot \hat{i}_0 \Rightarrow \hat{i}_0 \Big|_{\hat{u}_0 = U_{\text{inv,max}} = \text{const.}} \sim \frac{1}{f_{\text{ax}}} \quad (16)$$

This shows that the maximum possible bearing current amplitude is inversely proportional to its applied frequency, since the inverter voltage is limited. Usually it is limited by the inverter voltage rating. In this case additionally the modulation degree  $m_a$  for the required voltage space vectors of the torque and force generating voltage systems in the bearingless motor has to be considered. Taking into account that the fundamental amplitude of the applied voltage of a square-wave form is  $4/\pi \cdot U_{\text{DC}}$  the envelope of the peak current  $\hat{i}_{0,\text{max}}$  can be estimated according to (17) (see Fig. 9).

$$\hat{i}_{0,\text{max}} = (1 - m_a) \cdot \frac{2}{\pi^2} \cdot \frac{U_{\text{DC}}}{L_{\text{plant}}} \cdot \frac{1}{f_{\text{ax}}}; \quad \text{where } m_a = \sqrt{3} \cdot \frac{\hat{U}_{\text{cw}} + \hat{U}_{\text{ccw}}}{U_{\text{DC}}} \quad (17)$$

The black line in Fig. 9 shows the envelope of the operating area at the given conditions ( $U_{\text{DC}} = 150 \text{ V}$ ,  $L_{\text{plant}} = 15 \text{ mH}$ ,  $m_a = 0.73$ ).  $i_{0,\text{N}} = 0,9 \text{ A}$  and refers to the current necessary for rotor levitation at vertical operation.  $f_{\text{s,N}}$  refers to the rated speed of  $60\,000 \text{ min}^{-1}$ . It can be seen that for vertical as well as for horizontal operation the system can be operated without any problems as long as any imbalance force

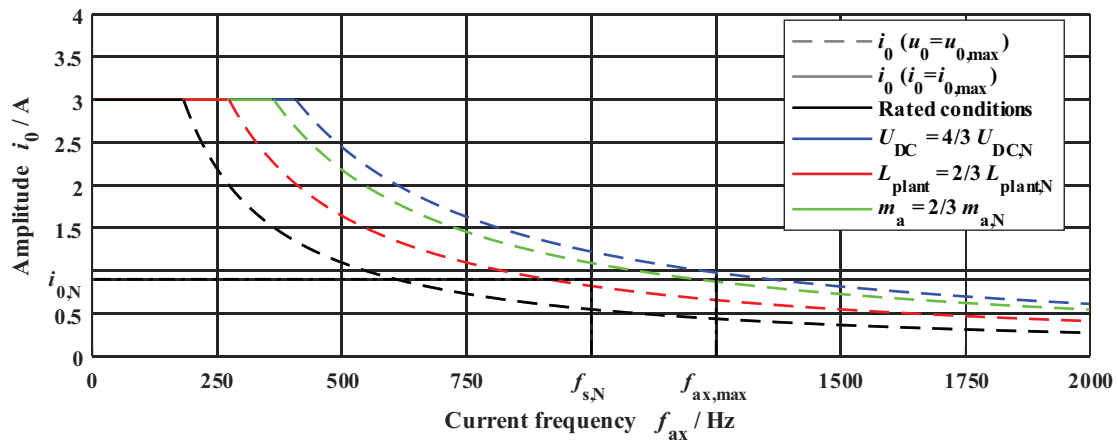


Fig. 9. Simulated operating area of the axial magnetic bearing system

excitation requires less than half the rated bearing current. However, this is not to expect since imbalance forces mainly act radially. Apart from that, there are several options to enlarge the operating area by adapting the system boundary conditions. The most effective is to increase the DC link voltage to increase the current slope and to decrease the modulation degree (blue line in Fig. 9). Another is to operate the drive at lower speeds which requires less modulation degree (green line in Fig. 9). Moreover a decrease in plant inductance yields higher current slopes. However, since  $L \sim N^2$  but  $F \sim N \cdot I$  a reduction in inductance by means of coil turn reduction is on the costs of moderately higher currents in order to achieve the same bearing force.

## CONCLUSIONS

A new method of operating the axial AMB for a cylindrical bearingless machine was introduced which relies on the feeding by the zero-sequence current between the two star points of the machine. Exemplary a 1 kW / 60 000 min<sup>-1</sup> PM synchronous machine is considered. It was shown that it is possible to manipulate artificially the electric potential of the star point of a three phase winding system by the adaption of the time spans for the passive voltage instants in a SVPWM. However, the voltage drop between the two star points depends on both potentials of the star points, leading to a coupling between the two current systems. It is explained, how this problem of five unknown phase currents can be separated into smaller problems of two and three dimensions. The operation of the system is dependent on the constraints, given by the BM as well as by the inverter capacity.

Firstly, it is shown that a zero-sequence current leads to torque and force ripple and to an increase in eddy current losses in the PM of the rotor. However, all these fields of interest are not crucial for currents  $i_0 < 3$  A. For the given AMB the rated current to compensate for the rotor weight is  $i_{0,N} = 0.9$  A. So it can be concluded that the constraints by the motor do not determine significantly the applicability of the method. Finally, it is demonstrated that the more crucial constraints are given by the inverter. For pure DC current requirements at steady state and in transient conditions it is shown that the motor currents are not influenced by the zero-sequence current, since the active time spans are calculated independently. For modulation degrees  $m_a > 0.866$  a third harmonic occurs in the zero-sequence current, prohibiting operations at speeds  $n > 1.25 \cdot n_N$  which is caused by the influence of the active voltage time spans on the star point potential. Finally, the step response and the sinusoidal current requirements yield suitable results for currents  $i_0 < 1$  A. Certainly the operating area can be enlarged by a higher DC link voltage, a smaller AMB inductance or if the modulation degree at rated operation is reduced.



Altogether it can be stated that the presented technique is applicable for active magnetic suspensions of high-speed drives, taking into account the mainly non-critical constraints by the bearingless machine and the inverter. It is topic of future investigations to realize the presented technique by a prototype.

## References

1. Chiba A, Fukao T, Ichikawa O, Oshima M, Takemoto M, Dorrell DG. *Magnetic Bearings and Bearingless Drives*. 1<sup>st</sup> ed. Oxford: Elsevier; 2005.
2. Bleuler H, Cole M, Keogh P, Larssonneur R, Maslen E, Nordmann R, Okada Y, Schweitzer G, Traxler A. *Magnetic Bearings – Theory, Design and Application to Rotating Machinery*. Schweitzer G, Maslen EH., editors. Dordrecht Heidelberg London New York: Springer; 2009.
3. Stölting HD, Kallenbach E, Amrhein W, editors. *Handbook of Fractional-Horsepower Drives*. Berlin Heidelberg New York: Springer; 2006.
4. Messenger G, Binder A. Evaluation of a Dual Half-Pitched Three-Phase Bearingless High-Speed Permanent Magnet Synchronous Motor Prototype. Proceedings of the 10<sup>th</sup> ETG/GMM-Symposium Innovative small Drives and Micro-Motor Systems (IKMT); 2015 Sep 14–15; p. 1–6. Cologne, Germany. Berlin Offenbach: VDE Verlag GmbH; 2015.
5. Schneider T, Binder A. Design and Evaluation of a 60 000 rpm Permanent Magnet Bearingless High Speed Motor. Proceedings of the 7<sup>th</sup> International Conference on Power Electronics and Drive Systems (PEDS); 2007 Nov 27–30; Bangkok, Thailand. IEEE; 2007. doi: 10.1109/peds.2007.4487669
6. Jastrzebski RP, Jaatinen P, Pyrhönen O, Chiba A. Design of 6-slot inset PM bearingless motor for high-speed and higher than 100 kW applications. Proceedings of the 2017 IEEE International Electric Machines and Drives Conference (IEMDC); 2017 May 21–24; p. 1–6. Miami (FL), USA. IEEE; 2017. doi: 10.1109/iemdc.2017.8002143
7. Wang T, Du G, Yu Z, Zhang F, Bai Z. Design and develop of a MW direct drive high-speed permanent-magnet machine for compression. Proceedings of the International Conference on Electrical Machines and Systems (ICEMS); 2013 Oct 26–29; p. 892–895. Busan, South Korea. IEEE; 2013. doi: 10.1109/icems.2013.6713160
8. Mitterhofer H, Amrhein W. Motion control strategy and operational behaviour of a high speed bearingless disc drive. Proceedings of the 6<sup>th</sup> IET International Conference on Power Electronics, Machines and Drives (PEMD); 2012 Mar 27–29; p. 1–6. Bristol, UK. IET; 2012. doi: 10.1049/cp.2012.0297
9. Bösch PN. *Lagerlose Scheibenläufermotoren höherer Leistung (Bearingless disk-like Motors of higher Power Classes)* [dissertation]. Zurich: Swiss Federal Institute of Technology (ETH); 2004.
10. Asama J, Oi T, Oiwa T, Chiba A. Investigation of integrated winding configuration for a two-DOF controlled bearingless PM motor using one three-phase inverter. Proceedings of the 2017 IEEE International Electric Machines and Drives Conference (IEMDC); 2017 May 21–24; p. 1–6. Miami (FL), USA. IEEE; 2017. doi: 10.1109/iemdc.2017.8002219
11. Grabner H, Silber S, Amrhein W. Feedback control of a novel bearingless torque motor using an extended FOC method for PMSMs. Proceedings of the IEEE International Conference on Industrial Technology (ICIT); 2013 Feb 25–28; p. 325–330. Cape Town, South Africa. IEEE; 2013. doi: 10.1109/icit.2013.6505693
12. Steinert D, Nussbaumer T, Kolar JW. Slotless Bearingless Disk Drive for High-Speed and High-Purity Applications. *IEEE Transactions on Industrial Electronics*. 2014; 61(11):5974-5986. doi: 10.1109/TIE.2014.2311379
13. Munteanu G, Binder A, Dewenter S. Five-axis magnetic suspension with two conical air gap bearingless PM synchronous half-motors. Proceedings of the International Symposium on Power Electronics Power Electronics, Electrical Drives, Automation and Motion (SPEEDAM); 2012 Jun 20–22, p. 1246–1251. Sorrento, Italy. IEEE; 2012. doi: 10.1109/speedam.2012.6264414

14. Kascak P, Jansen R, Dever T, Nagorny A, Loparo K. Levitation performance of two opposed permanent magnet pole-pair separated conical bearingless motors. Proceedings of the IEEE Energy Conversion Congress and Exposition; 2011 Sep 17–22; p. 1649–1656. Phoenix (AZ), USA. IEEE; 2011. doi: 10.1109/ecce.2011.6063980
15. Schleicher A, Werner R. Theoretical and experimental analysis of controllability of a novel bearingless rotary-linear reluctance motor with optimal chessboard toothing. Proceedings of the IEEE International Conference on Industrial Technology (ICIT); 2018 Feb 20–22; p. 540–545. Lyon, France. IEEE; 2018. doi: 10.1109/icit.2018.8352234
16. Sugimoto H, Srichiangsa T, Chiba A. Design of a high-speed single-drive bearingless motor. Proceedings of the IEEE International Electric Machines and Drives Conference (IEMDC); 2017 May 21–24; p. 1–6. Miami (FL), USA. IEEE; 2017. doi: 10.1109/iemdc.2017.8002300
17. Gasch R, Nordmann R, Pfützner H. *Rotordynamik (Rotor Dynamics)*. 2<sup>nd</sup> ed. Berlin, Heidelberg, New York: Springer; 2006.
18. Munteanu G, Binder A, Schneider T. Development and test of high-speed bearingless PM synchronous machines. *e & i Elektrotechnik und Informationstechnik*. 2011;128(3):75-80. doi: 10.1007/s00502-011-0810-1
19. Messenger G, Binder A. Six-axis Rotor Magnetic Suspension Principle for Permanent Magnet Synchronous Motor with Control of the Positive, Negative and Zero-Sequence Current Components. *Applied Computational Electromagnetics Society (ACES) Journal*. 2017;32(8):657-662.
20. Messenger G, Binder A. Analytical comparison of conventional and modified winding for high speed bearingless permanent magnet synchronous motor applications. Proceedings of the International Conference on Optimization of Electrical and Electronic Equipment (OPTIM); 2014 May 22–24; p. 330–337. Bran, Romania. IEEE; 2014. doi: 10.1109/optim.2014.6850951
21. Dietz D, Messenger G, Binder A. 1 kW / 60 000 min<sup>-1</sup> bearingless PM motor with combined winding for torque and rotor suspension. *IET Electric Power Applications*. Forthcoming 2018. doi: 10.1049/iet-epa.2018.0013
22. Schröder D. *Elektrische Antriebe – Regelung von Antriebssystemen*. 4<sup>th</sup> ed. Berlin Heidelberg: Springer Vieweg; 2015. doi: 10.1007/978-3-642-30096-7\_7
23. Binder A. *Elektrische Maschinen und Antriebe – Grundlagen, Betriebsverhalten*. 2<sup>nd</sup> ed. Heidelberg Dordrecht London New York: Springer; 2018.
24. Sequenz H. *Die Wicklungen elektrischer Maschinen*. 1<sup>st</sup> ed. Vienna: Springer; 1950.
25. Bergmann G. *Five-Axis Rotor Magnetic Suspension with Bearingless PM Motor Levitation Systems* [dissertation]. Darmstadt: Technical University; 2013.
26. Binder A. Analytical Calculation of Eddy-Current Losses in Massive Rotor Parts of High-Speed Permanent Magnet Machines. Proceedings of the International Symposium on Power Electronics Power Electronics, Electrical Drives, Automation and Motion (SPEEDAM); 2000 Jun 13–16, p. C2-1–C2-6. Ischia, Italy; 2000.
27. Stoll RL. The analysis of eddy currents. Oxford: Clarendon Press; 1974.
28. Greig J, Freeman EM. Travelling-wave problem in electrical machines. *Proceedings of the Institution of Electrical Engineers*. 1967;114(11):1681-1683, doi: 10.1049/piee.1967.0324

**Information about the authors:**

**Dietz Daniel**, M.Sc., Landgraf-Georg-Str. 4, 64283 Darmstadt, Germany  
E-mail: ddietz@ew.tu-darmstadt.de

**Binder Andreas**, Prof., Dr.-Ing. habil. Dr. h.c.;  
E-mail: abinder@ew.tu-darmstadt.de

**To cite this article:**

Dietz D, Binder A. Bearingless PM Synchronous Machine with Zero-Sequence Current Driven Star Point-Connected Active Magnetic Thrust Bearing. *Transportation Systems and Technology*. 2018;4(3):5-25. doi: 10.17816/transsyst2018435-25

UDC [УДК] 629.439.016.56  
DOI 10.17816/transsyst20184326-35

© **B. M. Lapidus**

Joint Scientific Council of JSC Russian Railways,  
UIC (International Union of Railways)  
(Moscow, Russia)

## MAGNETIC LEVITATION AS THE FUNDAMENTAL BASIS FOR SUPERFAST VACUUM LEVITATION TRANSPORT TECHNOLOGIES

**Abstract.** The article reviews the strategic trends of transport development that meet the modern requirements of the economy and society. It was revealed that the key trend is to increase the speed of traffic. To achieve breakthrough results in this direction, it is proposed to use magnetic levitation in combination with the use of a vacuum environment - the creation of vacuum-levitation transport systems. It is noted that the Joint Scientific Council of JSC Russian Railways formed the requirements for the creation of such systems and focused attention on the problem of the socio-economic efficiency of its creation. It was concluded that railway transport, in the interests of its strategic competitiveness, should be the initiator and active participant in the creation of vacuum-levitation transport systems, which, in turn, can become an important incentive for integrating the efforts of the world scientific community.

**Keywords:** social and economic trends, strategic trends in transport development, convergence of transport systems, magnetic levitation, vacuum-levitation transport systems, scientific priorities of speed increase, intermodal transportation, business cooperation of transport systems.

© **Б. М. ЛАПИДУС**

Объединенный ученый совет ОАО «РЖД»,  
Международный Союз железных дорог  
(Москва, Россия)

## МАГНИТНАЯ ЛЕВИТАЦИЯ – ФУНДАМЕНТАЛЬНАЯ ОСНОВА ДЛЯ СВЕРХСКОРОСТНЫХ ВАКУУМНО- ЛЕВИТАЦИОННЫХ ТРАНСПОРТНЫХ ТЕХНОЛОГИЙ

**Аннотация.** В статье проанализированы стратегические тренды развития транспорта, отвечающие современным требованиям экономики и общества. Выявлено, что ключевой тренд – повышение скорости движения. Для достижения прорывных результатов в этом



направлении весьма перспективно применение магнитной левитации в сочетании с использованием вакуумной среды – создание вакуумно-левитационных транспортных систем. Отмечено, что Объединенным ученым советом ОАО «РЖД» сформированы требования к созданию таких систем, сфокусировано внимание на проблеме социально-экономической эффективности их создания. Сделано заключение, что железнодорожный транспорт в интересах своей стратегической конкурентоспособности должен быть инициатором и активным участником создания вакуумно-левитационных транспортных систем, что, в свою очередь, может стать важным стимулом для интеграции усилий мирового научного сообщества.

**Ключевые слова:** социально-экономические тенденции, стратегические тренды развития транспорта, конвергенция транспортных систем, магнитная левитация, вакуумно-левитационные транспортные системы, научные приоритеты повышения скорости движения, интермодальные перевозки, бизнес-кооперация транспортных систем.

The global and economic tendencies which formed themselves at the end of XX and beginning of XXI century, demand drastic acceleration of transport communication. The establishment of new transport systems is a crucial task, successful solution of which will broadly determine increase of life quality and trade and economic efficiency of the regions, cities, and countries. When choosing a direction of research, one needs assess risks and possibilities associated therewith, and develop certain relative actions.

## STRATEGIC TENDENCIES IN TRANSPORT DEVELOPMENT






















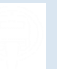



































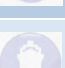




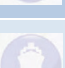




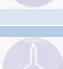
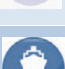



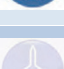
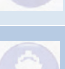



Macro-and microeconomic requirements for a transport system are characterised by factors which produce decisive influence on evolution of transport [1]. Among them, five factors are distinguished:

- increase of life quality of population;
- increase of human capital cost;
- deepening of interregional demographic disproportions;
- increase of demographic and industrial impact on environment;
- decrease of resource intensity of economy, perfection of raw materials processing techniques, increase of final products share in the transportation structure.

With these factors in mind, the global requirements for future transport systems are becoming speed acceleration, safety, namely environmental safety, energy efficiency, passenger services flexibility, and integration into multimodal transport systems.

Figure 1 shows today's modes of transport which hold leading positions or are aspirant to take leading positions at the transportation market. In terms of safety, namely environmental safety, the first position is held by railway transport, whereas remainder of positions is held by car, pipeline, aircraft, and maritime transports. The strategic benchmarks for railway transport are increase of service flexibility, provision of intermodality, and speed acceleration. Altogether, these strategic trends are most rapidly developing in car transport, which demonstrates aspiration to leadership in the growing segment of society's requirements for transport services.

Due to population growth, increase of human capital cost [2], and value of time, the demand and requirements for high-speed passenger transportation development are also on the rise. These tendencies are verified by boosting growth of high-speed railways (HSR) construction over the last decade [3]. In China alone, over 22 thousand kilometres of HSR were built, that is more than elsewhere in the world. According to UIC forecast, this dramatic development of HSR global network will continue in the future.

Tendencies	Leaders	Aspirants to leadership
Transportation acceleration	    	     
Cost reduction	    	     
Safety	    	     
Sustainability and energy efficiency	    	     
Service flexibility	    	     
Low maintenance and unmanned technologies	    	     
Multimodality	    	     

Modes of transport keys:



– railway transport



– air transport



– maritime transport



– road transport



– pipeline transport

– vacuum levitation transport

Fig. 1. Strategic tendencies in transport system development

As a modern tendency, the “borrowing” of one transport mode’s advantages by another for its subsequent development is considered. For instance, train speed is approaching that of aircraft, and load and passenger capacity of the latter are striving for that of railway counterparts. It was not by coincidence that the term “transport systems convergence” was introduced. And the technological borrowing of transport systems’ elements is called “synergetic evolution of transport systems”. There are projects that have been developed and implemented, where technological solutions of a train, car transport and even aircraft converge. Quite promising is the railway channel that unites maritime and railway transports (carrying of ships by rail), which enables covering hundreds of kilometres without the need to construct water channels. The air-and-railway projects, suggested by Tomsk (a city in Russia) scientist Boris Weinberg represent interest as well [6]. Today, the idea of “floating trains” is crystallised in such projects as magnetic levitation and vacuum levitation trains. In this regard, it is required that the projects of ET3 [7] and actively realised Hyperloop as well as the concept of “plain trains” should be emphasised [4].

At the same time, the tendency of XXI century is to achieve high speed together with the use of alternative energy sources, traction transmission mode, and artificial environment for traffic in transport systems.

### **PROSPECTS OF MAGNETIC LEVITATION IN COMBINATION WITH VACUUM ENVIRONMENT**

The application of magnetic levitation combined with vacuum seems promising for transport systems [8, 9]. These solutions foster overcoming the most energy-intensive hindrances to transport systems traffic – wheel-rail contact [12, 13], and air resistance [12, 13]. The application of evacuated environment with 100 times and more reduced pressure on transport, provides opportunity to double speed performance of the magnetic levitation system “train-infrastructure”. Whereas, the application of a deeper near-vacuum environment will enable achieving the speeds of five or six times higher than the maximum one [14].

The scientific basis for solving technical and technological, and economic issues is being actively developed in Russia at present. Basing on the findings of the studies conducted by JSC “Russian Railways” Joint Scientific Council, the technical requirements for development and vacuum levitation transport system (VLTS) have been designed, which are summarised in the monograph [5]. The viability of VLTS, namely in Russian conditions, has been proven, in

terms of potential competitiveness at medium distance (500–1000 km) and long distance transportation (over 1000 km), provided that there is logistics and digital cooperation of new transport system with conventional railway network.

As a result of the activity of JSC “Russian Railways” Joint Scientific Council [15 – 17], it was made possible to identify future technical requirements for VLTS construction. These must cover basic parameters of VLTS infrastructure and rolling stock, methods of air resistance reduction in vacuum, achieving movement using magnetic levitation, and creating of safety and risks assessment systems.

### SCIENTIFIC PRIORITIES FOR CONSTRUCTION OF VACUUM LEVITATION TRANSPORT

In the process of working out the concept, the following priorities were determined to achieve speeds of 1 000–12 000 km/h with 100 times reduction of resistance.

1. Determination of major infrastructure parameters:
  - proportion of sizes and dimensions;
  - terra-efficiency;
  - stations and passing loops;
  - minimal curvatures.
2. Ensuring traffic based on magnetic levitation: constructive solutions for propulsion, acceleration, and braking.
3. Provision of safety systems:
  - physiological hindrances;
  - incidents;
  - technological and man-induced risks.
4. Determination of major vehicle parameters:
  - geometric parameters;
  - aerodynamic form;
  - equipment;
  - materials.
5. Achieving resistance reduction:
  - near vacuum;
  - rarefied medium;
  - alternative physical principles of movement.
6. Reproduction of life supporting systems:
  - life supporting for passengers;

- heat profile;
  - sources and accumulators of energy.
7. Choosing principles, methods, and equipment to construct the near-vacuum infrastructure or to reduce resistance;
  8. Assessment of contingency and relevance of replacement of the near vacuum in the infrastructure of the transport system with light gas medium corresponding to relative resistance reduction objectives;
  9. Assessment of contingency of application of alternative physical principles and constructive solutions for additional reduction of resistance to the maglev system pod.
  10. Assessment of energy optimality in power supply systems relying on existing energy sources, and possibility to accumulate heat and kinetic energy during the train movement;
  11. Assessment calculations-based forecast of heat profile of vehicles and infrastructure for various movement modes within the speed range of 0–1 200 km/h;
  12. Constructive solutions for passengers' onboard life supporting systems.

## **IDENTIFICATION OF A NICHE IN THE MARKET FOR INNOVATIVE TRANSPORT SYSTEMS**

One of the crucial economic issues is to identify a commercial niche in the transport services market so as to make the projects profitable and promising. The main technology related prerequisite for mass operation of VLTS consists in promptest solving the fundamental task of achieving superconductivity.

However, in our time the efficiency of any transport system, e.g. HSR [18], is achieved not only through their commercial operation. A more weighty contribution is made by creation of social and economic effects and associated businesses for investors [19].

Let us consider systematised requirements for development of energy sources, routes, increase of travel distance, and speed in each segment of the market (Fig. 2). In segments from 150 to 500 km it is promising to develop competitiveness between conventional railway and maglev transport, whereas in segments with over 500 km – VLTS; after finalising physical principles of creating levitation and reducing cost of maglev transport system elements, the latter will be used on a broader scale. These risks are significant for railway operator companies, therefore railway science and railway management should be interested in introduction of maglev systems and VLTS. The formation of these systems must be perceived



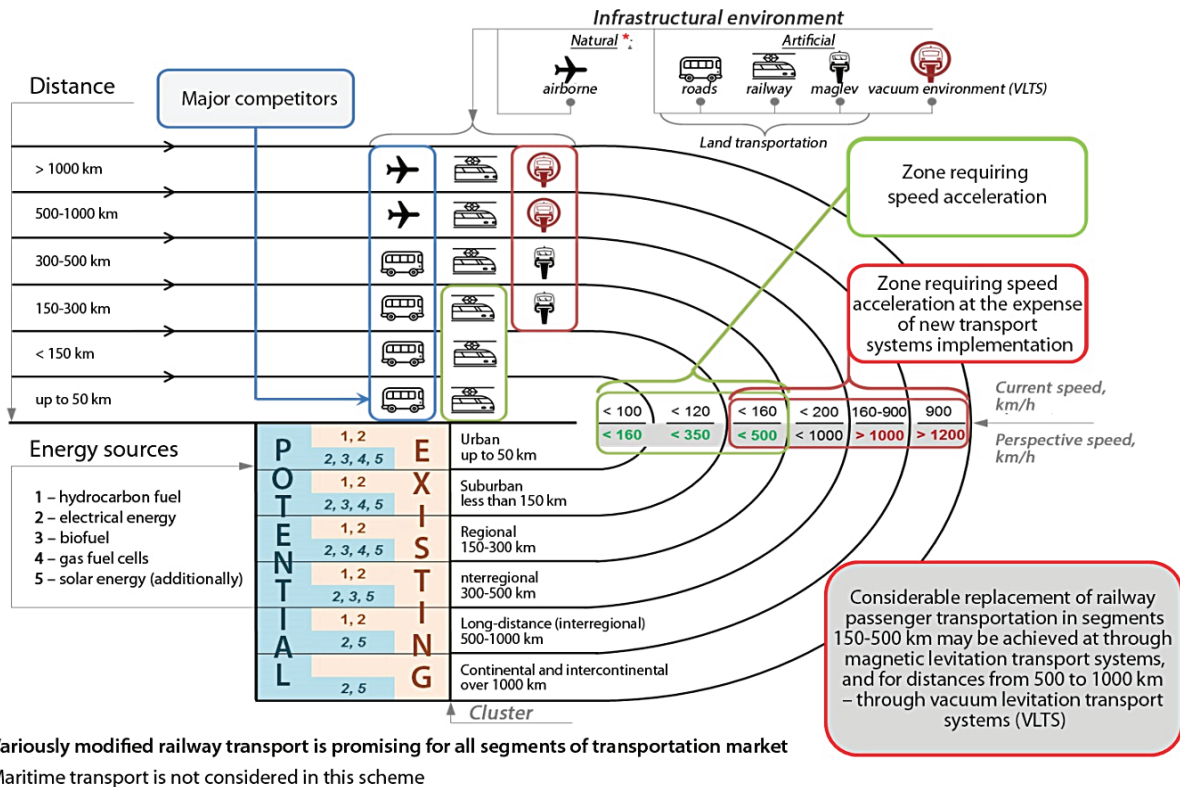


Fig. 2. Scheme of passenger transportation perspective development

as another stage of railway transport development. Other ways of thinking will inevitably result in drastic redistribution of business against the latter.

Thus, a key tendency in transport development, which addresses the social and economic challenges of today, is transportation speed increase. A revolutionary increase of transportation speed may be achieved using maglev in combination with vacuum environment, i.e. VLTS. The fundamental requirements for those are identified by JSC “RZD” Joint Scientific Council.

It is necessary to achieve convergence of VLTS and conventional railways, which will make implementation of maglev efficient and will serve for the benefit of railway business development. Firstly, construction of VLTS lines can be done above existing railway lines, i.e. the infrastructure cooperation is achievable. Secondly, realisation of intermodal transportation using VLTS lines and railway lines can provide an expanded logistics network and an immense transport services coverage. Thirdly, business cooperation: creation of VLTS may become a good business type and strategic investments into transport systems development.

The work over the promising maglev transport development projects must stimulate integration of the world society so as to accelerate in choosing the best constructive and technological solutions for XXI century transport.

**Библиографический список / References**

1. Лapidус Б.М., Мачерет Д.А. Методология оценки и обеспечения эффективности инновационных транспортных систем // Экономика железных дорог. – 2016. – № 7. – С. 16–25. [Lapidus BM, Macheret DA. Metodologiya ocenki i obespecheniya ehffektivnosti innovacionnyh transportnyh system. *Ehkonomika zheleznih dorog*. 2016;7:16-25. (In Russ.)].
2. Капелюшников Р.И. Сколько стоит человеческий капитал России? Часть I // Вопросы экономики. – 2013. – №1. – С. 27–47. [Kapelyushnikov RI. Russia's Human Capital: What Is It Worth? Part I. *Voprosy Ekonomiki*. 2013;1:27-47. (In Russ.)].
3. High Speed Rail: Fast Track to Sustainable Mobility. UIC Brochure, June 2015.
4. Лapidус Б.М., Лapidус Л.В. Железнодорожный транспорт: философия будущего. – М.: Прометей, 2015. – 232 с. [Lapidus BM, Lapisus LV. Zheleznodorozhnyi transport: filosofiya budushchego. Moscow: Prometey; 2015. 232 p. (In Russ.)].
5. Galen J. Suppes, A Perspective on Maglev Transit and Introduction of the PRT Maglev. *Transportation Research Record*. 1995;1496:103-111.
6. Вейнберг Б.П. Движение без трения. Доступно по: [http://veinberg.o7.ru/pdf/no\\_friction\\_motion.pdf/](http://veinberg.o7.ru/pdf/no_friction_motion.pdf/). Ссылка активна на 09.08.2018. [Veinberg BP. Dvizhenie bez treniya. Available from: [http://veinberg.o7.ru/pdf/no\\_friction\\_motion.pdf/](http://veinberg.o7.ru/pdf/no_friction_motion.pdf/). Accessed August 09, 2018. (In Russ.)].
7. Patent №USOO5950543A/ 14.09.1999. Daryl Oster. Available from: <https://patents.google.com/patent/US5950543A/en>.
8. Зайцев А.А., Юдкин В.Ф. Транспортная система для межстрановых и межконтинентальных перевозок на основе магнитной левитации // Русский инженер. – 2016. – № 4 (51). – С. 36–40. [Zaitsev AA, Yudkin VF. Transportnaya sistema dlya mezhstranovykh i mezhkontinental'nykh perevozok na osnove magnitnoi levitatsii. *Russkii inzhener*. 2016;4:36-40. (In Russ.)].
9. Зайцев А.А., Антонов Ю.Ф. Магнитолевитационная транспортная технология. – М.: ФИЗМАТЛИТ, 2014. – 476 с. [Zaitsev AA, Antonov YuF. Magnitolevitatsionnaya transportnaya tekhnologiya. Moscow: FIZMATLIT; 2014. 476 p. (In Russ.)].
10. Камчатный В.Г. Особенности динамики взаимодействия высокоскоростных объектов с рельсовой направляющей. // Испытания материалов и конструкций. – Нижний Новгород: Интелсервис. – 200 с. [Kamchatny VG. Osobennosti dinamiki vzaimodeistviya vysokoskorostnykh ob'ektov s rel'sovoi napravlyayushchei. *Ispytaniya materialov i konstruksii*. Nizhny Novgorod: Intelservis. 200 p. (In Russ.)].
11. Камчатный В.Г., Бутова С.В. Опыт реализации в РФЯЦ-ВНИИЭФ высокоскоростного движения объектов по рельсовым направляющим. Научно-технические проблемы // Бюллетень Объединенного ученого совета ОАО «РЖД». 2013. №2. С. 38–44. [Kamchatny VG, Butova SV. Experience of realization of high-speed objects transportation on guide rails in RFNC – VNIIEF. Scientific-technical issues. *Bulletin of Joint Scientific Council of JSC Russian Railways*. 2013;2:38-44. (In Russ.)].
12. Кирякин В.Ю., Лежава В.Ш., Новгородцева А.В., и др. Об оценке оптимальной скорости вакуумных поездов и выборе глубины вакуума // Бюллетень Объединенного ученого совета ОАО «РЖД». 2016. №5. С. 26–38. [Kiryakin VYu, Lezhava VSh, Novgorodtseva AV, et all. An estimate of the vacuum trains optimum speed and the choice of vacuum level. *Bulletin of Joint Scientific Council of JSC Russian Railways*. 2016;5:26-38. (In Russ.)].

13. Воробьев И.А., Кондратенко Р.О., Нестеров С.Б., Белоконев А.Н. Оценка характеристик вакуумной среды и энергетических параметров инфраструктуры для вакуумно-левитационного транспорта // Бюллетень Объединенного ученого совета ОАО «РЖД». – 2016. – № 4. – С. 18–25. [Vorob'ev IA, Kondratenko RO, Nesterov SB, Belokonev AN. Evaluation of the vacuum environment characteristics and energy infrastructure parameters for vacuum levitation transport. *Bulletin of Joint Scientific Council of JSC Russian Railways*. 2016;4:18-25. (In Russ.)].
14. Вакуумно-левитационные транспортные системы: научная основа, технологии и перспективы для железнодорожного транспорта: коллективная монография членов и научных партнеров Объединенного ученого совета ОАО «РЖД» / Под ред. Лapidуса Б.М., Нестерова С.Б. – М.: ООО «РАС», 2017. – 192 с. [Lapidus BM, Nesterov SB, editors. *Vakuumno-levitatsionnye transportnye sistemy: nauchnaya osnova, tekhnologii i perspektivy dlya zheleznodorozhnogo transporta: kollektivnaya monografiya chlenov i nauchnykh partnerov Ob»edinennogo uchenogo soveta ОАО “RZhD”*. Moscow: ООО RAS; 2017. (In Russ.)].
15. Кирякин В.Ю., Лежава В.Ш., Новгородцева А.В. Применение вакуумной среды для создания скоростных транспортных систем. Математическое моделирование обтекания объектов (метод дискретных вихрей) // Бюллетень Объединенного ученого совета ОАО «РЖД». – 2015. – № 6. – С. 28–36. [Kiryakin VYu, Lezhava VSh, Novgorodtseva AV. The use of a vacuum environment for creating highspeed transport systems. Mathematical modelling of flow around objects (the method of discrete vortices). *Bulletin of Joint Scientific Council of JSC Russian Railways*. 2015;6:28-36. (In Russ.)].
16. Зайцев А.А. Отечественная транспортная система на основе магнитной левитации // Бюллетень Объединенного ученого совета ОАО «РЖД». – 2015. – № 6. – С. 22–27. [Zaitsev AA. The domestic transport system based on magnetic levitation. *Bulletin of Joint Scientific Council of JSC Russian Railways*. 2015;6:22-27. (In Russ.)].
17. Воробьев И.А. и др. О возможностях, специфике, научных задачах по созданию вакуумной среды для транспортных систем // Бюллетень Объединенного ученого совета ОАО «РЖД». – 2016. – № 1–2. – С. 28–38. [Vorob'ev IA et al. The possibilities, specifics and scientific tasks of creating a vacuum environment for transport systems. *Bulletin of Joint Scientific Council of JSC Russian Railways*. 2016;1-2:28-38. (In Russ.)].
18. Лapidус Л.В. Социально-экономические эффекты высокоскоростного железнодорожного сообщения // Экономика железных дорог. – 2013. – № 12. – С. 58–63. [Lapidus LV. Sotsial'no-ekonomicheskie efekty vysokoskorostnogo zheleznodorozhnogo soobshcheniya. *Ekonomika zheleznnykh dorog*. 2013;12:58-63. (In Russ.)].
19. Мишарин А.С. ВСМ – новый импульс развития экономики // Пульс управления. – 2015. – № 4. – С. 6–9. [Misharin AS. VSM – novyi impul's razvitiya ekonomiki. *Pul't upravleniya*. 2015;4:6-9. (In Russ.)].

#### Information about the author:

**Boris M. Lapidus**, Doctor of Economics, professor;  
eLibrary SPIN: 6429-2736; ORCID: 0000-0002-4887-4255;  
E-mail: lapidusbm@mail.ru

**Сведения об авторе:**

Лapidус Борис Моисеевич, д.э.н., профессор;  
eLibrary SPIN: 6429-2736; ORCID: 0000-0002-4887-4255;  
E-mail: lapidusbm@mail.ru

**To cite this article:**

Lapidus BM. Magnetic Levitation as the Fundamental Basis for Superfast Vacuum Levitation Transport Technologies. *Transportation Systems and Technology*. 2018;4(3):26-35. doi: 10.17816/transsyst20184326-35

**Цитировать:**

Лapidус Б.М. Магнитная левитация – фундаментальная основа для сверхскоростных вакуумно-левитационных транспортных технологий // Транспортные системы и технологии. – 2018. – Т. 4. – № 3. – С. 26-35. doi: 10.17816/transsyst20184326-35

DOI 10.17816/transsyst20184336-43

© G. Lin<sup>1</sup>, X. Sheng<sup>2</sup>

<sup>1</sup> National Maglev Transportation Engineering R&D Center, Tongji University

<sup>2</sup> Shanghai Maglev Transportation Development Company Ltd.  
(Shanghai, China)

## APPLICATION AND FURTHER DEVELOPMENT OF MAGLEV TRANSPORTATION IN CHINA

**Abstract.** Since the high-speed maglev line in Shanghai was put into operation in 2003, it has been running safely for 15 years, maintaining the highest speed of public ground traffic 430 km/h and 99.8~99.9 % punctuality. Since 2001, China ministry of science and technology (MOST) has been supporting the research and development of high speed maglev transportation technology. In 2016, under the support of the MOST, China Railway Rolling stock Corporation (CRRC) started to lead the program of engineering research of Maglev. The aim of the program is to develop 600 km/h high speed Maglev system and 200 km/h medium speed maglev system. The newly developed high speed Maglev system could be tested, verified and applied on the planned Shanghai - Hangzhou high speed Maglev line. Since the operation opening of Changsha Maglev Airport Express Line in May 2016, Hunan province has planned to build more maglev line with top speed 100–160 km/h. Following the operation of urban maglev in Changsha and Beijing, the Qingyuan Maglev line in Guangdong province began to build at the end of 2017. The new maglev line will connect hot spring tourist attractions and Changlong theme park (animal park) in 2019. This paper introduces the application and construction of maglev transportation in China, recent R&D status, further plans and trend of development.

**Keywords:** High Speed Maglev, Urban Maglev, Transportation, Application.

### 1. OPERATION STATUS OF SHANGHAI MAGLEV DEMONSTRATION LINE

Shanghai Maglev Demonstration Line (SMDL) started its trial operation on a single track at the beginning of 2003, was began shuttle running on the double track in September of 2003 and completed the test and acceptance at the end of 2003. The year of 2004 witnessed its beginning of commercial operation according to the operation schedule. Currently the train runs at the highest speed of 430 km/h in the day and 300km/h in the morning and evening. Up to 21st June 2018, the maglev train on SMDL has covered a mileage of about 17.9 million kilometer and carried passengers of about 53.3 million person-times (Fig. 1).

In the past years, the maglev system has undergone bad weather such as hurricane, dense fog, heave rain and heavy snow, no operation has been interrupted



by extreme bad weather, nor accidents that injured people have happened. Statistical results of the past years since 2005 show that average operation punctuality rate reaches 99.85 % and 99.93 % of the operation schedule is fulfilled, as shown in Fig. 2 and Fig. 3. The system has reached to top availabilities as a passenger transportation system.

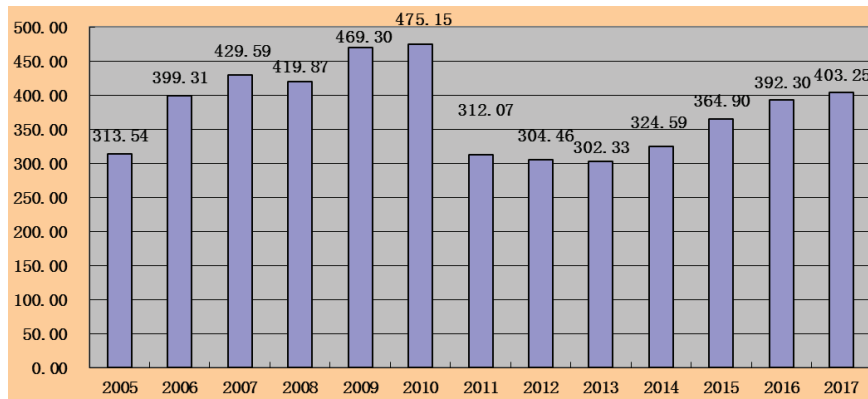


Fig. 1. Carried passengers on SMDL in the past years ( $\times 10$ Thousand)

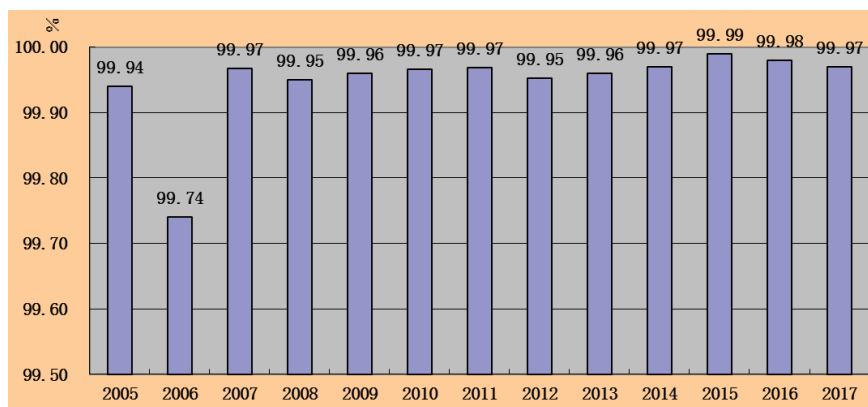


Fig. 2. Rate of punctuality on SMDL

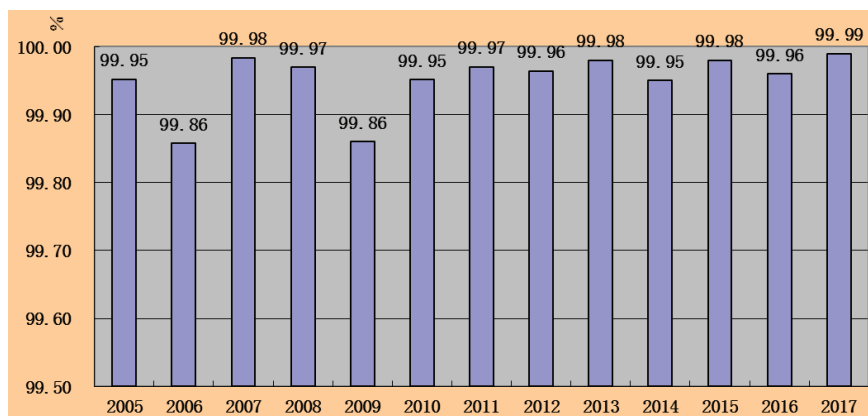


Fig. 3. Rate of schedule fulfillment

The over 15-year operation of SMDL proves that Transrapid Maglev technology is mature and applicable as a high speed transportation tool.

## 2. FURTHER RESEARCH ON HIGH SPEED MAGLEV

Till the end of 2017 a total mileage of 26,000 kilometers of high-speed railway network has been built and put into operation. According to the railway network development plan, till 2025 the high-speed railway mileage in operation in China will reach 38,000 kilometers, and the maximum operation speed for the main line should be 350 km/h. It seems that there is no need and no appropriate space to apply high speed maglev system in the short term future. The planning work of maglev application project in Shanghai and near Shanghai were braked because of opinion division in the decision – making level in 2011.

Also many experts still think, the high-speed railway with maximum speed 350 km/h and travel speed less than 300 km/h attracts passengers from the 500–800 km distance aircraft to track traffic. Between the capital Beijing economic circle and the Yangtze River Delta, between the Yangtze River Delta and the Pearl River Delta economic circle, the distance is above 1000 km, the three-hour fast comfortable travel, a day trip demand for business travelers will increase along with economic development. If the further lifting traffic speed to the 500 km/h through the maglev technology, travel speed can reach more than 430 km/h, which is between the wheel/rail high-speed railway and aviation, will help attract middle and long distance air travelers, thereby reduces traffic dependence on fossil energy, and reduces carbon emissions. It means that even with the high-speed railway network, still exist in the transportation development space and demand for high-speed maglev.

In order to keep operation of Shanghai Maglev Demonstration Line for a long term and promote the further application of maglev technology in China, the MOST has arranged maglev further development program in the “13th Five Year Plan” (2016–2020), and entrusted CRRC to organize implementation of the Maglev R&D task.

The new aim of the Maglev program are the development of 600 km/h high speed maglev train and 200 km/h medium speed maglev train. CRRC Qingdao Sifang Co., ltd. leads the research on high-speed maglev vehicle and the CRRC Zhuzhou Electric Locomotive Co., ltd leads the research on medium speed maglev vehicle. The exchange and cooperation between China and Germany are playing an important role in the promotion of the project.

The feasibility study of Shanghai-Hangzhou Maglev line (ca. 170 km long) was completed in March 2008, but it was suspended by the formal Ministry of

Railway (MOR) who preferred the high speed railway system at that time and was afraid of that the Maglev extending project would disturb the construction plan of high speed railway. Now the large network of high speed railway is completed or planned, the 10 year's suspended Shanghai - Hangzhou Maglev feasibility study was started again in May 2018 by China Railways Corporation. Because the reserved corridor is much higher urbanized than ten years before and the noise impact problem along the elevated track will be difficult to resolve, underground track with low pressure vacuum pipe concept will be studied in the feasibility study review. It should be possible to provide the running test condition for the newly developed 600 km/h high speed maglev operation systems in the first section of the application project. The newly developed high speed Maglev systems could be tested, verified and applied on the planned Shanghai - Hangzhou high speed Maglev line.

### 3. DEVELOPMENT AND APPLICATION OF URBAN MAGLEV TECHNOLOGY

#### 3.1 Background of Urban Maglev Development

China is in the rapid urbanization period. The urbanization reached 58.52 % in 2017. In 2030 the Chinese urbanization rate will reach 70 %, which means that each year there will be about 13 million population into the cities. Currently there are 13 cities with population of more than 10 million people, 88 cities with population of more than 5 million people. In Beijing, Shanghai and other large cities, there have been more and more serious traffic and environmental problems. The high-speed urbanization has brought serious challenges to the traffic development of large cities. Since 2000, Chinese auto market has developed rapidly and the auto possession increased to 217 million vehicles till end 2017, It has increased by 11.85 % than 2016. China has become the world's largest car market. Road congestion, air pollution, energy shortages makes the rapid growth of the auto being questioned.

In the past ten years, large cities gave priority to the development of rail transportation as the main measure to solve city traffic problems. Compared with the Subway and elevated light rail, The maglev transportation system has lower noise, smaller curve radius and higher slope, and suitable for elevated, and has about 50~60 % less cost than metro system.

Since 2010 some application urban maglev lines have been planned and from those Changsha airport Maglev line and Beijing S1 Maglev line and were built finally.



### 3.2 Urban Maglev Application Line

Changsha maglev project connects the airport and south station of high speed railway, has line length of 18.5 kilometers, all elevated, with three stations. 5 trains with 3-section configuration are put into operation in the early phase. The project was officially put into public operation in May 6th 2016.

Up to May 2018, the maglev train on Changsha line had covered a mileage of 2 million kilometer and carried passengers of about 6.2 million person times. Statistical results of the past 2 years show that average operation punctuality rate reaches 99.85 % and 99.95 % of the operation schedule is fulfilled.

Beijing maglev application line is called S1 line. The line whole length is 10.2 km with 8 stations. 10 trains with 6-section configuration are put into operation in the early phase of the project. This project has been started in October 2013 and put into public operation in at end of 2017 (Fig. 6).



Fig. 4. Changsha Maglev Line (source: China Railway Eryuan Engineering Group Co., Ltd)



Fig. 5. Changsha Maglev vehicle running on the bridge



Fig. 6. Beijing S1 Maglev vehicle in trial running

### 3.3 Further Urban Maglev Applications

Since public operation of Changsha maglev, the Hunan Maglev Transportation Development Co. has received visit guests related to urban planning from more than 70 cities in the world. Some urban maglev application line are planned in different cities especially in Qingyuan, Guangdong Province, Chengdu, Sichuan province and Zhangjiajie, Hunan povince and so on. The construction of Qingyuan line in Guangdong province was started at the end of 2017 and was expected to operate at the end of 2019. The whole length of first phase of Qingyuan Maglev line is 8.03 km with 3 stations. This Maglev project is designed as tourism special line which connects hot spring tourist attractions and Changlong theme park (animal park). The extension line to connect other tourist attractions and railway station is planned.



Fig. 7. Qingyuan Maglev tourism special line (source: Qingyuan Maglev Co.)



Fig. 8. Qingyuan Maglev track construction site (June 2018)

### 3.4 Further urban Maglev research and development

In order to meet the needs of Urban Maglev, the following research and development work is being carried out in the field of Maglev transportation research and development in China.

1) Increase the top speed

The new vehicle types with the highest running speed of 160–200 km/h are developed by 4 different groups.

2) Introduction of LSM propulsion and hybrid magnet levitation system

The long stator synchronous motor is applied by urban maglev vehicle. The permanent and electromagnetic hybrid magnet is introduced and studied for the new type of levitation system.

3) Reduce noise impact through improving the power rail and current pick-up.

4) Enhance the propulsion and braking system, increase the power of linear motor and propulsion inverter.

5) Reduction of weight of vehicle

Using composite material, new electronic devices and cooling methods to reduce the weight of vehicle;

6) Improve contact current collection system to adapt to higher speed, reduce noise and wear, prevent icing.

## 4. CONCLUSION

High speed maglev transportation system provides a technical and economical choice of land transportation mode within the speed range between high speed wheel-on-rail railway and aviation. In terms of the internationally accepted concept

of 3-hour comfort travelling, it is suitable for medium and long distance passenger transport. The high speed maglev will provide a new planning alternative for the comprehensive transportation system and improve its service quality and efficiency if it is introduced between the high speed wheel-on-rail and aviation systems. After 10 years' suspension, Shanghai – Hangzhou Maglev project feasibility study was restarted and it should be possible to provide the running test condition for the newly developed 600 km/h high speed maglev systems in the first section of the 170 km long line.

Under the background of vigorous development of rail transport in China's large and medium cities, there is a certain developing room for the urban Maglev system. The successful implementation and operation of Changsha Maglev project is promoting wide application of urban maglev in China and further research and development.

### ACKNOWLEDGEMENTS

This work is supported by the National Key Technology R&D Program of the 13<sup>th</sup> Five-year Plan, “Research on Key Technologies of Medium Speed Maglev Transportation System” (No.: 2016YFB1200601) and Hunan provincial science and technology major project, “Integrated Technology Engineering and High Reliability Operation Demonstration of Medium and Low Speed Maglev Train” (No.: 2015GK1001).

#### Information about the authors:

**Guobin Lin**, professor, Tongji University, Cao'an Road 4800, Tongxin Building 505, Shanghai, PR China;

ORCID: 0000-0002-6583-4896;

E-mail: 12154@tongji.edu.cn

**Xiongwei Sheng**, Senior Engineer,

ORCID: 0000-0002-1235-9104;

E-mail: 13901803668@163.com

#### To cite this article:

Lin G, Sheng X. Application and Further Development of Maglev Transportation in China. *Transportation Systems and Technology*. 2018;4(3)36-43. doi: 10.17816/transsyst20184336-43

UDC [УДК] 338.47:656(571.122)  
DOI 10.17816/transsyst20184344-64

© **P. V. Bolshanik**  
Yugra State University  
(Khanty-Mansiysk, Russia)

## FORECAST OF YUGRA TRANSPORT DEVELOPMENT

**Background:** The transport industry is leading in the overall structure of the country's economy. In parts of the regions, this industry can be a branch of specialization.

**Aim:** To forecast further development of the industry in the territory of Yugra.

**Method:** Analysis based on a questionnaire survey of organizations related to the transport industry in Yugra.

To analyze the further development of the transport industry of Yugra, the methods of SWOT analysis and rating ranking were used.

**Results:** The study revealed the main and secondary factors of the transport industry of Yugra. The analysis allowed to determine the strengths and weaknesses of transport, opportunities and threats to its development. On the basis of the analysis three rows of the forecast of transport development are given: pessimistic, moderate and optimistic.

**Conclusion:** Thus, based on the analysis of the data presented, the following conclusions can be drawn:

First, regional or inter-municipal highways, as well as the federal highway, perform a clearly expressed system-forming, supporting role in the common network of Yugra roads – on 8 km of these roads 8.8 km of private and local roads (for example, in Russia this ratio is 2.8 km);

These roads, in comparison with the average indicators for regional or intermunicipal motorways of Russia, have higher loads, both from single types of motor transport, and the total load from all types of motor transport.

Secondly, measurements of traffic on the bridge over the Ob River in Surgut showed that 44 % of passenger cars and 69 % of trucks, as well as 54 % of buses in the transport stream, consisted of transport from 32 other regions of the country.

Taking into account that Rosstat cites the volumes of cargo transportation by organizations in the place of their registration, it is possible to assume with full justification that the actual volume of transported goods along the roads of Yugra is much larger. Above and the dynamics of growth in the volumes of goods transported by road.

Thirdly, the industrial orientation of economic development predetermines the vastness of economic ties between Yugra and other regions of the country, which places regional inter-regional importance for the main regional roads, and therefore the construction and maintenance of such highways should be carried out not only at the expense of the budget of the Autonomous Okrug, but also of the federal budget.

**Keywords:** transport, forecast, factors, trends, SWOT-analysis.

© П. В. Большаник

Югорский государственный университет  
(Ханты-Мансийск, Россия)

## ЭВОЛЮЦИЯ, ПРОГНОЗ И ПРЕОБЛАДАЮЩИЕ ТРЕНДЫ РАЗВИТИЯ ТРАНСПОРТА ЮГРЫ

**Введение:** Транспортная отрасль является ведущей в общей структуре экономики страны. В части регионов эта отрасль может быть отраслью специализации.

**Цель:** Дать прогноз дальнейшего развития отрасли на территории Югры.

**Метод:** Анализ на основании анкетного опроса организаций, имеющих отношение к транспортной отрасли в Югре.

Для анализа дальнейшего развития транспортной отрасли Югры были использованы методы SWOT-анализа и рейтингового ранжирования.

**Результаты:** Проведенное исследование выявило основные и второстепенные факторы развития транспортной отрасли Югры. Анализ позволил определить сильные и слабые стороны транспорта, возможности и угрозы его развития. На основании проведенного анализа даны три ряда прогноза развития транспорта: пессимистический, умеренный и оптимистический.

**Выводы:** Самой сильной стороной транспортного комплекса Югры является высокий транзитный потенциал территории округа. Самыми слабыми сторонами являются дороговизна прокладки дорог в условиях болотистой местности и холодного климата и большая зависимость транспорта от нефтегазодобывающей отрасли.

Наиболее соответствующими сильным и слабым сторонам транспортной системы округа являются такие возможности, как: становление национальных сетей в сфере логистики, появление альтернативных видов транспорта, появление новых технологий строительства дорог.

Наиболее опасными угрозами, которые накладываются на слабые стороны транспортного комплекса, являются: стагнация добычи полезных ископаемых и возрастание дефицита бюджета Югры.

**Ключевые слова:** транспорт, прогноз, факторы, тенденции, SWOT-анализ.

---

Исследование выполнено при финансовой поддержке РФФИ и Правительства ХМАО-Югры, соглашение №17-12-86010/17-ОГОН «Долгосрочное прогнозирование эволюции экономики ресурсодобывающего региона с учетом пройденного пути и особенностей институциональной среды (на примере Ханты-Мансийского автономного округа-Югры)».

## INTRODUCTION

Transport industry is leading in the overall structure of the country's economy. In some regions this industry can be a branch of specialisation. Therefore, it is relevant to consider issues regarding role and significance of transport in Yugra economy and give forecast of its further development.

## TODAY'S STATE OF YUGRA TRANSPORT

Considerable influence on transport development dynamics is exerted by geographical factors, which to a large extent determine current state of transport complex of Yugra. These are:

- vast territory of the Autonomous Okrug (District);
- uneven distribution of transport infrastructure facilities and transport network discrepancy;
- high concentration of natural resources (hydrocarbon);
- availability of navigable waterways running through the territory of the Okrug (largest river mainlines – Ob, Irtysh; shorter rivers – Konda, Kazym, Severnaya Sosva, Agan, Tromyagan, Vakh, Nazym, etc.);
- specifics of natural conditions (climate, seasonal nature of transport availability, etc.);
- proximity of federal transport ways of federal significance, etc. [1].

The peculiarity of roads in Khanty-Mansiysk Okrug (Yugra) is predominance of non-public roads (Table 1).

The Tyumen – Khanty-Mansiysk federal road, regional and intermunicipal roads of the Okrug ensure that transport from private and local roads enter the country's transport system, and transport access of sectors of economy and inhabitants to railway stations, river ports, and airports. This is what determines their system-forming, supporting role in Yugra road network.

In the entire length of regional and municipal hard surface public roads in Yugra the III class roads prevail, whereas in the Russian Federation it is the IV class roads (Table 1) [2].

As of January 1<sup>st</sup>, 2016 the density of roads of regional and municipal importance in Yugra was 5.5 and 4.2 times respectively less than those in Russia and Ural Federal Okrug. At the same time, the density of winter roads and ice passages of municipal importance in Yugra was 4.8 and 2.3 times higher (Table 2). There is a considerable discrepancy in length of roads in districts of the Okrug.

The federal highway, as well as regional and intermunicipal roads perform structure-forming role in the road network of Yugra. It is them that are joined

Table 1. Length of roads at the beginning of 2015, km.

Federal Subject	Length of roads			Hard surface roads out of the total length					
	Total	Including		Total	Public				Non-public
		Public	Non-public		Total	Federal	Regional and Municipal	Local	
Russia	1612139	1451249	160890	1133687	1023849	51523	473896	498429	10983
UFO*	128728	95451	33277	89907	70616	3291	35918.6	31406.6	19291
Yugra	27074	6692	20382	17138	5520	345	2708	2467	11618

UFO\* stands for Ural Federal Okrug (District)

Table 2. Density of roads as of January 1<sup>st</sup>, 2015, in km/thousand km<sup>2</sup>

Federal Subject	Federal, Regional or Intermunicipal roads	Regional or Intermunicipal Roads	Winter Roads and Ice Passages
Russia	32.76	29.75	1.34
UFO	24.16	22.35	2.19
Yugra	5.76	5.11	4.81

Note: the data used were provided by: Rosstat – volume of freight transported and freight turnover of all industries' organisations; RADOR – length of public roads by federal subjects of Russia.

by local and private roads. Therefore, with some conditions, as assessment of compatibility for forming of transport flow and impact of road transport on regional and municipal roads, a number of indicators per one kilometre of roads in Russia, Ural Federal Okrug and Yugra were considered (Table 2). Let us note that ratios between federal and regional (including intermunicipal) roads differ insignificantly and make: 1 to 9 for Russia, 1 to 12 for Ural Federal Okrug, and 1 to 8 for Yugra [3]. It means the indicators given below are compatible with each other and relatively correct.

## VOLUME OF FREIGHT TRANSPORTED BY ROADS

The leading position in Russia of Yugra in development of industry and resource-based specialization of its economy predetermine the largest (as compared to other regions of Russia) volumes of road transported freight. These volumes are comparable to analogous indicators in federal okrugs (districts), and even superior in some of them [4].



If the volumes of freight transported in UFO in 2014 as compared to 2005 almost remained the same, with those even decreased in Russia, then in Yugra they have increased significantly, which indicates growth in car flow and loads on roads (Fig. 1).

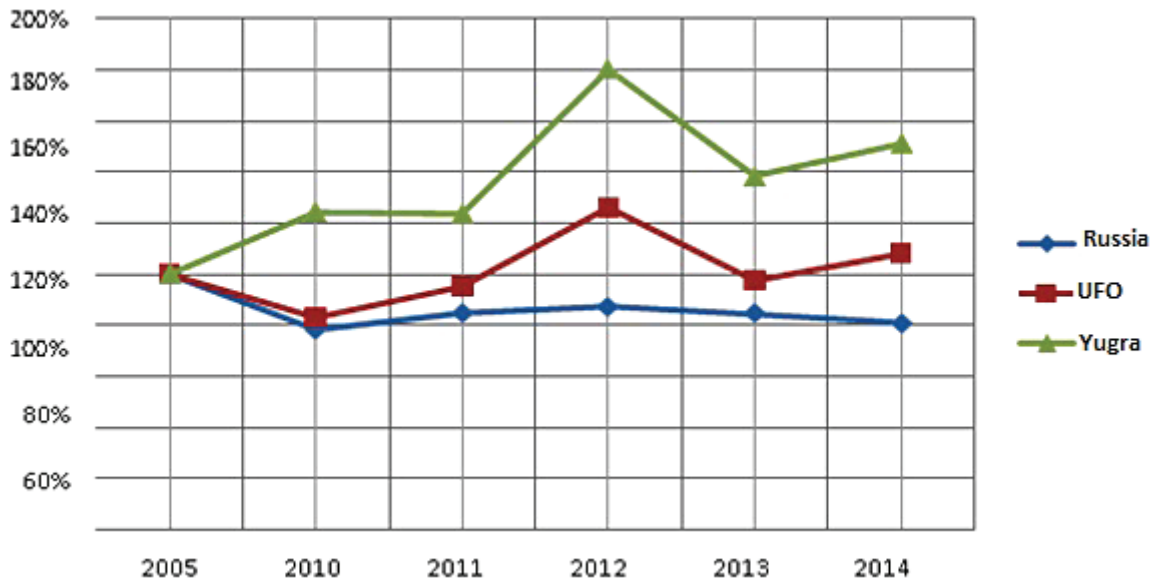


Fig. 1. Volumes of road transported freight by various industries' organisations as compared to 2005 (the data of 2005 have been assumed as 100 %) [4]

So, by volume of car transport, freight turnover and its volume, Yugra roads are considerably ahead of average Russia's and regional indices, which signifies intense loads on existing road network [5, 6, 7, 8].

## FACTORS INFLUENCING YUGRA TRANSPORT DEVELOPMENT

The influence of social factors is most seen in water transport performance. It ensures communication with those settlements which do not have any other transport network. During navigation season, water transport in Yugra territory is one of the major transport ensuring passenger transportation and various cargo delivery.

The most important task relating to maintaining continuous operation of water transport is Okrug's budget financing maintenance works aimed at maintaining passes of small and minor rivers in navigable state.

The scientific and technical progress factor primarily reflects itself in the state of all transport fleet. A strong wear of rolling stock is observed. To overcome increased wear is possible not only at the expense of imported equipment procurement, but

also through new technologies used to upgrade the existing equipment. In this regard, upgrade and new technologies in electric locomotives repair led to 14.2 % reduction in failure, therefore strength reserves of electric locomotives fleet enable its reliable operation for the next 10–15 years.

Location factor reflects itself primarily in configuration of the main transport network which does not meet the today's and tomorrow's freight and passenger flows. Yugra is faced with great difficulties in development road transport, since the main highway Surgut–Pyt-Yakh–Demyanskoye–Tobolsk connecting Yugra with southern parts of Tyumen Oblast (Region) is intensely congested, does not have required capacity, and is in unsatisfactory technical state. Every time the roadbed deteriorated due to natural processes, Yugra would be cut from the mainland. The role of connector with other parts of Russia is partially performed by the Perm–Sovetsky–Khanty-Mansiysk–Nizhnevartovsk highway, but the section running through Tomsk Oblast has not been laid yet. In the perspective, the freight and passenger flow through mainlines is expected to rise. This will be caused by booming development of Yamal-Nenets Autonomous Okrug and commissioning of the Sabetta Port. Currently, the role of meridian transport corridor is performed by the Urengoi–Surgut–Tobolsk–Tyumen Highway. This is highway having no other alternatives, therefore it is vital to construct the second and the third meridian corridors: the Tyumen–Urai–Sovetsky–Nyagan–Beloyarsky–Nadym Highway and the Agirish–Obskaya–Salekhard Railway.

Climate conditions, swampy areas, abundance of rivers have determined certain features of use of road transport. When approving and drawing up the route, one should consider such potential damages as destruction and gouges of parts of road surface, roadbed subsidence, and destruction of barriers, etc. Also, in some options it is possible to draw up fully-fledged logistical schemes engaging water transport, several lorries and handling in storage facilities.

The leading role of Yugra's industry development in Russia has triggered (for a number of regional and intermunicipal roads) increase in transport intensity, which is two and over times more than the permissive one, set by norms for road categories, and this requires urgent measures to reconstruct these roads. The situation with the bridge across the Ob is particularly serious. Its actual traffic density in 2014 was 2.4 times bigger than the designed one, whereby the peak intensity in August 2014 was 3 times bigger than the designed one for 2015, which was set in bridge project documentation for. In order to provide passage over the Ob, it is vital to construct another bridge [9].

In terms of freight transportation by car Yugra is far ahead among other regions of Russia. The Okrug accounts for almost half of the freight volume transport in UFO, thus excelling Far-Eastern and North Caucasian Federal Okrugs

(Districts). At the same time, in relation to UFO and the rest of Russia Yugra is characterised by positive dynamics of growth in volume of road transported freight. On the basis of the fact that federal, regional and intermunicipal roads are structure-forming, in 2014 one kilometre of these roads in Yugra serviced 6.4 and 7.1 times more transported freight than in UFO and the rest of Russia [10, 11].

## STUDY METHODS

In order to identify dominating tendencies in transport, we developed a questionnaire for organisations relating to transport industry in Yugra. This method was tested in the previous study of the author [12]. A total of 15 organisations directly engaged in transport industry have taken part in the questionnaire. The questionnaire was filled in by respondents who work in the most sectors of transport branch of the region, except for pipeline and railway transport. However, the majority of the respondents were from road transport (86.7 %). The questionnaire covered respondents from various parts of the region: Ninzhnevartovsk, Khanty-Mansiysk, Sovetsky, Yugorsk, Nyagan, Urai, Langepas, and Megion, with the answers being mainly from the capital city of the region – Khanty-Mansiysk. Generally, the majority of the respondents were average business representatives (54 %), then small businesses (31 %), and large ones (15 %). Also, representatives of very large and very small businesses were also questioned. Among the questioned, there were those being indirectly connected with transport industry. Among them, the share of transport services customers is 50 % of respondents, of transport services providers – 17 % of respondents. The remainder delivers various transport services. The dominating age of the respondents' businesses was: from 3 to 10 years old – 34 %, from 1 to 3 and emergence stage – 25 % each, from 10 to 20 years old and over – 8 % each. The managers made 31 % of respondents, average managers – 46 %, the rest – business owners. The majority of the questioned (60 %) consider that in recent years, sustainable tendencies in development of various sub-branches of the transport industry have emerged in Yugra. Part of the respondents (13.3 %) think that such tendencies have not shaped themselves, and part of the respondents consider that it is complicated to identify such tendencies (26.7 %).

According to participants' assessments, in sub-branches, the following tendencies are active (Table 3):

In general, development of transport in Yugra shows positive tendency (46.7 %) (Fig. 2).

The shown tendencies, according to the respondents, are relatively stable (53.3 %) and sufficiently sustainable (40 %). The greatest discrepancy was shown

Table 3. Assessment of availability, direction and influence ration of intra-sectoral factors, %

Dominating tendencies	Transport industry sub-branches			
	Road	Water	Air	Railway
Sharp exponential growth	6.6	–	6.6	–
Continuous fast growth	33.4	–	6.7	6.7
Gradual expansion of volume of structure of production	40	–	6.7	20
Stability (maintaining the same level)	13.4	20	53.4	60
Stagnation (gradual reduction in production)	–	40	20	6.7
Crisis (sharp downturn in volumes)	–	33.4	–	–
Sharp chaotic oscillations	6.6	6.6	6.6	6.6

Source: calculated by the author using questionnaire results.

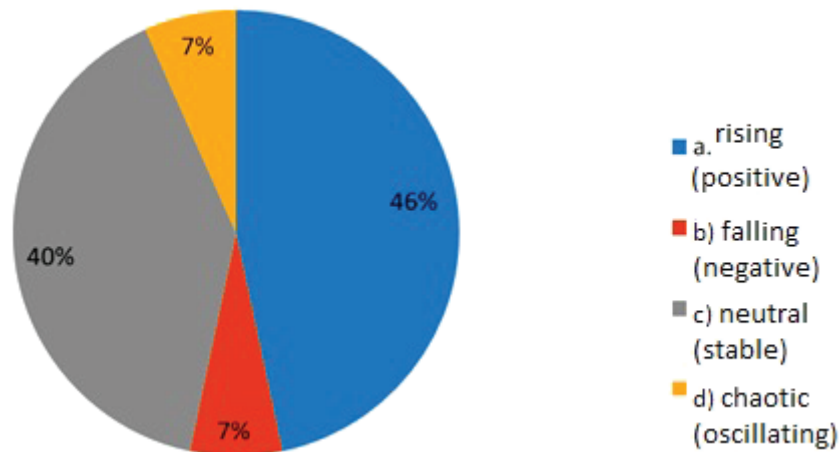


Fig. 2. Respondents' answers about dominating tendency  
Source: calculated by the author using questionnaire results

in forecasts. According to the respondents, in case the tendency is subject to change in the near 10 years, it will more likely to:

- stable – 40 %;
- positive – 33.3 %;
- oscillating – 20 %;
- negative – 6.7 %.

The most important factor indicated by the respondents was dependency on the main economy branch of Yugra.

The significant factors having equal rate of influence were considered to be:

- overall state of Russia's economy;
- regulatory base state.

As the less significant ones, the following factors were indicated:

- competitiveness rate;
- science and technology factor.

The influence of the “sanctions and counter-sanctions” factor on transport industry state was seen as non-significant (Fig. 3).

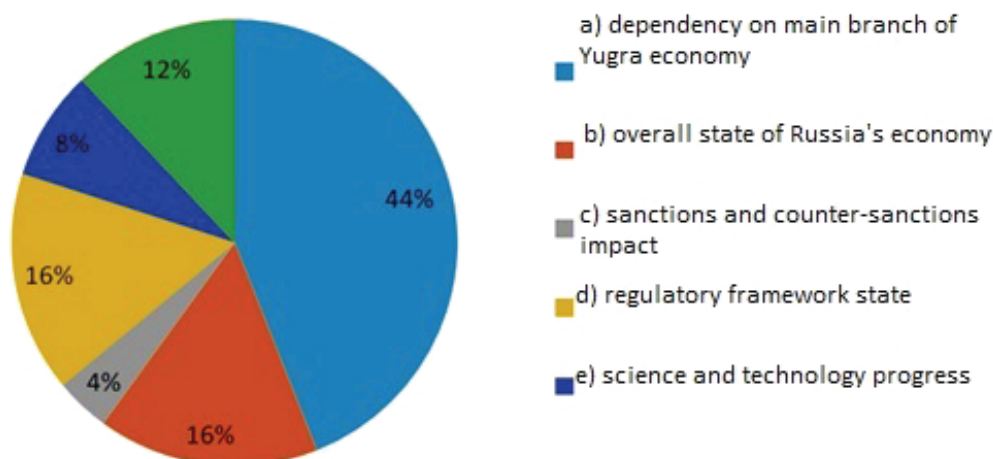


Fig. 3. Factors identifying dominating tendency in transport industry.

Source: calculated by the author using questionnaire results

Evaluation of factors that most determine the dominating tendency in transport industry give the following results: the dominating influence is exerted by interregional factors (57.9 %), all-Russian factors (26.3 %), intra-sectoral factors (15.8 %). None of the respondents maintains that common global factors influence transport industry development.

Interesting results were obtained after questionnaire on the reasons which may influence change of dominating factor in transport industry development (Table 4).

Table 4. Evaluation of influence of factors on possible change of transport industry development, %

№	Factors	Share
1	Change over economic policy	40.7
2	Change of raw materials prices	26.0
3	Change of final products prices	11.1
4	Administration of new sanctions and counter-sanctions	11.1
5	Change of legislation	7.4
6	Withdrawal of sanctions and counter-sanctions	3.7

Source: calculated by the author using questionnaire results.

To analyse further development of transport in Yugra, SWOT analysis and rankings methods were used.

The list of strengths and weaknesses of, opportunities for and threats to Yugra transport systems is given in Table 5.

*Table 5. Strengths and weaknesses of, opportunities for and threats to Yugra transport development*

<b>Strengths</b>	<b>Weaknesses</b>
S1. Well-developed riverways network S2. Proximity of transport passages of federal level S3. Investment attractiveness of Yugra economy S4. High transit potential of Yugra territory	W1. Large distances between inhabited areas, low population density W2. Lack of connectivity of transport system W3. High cost of road construction in swampy areas and harsh climate W4. Large unit cost of transport infrastructure maintenance W5. Great dependency of transport on oil extracting industry
<b>Opportunities</b>	<b>Threats</b>
O1. Delivery of large-scale infrastructure investment projects O2. Rise of national logistics networks, strengthening of interregional relations O3. Exploration and development of new deposits O4. Emergence of alternative transport modes O5. Reduction in resources consumption on transport due to development of energy efficient production and green energy sector O6. Emergence of new road construction technologies	T1. Contingency of reduction in federal investment programmes in transport industry T2. Increase in competitiveness with neighbouring regions T3. Oil extraction stagnation T4. Increase in Yugra budget deficit T5. Extension of sanctions

The strongest side of transport industry in Yugra lies in the territory's high transit potential. The weakest are high cost of road construction in swampy areas and severe climate as well as great dependency of transport on oil and gas extracting industry.

The opportunities that most correspond to strong and weak sides of transport system are: rise of national logistics networks, emergence of alternative transport modes and new road construction technologies. SWOT analysis of Yugra transport system development is given in Table 6.

The greatest threats overlapping weaknesses of transport industry are: natural resources extraction stagnation and increase in Yugra budget deficit [1].

Long-term priorities of SWOT-analysis are:

Table 6. SWOT-analysis of Yugra transport system development

Indicators		Opportunities						Threats					Total
		O1	O2	O3	O4	O5	O6	T1	T2	T3	T4	T5	
Strengths	S1	+1	+2	+1	0	+1	0	0/0	0/0	0/0	0/0	0/0	+5
	S2	+2	+2	0	0	0	0	0/0	+1/0	0/0	0/0	0/0	+5
	S3	+3	+3	+2	+3	0	0	+2/0	+1/-1	0/-3	+1/-1	0/-3	+7
	S4	+3	+3	0	+3	0	+3	+2/0	+1/0	0/0	+1/0	0/0	+16
Weaknesses	W1	-3/+1	-2/+1	0/+1	0/+3	0/+2	0/0	0	-1	-2	-1	0	-1
	W2	-2/+3	-1/+2	-1/+1	0/+3	0/0	0/0	-2	-2	-1	-1	0	-1
	W3	-3/0	-3/0	-3/0	0/0	0/0	0/+3	-3	0	0	-3	0	-12
	W4	0/0	-2/0	-2/0	0/+2	0/0	0/+3	-3	0	-2	-3	0	-7
	W5	-2/+2	0/+3	0/-1	-3/+1	-3/0	0/+1	0	-1	-3	-3	-1	-10
Total		+5	+11	-2	+13	0	+10	-4	-2	-11	-10	-4	X

**SO** – prioritised actions which need to be taken in order to exploit strengths to increase and ultimately use opportunities:

S3O1, S3O2 – increase in investment attractiveness of Yugra transport industry at the expense of delivery of large-scale infrastructure projects and their linking to national logistics networks;

S4O1, S4O2 – delivery of large-scale infrastructure projects, including those allowing for linking to national logistics networks to exploit high transit potential of the territory;

S3O4, S4O4 – development of alternative modes of transport which would enhance investment attractiveness of transport industry of Yugra and exploit high transit potential of the territory;

S4O6 – development of new road construction technologies to exploit transit potential of the territory.

**WO** – prioritised actions which need to be taken to overcome weaknesses and use opportunities:

W1O1, W1O4 – delivery of large-scale infrastructure projects, including development of alternative transport modes, to overcome such weaknesses as large distances between inhabited areas and low population density;

W2O4 – development of alternative modes of transport to overcome lack of connectivity in transport system;

W3O1, W3O2, W3O4 – search for ways to reduce cost of road construction to avoid lost opportunities caused by economic irrelevance such as new infrastructure projects, linking to national logistics networks, and exploration and development of new deposits;

W3O6, W4O6 – development of new road construction technologies to reduce their construction cost and transport infrastructure maintenance cost;

W5O2, W5O4, W5O5 – decrease in dependency on oil and gas extracting industry at the expense of linking to national logistics networks, development of alternative modes of transport and alternative energy sector;

**ST** – *prioritised actions that use strengths to avoid threats, and prioritised actions to prevent losses of strengths under influence of threats:*

S3T3 – Yugra economy diversification, including its transport infrastructure, to avoid stagnation of oil extraction and additional sanctions, which may lead to decrease in investment attractiveness of Yugra.

**WT** – *prioritised actions which overcome weaknesses, to prevent catastrophic consequences of identified threats:*

W3T1, W4T1 – search for reserves to reduce road construction expenditures, transport infrastructure maintenance, so as to overcome consequences of potential reduction in federal investment programmes in transport industry;

W5T3 – search for opportunities to reduce dependency of transport complex on oil and gas extracting industry, so as to overcome consequences of oil extraction stagnation;

W3T4, W4T4, W5T4 – search for reserves to reduce road construction cost, transport infrastructure maintenance cost, and dependency on gas and oil extracting industry, to overcome potential budget deficit.

Evaluation of degree of priority of development of most promising modes of global transport is given in Table 7.

Table 7. Evaluation of degree of priority of most promising transport modes

Transport modes	Potential to acquire the greatest social and economic budget effect	Correspondence to basic technological and organisational priorities	Correspondence to prioritised areas (axes) of transport complex development	Degree of influence of transport complex development on improvement of other directions of social and economic development of Yugra	Total priority ranking
Water	3	1	3	5	12
Air	5	3	1	5	14
Road	10	5	10	10	35



Pipeline	3	3	1	3	10
Railway	8	10	8	8	34

The most overriding modes of global transport in Yugra are road and railway transport. Road transport enables acquiring maximum social and economic, and budget effects, it corresponds to prioritised areas (axes) of development, and exerts the greatest influence on development of other directions of social and economic development of Yugra. Railway transport is slightly inferior to the mentioned indicators, but best corresponds to basic technological and organisational priorities, as it provides sound connectivity of Yugra and mainland [13].

### YUGRA TRANSPORT COMPLEX DEVELOPMENT FORECAST

Long-term forecast of freight traffic builds on forecast of volumes of freight by its types, taking into account the tendencies that formed in major economy branches of Yugra. The forecast was given in three options: pessimistic, in case current negative tendencies in development of gas and oil extracting industry remain unchanged and lack of large-scale infrastructure projects for development of other economy branches; moderate, in case of partial delivery of infrastructure projects; and optimistic, in case of overcoming negative tendency in gas and oil extracting industry development and realising large-scale infrastructure projects of regional and federal levels, such as construction of the Tyumen–Urai–Sovetsky–Nyagan–Beloyarsky–Nadym Highway, bridges across the Ob in Surgut and Oktyabrsky districts, the Priobye–Igrim, the Igrim–Saranpaul, the Agirish–Obskaya–Salekhard highways, the Polunochnoye – Obskaya – Salekhard Railway, the Northern Latitudinal Railway passing through Obskaya, Salekhard, Nadym, Pangody, Novyi Urengoi, Korotchaevo, Sabetta Port and development of Northern Sea Route, and finally realisation of complex investment project of Subpolar Ural development (Table 8) [14].

In case of pessimistic scenario, it is supposed that the volume of freight transported may decline, which can be brought about primarily by oil extraction, consequently associated gas, construction materials and equipment for deposits.

In case of optimistic scenario, it is supposed that oil extraction may fall insignificantly, which can be partially compensated for by development of new deposits and application of new technologies? Besides, in optimistic scenario the option is considered that the volume of freight may rise due to development of Subpolar Ural and setup of West-East and North-South transit transportation.

Table 8. Long-term forecast of freight volume, million tonnes

Type of freight	Basic figure (2014)	Forecast up to 2030		
		<i>Pessimistic</i>	<i>Moderate</i>	<i>Optimistic</i>
<b>Freight of Yugra</b>				
Oil	248	195	211	228
Associated gas	45	35	38	41
Petroleum products	1.55	2	2	2
Construction materials for buildings and accommodation erection	13.24	18	29	18
Construction materials to be used in deposit construction works (including site access roads)	73.04	48	54	60
Construction materials for repair and construction of regional and municipal roads	2.33	3.5	4.4	5.8
Timber	1.6	1.6	3.2	7
Food and consumer goods	3.22	3.58	3.58	3.58
Industrial goods	6.45	7	7	7
Oil and gas extracting equipment	3.65	2.4	2.7	3
Other types of freight	47.84	71.76	71.76	71.76
<b>Transit freight (excluding gas transit from Yamal-Nenets Autonomous Okrug)</b>				
Delivery of equipment and materials for Yamal peninsula deposits	3.69	1.49	1.49	1.49
Transit (transshipment) of freight for Yamal	27.98	34.98	35.38	34.98
Transit of LNG and petroleum products to Sabetta Port	0.00	0.00	3.00	10.00
Delivery of equipment and materials for deposit in northern Tomsk Oblast	1.49	7.47	7.47	7.47
Transit freight by Northern Latitudinal Railway	0.00	0.00	3.79	37.95
<b>New types of freight due to development of Subpolar Ural</b>				
Construction materials	0.00	0.00	3.00	14.00
Run-of-mine	0.00	0.00	2.00	18.40
Brown coal	0.00	0.00	6.00	10.00
Mining industry equipment and machinery	0.00	0.00	0.10	0.50
<b>Total</b>	<b>479.32</b>	<b>434</b>	<b>491</b>	<b>584</b>

In moderate scenario, estimation of volume of freight is more conservative. The structure of freight transportation at the directions given above is presented in Table 9 below.

Table 9. Structure of freight transportation at certain directions, million tonnes

Direction of transportation	Basic figure (2014)	Forecast up to 2030		
		<i>Pessimistic</i>	<i>Moderate</i>	<i>Optimistic</i>
Internal radial transportation	17.91	26–27	29–30	37–38
To Yugra	118.26	108–109	126–127	122–123
From Yugra	309.99	255–256	283–284	325–326
South-North/North-South transit	31.66	36–37	39–40	46–47
West-East/East-West transit	1.49	7–8	12–13	52–53
Total	479.32	434–435	491–492	584–585

In pessimistic scenario, the structure of transportation for each direction changes insignificantly, with the volume of transportation out of Yugra and internal radial transportation increased.

In optimistic scenario, the volume of transportation increases three times as compared to the pessimistic one. Also, the volume of internal radial transportation increases sharply (more than twice), and the import to Yugra hardly increases.

In moderate scenario, the evaluation of transit volumes is also conservative. The structure of transportation for transport modes is given in Table 10.

Table 10. Structure of freight transportation by transport modes, million tonnes.

Transport mode	Basic figure (2014)	Forecast up to 2030		
		<i>Pessimistic</i>	<i>Pessimistic</i>	<i>Pessimistic</i>
Freight sent by railway	13.80	16–17	25–26	63–64
Freight received by railway	15.00	17–18	23–24	61–62
Road transport	223.9	209–210	234–235	235–236
Internal water transport	3.36	4–5	4–5	4–5
Pipeline transport	236.26	185–186	201–202	218–219
Other transport modes	0.1	0.2	0.3	0.5
Total	479.32	434–435	491–492	584–585

In pessimistic scenario the structure of transportation by transport modes changes inconsiderably.

In optimistic scenario, almost 4 times increase in transportation by railway is observed, since it is railway transport that will carry natural resources from

Subpolar Ural, and will be a part of transit transportation in both latitudinal and meridian directions.

In moderate scenario, the role of railway transport is limited, since it may turn out that the volume of freight is not sufficient.

Long-term passenger transportation forecast.

The forecast of passenger transportation is more dependent on Yugra population growth, than on infrastructure projects delivery. Considering that the population of Yugra is forecast to grow up to 1791 thousand people by 2030, the volume of transportation will grow proportionally. The structure of passenger transportation by directions is given in Table 11.

Table 11. Structure of passenger transportation by directions, million people.

Direction of transportation	Basic figure (2014)	Forecast up to 2030
Within settlements	92.80	93–94
Internal radial municipal transportation	1.57	1.6–1.65
To Yugra	2.55	3.5–4.0
From Yugra	2.48	3.5–4.0
South-North/North-South transit	1.10	1.5–1.8
West-East/East-West transit	0	0.6–0.8
Passenger transported (sent) in total	100.5	104–105

The population growth will trigger increase in transportation in all directions, but due to motorisation rate increase, it will not be that fast [15]. Due to development of the latitudinal transport corridor, a new type of passenger transportation will emerge, that is West-East (and reverse) transit. The structure of passenger transportation by transport modes is given in Table 12 [1].

Table 12. Structure of passenger transportation by transport mode, million people.

Transport mode	Basic figure (2014)	Forecast up to 2030
Railway	2.4	4.0–5.0
Road transport (buses, shuttles, taxis)	89.1	93–94
Internal water transport	0.4	0.3
Others (air, non-public, etc.)	8.6	6–6.5
Passenger carried (sent) – total	100.5	104–105

The dominance in the structure will be retained by road transport; at the expense of increase in connectivity, railway transport volume will rise. The share of other types of transport will fall owing to road network development.

The main directions and activities of development and technical refurbishment of transport complex should be:

- transition of transport modes to natural gas-based fuel;
- transition of transport modes to electric traction;
- implementation of satellite navigation and monitoring systems;
- implementation of autopilot systems on road transport;
- expansion of Wi-Fi and mobile phone networks;

All activities must be undertaken with maximum use of scientific and technical potential.

## CONCLUSIONS

Thus, on the basis of analysis of the data presented, one can make the following conclusions.

*Firstly*, regional and municipal roads as well as the federal road have an express fundamental structure-forming role in Yugra road network: one km of these roads accounts for 8.8 km of privately owned and local roads. In the rest of Russia, this relation is 2.8 km, for instance.

As compared to average regional and intermunicipal roads of Russia, these roads have higher loads from both single transport units and total loads from all types of road transport.

*Secondly*, road transport flow is predominantly composed of other regions' transport.

Since the Rosstat (Russia's Statistics Agency) provides data on volumes of freight transportation by organisations' legal addresses, the actual volume of freight transported by roads is much higher. The dynamics of growth of freight transportation by roads is higher as well.

*Thirdly*, the industrial focus of Yugra economy development predetermines its multiple connections with other regions of Russia, which gives major regional roads interregional importance and, consequently, construction and maintenance of these roads should be provided not only at the expense of the Autonomous Okrug budget, but the expense of the federal one.

*Fourthly*, the dominating factors influencing development of transport complex in Yugra are nature and climate conditions, geographical location and location of town-forming enterprises in the territory of the Okrug.

The key agents responsible for Yugra transport complex development are:

- 1) Yugra government, whose interests consist in providing transport accessibility for all inhabited areas, industry branches development, small and average businesses;
- 2) cities' and municipalities' administration, interested in solving local transport problems;
- 3) business representatives, who can be divided into three groups:
  - VINKs (Vertically Integrated Oil Companies), interested in decrease in investment and operational expenditures for road network and transport infrastructure;
  - big investors, including logistics companies of national level, interested in attraction of profit from transit transportation;
  - small and average transport and related businesses, interested in continuous transport services.

## ACKNOWLEDGMENT

The study was conducted with financial support of RFBR and the Government of Khanty-Mansiysk Autonomous Okrug (Yugra), Agreement №17-12-86010/17-ОГОН (OGON) “Long-Term Forecast for Evolution of Economics of Resources Extracting Region, Considering the Path Completed and Peculiarities of Institutional Environment (by the example of Yugra)”.

## Библиографический список / References

1. Отчет о научно-исследовательской работе по теме: Создание распределенной модели данных об отраслях экономики Ханты-Мансийского автономного округа - Югры и разработка на ее основе проекта Стратегии социально-экономического развития Ханты-Мансийского автономного округа – Югры до 2020 года и на период 2030 года. Четвертый этап (отчет в 4 книгах). Книга 2. Стратегия социально-экономического развития Ханты-Мансийского автономного округа – Югры до 2020 года и на период 2030 года. Часть 6. Транспортный комплекс и транспортная инфраструктура. Режим доступа: <http://us86.ru/?p=3969>. Дата обращения: 14.06.2018. [Otchet o nauchno-issledovatel'skoj rabote po teme: Sozdanie raspredelennoj modeli dannyh ob otrasljah jekonomiki Hanty-Mansijskogo avtonomnogo okruga – Jugry i razrabotka na ee osnove proekta Strategii social'no-jekonomicheskogo razvitija Hanty-Mansijskogo avtonomnogo okruga - Jugry do 2020 goda i na period 2030 goda. Chetvertyj jetap (otchet v 4 knigah). Kniga 2. Strategija social'no-jekonomicheskogo razvitija Hanty-Mansijskogo avtonomnogo

- okruga – Jugry do 2020 goda i na period 2030 goda. Chast' 6. Transportnyj kompleks i transportnaja infrastruktura. Available from: <http://us86.ru/?p=3969>. (InRuss.).
2. Альметова З. В. Развитие транзитного потенциала уральского региона. Современные проблемы транспортного комплекса России. – 2012. – № 2. Режим доступа: [elibrary.ru/contents.asp?issueid=1026892](http://elibrary.ru/contents.asp?issueid=1026892). Дата обращения: 14.05.2018. [Al'metova ZV. Razvitie tranzitnogo potentsiala ural'skogo regiona. Sovremennye problemy transportnogo kompleksa Rossii. 2012;(2). Available from: [elibrary.ru/contents.asp?issueid=1026892](http://elibrary.ru/contents.asp?issueid=1026892)(InRuss.)].
  3. Транспорт в Тюменской области (2010–2014): Стат. сб. / Территориальный орган Федеральной службы государственной статистики по Тюменской области. – Тюмень: 2015. – 285 с. [Transport v Tjumenskoj oblasti (2010 – 2014): Stat. sb. Territorial'nyj organ Federal'noj sluzhby gosudarstvennoj statistiki po Tjumenskoj oblasti. Tyumen. 2015: 285. (InRuss.)].
  4. Транспорт в России, 2002. / Росстат. – Режим доступа: <http://www.gks.ru>. Дата обращения: 14.06.2018. [Transport v Rossii, 2002. Rosstat. Available from: <http://www.gks.ru> (InRuss.)].
  5. Постановление Правительства Ханты-Мансийского автономного округа – Югры № 152-п от 20 мая 2016 г. «О нормативах финансовых затрат на содержание, ремонт и капитальный ремонт автомобильных дорог регионального или межмуниципального значения за счет средств Дорожного фонда Ханты-Мансийского автономного округа – Югры и правилах их расчета». Режим доступа: <http://publication.pravo.gov.ru/Document/View/8600201605240010>. Дата обращения: 14.05.2018. [Postanovlenie Pravitel'stva Hanty-Mansijskogo avtonomnogo okruga – Jugry № 152-p 20 maja 2016 g. “O normativah finansovyh zatrat na sodержanie, remonti capital'nyj remont avtomobil'nyh dorog regional'nogo ili mezhmunicipal'nogo znachenija za schetsredstv Dorozhnogo fonda Hanty-Mansijskogo avtonomnogo okruga – Jugry i pravilahih rascheta”. Available from: <http://publication.pravo.gov.ru/Document/View/8600201605240010> (InRuss.)].
  6. Иванкив В.М., Сафронов К.Э. Комплексное использование автовокзалов для обслуживания вахтовых и междугородных перевозок в ХМАО-Югра // Дорожно-транспортный комплекс как основа рационального природопользования: материалы междун. науч.-техн. конф. – Омск: Изд-во СибАДИ, 2004. – Книга 2. – С. 5. [Ivankiv VM, Safronov KJe. Kompleksnoe ispol'zovanie avtovokzalov dlja obsluzhivaniya vahtovyh i mezhdugorodnyh perevozok v HMAO-Jugra. Mezhdun. nauch.-tehn. Konf “Dorozhno-transportnyj kompleks kak osnova racional'nogo prirodo-pol'zovanija”. (Conference proceedings) Omsk: Izd-vo SibAdI; 2004; 2: 5.(InRuss.)].
  7. Территориальный орган федеральной службы государственной статистики по Ханты-Мансийскому автономному округу – Югре. – Режим доступа: <http://khmstat.gks.ru>. Дата обращения 14.06.2018. [Territorial'nyj organ federal'noj sluzhby gosudarstvennoj statistiki po Hanty-Mansijskomu avtonomnomu okrugu – Jugre. Available from: <http://khmstat.gks.ru> (InRuss.)].
  8. Владимирова Т.А., Короткова Е.А., Позднякович С.Л. и др. Концепция стратегии создания системы наземного транспорта в Ханты-Мансийском автономном округе // Инвестиции и инновации. – 2008. – № 1. – С. 62–70. [Vladimirova TA, Korotkova EA,

- Pozdnjakovich SL, et al. Konceptcija strategii sozdanija sistemy nazemnogo transporta v Hanty-Mansijskom avtonomnom okruge. Investicii i innovacii. 2008;1: 62–70.(InRuss.).
9. Исследование современных и прогноз перспективных пассажиропотоков в г. Сургуте для оценки потенциального спроса на услуги муниципального пассажирского автотранспортного предприятия СГМУП «СПОПАТ», Ленгипрогор, Санкт-Петербург, 2006. [Issledovanie sovremennyh i prognoz perspektivnyh passazhiropotokov v Surgute dlja ocenki potencial'nogo sprosa na usluzi municipal'nogo passazhirskogo avtotransportnogo predpriyatija SGMUP SPOPAT. Lengiprogor. St-Petersburg; 2006. (InRuss.).]
  10. Основные показатели транспортной деятельности в России. 2010: Стат. сб./Росстат. – М., 2010. – Режим доступа: <http://www.gks.ru>. Дата обращения: 14.06.2018. [Osnovnye pokazateli transportnoj dejatel'nosti v Rossii. 2010: Stat. sb. Rosstat. – Moscow, 2010. – Available from: <http://www.gks.ru>.(InRuss.)]
  11. Постановление Правительства Ханты-Мансийского автономного округа – Югры № 166-п от 24 мая 2012 г. «О нормативах финансовых затрат на содержание, ремонт и капитальный ремонт автомобильных дорог регионального или межмуниципального значения за счет средств Дорожного фонда Ханты-Мансийского автономного округа – Югры и правилах их расчета» Режим доступа:<http://publication.pravo.gov.ru/Document/View/8600201605240010>. Дата обращения: 14.05.2018. [Postanovlenie Pravitel'stva Hanty-Mansijskogo avtonomnogo okruga – Jugry № 166-p ot 24 maja 2012 g. “O normativah finansovyh zatrat na sodержanie, remont i kapital'nyj remont avtomobil'nyh dorog regional'nogo ili mezhmunicipal'nogo znachenija za schet sredstv Dorozhnogo fonda Hanty-Mansijskogo avtonomnogo okruga – Jugry i pravilah ih rascheta” Available from: <http://publication.pravo.gov.ru/Document/View/8600201605240010>. (In Russ.)].
  12. Большаник П.В., Евланов Е.А., Исламутдинов В.Ф. и др. Исследование эволюции, институциональных условий и факторов развития отраслей экономики северного ресурсодобывающего региона (на примере Ханты-Мансийского автономного округа-Югры) / Под. науч.ред.д.э.н., доцента В.Ф. Исламутдинова – Ханты-Мансийск: ООО «Печатный мир г.Ханты-Мансийск», 2017. – 446 с. [Bol'shanik PV, Evlanov EA, Islamutdinov VF, et al. Issledovanie jevoljucii, institucional'nyh uslovij i faktorov razvitija otraslej jekonomiki severnogo resursodobyvajushhego regiona (na primere Hanty-Mansijskogo avtonomnogo okruga-Jugry). Hanty-Mansijsk: ООО “Pечатnyj mir g.Hanty-Mansijsk”; 2017. 446 p. (In Russ.)].
  13. Транспортная стратегия Российской Федерации на период до 2030 года. Проект. Министерство транспорта Российской Федерации. Москва. Режим доступа: <http://www.mintrans.ru>. Дата обращения: 14.06.2018. [Transportnaja strategija Rossijskoj Federacii na period do 2030 goda. Proekt. Ministerstvo transporta Rossijskoj Federacii. Moskva. Available from: <http://www.mintrans.ru>. (In Russ.)].
  14. Приложение 2 к распоряжению Правительства Ханты-Мансийского автономного округа – Югры от 22 марта 2013 года № 101-рп. Режим доступа: <https://depeconom.adhmao.ru/deyatelnost/innovacionnaya-politika/normativnaya-pravovaya-baza/296924/rasporyazhenie-pravitelstva-khanty-mansijskogo-avtonomnogo-okruga-yugry-ot-22-marta-2013-goda-101-rp>. Дата обращения 14.06.2018. [Prilozhenie 2 k rasporyazheniju



Pravitel'stva Hanty-Mansijskogo avtonomnogo okruga – Jugry ot 22 marta 2013 goda № 101-рр. Available from: <https://depeconom.adhmao.ru/deyatelnost/innovatsionnaya-politika/normativnaya-pravovaya-baza/296924/rasporyazhenie-pravitelstva-khanty-mansijskogo-avtonomnogo-okruga-yugry-ot-22-marta-2013-goda-101-рр.> (InRuss.).

15. Гудков В.А., Миротин Л.Б. Технология, организация и управление пассажирскими автомобильными перевозками. – М.: Транспорт, 1997 г. – 254 с. [Gudkov VA, Mirotin LB. Tehnologija, organizacija i upravlenie passazhirskimi avtomobil'nymi perevozkami. Moscow: Transport; 1997. 254 p. (In Russ.)]

**Information about the author:**

**Petr V. BOLSHANIK**, Candidate of Geographical Sciences (PhD); address: 628011, Khanty-Mansiysk, 41 Svetlaya St., Flat 9;  
ELibrary SPIN code 4550-0033; ORCID: 0000-0002-9118-2684;  
E-mail: bolschpetr@mail.ru

**Сведения об авторе:**

**БОЛЬШАНИК Петр Владимирович**, кандидат географических наук; адрес: 628011, Ханты-Мансийск, ул. Светлая, д. 41 кв. 9;  
eLibrarySPIN-код 4550-0033; ORCID: 0000-0002-9118-2684;  
E-mail: bolschpetr@mail.ru

**To cite this article:**

Bolshanic P.V. Forecast of Yugra Transport Development. *Transportation Systems and Technologies*. 2018;4(3):44-64. doi: 10.17816/transsyst20184344-64

**Цитировать:**

Большаник П.В. Эволюция, прогноз и преобладающие тренды развития транспорта Югры // Транспортные системы и технологии. – 2018. – Т. 4. – № 3. – С. 44–64. doi: 10.17816/transsyst20184344-64

DOI 10.17816/transsyst20184365-71

© **R. Rampelmann, R. Köhler**  
Thyssenkrupp Transrapid GmbH  
(Munich, Germany)

## SERVICE EXPERIENCES MAGLEV VEHICLES SHANGHAI

**Abstract:** In the late 1990s thyssenkrupp Transrapid GmbH successfully qualified the Maglev Vehicle TR08 and obtained the type approval certificate. Based on that design, in 2001–2003 three five-car vehicles for the first commercial high speed Maglev Line in Shanghai have been manufactured and set into operation. The VIP-Run took place over 15 years ago and the commercial operation has been running for almost 15 years at great availability.

The Transrapid system concept of small autonomous redundant electronics based modules facilitates significantly smooth maintenance - diagnosis, testing and system inspection.

Thanks to intelligent diagnostics, the use of easily interchangeable plug-in units, the dimensioning of the spare parts inventory according to the expected failure rates and the replenishment lead time, the maintenance efforts are still within the forecast range at the beginning of the project. Furthermore, the maintenance concept is essentially unchanged since the beginning.

There are no special materials that are subject to a potential shortage or price leap, but all according to normal industrial base.

Thanks to the low level of stress to components on board, most electrical and electronic units are still on-board as original equipment, which are 15 years old and at no end of life is visible.

But in case of repair or replacement, the challenge is the adaptation to the volatile market of electronic components. This includes the necessary lead-time for adaptive development and qualification, which has to be considered.

On the side of the vehicle supplier, a small smart team of electronics experts is managing obsolescence and compensates discontinuation.

The paper tells how it works and appreciates trustful cooperation of the supplier in Europe with the operator in China.

**Keywords:** Maglev vehicle, Service, Spare parts strategy, Maintenance, Obsolescence, Electronic components.

## INTRODUCTION

The article first provides the key data of the Shanghai Maglev Transportation Project, then highlights some main features of the Transrapid system and especially the vehicle to end with a detailed description of the maintenance procedures and experiences for the vehicles up to now.

## SHANGHAI MAGLEV TRANSPORTATION PROJECT

The Shanghai project is in all, a real story of success. In only three years, the total project, from the signing of contracts to the start of commercial operation, was finished. Fig. 1 shows the timeline for the realization of the Shanghai Project.

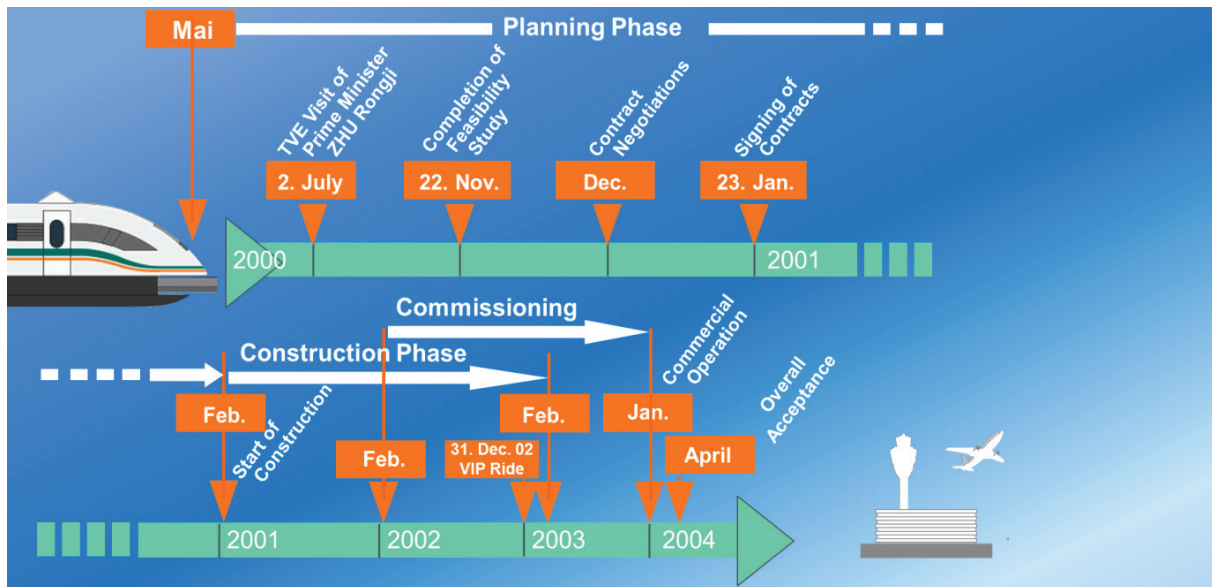


Fig. 1. Timeline of the Shanghai Maglev Project

Fig. 2 shows the track scheme and the main data. The technical layout like platform length and maintenance tracks is made for eight car trains. The operation control system and the propulsion system allow a frequency of one train every ten minutes. So the system is ready for further increase in passenger demand. For the time being five car trains and fifteen minute headway are used for operation.

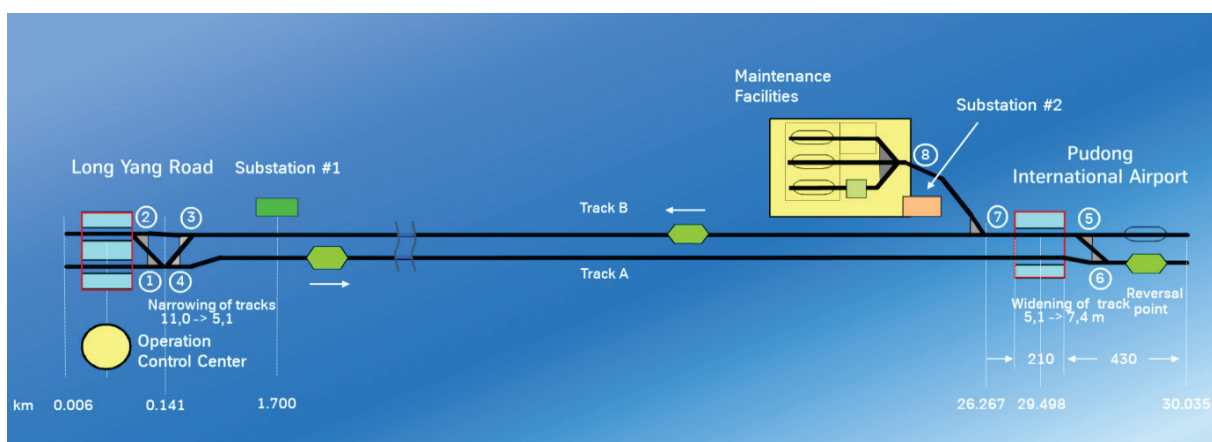


Fig. 2. Track scheme of the Shanghai Maglev Project

## TRANSRAPID SYSTEM CONCEPT

Fourteen years of operation after acceptance in April 2004 and sixteen years of system operation after start of commissioning in September 2002 represent a time period already nearing half of the 35 years life span Maglev vehicles are designed for. This is now a good time to have a technical review and outlook.

There is one basic principle of the system design which is still absolutely valid: the redundancy in such a way that any failure in any active component (vehicle, propulsion, or operations control) allows to continue service for a tolerable predefined time and that there is no need to stop the system running.

Also the key functions of levitation, guidance, and eddy-current safety brake are based on active safe-life strategy. So it never occurred that a vehicle stopped and could not become levitating due to failure.

Now, the actual experience with Transrapid vehicles and many other electronic applications have clearly proven the benefit and availability of systems mainly based on electronics. In fact, today many experts state electronics being a precondition to achieve extreme reliability and availability.

Another important design feature is the diagnosis system for the precise detection of failures to reduce maintenance time by clearly indicating the type and location of a failure

Dominant use of quickly replaceable slide-in units with short replacement time reduces maintenance measures and time at system level to a minimum, defective components are tested and repaired off-line without influencing system availability.

Fig. 3 shows the exchange of a slide-in unit that can be handled by two persons and is accomplished very quickly.



Fig. 3. Exchange of Slide-in Unit

Independence of subsystems, no relevance of combinations of failures of components of different subsystems, clear definition of structure and components allows assignment of failures to the responsible subsystem

## **MAINTENANCE STRATEGY AND MEASURES FOR THE VEHICLES**

The maintenance program defines the scheduled and unscheduled maintenance measures required to ensure safety, availability and performance of the system. The maintenance measures are based on fault tree/failure effect/maintenance analysis (including defined mitigation measures), inspection/test results, and manufacturer's specifications for components.

Vehicle maintenance measures executed in the maintenance area are:

- short term maintenance: daily executed measures
- long term maintenance: measures executed in longer time intervals and needing longer time

The technical prerequisites for the status-based maintenance strategy are subsystem diagnosis, failure tolerant, redundant design and inspection procedures.

The long term experience from the Shanghai project has shown that the inspection work that was done in the beginning did not reveal failures before the diagnosis systems disclosed them.

Typical intervals for electronic vehicle components maintenance derived from safety analyses and required to ensure safety of redundant active vehicle functions are daily and annual maintenance.

Scheduled daily vehicle maintenance measures and replacement of defective components can be completed in most cases within a time of maximum 1 hour.

Replacement of a defective electronic unit is expected to occur on the average every two weeks in a 5-car-vehicle with a MTBF target figure of 100 000 h and a total of about 1 250 electronic units. The dominant use of slide-in units enables short replacement time of typically below 15 minutes.

## **NECESSARY SPARE PARTS AND EQUIPMENT FOR VEHICLE MAINTENANCE**

- Set of spare parts to be located in the warehouse of the Maintenance Centre, including a defined amount of complete units, subcomponents and single parts, types and numbers is based on experience with life time, reliability, recovery time and lead time for spare part supply

- A set of special tools in the Maintenance Centre for assembly on site and execution of required maintenance measures
- Set of maintenance equipment including testing devices to check electronic units and to do inspection items
- Diagnosis database system to receive, transmit and store diagnostic messages, which are sent on-line from cruising vehicles in case of a component failure

### **THE MAINTENANCE DATA SYSTEMS (MAINTENANCE MANAGEMENT SYSTEM)**

- control data for train movements and safeguarding in the maintenance area
- maintenance program data and maintenance handbook
- diagnostic data display and recording
- line operation display information
- maintenance measures data recording
- configuration data and life cycle of subsystems and components
- spare parts and materials data

### **DAILY MAINTENANCE**

After arrival of a vehicle in the maintenance center the following steps are carried out:

- complete deactivation of vehicle and shut-down of external power supply, e.g. power rails;
- general visual check, taking about 30 min;
- replacement of defective components;
- daily preventive measures as e.g. exchange or replenishment of operation resources;
- vehicle activation and execution of defined safety-related daily function tests (especially brake test) before restart to station platform to resume scheduled operation.

### **ANNUAL MAINTENANCE ELECTRONIC COMPONENTS**

Annual scheduled maintenance includes component function tests to detect specific failures. Examples are

- in-circuit measurements;

- tests of safety-related control functions to check the component's reactions on failure conditions which don't occur and thus can't be detected in regular operation;
- servicing of batteries to restore nominal battery conditions and extend battery lifetime (performed quarterly).

These scheduled annual component tests are carried out at dedicated test benches. The availability of the vehicle for planned operation is only influenced by the necessity to replace the components to be tested by spare parts. This can be done depending on spare part policy and maintenance strategy by

- replacing all vehicle components to be tested (this may need more time on the long term maintenance track, more spare parts and using a long term spare train) or;
- replacement zone by zone or for a defined number of vehicle sections in consecutive night breaks, which also can be done on the short term maintenance track with regular fade-out and fade-in.

## ANNUAL MAINTENANCE MECHANICAL COMPONENTS

Maintenance measures derived for mechanical components are mainly preventive measures carried out in regular intervals. These measures, included in the maintenance program are mainly

- daily visual check as part of daily measures (see above);
- regular inspection, a comprehensive inspections is carried out at the long term maintenance track of the maintenance hall;
- exchange of operating resources like air filters for air-conditioning systems and, if required after five to ten years service life, exchange of minor wearing parts like rubber bearings;
- measurement of geometrical dimensions with respect to defined tolerances.

Long term measures requiring several days are performed after exchange of a vehicle against the long term reserve.

## MAINTENANCE PROGRAM AND INSTRUCTIONS

The maintenance program developed for the vehicles of the Shanghai Maglev Transportation Project consists of maintenance instructions for a total number of about 400 different scheduled and 60 unscheduled measures, including visual checks mostly for longer intervals up to 10 years, function tests, unscheduled

measures in case of diagnostic message after replacement of the component and replacement of operating resources.

In case of unexpected failures or malfunctions that are not covered by the maintenance routines there is an ongoing cooperation between the operator in Shanghai and the vehicle supplier in Germany. This long term product support is ensured by yearly inspections that are performed together and a steady contact in case of extraordinary events.

## CONCLUSION

The long term experience with maintenance of the Transrapid Maglev in Shanghai shows that the maintenance programs and measures that were defined at the beginning of the project are still valid and sufficient for the safe and reliable function of the system.

The high reliability of the individual components of the vehicle keeps the overall effort low. For the supply of spare parts, the challenge is the design adaptation to the volatile market of electronic components. The necessary lead-time for that adaptation and required qualification has to be considered.

On the side of the vehicle supplier, a small smart team of electronics experts is managing obsolescence and compensates discontinuation.

## References

1. Lin G, Sheng X. Application and Development of Maglev Transportation in China. Proceedings of the 23<sup>rd</sup> International Conference on Magnetically Levitated Systems and Linear Drives Maglev2016, Vol. 2; 2016 Sep 23–25; Berlin. Berlin: The International MaglevBoard; 2016.

### Information about the authors:

**Reinhard Rampelmann,**

E-mail: [info.transrapid@thyssenkrupp.com](mailto:info.transrapid@thyssenkrupp.com)

**Reiner Köhler,**

E-mail: [info.transrapid@thyssenkrupp.com](mailto:info.transrapid@thyssenkrupp.com)

### To cite this article:

Rampelmann R, Köhler R. Service Experiences Maglev Vehicles Shanghai. *Transportation Systems and Technology*. 2018;4(3):65-71. doi: 10.17816/transsyst20184365-71





UDC [УДК] 656.34  
DOI 10.17816/transsyst20184372-79

© E. Yu. Sundukov<sup>1</sup>, L. F. Selivanov, V. E. Sundukova<sup>2</sup>

<sup>1</sup>Komi scientific center of the Russian Academy of Sciences

<sup>2</sup>Syktyvkar forest institute  
(Syktyvkar, Russia)

## THE MAGLEV-SYSTEMS ON THE BASIS OF TRESTLE OF ARCH TYPE

**Aim:** To show that the trestle of arch type allows to realize various limiters of movements of the levitating vehicles.

**Methods:** Patent search, comparison with analogs, system approach.

**Results:** Options of designs of trestles for freight and passenger traffic are offered.

**Conclusion:** In all cases it is necessary to look for a compromise between achievement of the goal of functioning of maglev-system and costs of its construction and service.

**Keywords:** Maglev-systems, Trestle of arch type, Driving on a ceiling, Driving along a beam, Safe distance

© Е. Ю. Сундуков<sup>1</sup>, Л. Ф. Селиванов, В. Е. Сундукова<sup>2</sup>

<sup>1</sup>Коми научный центр Российской академии наук

<sup>2</sup>СЫКТЫВКАРСКИЙ ЛЕСНОЙ ИНСТИТУТ  
(СЫКТЫВКАР, РОССИЯ)

## МАГЛЕВ-СИСТЕМЫ НА ОСНОВЕ ЭСТАКАДЫ АРОЧНОГО ТИПА

**Цель:** Показать, что при помощи арочной эстакады можно реализовать применение различных типов ограничителей перемещений магнитнолевитирующих транспортных средств.

**Методы:** Патентный поиск, сравнение с аналогами, системный подход.

**Результаты:** Предложены варианты конструкций эстакад для пассажирских и грузовых перевозок.

**Выводы:** Во всех случаях конструирования маглев-систем арочного типа необходимо искать компромисс между затратами на строительство и достижением цели функционирования системы.

**Ключевые слова:** Маглев-системы, Эстакада арочного типа, «езда по потолку», «езда вдоль балки», безопасное расстояние.



## INTRODUCTION

We will call the guideway having an arch in cross section by trestle of an arch type. The arch trestle can be both by “opened”, and by “closed”. The monorail road in the city of Vappertel can be an example of the transport system with an opened trestle of arch type. The closed arch trestle (fig. 1) will allow to provide protection of vehicles against a rain, snow, strong wind gusts and other atmospheric phenomena. In Fig. 1: 1 – directly a trestle, 2 – the magnetic (electromagnetic) devices for propulsion of vehicles, 3 – the magnetic (electromagnetic) devices for levitation of vehicles are designated. Devices 3 can be replaced with aluminum rails.

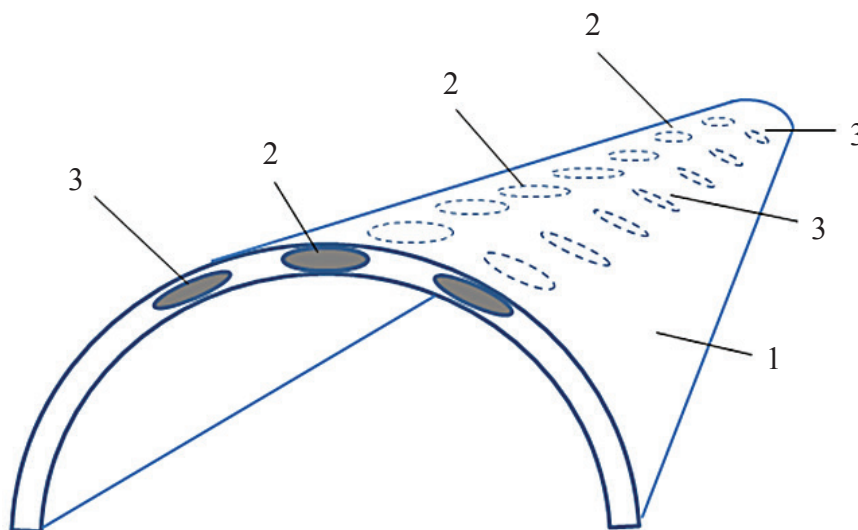


Fig. 1. The closed trestle of arch type

## THE TRESTLE OF ARCH TYPE FOR CARGO TRANSPORT

In the cargo transport systems various decisions which are directed to reduction of cost of construction and operation of maglev-system can be applied.

The arch trestle allows to realize limiters of movements (LMV) of two types [2]. Partially envelope LMV can be formed in the top part of an arch trestle (“the driving on a ceiling”). Partially enveloped LMV can be formed on surface of an arch trestle («the driving on a roof»).

Implementation of these assumptions for transit of containers is shown in Fig. 2. Conditionally we will call suspended container 7 (upper) “by empty”, hung container 4 (lower) – “by loaded”. It is desirable that containers 4 and 7 had a streamline shape.

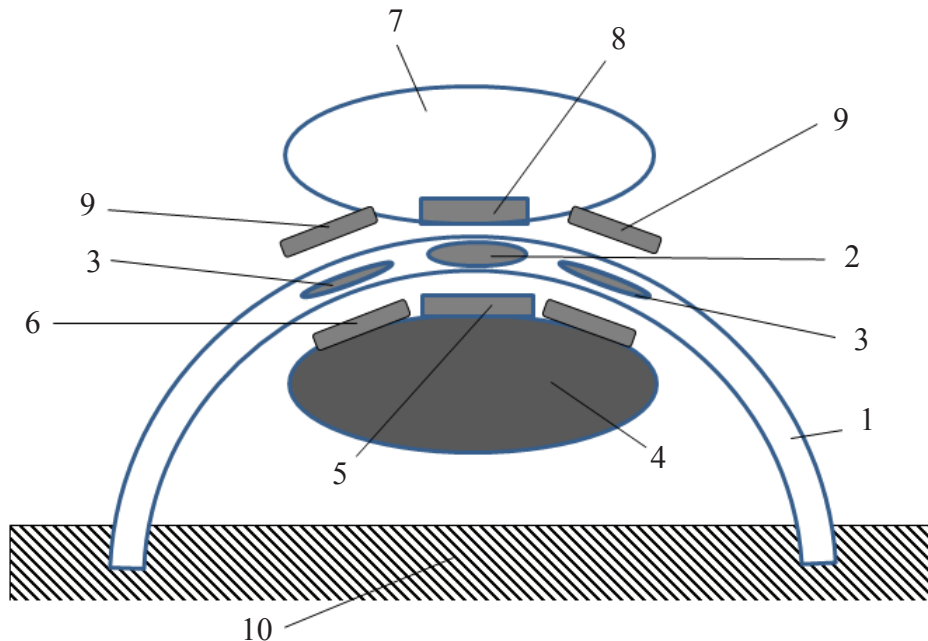


Fig. 2. The arch trestle for transportation of containers: 1 – the arch trestle; 2 – the round (coil) of a step's electromagnetic engine; 3 – the round (coil) of limiters of movements; 4 – the loaded container; 5, 8 – the magnetic sources for move of containers; 6, 9 – the magnetic sources for levitation of containers; 7 – the empty container; 10 – a supporting surface

Loaded container 4 levitates in the top part of an internal surface of trestle 1 as a result of interaction of coils 3 stator windings of the guideway and the magnetic sources 6 established on a container. Movement of container 4 will be carried out when passing electric current to coil 2 and his interaction with source of the magnetic field 5 which is also established on a container.

Empty container 7 can be moved into the opposite direction of movement of container 4 on external surface of trestle 1. His magnetic sources 8 and 9 in this case have to have different polarity to magnetic sources 5 and 6 of the loaded container 4.

Thus, it is possible to use both poles of a stator winding of the electromagnetic engine.

It is better to show the directions of movements of containers 4 and 7 concerning the trestle 1 in a longitudinal section (Fig. 3). When electric current feeds certain rounds 2, there are electromagnetic lines 11 under the influence of which the loaded container moves in direction 12 and the empty container in direction 13.

Together with an arch trestle other designs can be used. For example, a beam can be used together with an arch trestle for transportation of ballons or minitanks.

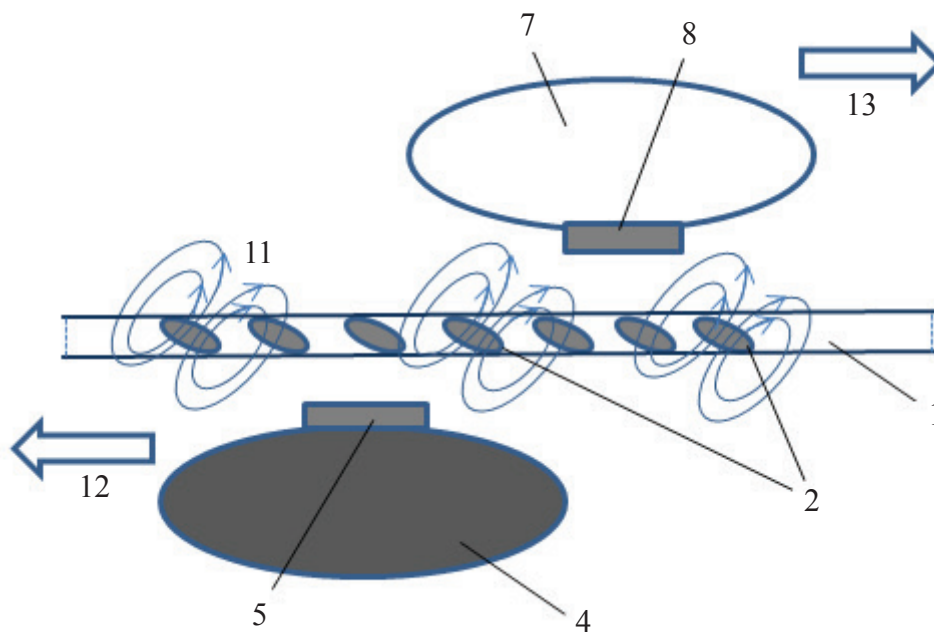


Fig. 3. The movement of containers concerning a trestle

In Fig. 4 it is shown that arch trestle 1 is combined with beam 12 which is established under trestle. Beam 12 has coil 2 for propulsion and coils 3 for levitation of ballons, for example, if oil or liquefied natural gas are transported.

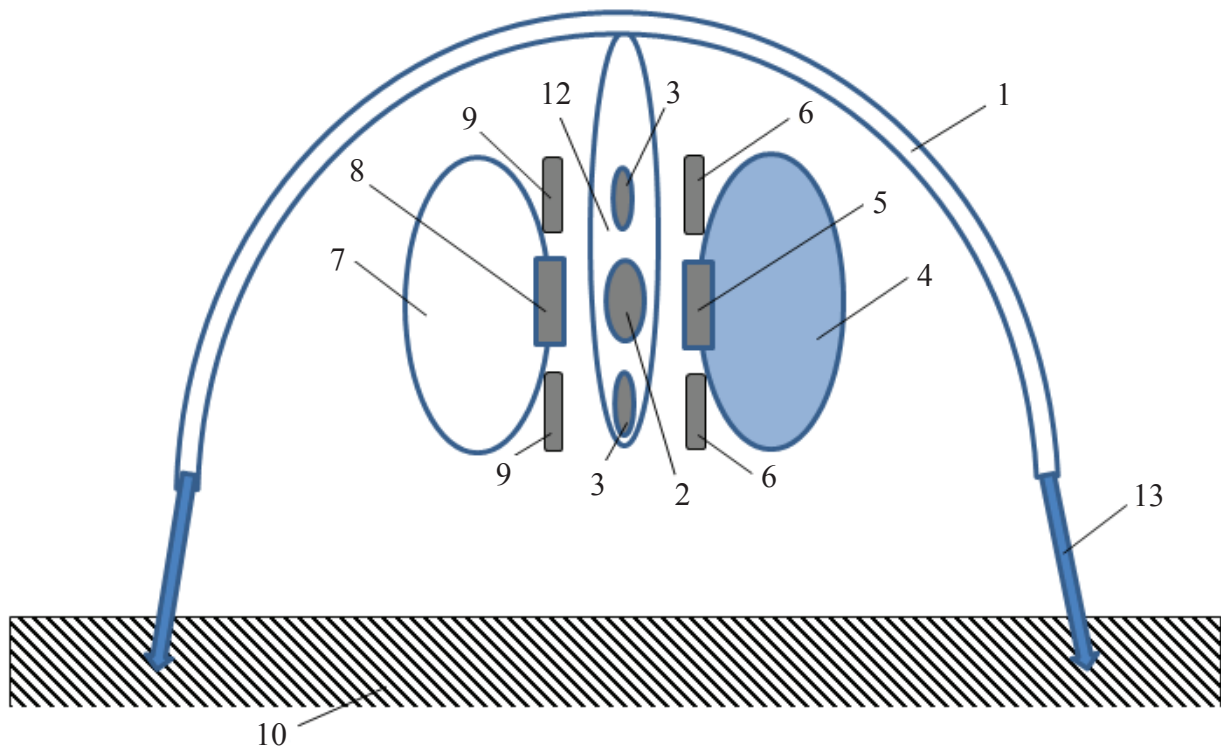


Fig. 4. An arch trestle, established on piles, with a beam

Filled ballon 4 has magnetic sources 5 and 6. Cylinder 4 levitates concerning beam 12 (sideways from it) thanks to magnetic interaction of coils 3 with sources 6.

Empty ballon 7 has magnetic sources 8 and 9. It levitates on the other side of beam of 12 thanks to magnetic interaction of coils 3 with sources 9.

Ballons 4 and 7 can move in identical or opposite directions depending of polarity of sources 5 and 6, when an electric current feeds coil 2.

Arch trestle 1 may is established on piles 13.

## THE ARCH TRESTLE FOR PASSENGER TRAFFIC

For passengers the main thing to ensure safety and comfort. Protection against electromagnetic radiations can be reached by an arrangement of a passenger cabin at a «safe distance» B from a stator winding of the guideway (Fig. 5). However, it will lead to increase of trestle height and cost of her construction.

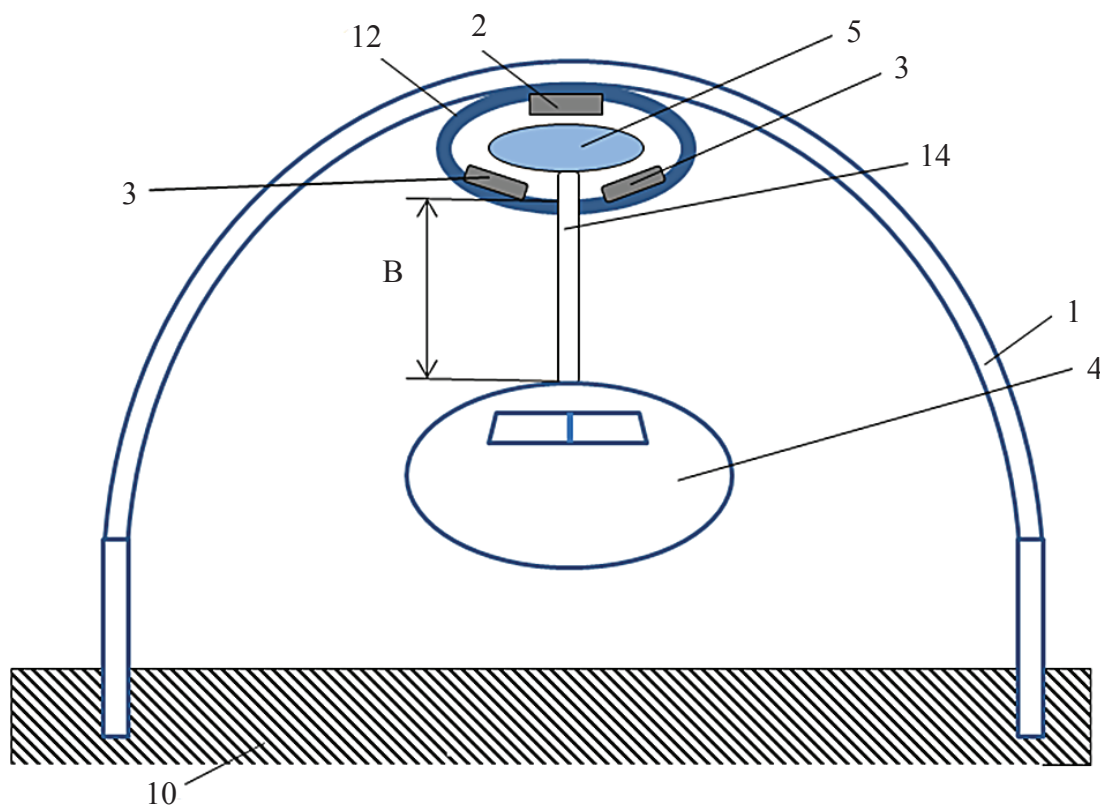


Fig. 5. The passenger maglev-system of arch type: 1 – the arch trestle; 2 – the coil of a step's electromagnetic engine; 3 – the coils for levitation of cabin; 4 – the passenger cabin; 5 – the magnetic source for levitation and propulsion of cabin; 10 – a supporting surface; 12 – a beam for coils of stator winding and magnetic source; B – «safe distance»

Some actions, for example, installation of protective screen, allow to reduce a «safe distance». As the result the cost of construction of a trestle falls, but the cost of a vehicle increases.

In Fig. 6 the protective screen is designated by position 15, other designations same, as in Fig. 5.

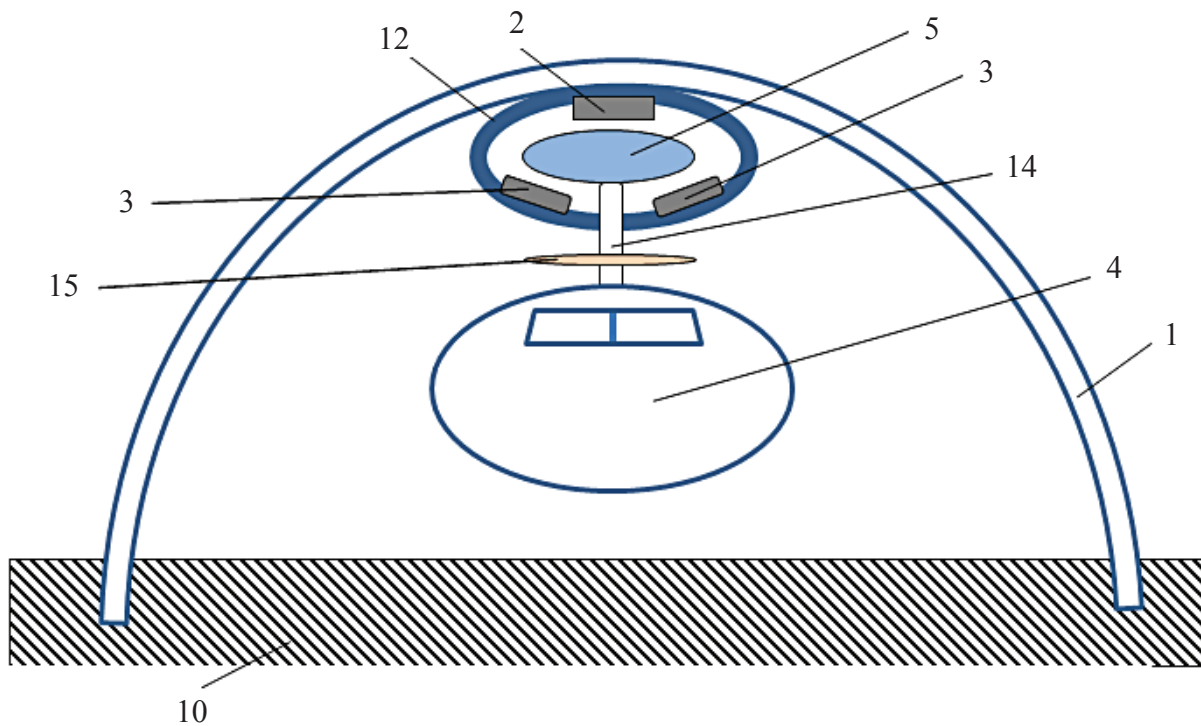


Fig. 6. The passenger maglev-system of arch type: 1 – the arch trestle; 2 – coil of a step's electromagnetic engine; 3 – the coils for levitation of cabin; 4 – the passenger cabin; 5 – the magnetic source for levitation and propulsion of cabin; 10 – a supporting surface; 12 - a beam for movement of a magnetic source; 14 – a frame; 15 – a protective screen

Movement of source 5 in beam 12 under influence of magnetic fields from rounds 2 and 3 can be described by means of the models presented in literature [3].

For the purpose of reduction of cost of a trestle not many-placed vehicles [4], but individual passenger cabins, calculated on three-four passengers, are offered.

This system has similarity to other maglev-systems [5, 6], they differ in engine type.

We suggest using for movement of vehicles the step's electromagnetic engine with the inclined rounds of a stator winding [6] that will allow to set various speeds of the movement of vehicles. At the same time there is no problem of increase in a gap of a levitation at an inclination of rounds. For secure wheel support can be used.

## CONCLUSION

The Maglev-systems on the basis of trestle of arch type can find application for transportation of goods and passengers.

In all cases it is necessary to look for a compromise between achievement of the goal of functioning of maglev-system and costs of its construction and service.

## БИБЛИОГРАФИЧЕСКИЙ СПИСОК / REFERENCES

1. Козорез В.В. Динамические системы магнитно-взаимодействующих свободных тел. – Киев: Наук. думка, 1981. – 140 с. [Kozorez VV Dinamicheskie sistemy magnitno-vzaimodejstvuyushhikh svobodnykh tel. – Kiev: Nauk. dumka, 1981. (In Russ.)]
2. Sundukov E. The stator winding with the inclined rounds. Possible applications. *Maglev Solutions for People, Cities, and Regions?* 2016;1:9-14.
3. Витков Г.А. Новый класс сил сопротивления в сплошных средах. – Тверь: ТГТУ, 1997. – 352 с. [Vitkov GA. Novyj klass sil soprotivleniya v sploshnykh sredakh. Tver': TGTU, 1997. (In Russ.)].
4. Cavagnaro M, Delle V. Saving Money with Maglev. An Urban Transport Revolution. *Maglev Solutions for People, Cities, and Regions?* 2016;1:15-24.
5. Патент РФ на изобретение № 2549317/ 27.04.2015. Бюл. № 12. Ким К.К., Титова Т.С. Транспортная система на электродинамическом подвесе. Режим доступа: <http://www.findpatent.ru/patent/254/2549317.html>. Дата обращения: 31.05.2018. [Patent RUS № 2549317/ 27.04.2015. Byul. № 12. Kim KK, Titova TS. Transportnaya sistema na ehlektrodinamicheskom podvese. Available from: <http://www.findpatent.ru/patent/254/2549317.html> (In Russ.)].
6. Maglev.net [Internet]. Skytran is coming to Tel-Aviv, Inc.; [updated 2014 January 1; cited 2018 Jul 9]. Available from: <http://www.maglev.net/skytran>.
7. Патент РФ на полезную модель № 168039/11.01.2016. Бюл. № 2. Сундуков Е.Ю., Малащук П.А., Тарабукина Н.А. Транспортная система с шаговым электромагнитным двигателем и колесными опорами. Режим доступа: [http://www1.fips.ru/fips\\_servl/fips\\_servlet](http://www1.fips.ru/fips_servl/fips_servlet). Дата обращения: 31.05.2018. [Patent RUS № 168039/11.01.2016. Byul. № 2. Sundukov EY, Malashhuk PA, Tarabukina NA. Transportnaya sistema s shagovym ehlektromagnitnym dvigatelem i kolesnymi oporami. Available from: [http://www1.fips.ru/fips\\_servl/fips\\_servlet](http://www1.fips.ru/fips_servl/fips_servlet) (In Russ.)].

### Information about the authors:

**Evgeny Sundukov**, senior research associate; address: 167982, Syktyvkar, ul. Kommunisticheskaya, 26  
eLibrary SPIN: 8735-7995; ORCID: 0000-0003-0141-8292;  
E-mail: jek-sun@mail.ru

### Leonid Selivanov,

ORCID: 0000-0003-1864-056X;  
E-mail: l.seliwanov@yandex.ru



**Veronika Sundukova**, student;  
ORCID: 0000-0002-9367-5693;  
E-mail: v.sunduckova@yandex.ru

**Сведения об авторах:**

**Сундуков Евгений Юрьевич**, кандидат экономических наук, доцент;  
телефон: +7(821) 2242593; адрес: 167982, Сыктывкар, ул. Коммунистическая, д. 26;  
eLibrary SPIN: 8735-7995; ORCID: 0000-0003-0141-8292;  
E-mail: jek-sun@mail.ru

**Селиванов Леонид Федорович**,  
ORCID: 0000-0003-1864-056X;  
E-mail: l.seliwanov@yandex.ru

**Сундукова Вероника Евгеньевна**, студент;  
ORCID: 0000-0002-9367-5693;  
E-mail: v.sunduckova@yandex.ru

**To cite this article:**

Sundukov EY, Selivanov LF, Sundukova VE. The maglev-systems on the basis of trestle of arch type. *Transportation Systems and Technology*. 2018;4(3):72-79. doi: 10.17816/transsyst20184372-79

**Цитировать:**

Сундуков Е.Ю., Селиванов Л.Ф., Сундуков В.Е. Маглев-системы на основе эстакады арочного типа // Транспортные системы и технологии. – 2018. – Т. 4. – № 3. – С.72–79. doi: 10.17816/transsyst20184372-79



DOI 10.17816/transsyst20184380-89

© R. Appunn<sup>1</sup>, J. Frantzheld<sup>1</sup>, M. Jetter<sup>2</sup>, F. Löser<sup>1</sup>

<sup>1</sup>thyssenkrupp Transrapid GmbH  
(Munich, Germany)

<sup>2</sup>thyssenkrupp Elevator AG  
(Filderstadt, Germany)

## MULTI<sup>®</sup>-ROPE-LESS ELEVATOR DEMONSTRATOR AT TEST TOWER ROTTWEIL

**Background:** The world's first linear motor driven passenger elevator system MULTI<sup>®</sup> started test operation at test tower Rottweil, Germany. A full scale showcase has been installed, the commissioning is finished and extensive testing activities are performed. The new test tower in Rottweil provides the perfect test and certification environment to get this ground-breaking product onto the market.

The propulsion of the cars is based on an ironless long-stator linear motor with distributed active drive, motor and sensor elements. This technology allows cars to move individually in the same elevator shaft without any ropes. The same type of linear motor will also be used to exchange cars horizontally from one shaft to another. Herewith a movement of the cars in a loop or any vertical and horizontal travel path can be realized. The testing procedures to characterize the operation of the MULTI<sup>®</sup> include measurements of electrical, mechanical and thermal quantities.

Smart energy management feeds power of descending cars for rising cars. To overcome the high power demand for acceleration cars, an energy buffering system is installed.

**Aim:** This paper focuses on the power and energy management of the MULTI<sup>®</sup> demonstrator. The benefit of intelligent buffering strategy is depicted.

**Methods:** Full scale prototype, numerical simulation, testing and measurement.

**Results:** This paper presents first measurement results of the MULTI<sup>®</sup> demonstrator mainly focusing on the power and energy characteristics of the propulsion system.

**Conclusion:** Using an energy buffering system, the peak input power of the MULTI<sup>®</sup> can be reduced to 50 % of the peak power level without energy buffer. The power from downward moving cars is recuperated and used for upward driving cars, balanced by the energy buffer without stressing the grid.

**Keywords:** Ropeless elevator system, ironless linear motor, linear drive, multiple car operation, energy buffer.

## INTRODUCTION

MULTI<sup>®</sup> represents a completely new and innovative transportation system of thyssenkrupp Elevator [1] – a ropeless elevator that can move through a building not only vertically but also horizontally – a system to revolutionize high building construction. MULTI<sup>®</sup> in comparison to conventional and modern elevator systems provides the following main benefits (compare Fig. 1).



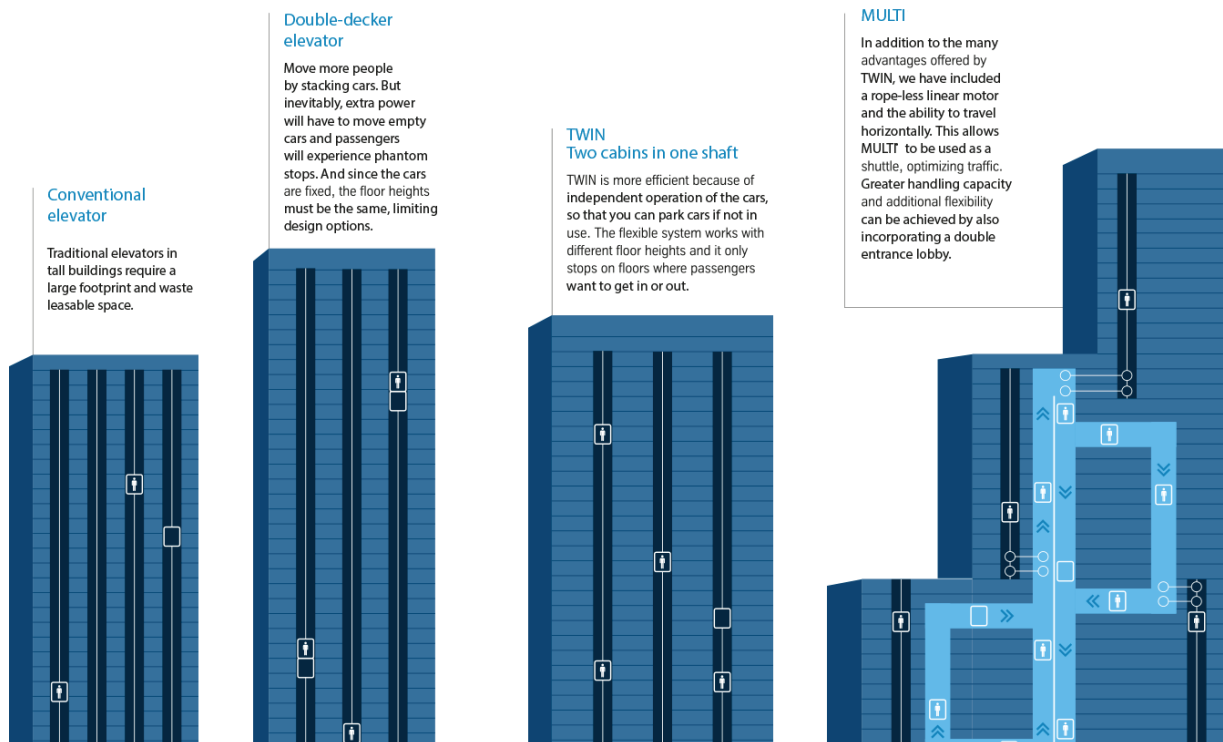


Fig. 1. Comparison of elevator technologies

### ***Significantly increased transport capacity with shorter waiting times***

In one year alone, New York City office workers spent a total of 16.6 years waiting for elevators, compared to only 5.9 years spent travelling in them [2]. The best way to save people's valuable time is to find solutions that cut waiting times rather than only speed up elevators. With MULTI®'s multiple cars in a single shaft passengers never wait more than 15 to 30 seconds for a lift.

### ***Substantially reduced mass***

Advances in lightweight design, including new lightweight carbon composites, to reduce MULTI®'s cabin and door weight by up to 50 % are integrated. Eliminating the ropes and counterweights of conventional elevators also decreases the mass to be moved during an elevator trip.

### ***Much smaller footprint***

With one car per shaft, traditional elevators take up more and more space as buildings increase in height [3, 4]. MULTI® consolidates multiple carriages into fewer shafts. It reduces the elevators' footprint by up to 50 % while increasing passenger throughput by at least as much. MULTI® may also help reduce the building's overall size, external surface area and total energy consumption.

### ***No more constraints in building height and shape design***

With MULTI®'s rope-free system, architects and developers are no longer restricted in their designs by concerns about elevator shaft height and vertical alignment. MULTI® opens the door to design possibilities in all directions.

## SHOWCASE AT TEST TOWER ROTTWEIL

The new 246-metre-high elevator test tower in Rottweil, southern Germany is specially configured for the elevator technology of tomorrow: in the twelve shafts within the tower, which have a diameter of 21 meters, the engineers can test elevators at speeds of up to 18 m/s. Three shafts with a height of 80 meters are used for the testing of the innovative MULTI<sup>®</sup> system.

Two of these shafts form a loop for upward and downward movement of elevator cars. In the third shaft garages are located for parking and maintenance of cars. Fig. 2 gives an overview of the testing scope.

Scope	
Travel height	80 m
Number of shafts	2
Shaft Dimension (WxD)	9,1 x 3 m
Number of Cars	3
Car weight	1680 kg
Number of Exchanger	4
Guide Rail Type	T140-2/B
Installation tolerance	<0,5mm
Nominal speed	5 m/s
Number of Inverters	~300
Number of Coil units	~600
Shuttle mode (clockwise)	Yes
Crane & Gondola	Yes

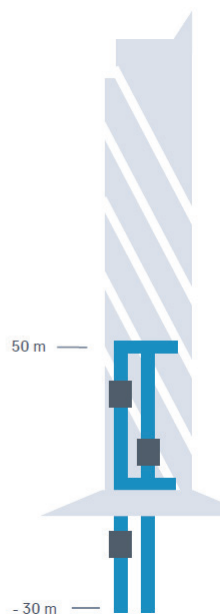


Fig. 2. MULTI<sup>®</sup> Showcase scope definition and foto of test tower Rottweil

### *Guiding system*

A cantilever concept is chosen as guide rail concept. This concept is shown in Fig. 3, where the linear drive is mounted centrally behind the car (hence cantilever solution). The chassis consists of a sledge (rotational part) and a car frame (static part). The car frame carries the cabin containing the payload (passengers) via a suspension system to isolate the payload from vibrations resulting from drive and roller guiding. The sledge contains the magnet yoke (movable part of the linear motor) which can be rotated by 90 degrees at a swivel platform.

### *Exchanger*

Four exchangers are located at intersections of vertical and horizontal shafts. An exchanger is a direct driven swivel device, which rotates the sledge including the

linear motor, while the cabin remains vertical by an interlock. In horizontal position the linear motor now drives the car horizontally to the next exchanger, where the sledge is turned back in vertical direction. Herewith a transition from a vertical to a horizontal shaft and vice versa is realized. The principle is shown in Fig. 4.

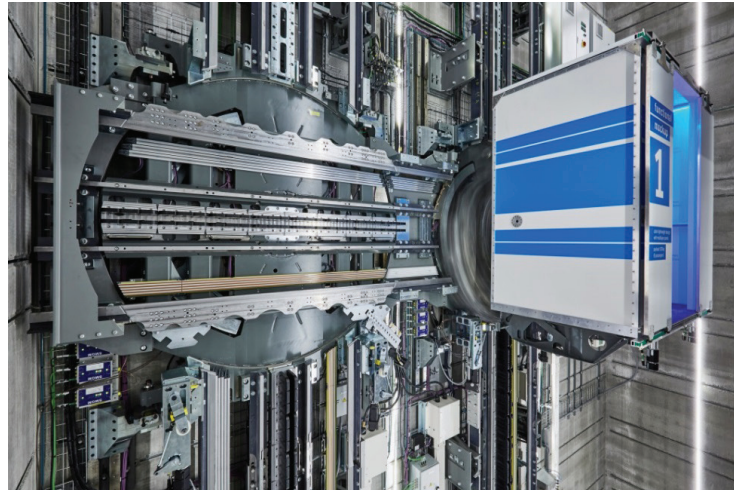


Fig. 3. MULTI® Showcase (Rottweil, Germany)

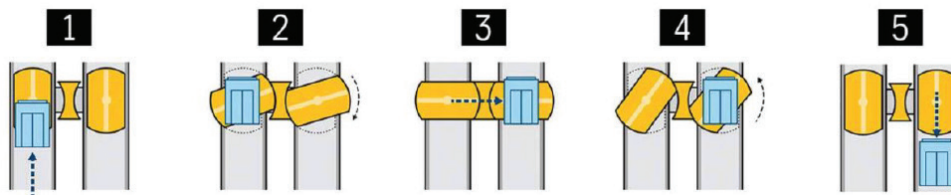


Fig. 4. Horizontal transition between shafts

## PROPULSION SYSTEM

The MULTI® elevator system operates multiple cars along several shafts distributed in a building. Linear drive technology [5] is applied for the movement of the cars. The propulsion system with its subcomponents is described in this section.

### *Linear motor*

An ironless long-stator linear synchronous motor concept is applied. The primary part consists of multiple coil units in double array configuration placed along the shaft. The secondary part is a permanent magnet yoke fixed at the car. Fig. 5 shows the configuration. Compact, IGBT-based inverter units (motor controllers) are distributed along the shafts. Each motor controller drives a 3-phase current to a dedicated coil unit. In double array configuration, eight motor controllers and coil units act on a single car.

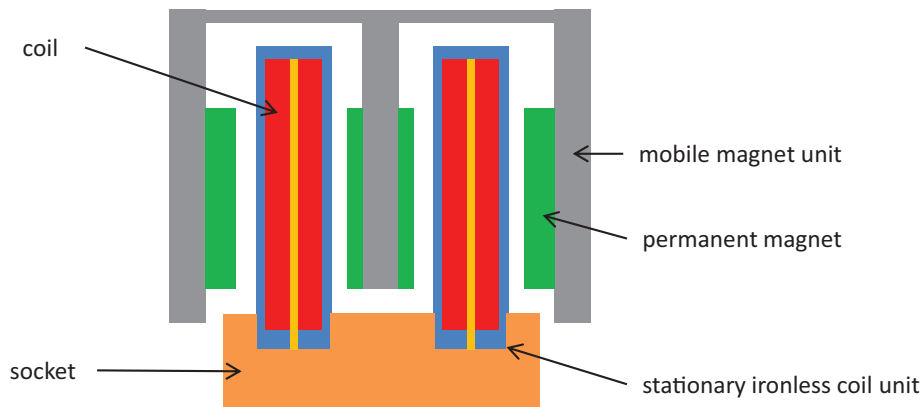


Fig. 5. Linear motor topology

### ***Position sensor***

For the MULTI<sup>®</sup> system, position sensors are required to measure the relative position of the magnet yoke on the car with respect to the coil units. The position information is required to perform position control (motion control) of the cars and for the commutation of the motor currents.

A customized sensor based on inductive influence of the scale (mounted on the car) on the sensor heads (distributed along the shaft) is utilized. The relative position accuracy is in the range of several  $\mu\text{m}$ , to match the requirements of the position control.

### ***Braking system***

The cars are equipped with two mechanical braking systems, the operation brake and the safety gear. The operation brake is only active at the stopping positions at the different floors. The safety gear is for emergency situations.

### ***Power distribution***

At Testtower Rottweil the MULTI<sup>®</sup> demonstrator has four independent power supplies. Herewith a fourfold redundancy is achieved. The power supplies consists of bidirectional rectifiers (active front ends), which feed DC-power to busbars, distributed along each elevator shaft. The DC-based system offers a higher efficiency and requires less space inside the shaft when compared to an AC-system. Motor controllers controlling coil units are supplied from these busbars. The coil units are generating the mechanical force through a yoke which is equipped with permanent magnets. The yoke is mechanically connected to an elevator car.

To reduce the installed power required for operation and to increase overall efficiency, an energy buffering system is applied. According to the redundancy concept of the MULTI<sup>®</sup>, each busbar should be equipped with a single energy buffer (compare Fig. 6). This means each energy buffer is connected in parallel to each power supply. An energy buffering strategy is applied to control the power flow of the system.

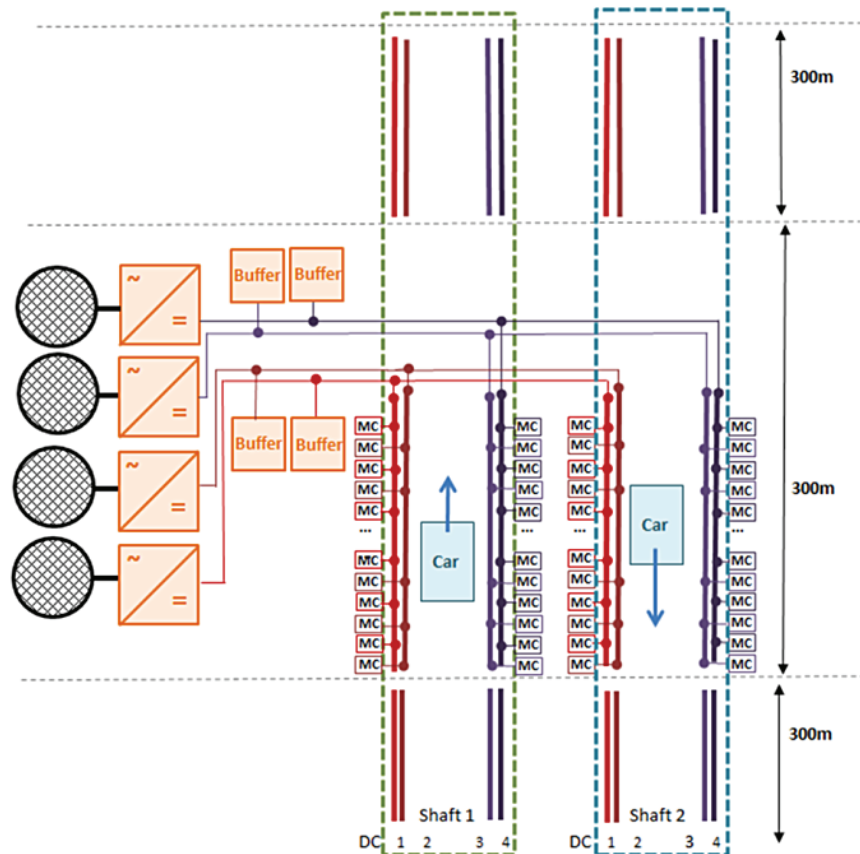


Fig. 6. Power distribution system

### ***Energy buffer***

In elevator operation, high input power is required for rising cars if no other car is lowering at the same time. To reduce these power peaks an energy buffer is applied. The energy buffer consists of a DC/DC-converter and supercapacitor arrays. The DC/DC-converter steps the DC-Link voltage down to the operating range of the supercapacitors. An active cell balancing strategy is applied to harmonize the voltages of the supercapacitor cells.

The energy buffer is connected in parallel to the DC-link, physically realized by power transmission cables. The power flow from DC-link to the energy buffer is controlled by a power management strategy. A real-time Ethernet communication is utilized. A current control is applied, since the DC-link voltage is already controlled by the active front end. Fig. 7 gives a schematic overview of the connection of the energy buffer.

### ***Energy buffering strategy***

The operation strategy of the energy buffer is defined as follows. Depending on the measured current demand of the MULTI<sup>®</sup> and the actual energy level of the buffer, the system either feeds power to the DC-link or is loaded by power from the DC-link. The target of the strategy is to reduce the peak input power of the system

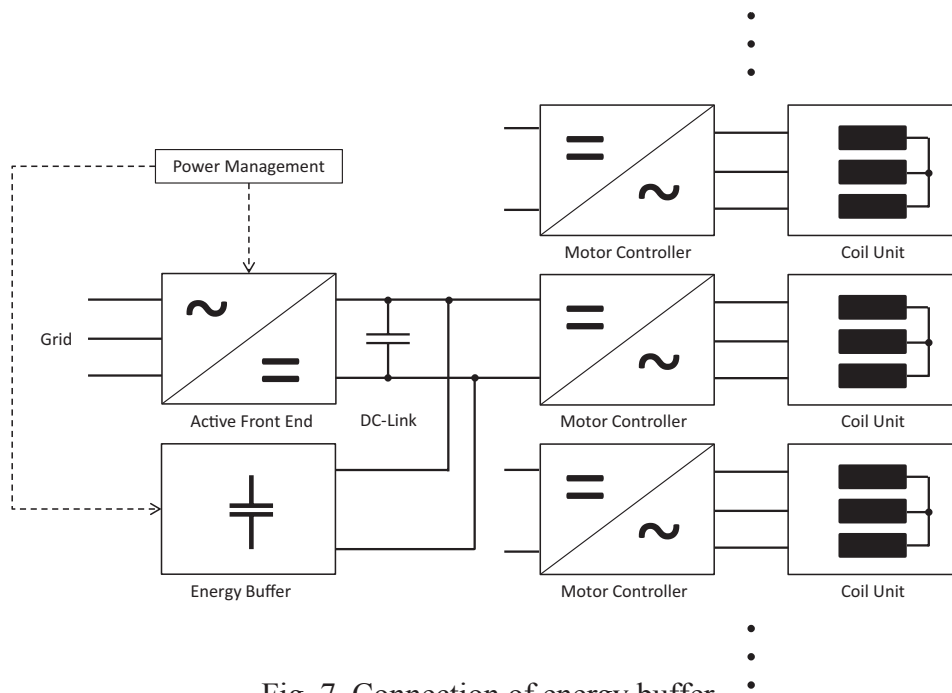


Fig. 7. Connection of energy buffer

and maintain a long term energy buffer target level of 50 %. Several thresholds can be defined to specify the behavior of the buffering system. Following the different decision paths, set values for the current control are generated. The operation strategy is implemented in the MULTI<sup>®</sup> power management.

## MEASUREMENT RESULTS

Various test runs are currently performed to analyze the power characteristics of the MULTI<sup>®</sup> and the influence of the energy buffering system. Speed, acceleration, weight and number of cars moving vertically or horizontally have been varied to cover relevant driving situations. Exemplary two test scenarios are presented in the following sections.

### *Example scenario 1: Shuttle operation up and down, no exchange*

The test run is done with two cars ( $m_1 = m_n$ ,  $m_2 = 0.75 m_n$ ) in two shafts with a speed of 5 m/s and an acceleration of 1.2 m/s<sup>2</sup>. The cars are moved as shuttle upwards and downwards (yo-yo). The movement consists of three full shuttle moves.

The measured input power of one power supply system is shown. The input power with and without energy buffer is depicted on the left chart in Fig. 8. The peak power without buffer is defined as 100 %. 40 % of this peak power are fed back during the downwards movements. A stand-by load of 8 % is measured. The input power with energy buffer differs significantly from the case without energy buffer. The peak input power is reduced to 50 %.

From the measured input current at the output of the active front end and the energy buffer current, the current demand of the MULTI<sup>®</sup> is calculated. Hereof a current offset is subtracted to take the standby losses into account. Based on this current demand, the current control of the energy buffer is carried out. The current demand is covered by the grid and also by the energy buffer.

The amount of energy stored in the buffer and the power of the buffer are depicted on the right chart in Fig. 8. The buffer is initially charged to 50 % of the maximum energy level. After the upwards movement the buffer is reduced to 32 %. After the following downward movement it is recharged completely. During every charge/discharge operation 95 % and 100 % of buffer power are transferred, respectively. The power circulates with the dynamic of the car movements.

The shuttle test operation is an extreme load condition for the MULTI<sup>®</sup>, which does not occur in real life operation. In addition to the characterization of the power demand, this test case is done to determine the thermal behavior of the linear drive.

### ***Example scenario 2: Showcase operation, circulation with exchange***

A circulation test run with three cars ( $m_1 = m_n$ ,  $m_2 = 0.75 m_n$ ,  $m_3 = 0.6 m_n$ ) in both vertical and horizontal shafts (loop) with a vertical speed of 5 m/s and a horizontal speed of 0.2 m/s is done. The maximum acceleration is 1.2 m/s<sup>2</sup> and 0.4 m/s<sup>2</sup>, respectively.

The measured input power of one power supply system is shown. The input power with and without energy buffer during the showcase scenario is depicted on the left chart in Fig. 9. Depending on the respective movements of the three cars, a different input power can be observed. The measured peak power without energy buffer is indicated as 100 %. In maximum 21 % of this peak power is fed back to the grid. The input power with energy buffer differs significantly from the case without energy buffer. The peak input power is reduced to 40 %.

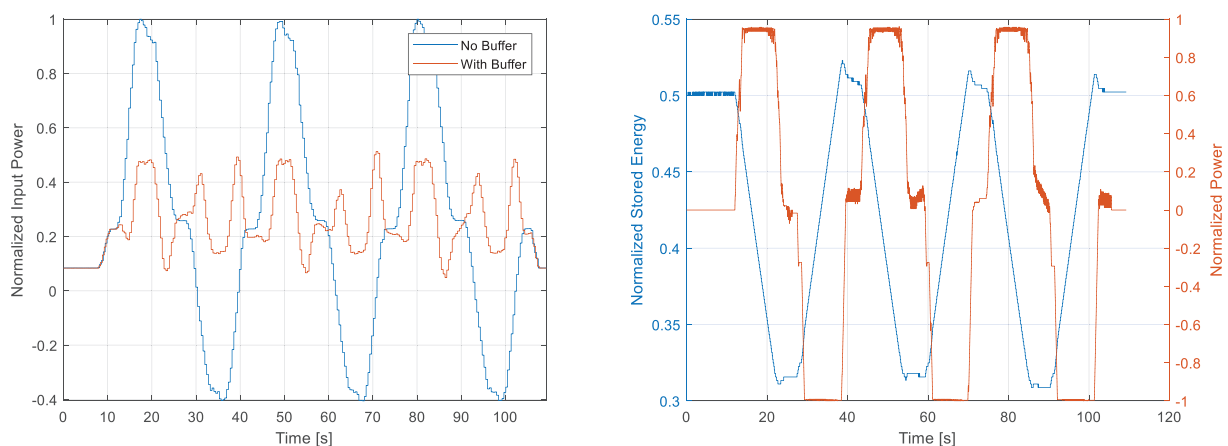


Fig. 8. Normalized measured power / energy of shuttle operation



The amount of energy stored in the buffer and the power of the buffer are depicted on the right chart in Fig. 9. The buffer is initially charged to 50 % of the maximum energy level. After the first downwards movement the buffer is charged above 54 %. After the following upward movement it is discharged to 45 %. During the following downwards and upwards movements the cycle is repeated. Since there are long standstill periods and horizontal movements in this scenario, the energy buffer is recharged completely every time. The maximum charge/discharge power is 80 % and 30 % of nominal buffer power, respectively.

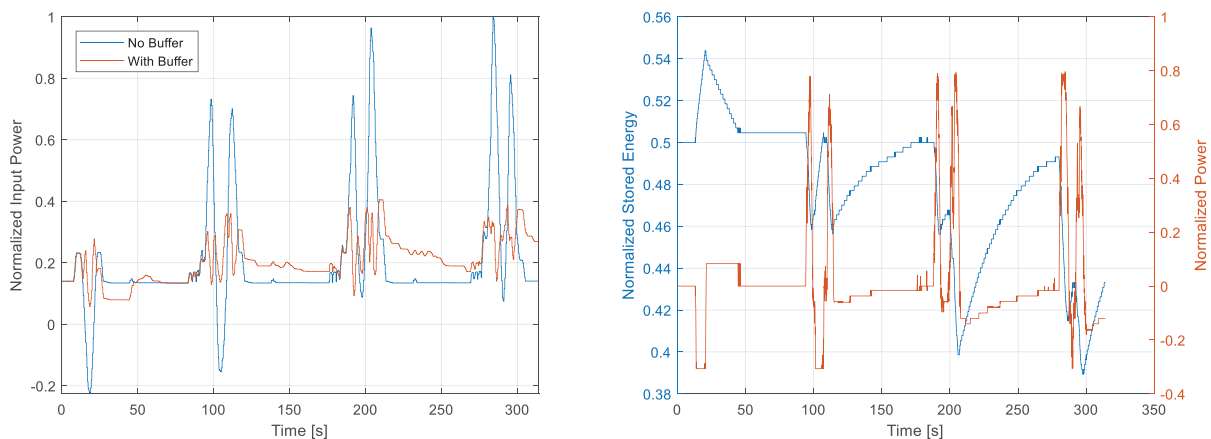


Fig. 9. Normalized measured power / energy of showcase operation

The power demand of the MULTI<sup>®</sup> during the showcase scenario is very low compared to the shuttle scenario. At maximum one car is moving upwards, while the other cars are at standstill, moving horizontally or downwards.

## CONCLUSIONS

A full scale demonstrator, the MULTI<sup>®</sup> Showcase has been commissioned at Testtower Rottweil and extensive testing has been performed. The propulsion system including multi-redundant power supply, power distribution and energy buffering is proofed fully operational. Using an energy buffering system, the peak input power of the MULTI<sup>®</sup> can be reduced to 50 % of the peak power level without energy buffer. The power from downward moving cars is recuperated and used for upward driving cars, balanced by the energy buffer without stressing the grid.

The applied linear drive technology with its multiple coil units and motor controllers provides both vertical and horizontal movement of three cars in one loop at a high ride comfort. Mechanical vibrations and the thermal characteristics of the linear motor are within the specified range. A highly redundant control system

guarantees in combination with an overall safety system a safe ride. In the ongoing project phase the MULTI® is subject to safety assessment for passenger transportation.

## References

1. Appunn R, Frantzheld J, Gerstenmeyer S, Jetter M, Löser F. MULTI® - New Technology of a People Transportation System for mid and high-rise Buildings. MAGLEV 2016, The 23rd International Conference, Berlin, 2016.
2. Dong J, Zafar Q. Elevator scheduling (Internet). Columbia University, New York; 2010. Available from: <http://www.columbia.edu/~cs2035/courses/ieor4405.S13/p14.pdf>.
3. Ishii T. Elevators for skyscrapers. *IEEE Spectrum*. 1994;31(9):42-46. doi: 10.1109/6.309960
4. Strakosch GR. *The Vertical Transportation Handbook*. John Wiley & Sons, Inc., New York; 1998. doi: 10.1002/9780470172865
5. Platen M. *Entwicklung eines Synchron-Linearantriebs für ein vertikales Transportsystem* [dissertation]. Aachen (Germany): RWTH Aachen University; 2001.

### Information about the authors:

**Appunn Rüdiger**, Doctor of Engineering;  
ORCID: 0000-0003-3487-6724;  
E-mail: [ruediger.appunn@thyssenkrupp.com](mailto:ruediger.appunn@thyssenkrupp.com)

**Frantzheld Jürgen**, Doctor of Engineering;  
ORCID: 0000-0003-2860-8723;  
E-mail: [juergen.frantzheld@thyssenkrupp.com](mailto:juergen.frantzheld@thyssenkrupp.com)

**Jetter Markus**,  
ORCID: 0000-0003-4939-8446;  
E-mail: [markus.jetter@thyssenkrupp.com](mailto:markus.jetter@thyssenkrupp.com)

**Löser Friedrich**, Doctor of Engineering;  
ORCID: 0000-0002-4341-1032;  
E-mail: [friedrich.loeser@thyssenkrupp.com](mailto:friedrich.loeser@thyssenkrupp.com)

### To cite this article:

Appunn R, Frantzheld J, Jetter M, Löser F. MULTI® – Rope-less Elevator Demonstrator at Test Tower Rottweil. *Transportation Systems and Technology*. 2018;4(3):80-89. doi: 10.17816/transsyst20184380-89

DOI 10.17816/transsyst20184390-101

© M. Kato, K. Hirata  
Osaka University  
(Osaka, Japan)

## CONTROL OF THREE-DEGREE-OF-FREEDOM RESONANT ACTUATOR DRIVEN BY NOVEL VECTOR CONTROL

**Abstract.** This paper presents a novel vector control method for three-degree-of-freedom resonant actuator in order to improve its controllability. The effectiveness of the presented method is verified through electromagnetic field analysis using 3-D finite element method:

**Issue:** A three-degree-of-freedom resonant actuator has a great potential to broaden the application range of linear oscillatory actuators because it has a lot of advantages: high efficiency, simple structure, etc. However, this actuator has low controllability because the magnetic structure of each axis is not independent.

**Aim:** To establish a novel vector control technique suitable for our actuator.

**Methods:** Electromagnetic analysis employing 3-D finite element method.

**Results:** In this study, the novel vector control theory was constructed on the basis of four-phase system. The new dq model was achieved by considering 3-D coordinate transformation. The proposed method is able to decrease the influence of thrust interference from other axis and achieved higher controllability.

**Conclusion:** The results of the study will contribute to a practical use of the three-DOF resonant actuator.

**Keywords:** linear actuators, linear oscillatory actuators, vector control, multi degree-of-freedom actuators, finite element analysis, four-phase system, dq transformation.

### INTRODUCTION

Linear resonant actuators (LRAs) [1–5] have been used in a wide range of applications because they can reciprocate in a comparatively short stroke in spite of their compact size and lightweight. In order to broaden the application range of LRAs, various kinds of multi-degree of freedom (DOF) resonant actuators have been developed [6, 7]. Authors have also proposed a two degree-of-freedom resonant actuator that was able to be independently driven in x- and z-axes by vector control [8–10]. Additionally, authors have designed a three-DOF resonant actuator driven by conventional vector control [11]. However, the previous control method did not completely control the thrusts in three directions ( $x$ ,  $y$ , and  $z$ ) because the magnetic circuit for each axis was not independent.

In order to improve controllability of the thrust, this paper proposes a novel vector control method using a four-phase system. Four fundamental voltage vectors ( $V_x$ ,  $W_x$ ,  $V_y$  and  $W_y$  phases) are defined in a stationary three-dimensional (3-D) coordinate systems. 3-D rotation using Euler angles achieved a spatial dq transformation. Electromagnetic field analysis by 3-D finite element method suggested that  $x$ - and  $y$ -axes thrust did not affect each other strongly when the proposed vector control was applied. Finally, the effectiveness of the proposed method was validated by comparing with the conventional method.

### THREE-DOF RESONANT ACTUATOR AND OPERATING PRINCIPLE

The basic structure of the three-DOF resonant actuator is shown in Fig. 1. This actuator mainly consists of a mover, a stator, and resonance springs in the  $x$ -,  $y$ -, and  $z$ -directions that support the mover. The mover is composed of a cross-shaped laminated yoke with five excitation coils (45 turns). This actuator is assumed to move with a range of  $\pm 1.2\text{mm}$  in the  $x$ - and  $y$ -directions and  $\pm 0.5\text{mm}$  in the  $z$ -direction, respectively. Resonance frequencies in  $x$ -,  $y$ -, and  $z$ -axes drive are set to be 41, 42, and 175 Hz, respectively. The specification of this actuator is shown in Table 1.

When a sectional view of the actuator in  $x$ - $z$  plane is focused, the magnetic structure is similar to those of four-pole three-phase permanent magnet synchronous motors. Therefore, this actuator is operated by vector control. The mover is driven in  $x$  and  $z$  axes independently when the field current element  $I_{dx}$  and the torque current element  $I_{qx}$  are assigned as the  $z$ - and  $x$ -axes thrust elements, respectively.

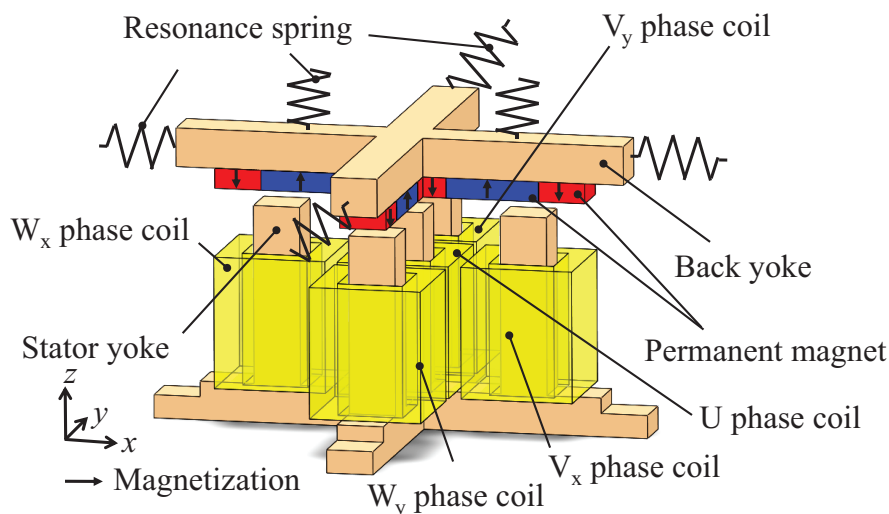


Fig. 1. Basic structure of three-DOF resonant actuator

Table 1. Specification of three-DOF resonant actuator

Parameter	Value		
	x-axis	y-axis	z-axis
Mass of mover [g]	214.89	55.38	21.22
Spring constant [N/mm]	14.89	3.22	29.15
Viscous damping coefficient [Ns/m]	0.997	0.44	0.528
Dimensions [mm]	31 x 31 x 18.8		
Remanence of magnet [T]	1.4		
Coil resistance [ $\Omega$ ]	0.24		

Because of the symmetry of magnetic circuits in  $x$ - and  $y$ -direction, the mover is also independently driven in  $y$  and  $z$  axes when the  $I_{dy}$  and  $I_{qy}$  are assigned as the  $z$ - and  $y$ -axes thrust elements, respectively. This actuator is a non-salient pole type and the thrust equation under the vector control is given as follow:

$$\begin{bmatrix} F_z & F_x & F_y \end{bmatrix}^T = \varphi \begin{bmatrix} I_{dx} + I_{dy} & I_{qx} & I_{qy} \end{bmatrix}^T \quad (1)$$

where  $F_x$ ,  $F_y$ , and  $F_z$  are the thrust of the  $x$ -,  $y$ -, and  $z$ -axes, respectively, and  $\varphi$  is the armature interlinkage flux from the permanent magnet. A phase angle of each axis between the stator and the mover is given as follow:

$$\theta_j = \frac{j}{l} \pi \quad (2)$$

where  $l$  is the distance between north and south poles, and  $j$  is the axis of the mover. From the equations (1) and (2), the current of each phase is determined by the inverse d-q transformation, as follow:

$$\begin{bmatrix} I_U \\ I_{V_j} \\ I_{W_j} \end{bmatrix} = \sqrt{\frac{2}{3}} \begin{bmatrix} \cos \theta_j & -\sin \theta_j \\ \cos(\theta_j - 2/3\pi) & -\sin(\theta_j - 2/3\pi) \\ \cos(\theta_j + 2/3\pi) & -\sin(\theta_j + 2/3\pi) \end{bmatrix} \begin{bmatrix} I_{dj} \\ I_{qj} \end{bmatrix} \quad (3)$$

where  $I_U$  is the current of U phase coil, and  $I_{V_j}$  and  $I_{W_j}$  are the current of  $V_j$  and  $W_j$  ( $j = x, y$ ) phase coils, respectively.

## EVALUATION OF THRUST INTERFERENCE

In this chapter, thrust interference is evaluated by electromagnetic field analysis using 3-D finite element method (FEM). Fig. 2 shows the FEM model except air region. The number of tetrahedron elements and edges are approximately 1,554 000 and 1,799 000, respectively. CPU time per one step was about 10 minutes. Fig. 3 shows the analyzed current thrust characteristics in  $x$ -direction when magnetomotive force of 45 A is applied to each excitation coil ( $U$ ,  $V_x$ ,  $W_x$ ,  $V_y$ , and  $W_y$  phase). Out of five thrust waveforms, the waveforms in the  $U$ ,  $V_x$ , and  $W_x$  phase coils are sinusoidal and the phase differences of these waveforms are approximately 120 degrees in electrical angle. This result means that the actuator is able to operate in the  $x$ -axis if the three coils are excited on the basis of normal vector control theory. Fig. 4 shows the analyzed current thrust characteristics in  $z$ -direction. Thrust waveforms of  $U$ ,  $V_x$ , and  $W_x$  phase coils are also sinusoidal as thrust waveforms in  $x$ -direction mentioned above.

Next, the mutual thrust interference is evaluated when the vector control which is described at the previous section is employed. Fig. 5, 6 show the static thrust characteristics when only one target current is set. In Fig. 5, the  $x$ -axis thrust is almost constant with respect to the displacement in the  $x$ - and  $y$ -directions. However, the undesirable thrust in the  $z$ -axis is generated though  $d$ -axis targets  $d_x$  and  $d_y$  are zero, respectively. This is because the thrust characteristics of  $U$ ,  $V_x$ , and  $W_x$  phase coils are not complete sine wave due to the end effect. Similarly in Fig. 6, the  $z$ -axis thrust is almost constant with respect to the displacement in  $x$ - and  $y$ -directions and the undesirable  $x$ -axis thrust is slightly generated. From these

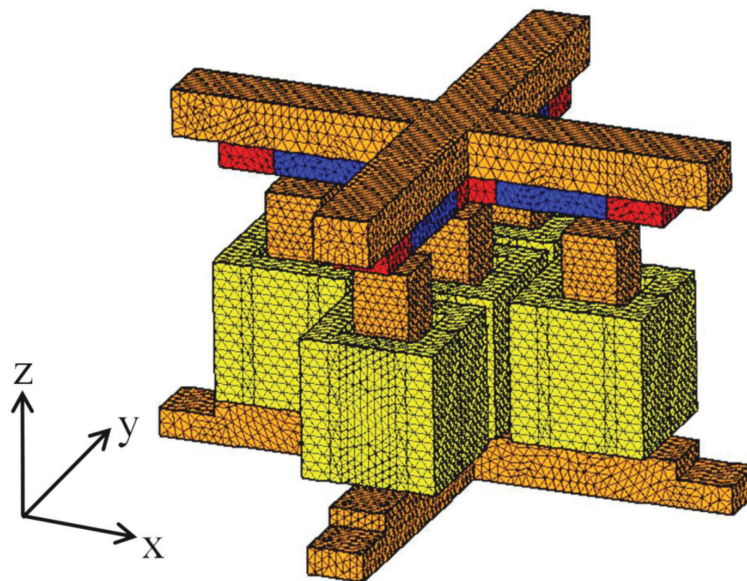
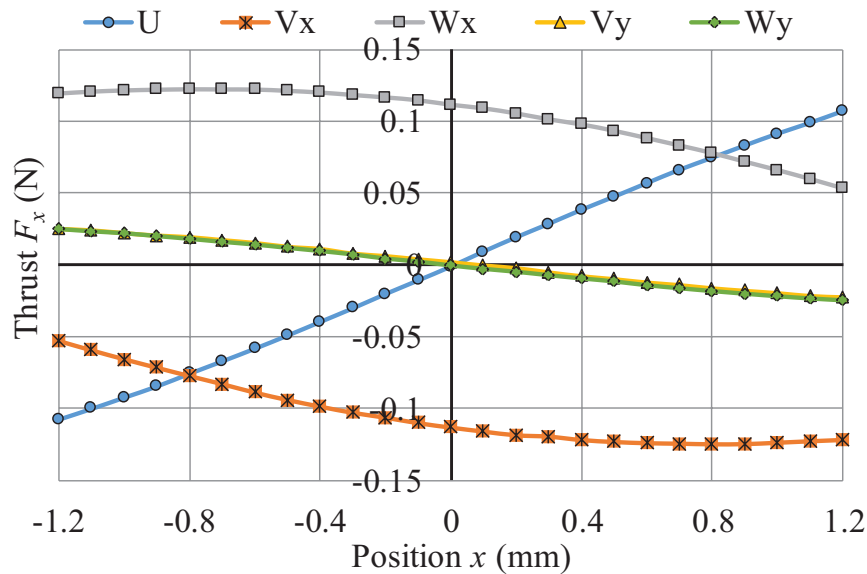
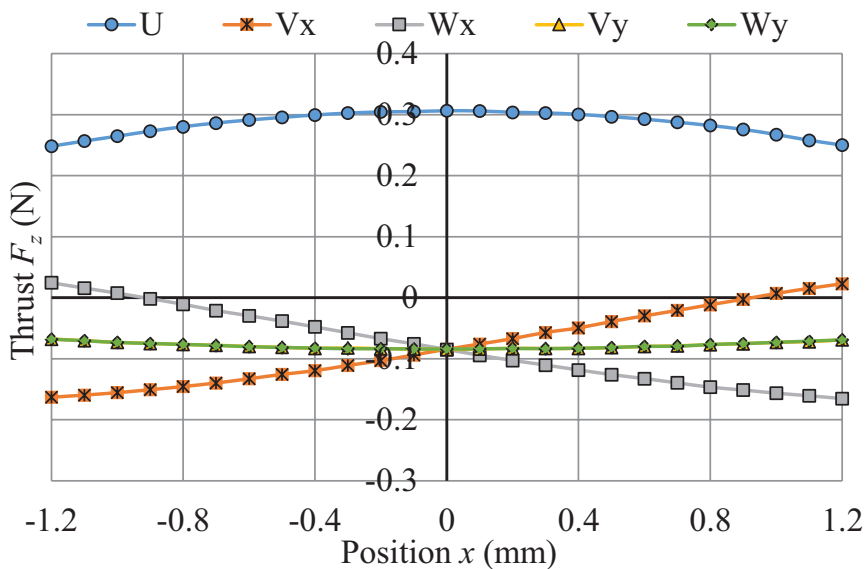
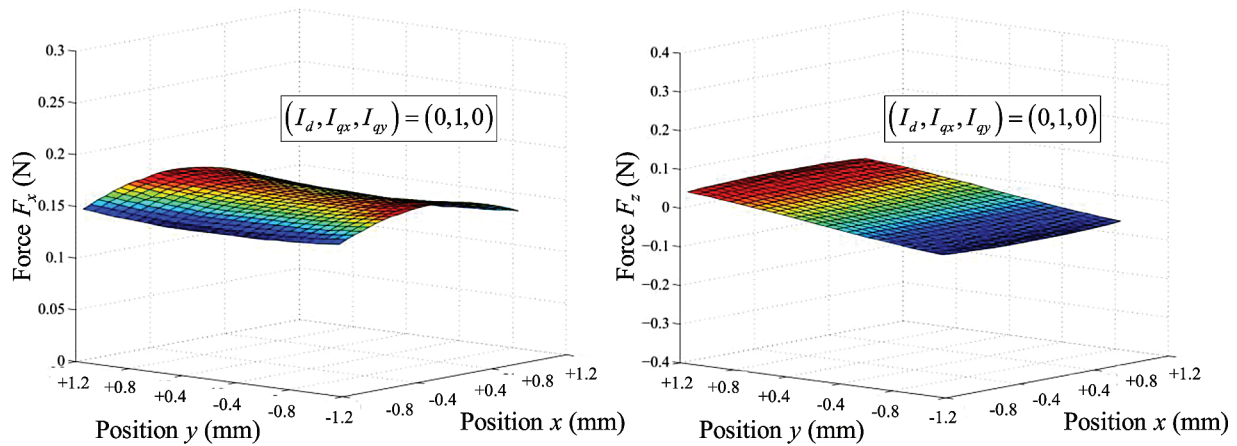
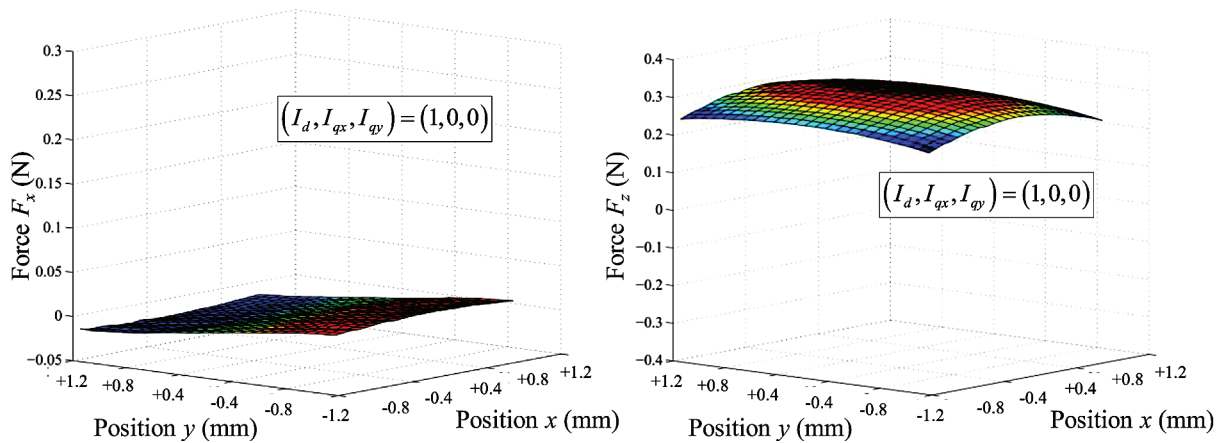
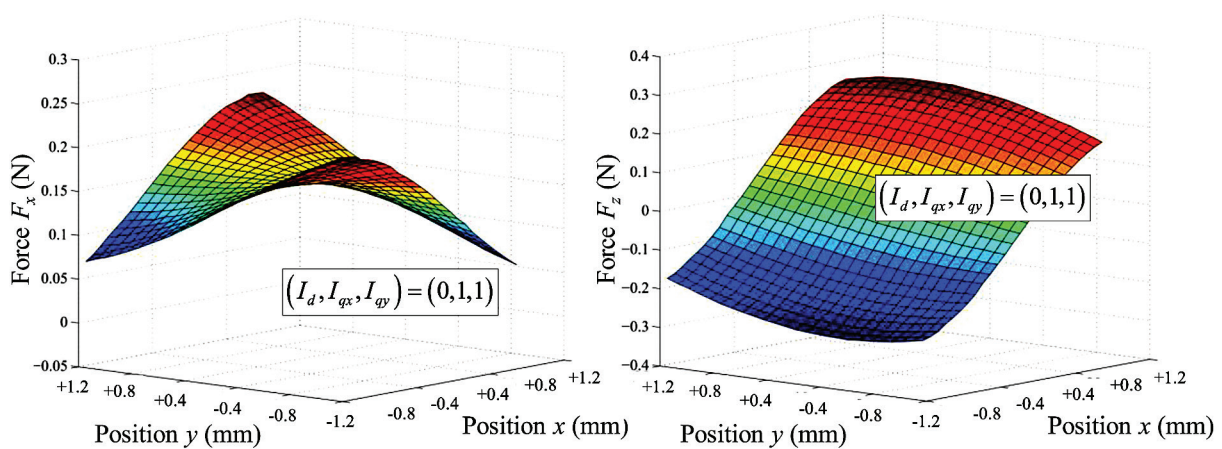


Fig. 2. FEM model

Fig. 3. Current thrust characteristic ( $x$ -axis)Fig. 4. Current thrust characteristic ( $z$ -axis)

results, the mutual thrust interference is tiny when the target direction of thrust is single.

Fig. 7 shows the static thrust characteristics when two target currents are simultaneously set. The  $x$ - and  $z$ -axes thrusts severely vary with respect to the displacement in the  $x$ - and  $y$ -directions. This is because  $V_y$  and  $W_y$  phase coils, which are originally used for  $y$ -axis operation, generate the thrust in the  $x$ -direction, as shown in Fig. 5. Moreover, the  $y$ -axis target current affects the  $z$ -axis thrust.

Fig. 5. Thrust characteristics under only one target current ( $q_x = 1$ )Fig. 6. Thrust characteristics under only one target current ( $d_x = 1$ )Fig. 7. Thrust characteristics under two target currents ( $q_x = q_y = 1$ )



Therefore, when the actuator is operated to oscillate in two or three directions, the thrust equation (3) is not suitable for obtaining a target thrust precisely.

## NOVEL VECTOR CONTROL THEORY

As described in the previous chapter, the conventional vector control is not completely able to control the thrust of the actuator because U phase coil is shared. When a sectional view of the actuator in  $x$ - $z$  plane is focused, three-phase system under the vector control corresponds to “three” actions. Two of the three are torque current ( $x$ - or  $y$ -axis drive) and field current ( $z$ -axis drive). The rest one is a condition that the sum of three-phase currents is constrained to zero. This suggests that the numbers of phases and actions are identical. On the basis of this concept, four-phase system is theoretically desirable for three-DOF resonant actuator because four-phase system corresponds to three operational actions ( $x$ -,  $y$ -, and  $z$ -axes drive) and one constraints that the sum of four-phase currents is zero.

Fig. 8 shows the schematic diagram of space vectors in the novel vector control using four-phase system.  $U_x$ ,  $V_x$  and  $W_x$  phase vectors are defined in  $\alpha\beta$  plane and  $U_y$ ,  $V_y$  and  $W_y$  phase vectors are defined in  $\alpha\gamma$  plane. These six vectors are integrated in the  $\alpha\beta\gamma$  space. However,  $U_x$  and  $U_y$  phase vectors are arranged in order to cancel each other. As a result, four phase vectors are defined in the  $\alpha\beta\gamma$  space. Since  $\alpha\beta$  plane are orthogonal to  $\alpha\gamma$  plane, the four phase vectors work as basis vectors of the proposed control.

Next, we form a novel dq transformation matrix. The transformation matrix from a four-phase stationary reference frame to a three-axis orthogonal stationary reference frame is represented by the following equation which contains three unknowns:

$$\begin{bmatrix} I_\alpha \\ I_\beta \\ I_\gamma \\ I_0 \end{bmatrix} = k \begin{bmatrix} \cos\theta_{un} & \cos\theta_{un} & -\cos\theta_{un} & -\cos\theta_{un} \\ \sin\theta_{un} & -\sin\theta_{un} & 0 & 0 \\ 0 & 0 & \sin\theta_{un} & -\sin\theta_{un} \\ a & a & a & a \end{bmatrix} \begin{bmatrix} I_{V_x} \\ I_{W_x} \\ I_{V_y} \\ I_{W_y} \end{bmatrix} = \begin{bmatrix} I_{V_x} \\ I_{W_x} \\ I_{V_y} \\ I_{W_y} \end{bmatrix} \quad (4)$$

$$= \begin{bmatrix} \alpha\beta\gamma \\ \mathbf{C}_{VWVW} \end{bmatrix} \begin{bmatrix} I_{V_x} \\ I_{W_x} \\ I_{V_y} \\ I_{W_y} \end{bmatrix}$$

where,  $I_\alpha$ ,  $I_\beta$ , and  $I_\gamma$  are the  $\alpha\beta\gamma$  orthogonal reference frame quantities,  $I_0$  is the zero sequence current,  $I_{vx}$ ,  $I_{wx}$ ,  $I_{vy}$ , and  $I_{wy}$  are the four-phase stationary reference frame quantities.  $\theta_{un}$  is the unknown angle between the  $\alpha$ -axis and  $W_x$  phase vector. The unknown coefficients  $a$  and  $k$  are required to satisfy power invariance before and after the transformation. In order to satisfy it, the product of the matrix  $[\alpha\beta\gamma C_{vwvw}]$  and its transpose matrix  $[{}^{vwvw}C_{\alpha\beta\gamma}]$  needs to be identity matrix. Therefore, the following equation is obtained and three unknown values are identified:

$$[\alpha\beta\gamma C_{vwvw}] [{}^{\alpha\beta\gamma} C_{vwvw}]^T = k^2 \begin{bmatrix} 4\cos^2 \theta_{un} & 0 & 0 & 0 \\ 0 & 2\sin^2 \theta_{un} & 0 & 0 \\ 0 & 0 & 2\sin^2 \theta_{un} & 0 \\ 0 & 0 & 0 & 4a^2 \end{bmatrix} =$$

$$= [\mathbf{I}] \begin{cases} \theta_{un} \cong 125 \text{ deg.} \Leftrightarrow \cos \theta_{un} = -\frac{1}{\sqrt{3}} \\ k = \frac{\sqrt{3}}{2} \\ a = \frac{1}{\sqrt{3}} \end{cases} \quad (5)$$

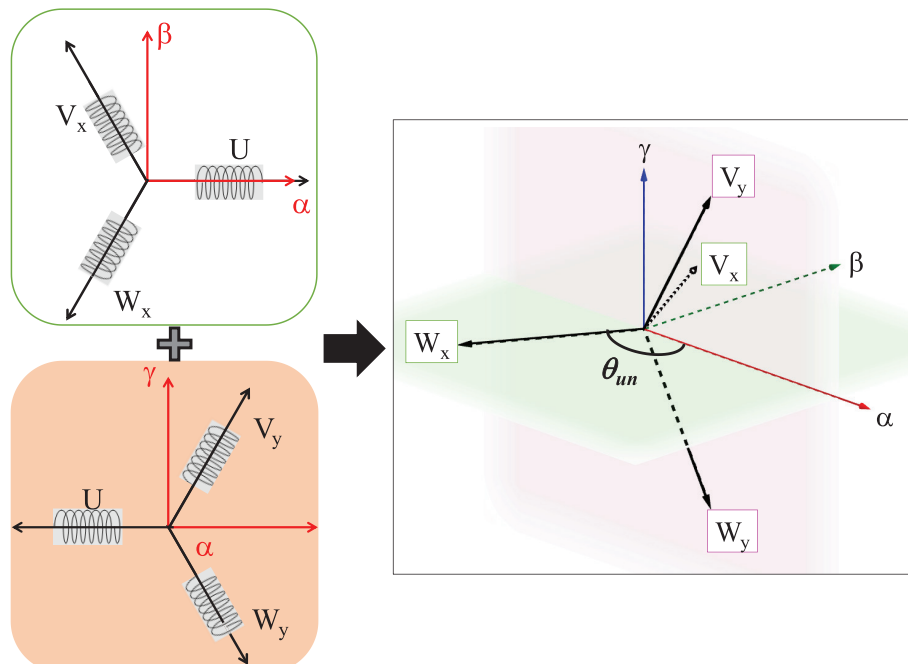


Fig. 8. Schematic diagram of novel vector control theory

This result suggests that the four-phase system has a slightly different angle (125 deg.) from that of the normal three-phase system (120 deg.). Next, dq transformation for three-DOF resonant actuator is introduced. The proposed vector control employs Euler angles representation in order to express the two electrical angles  $\theta_x$  and  $\theta_y$ . Fig. 9 shows the schematic diagram of dq transformation by Euler angles. The  $\alpha\beta\gamma$  reference frame is converted to  $\alpha'\beta'\gamma$  reference frame by rotating around  $\beta$ -axis by  $\theta_y$ , as shown in Fig. 9b. After that, The  $\alpha'\beta'\gamma$  reference frame is converted to d-q<sub>x</sub>-q<sub>y</sub> rotational reference frame by rotating around  $\gamma'$ -axis by  $\theta_x$ , as shown in Fig. 9c. The transformation matrix from a three-axis stationary reference frame to a three-axis rotational reference frame is expressed by the following equation.

$$\begin{bmatrix} I_d \\ I_{q_x} \\ I_{q_y} \\ I_0 \end{bmatrix} = \begin{bmatrix} \cos\theta_x \cos\theta_y & \sin\theta_x & \cos\theta_x \sin\theta_y & 0 \\ -\sin\theta_x \cos\theta_y & \cos\theta_x & -\sin\theta_x \sin\theta_y & 0 \\ -\sin\theta_y & 0 & \cos\theta_y & 0 \\ 0 & 0 & 0 & 1 \end{bmatrix} \begin{bmatrix} I_\alpha \\ I_\beta \\ I_\gamma \\ I_0 \end{bmatrix} = \begin{bmatrix} I_\alpha \\ I_\beta \\ I_\gamma \\ I_0 \end{bmatrix} \quad (6)$$

$$= \begin{bmatrix} \text{dq} \mathbf{C}_{\alpha\beta\gamma} \end{bmatrix} \begin{bmatrix} I_\alpha \\ I_\beta \\ I_\gamma \\ I_0 \end{bmatrix}$$

From equations (5) and (6), The dq transformation matrix is obtained:

$$\begin{bmatrix} I_d \\ I_{q_x} \\ I_{q_y} \end{bmatrix} = \frac{\sqrt{3}}{2} \times \begin{bmatrix} c\theta_x c\theta_y c\theta_{un} + s\theta_x s\theta_{un} & c\theta_x c\theta_y c\theta_{un} - s\theta_x s\theta_{un} & -c\theta_x c(\theta_y + \theta_{un}) & -c\theta_x c(\theta_y + \theta_{un}) \\ -s\theta_x c\theta_y c\theta_{un} + c\theta_x s\theta_{un} & -s\theta_x c\theta_y c\theta_{un} - c\theta_x s\theta_{un} & s\theta_x c(\theta_y + \theta_{un}) & s\theta_x c(\theta_y - \theta_{un}) \\ -s\theta_y s\theta_{un} & -s\theta_y s\theta_{un} & s(\theta_y + \theta_{un}) & s(\theta_y + \theta_{un}) \end{bmatrix} \times \begin{bmatrix} I_{V_x} \\ I_{W_x} \\ I_{V_y} \\ I_{W_y} \end{bmatrix} \quad (7)$$

where, s and c are the abbreviations for sine and cosine, respectively.

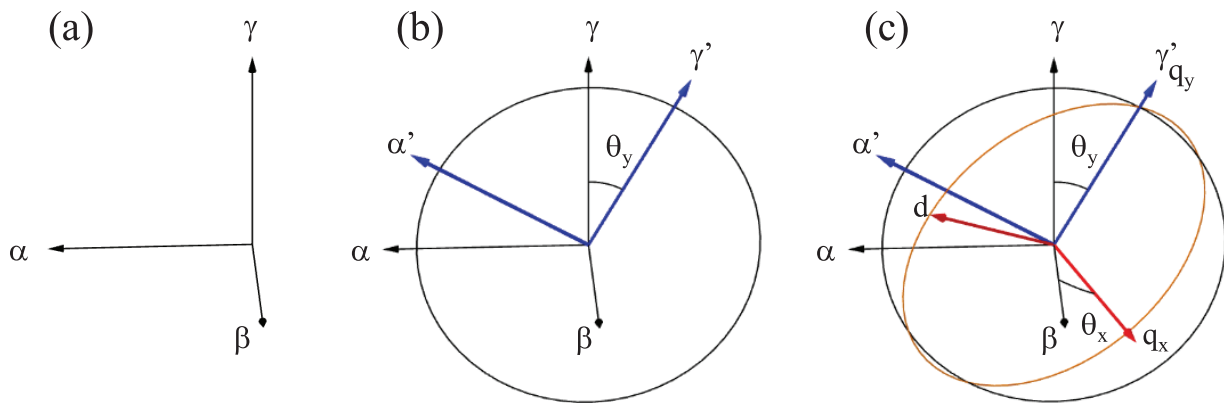
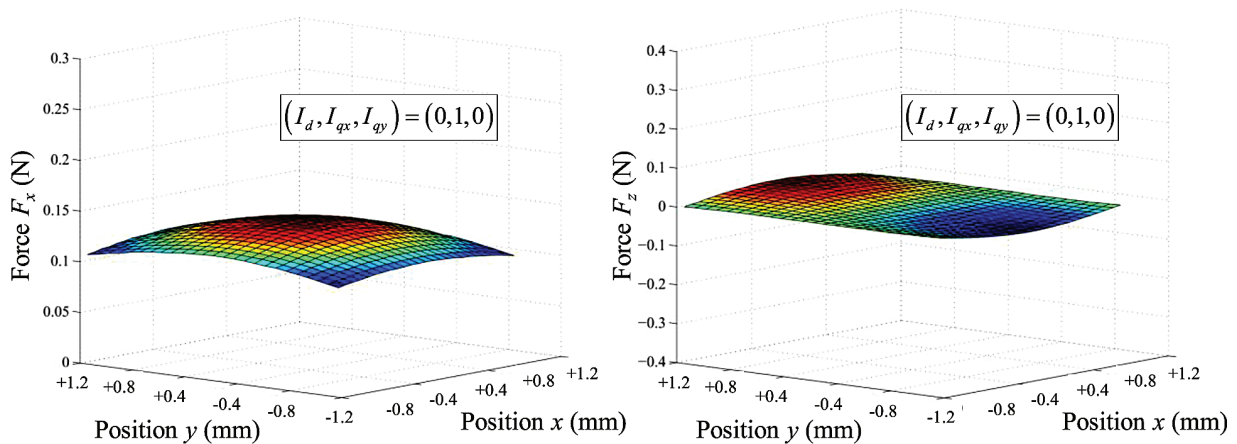


Fig. 9. 3-D dq transformation by Euler angles representation

## PERFORMANCE COMPARISON

The proposed vector control theory is applied to the three-DOF resonant actuator in order to confirm its effectiveness. Fig. 10 shows the static thrust characteristics when only one target current is set under the proposed control. In this case, the  $x$ -axis thrust is almost constant with respect to  $x$ - and  $y$ -axes displacements and this result is the same as that shown in Fig. 5. Similarly, the  $z$ -axis thrust is almost zero because the target current  $I_d$  equals zero. Fig. 11 shows the static thrust characteristics when two target currents are set simultaneously under the proposed control. It can be seen from the comparison between Fig. 11, 7 that the proposed vector control is able to decrease the thrust interferences from the other target current.

Fig. 10. Thrust characteristics under the proposed vector control ( $q_x = 1$ )

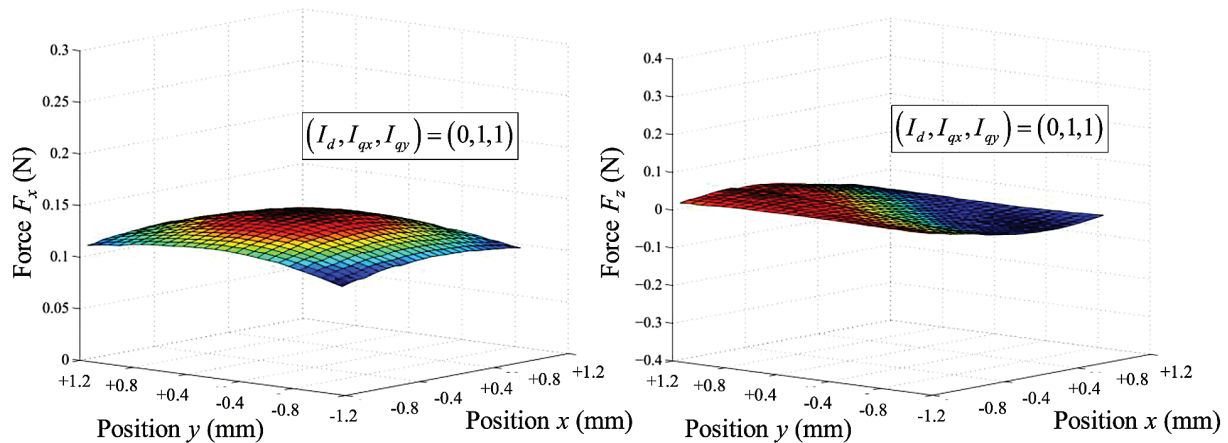


Fig. 11. Thrust characteristics under the proposed vector control ( $q_x=q_y=1$ )

## CONCLUSION

In this paper, we propose a novel vector control theory to improve a controllability of our three-DOF resonant actuator. The proposed control have an originality in that a four-phase system was used, not a combination of two sets of three-phase system. A dq transformation matrix for this actuator was successfully derived on the basis of a new phase angle (125 deg.) and 3-D rotation by Euler angles representation. As a result, the proposed control decreased the thrust interference from the other target current and its effectiveness was validated.

There are already several studies dealing with d-q transformation theory of multiphase induction motors [12, 13]. However, we were not able to confirm any studies for multi-DOF electromagnetic actuators. Moreover, the proposed method have a great potential to apply to a two-DOF spherical actuator [14] because its magnet arrangement is similar to that of the three-DOF resonant actuator.

## REFERENCES

1. Hirata K, Yamamoto T, Yamaguchi T, Kawase Y, Hasegawa Y. Dynamic analysis method of two-dimensional linear oscillatory actuator employing finite element method. *IEEE Trans. Magn.* 2007;43(4):1441-1444. doi: 10.1109/tmag.2007.891407
2. Jang SM, Choi JY, Jeong SS. Electromagnetic analysis and control parameter estimation of moving-coil linear oscillatory actuator. *Journal of Applied Physics.* 2006; 99, 08R307. doi: 10.1063/1.2165606
3. Lee H, Moon H, Wang S, Park K. Iron loss analysis of linear oscillating actuator for linear compressor. *International Journal for Computation and Mathematics in Electrical and Electronic Engineering.* 2006;25(2):487-495. doi: 10.1108/03321640610649140
4. Utsuno M, Takai M, Mizuno T, Yamada H. Comparison of the losses of a moving-magnet type linear oscillatory actuator under two driving methods. *IEEE Trans. Magn.* 2002;38(5):3300-3302. doi: 10.1109/tmag.2002.802291

5. Zhu ZQ, Chen X, Howe D, Iwasaki S. Electromagnetic modeling of a novel linear oscillating actuator. *IEEE Trans. Magn.* 2008;44(11):3855-3858. doi: 10.1109/tmag.2008.2001323
6. Yamaguchi T, Kawase Y, Sato K, Suzuki S, Hirata K, Ota T, Hasegawa Y. Trajectory analysis of 2-D magnetic resonant actuator. *IEEE Trans. Magn.* 2009;45(3):1732-1735. doi: 10.1109/tmag.2009.2012800
7. Suzuki S, Kawase Y, Yamaguchi T, Shibayama Y, Hirata K, Ota T. 3-D finite element analysis of dynamic characteristics of spherical resonant actuator. *Proc. of International Conference on Electrical Machines.* 2010; Roma, Italy. doi: 10.1109/icelmach.2010.5608213
8. Yoshimoto T, Asai Y, Hirata K, Ota T. Dynamic characteristics of novel two-DOF resonant actuator by vector control. *IEEE Trans. Magn.* 2012;48(11):2985-2988. doi: 10.1109/tmag.2012.2198203
9. Yoshimoto T, Asai Y, Hirata K, Ota, T. Simplified position estimation using back-EMF for two-DOF linear resonant actuator. *IEEE Trans. Magn.* 2014;50(2):7023804. doi: 10.1109/tmag.2013.2282496
10. Yoshimoto T, Asai Y, Hirata K, Ota T. Dynamic characteristic analysis and experimental verification of 2-DoF resonant actuator under feedback control. *Journal of the Japan Society of Applied Electromagnetics and Mechanics.* 2015;23(3):521-526. doi: 10.14243/jsaem.23.521
11. Kato M, Hirata K, Fujita K. Dynamic Characteristics of Three-Degree-of-Freedom Resonant Actuator. *International Journal for Computation and Mathematics in Electrical and Electronic Engineering.* 2018;37(6): to be published.
12. Leila P, Hamid T. Five-Phase Permanent-Magnet Motor Drives. *IEEE Trans. Ind. Appl.* 2005;41(1):30-37. doi: 10.1109/tia.2004.841021
13. Emil L. Multiphase Electric Machines for Variable-Speed Applications. *IEEE. Trans. Ind. Electron.* 2008;55(5):1893-1909. doi: 10.1109/tie.2008.918488
14. Tsukano M, Sakaidani Y, Hirata K, Niguchi N, Maeda S, Zaini A. Analysis of 2-Degree of Freedom Outer Rotor Spherical Actuator Employing 3-D Finite Element Method. *IEEE Trans. Magn.* 2013;49(5):2233-2236. doi: 10.1109/tmag.2012.2237390

#### Information about the authors:

**Kato Masayuki**, Master of Engineering, Doctor-course Student;  
Yamadaoka 2-1, Suita-shi, Osaka-fu, Japan, 5650871  
ORCID: 0000-0002-0856-1588;  
E-mail: masayuki.kato@ams.eng.osaka-u.ac.jp

**Hirata Katsuhiko**, Doctor of Engineering, Professor;  
ORCID: 0000-0002-5597-5265;  
E-mail: k-hirata@ams.eng.osaka-u.ac.jp

#### To cite this article:

Kato M, Hirata K. Control of Three-Degree-of-Freedom Resonant Actuator Driven by Novel Vector Control. *Transportation Systems and Technology.* 2018;4(3):90-101. doi: 10.17816/transsyst20184390-101

DOI 10.17816/transsyst201843102-116

© X. H. Wang, Y. Jin, Y. Lin, D. Q. Lu, F. Qin

National Maglev Engineering Technology Center, Tongji University  
(Shanghai, China)

## SPEED INCREASING SCHEME BY USING 3000V DC POWER SUPPLY FOR LOW-SPEED MAGLEV

**Background:** Low-speed maglev is usually designed to run at a maximum speed of about 100~110 km/h, the system does not have any advantage to the traditional urban railway transportation system at the aspect of running speed.

**Aim:** Increase the speed of low-speed Maglev is an urgent task for future promotion.

**Methods:** This paper presents a speed increasing scheme by using 3000 V DC power supply instead of original 1500 V DC.

**Results:** Under this condition, the max output voltage of propulsion inverter could be doubled. For reason that the insulation of linear induction motor has enough margin, only small adjustment of motor is needed to adapt the doubled voltage.

**Conclusion:** To calculate the performance of low-speed maglev while using 3000 V DC, a T-model circuit of single-sided linear induction motor is built, and the result shows that the maximum running speed could be increased to over 160 km/h. This scheme provides a promising way for speed increasing, and it's a simple and economical approach to enhance the competitiveness of low-speed maglev.

**Keywords:** Low-speed maglev, Speed increasing, Maximum speed, Over voltage, SLIM, T-model circuit, 160 km/h, End-effect

### INTRODUCTION

Low-speed maglev has made great progress in engineering application. Changsha maglev express, as the longest low-speed maglev line in the world, came into commercial operation in 2016 [1], and Beijing subway line S1 came into commercial operation at the end of 2017. These projects have verified that low-speed maglev has some merits when compared with the traditional urban railway, such as low noise, low vibration, excellent adaptability for smaller radius curves and larger slopes. As a result, several cities in China now plan to use low-speed maglev in urban transportation. But there still has a troublesome problem hard to overcome in the promotion of this technology. The suspending force of electromagnet has a limitation and couldn't be improved considerably, as a consequence, the passenger capacity of low-speed maglev is significantly lower than that of the metro and the light railway, which means this technology perhaps is more suitable for suburb transportation, which needs a higher running speed due to the longer distance

between stations. Therefore, if low-speed maglev couldn't significantly increase the running speed, its future would be pessimistic.

For decades, low-speed maglev in different countries is usually designed to run at a maximum speed of 100~110 km/h, which is similar to that of the metro. The Low-speed maglev line located at AICHI, Japan as the first commercial running maglev line in the world, based on the HSST 100L system has a maximum speed of 100 km/h [1]. The UTM-02 system of Korea put into service in 2016 at Incheon International Airport, has a maximum speed of 110 km/h [3]. Changsha maglev express's highest speed is 100 km/h [2]. However, there is still no proper rail transportation form to fill the blank of 140~200 km/h, neither do maglev, nor metro.

As mentioned above, to speed up the low-speed maglev to the so called 'medium-speed maglev', performance studies of single-sided linear induction motor (SLIM) of low-speed maglev is necessary. Reference [3] provided one useful function expression  $f(q)$  according to the SLIM secondary eddy current average value. This paper supposed that the air-gap flux linkage increased in the exponential function form from the entrance end to the exit end, it is affected by the SLIM running speed, secondary resistance and some other structure parameters. The per-phase simplified model can be used to calculate the output thrust force, efficiency conveniently. Reference [4] deduced a two-axis models to predict the SLIM dynamic performance, which can be applied in vector control of direct torque control. Reference [5] derived an equivalent circuit model from the pole-by-pole method, based on the winding functions of the SLIM primary winds. Reference [6] based on the results of reference [5], divided the SLIM air-gap flux density into three components. Then these three components were derived and get the inductance, secondary resistance and other parameters. A field theory analysis is performed to build a combined-parameter SLIM model in Reference [7]. The paper estimated the end-effect, the skin effect, and the back-iron saturation. Several different models were built from the electromagnetic relation in the air gap through a Fourier-series approach [8, 9, 10]. However, there are very few researches focused on speed increasing scheme for the SLIM of low-speed maglev. CRRC Zhuzhou Institute LTD. China is now developing on 'low-speed maglev 2.0' whose maximum speed is designed at 160 km/h. The primary approach used in the project is to redesign the linear induction motor by extending the length and width of iron cores so as to improve the thrust force [13]. Consequently, the motor is getting much heavier, and this kind of design challenges the electromagnetic suspending system, weakens the adaptability of line curve. Furthermore, the vehicle structure has to be redesigned totally. Obviously, there are tremendous works need to be done before finally achieving the goal speed.

This article presents a different way for speed increasing. As 3000 V DC is another electric tracking voltage in IEC standard, 3000 V DC power supply was



adopted instead of original 1500 V DC. Then the output voltage of the vehicular propulsion inverter was doubled. A preliminary analysis was performed to confirm the motor insulation has enough margin to endure the doubled voltage. Therefore, little modification is needed for the linear motor and vehicle structures. The key benefits of this approach is that motor voltage can keep rising with speed for longer time, and appearance of the constant power area is delayed. A mathematical model of SLIM based on T-model considering the end-effect was built to calculate the performance of the propulsion system, and the result showed that the maximum running speed exceeded 165 km/h when 3 sections formation adopted. The result can contribute to the exploration of a new feasible scheme for the application of ‘medium-speed maglev’.

### MODELING OF THE SLIM

The SLIM used in Low-speed maglev is shown in Fig. 1. The SLIM primary can be simply regarded as rotary cut-open stator and then rolled flat. The Secondary, similar with rotary induction motor (RIM) rotor, often consists of a sheet conductor, such as copper or aluminum, with a solid back iron acting as return path for the magnetic flux. The thrust force corresponding to the RIM torque can be produced by the reaction between the air-gap flux density and the eddy current in the secondary sheet [15].

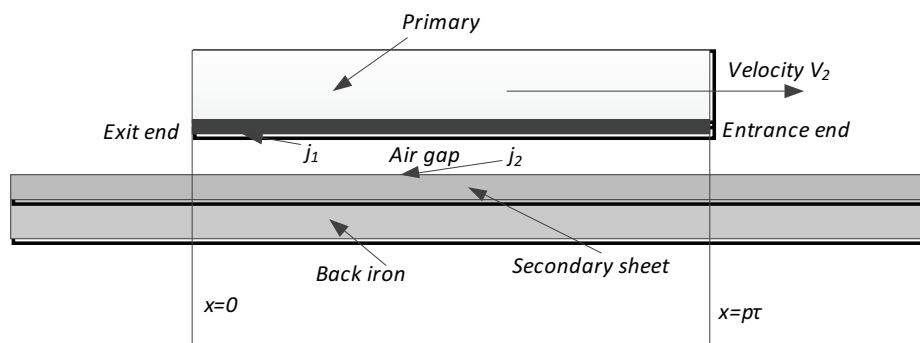


Fig. 1. Longitudinal structure view of SLIM

The SLIM special structure means that its performance is a little different from that of an RIM. As we know, in the RIM, an accurate equivalent circuit model can be derived easily by simplifying the geometry per pole. Unfortunately, it is not as straightforward as for RIM to gain the equivalent circuit for a SLIM.

In Fig. 1  $v_2$  is the primary moving speed,  $j_1$  is the primary equivalent current, and  $j_2$  is the secondary equivalent current. In terms of 1-D analysis, we can calculate the phase currents and excitation voltages. The air gap flux linkage can be obtained

using Maxwell's field equations and solved using the complex power method with a conformal transformation which considers the effects of the half-filled slots, magnetic saturation, and back-iron resistance. By using the equal complex power relationship between the magnetic field and the electrical circuit, we can obtain several circuit parameters, such as mutual inductance  $L_m$ , secondary resistance  $R_r$ , primary leakage inductance  $L_{1s}$ , secondary leakage inductance  $L_{1r}$ , longitudinal end effect coefficients  $C_r$  and  $C_x$ . The comprehensive derivations of the four coefficients can be referred to [15]. The T-model equivalent circuit is shown in Fig. 2, where the secondary equivalent resistance  $R_r$  consists of the secondary conducting sheet resistance  $R_{2sheet}$  and the secondary back iron  $R_{2back}$ . Some brief conclusions are summarized in the following paragraphs.

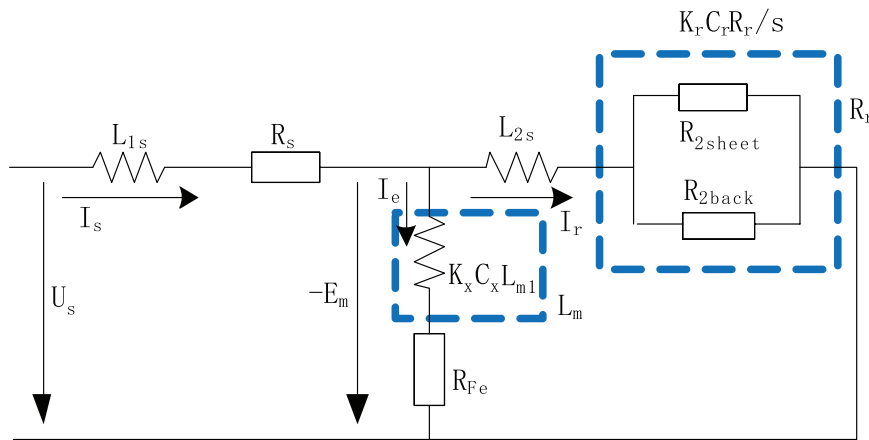


Fig. 2. The T-model circuit for SLIM

The longitudinal end effect coefficients  $K_r$  and  $K_x$  are denoted by

$$K_r = \frac{sG}{(2p_e \tau \sqrt{1 + (sG)^2})} \frac{C_1^2 + C_2^2}{C_1} \quad (1)$$

$$K_x = \frac{1}{(2p_e \tau \sqrt{1 + (sG)^2})} \frac{C_1^2 + C_2^2}{C_1} \quad (2)$$

where  $\tau$  is the primary pole pitch, and  $p_e$  is the number of pole pairs.  $C_1$  and  $C_2$  are functions of the slip and machine structure parameters, described as follows,

$$\begin{aligned} C_1 = & p\tau \cos \delta_s - N_L \times [\alpha_1^{-1} e^{-p\tau/\alpha_1} \sin(\delta_s - \beta + S_L p\tau) \\ & + S_L e^{-p\tau/\alpha_1} \cos(\delta_s - \beta + S_L p\tau) \\ & - \alpha_1^{-1} \sin(\delta_s - \beta) - S_L \cos(\delta_s - \beta)] \end{aligned} \quad (3)$$

$$\begin{aligned} C_2 = & p\tau \sin \delta_s - N_L \times [-\alpha_1^{-1} e^{-p\tau/\alpha_1} \cos(\delta_s - \beta + S_L p\tau) \\ & + S_L e^{-p\tau/\alpha_1} \sin(\delta_s - \beta + S_L p\tau) \\ & + \alpha_1^{-1} \cos(\delta_s - \beta) - S_L \sin(\delta_s - \beta)] \end{aligned} \quad (4)$$

Parameters in (1) and (2) are calculated as below,

$$\begin{aligned}\alpha_1 &= \frac{\tau g_e}{g_e X - \mu_0 \sigma_e v_2} \\ S_L &= k - \frac{\pi}{\tau_e}, \quad M_L = (\alpha_1^{-1})^2 + S_L^2 \\ N_L &= \frac{\alpha_1 \pi \tau_e}{M_L \tau \sqrt{\tau_e^2 + (\pi \alpha_1)^2}} \\ \delta_s &= \tan^{-1}\left(\frac{1}{S_L G}\right), \quad \beta = \tan^{-1}\left(\frac{\pi \alpha_1}{\tau_e}\right)\end{aligned}\quad (5)$$

For the existence of half-filled slots in the primary ends, the expression of the primary equivalent sheet current  $J_1$  can be divided into three regions, i.e., entrance half-filled, full-filled, and exit half-filled slots. Then, the expressions of the air-gap flux density can be gained. According to the electric machinery theory and complex power conversion algorithm, the air-gap effective electromotive force  $E_m$ , air-gap reactive power  $Q_3$ , secondary active power  $P_2$ , mutual inductance and secondary resistance can be deduced by taking the half-filled slots into consideration. By the comparison of these expressions without half-filled slots, the number of equivalent pole pairs  $p_e$  is expressed by

$$p_e = \frac{(2p - 1)^2}{4p - 3 + \varepsilon / (m_1 q)} \quad (6)$$

where  $p$  is the actual number of the pole pairs,  $m_1$  is the number of primary phases,  $q$  is the number of coil sides per phase per pole, and  $\varepsilon$  is the length of the short pitch.

The transversal-edge-effect coefficients are calculated by

$$C_r = \frac{sG[R_e^2[T] + I_m^2[T]]}{\text{Re}[T]} \quad (7)$$

$$C_x = \frac{[R_e^2[T] + I_m^2[T]]}{I_m[T]} \quad (8)$$

where  $T$  is the function of the slip, goodness factor, and motor structure parameters,  $Re$  and  $I_m$  are the real and imaginary parts of complex  $T$  respectively. Here,  $T$  is expressed by

$$T = j \left[ \gamma^2 + (1 - \gamma^2) \frac{\lambda}{0.5 l_\delta \alpha} \text{th}(0.5 l_\delta \alpha) \right] \quad (9)$$

where  $\alpha$  is the ratio of  $c$  to  $\tau$ ,  $\gamma$  and  $\lambda$  can be obtained by

$$\lambda = \frac{1}{1 + \frac{1}{\gamma} \text{th}(0.5 l_\delta \alpha) \text{th}[0.5 K(c_2 - l_\delta)]} \quad (10)$$

$$R^2 = \frac{1}{1 + jsG} \quad (11)$$

where  $K$  is the function of the slip and motor structure parameters and  $c_2$  is the width of the secondary sheet.

The five parameters in T-model circuit, respectively named as the primary resistance  $R_s$ , primary leakage inductance  $L_{1s}$ , secondary resistance  $R_r$ , secondary leakage inductance  $L_{1r}$ , and exciting inductance  $L_m$ , can be calculated as follows.

The primary resistance  $R_s$  is

$$R_s = \rho_{Cu} \times 2l_{av} W_1 / S_{Cu} \quad (12)$$

where  $\rho$  is the resistivity of copper,  $l_{av}$  is half the average length of the primary winding coil,  $W_1$  is the number of turns in series of the primary per phase, and  $S_{Cu}$  is the effective cross-sectional area of the primary winding conductor.

The primary leakage inductance  $L_{1s}$  is

$$L_{1s} = 0.025 W_1^2 \frac{l_\delta}{q} \left( \frac{\lambda}{p} + \frac{\lambda_t + \lambda_e + \lambda_d}{p_e} \right) \quad (13)$$

where  $\lambda_s$  is the primary slot leakage magnetic conductance,  $\lambda_e$  is the primary winding end leakage magnetic conductance, and  $\lambda_d$  is the primary harmonic leakage magnetic conductance.

The secondary resistance is composed of two parts, which is sheet and back resistance, because the flux can penetrate through the aluminum or copper sheet and enter the back iron. The depth of the flux density into the back iron  $d_{Fe}$  is

$$d_{Fe} = \sqrt{\frac{2\rho_{Fe}}{s\omega_e \mu_{Fe}}} \quad (14)$$

where  $\rho_e$  is the back iron resistivity,  $\mu_{Fe}$  is the permeability of the back iron, and  $\omega_e$  is the primary synchronous angular frequency. The resistance of the secondary conducting sheet  $R_{2sheet}$  is

$$R_{2sheet} = 4m_1 \rho_{sheet} \frac{(W_1 K_{W1})^2}{2p_e} \frac{l_\delta}{d\tau} \quad (15)$$

where  $\rho_{sheet}$  is the resistivity of the secondary conductance sheet and  $K_{W1}$  is the primary winding coefficient.

The resistance of the secondary back iron  $R_{2back}$  is

$$R_{2back} = 4m_1 \rho_{Fe} \frac{(W_1 K_{W1})^2}{2p_e} \frac{l_\delta}{d_{Fe} \tau} \quad (16)$$

Therefore, the secondary equivalent resistance  $R_r$  is

$$R_r = \frac{R_{2sheet} R_{2back}}{R_{2sheet} + R_{2back}} \quad (17)$$

The secondary leakage reactance is

$$L_{1r} = \frac{R_r}{2\pi f_s s} B_1 sh(2Kd) \quad (18)$$

where  $f_s$  is the primary frequency and  $B_1$  is the function of the slip, primary frequency, and machine structure parameters.

The exciting inductance is

$$L_{m1} = 4m_1\mu_0(W_1K_{W1})^2 \frac{l_\delta V_s}{4\pi^2 f_s g_e p_e} \quad (19)$$

where  $V_s$  is the synchronous velocity of the primary side and  $g_e$  is the equivalent air-gap width.

The iron loss in the SLIM is composed of the primary yoke, primary tooth, and secondary back iron losses. These three parts can be calculated as follows.

The primary yoke iron loss  $P_{Fe}$  is

$$P_{Fe} = P_{10/50} B_y^2 \left(\frac{f_s}{50}\right)^{1.3} W_y \quad (20)$$

The primary tooth iron loss  $P_{Fe}$  is

$$P_{Feb} = P_{10/50} B_b^2 \left(\frac{sf}{50}\right)^{1.3} W_b \quad (21)$$

Hence, the total iron loss  $P_{Fe}$  is

$$P_{Fe} = P_{Fet} + P_{Fey} + P_{Feb} \quad (22)$$

In (20)–(21),  $P_{10/50}$  is the iron loss value under 1.0 T and 50 Hz;  $B_y$ ,  $B_t$  and  $B_b$  are the primary yoke, primary tooth and secondary back iron flux densities respectively;  $W_y$ ,  $W_t$  and  $W_b$  are the primary yoke, primary tooth and secondary back iron weights respectively; and  $sf$  is the slip frequency in the secondary. According to the electromagnetic design methods in [11],  $B_y$ ,  $B_t$  and  $B_b$  can be calculated as follows,

$$B_y = \sqrt{2} \phi_g / (2l\delta K_{lam} h_y) \quad (23)$$

$$B_t = B_g t_1 / (K_{lam} t_2) \quad (24)$$

$$B_b = \phi_g / (c_2 K_{lam} h_b) \quad (25)$$

where  $\phi_g$  is the flux root-mean-square value per pole pair,  $K_{lam}$  is the silicon steel stacking factor,  $h_y$  is the primary height,  $B_g$  is the leakage air-gap flux density,  $t_1$  is the pitch of the primary teeth,  $t_2$  is the width of the primary teeth, and  $h_b$  is the height of the secondary back iron.

The iron loss resistance  $R_{Fe}$  in series with the excitation branch can be calculated by

$$R_{Fe} = P_{Fe} / I_e^2 \quad (26)$$

where  $I_e$  is the field current.

Besides the edge-effect, the skin-effect, big air-gap and thick secondary conductor are also very influential to SLIM's performance when running at a relative high speed. In order to get more accurate circuits, a skin-effect coefficient is calculated to adjust the secondary leakage inductance by using 2-D electromagnetic field theory in [15]. The skin-effect coefficient is

$$k_f = \frac{1 + (B \sinh 2k\delta)^2}{A[1 + (B \sinh 2kd)^2]} \quad (27)$$

where  $d$  is the thickness of secondary conductor sheet. Coefficients  $A$  and  $B$  are calculated as follows

$$A = \cosh^2 k\delta' + \left( \frac{k\rho_{sheet} \operatorname{sh}nhk\delta'}{s\omega_e \mu_0 d} \right)^2 \quad (28)$$

$$B = \frac{s\omega_e \mu_0 d}{2k\rho_{sheet}} \left[ 1 + \left( \frac{k\rho_{sheet}}{s\omega_e \mu_0 d} \right)^2 \right] \quad (29)$$

where  $s$  is the slip of SLIM,  $\mu_0$  is the air relative permeability,  $\delta'$  is the equivalent air-gap.

## PERFORMANCE CALCULATION

After approximate analysis of the four coefficients and parameter calculations, the SLIM T-model equivalent circuit indicated in Fig. 2 is got. The model is similar to that of RIM. The influence of longitudinal and transversal end-effect and half-filled slots can be estimated by corresponding coefficients. Therefore, it is very convenient to analyze the performance of the SLIM in a similar way to RIM. Main performance index calculation is showed as follows.

The secondary current is

$$I_r = I_s \times \frac{R_{Fe} + j\omega_e L_m}{R_{Fe} + j\omega_e L_m + R_r + j\omega_e L_{2r}} \quad (30)$$

The output mechanical power is

$$P_m = I_r^2 \left( \frac{1-s}{s} K_r C_r R_r \right) \quad (31)$$

The power factor is

$$\cos \varphi = \cos \left( \operatorname{atan} \left( \frac{\operatorname{Im} \left( R_s + j\omega_e L_{1s} + \frac{(R_{Fe} + j\omega_e L_m)(R_r + j\omega_e L_{2r})}{R_{Fe} + j\omega_e L_m + R_r + j\omega_e L_{2r}} \right)}{\operatorname{Re} \left( R_s + j\omega_e L_{1s} + \frac{(R_{Fe} + j\omega_e L_m)(R_r + j\omega_e L_{2r})}{R_{Fe} + j\omega_e L_m + R_r + j\omega_e L_{2r}} \right)} \right) \right) \quad (32)$$

The input voltage of the SLIM is

$$U_s = I_s \times \left( R_s + j\omega_e L_{1s} + \frac{(R_{Fe} + j\omega_e L_m)(R_r + j\omega_e L_{2r})}{R_{Fe} + j\omega_e L_m + R_r + j\omega_e L_{2r}} \right) \quad (33)$$

The efficiency of the SLIM is

$$\eta = P / (U I \cos \varphi) \quad (34)$$

The output thrust force of single SLIM is

$$F_x = P_m / v_2 \quad (35)$$

## INSULATION ANALYSIS

When 3000 V DC is adopted as input voltage from the power rail, the maximum output voltage of the vehicular propulsion inverter doubles to 2200 V AC, each SLIM's maximum input voltage rises to 440 V AC, and the maximum phase voltage is 254 V. Through the control of the inverter, the maximum input current is still limited to 300 A, therefore main size of SLIM wouldn't change a lot, the mechanical interface could keep unchanged.

From the design experience, we know that usually the weakest part of machine insulation system is the turn-to-turn insulation. At this point, the test line in Shanghai and the commercial line in Changsha all use polyimide film (PI) as the main turn-to-turn insulation. 2 layers of PI using 1/2 lapping method wrapped up around the primary aluminum winding coil, each layer's thickness is 0.06mm and the total turn-to-turn insulation thickness is 0.12 mm. The insulation strength of the common industrial PI reaches 200 kV/mm [16], the corona-resistance reaches about 2 kV/mm. On condition of using PI thickness of 0.12 mm, the insulation strength of the primary coil is no less than 20 kV and corona-resistance is no less than 2 kV. The insulation capability is significantly higher than the doubled input voltage of SLIM. Even when the voltage of the first turn of motor could reach nearly 80 % of terminal voltage in a PWM control system [17], there is still enough voltage margin to the insulation limitation.

## SLIP FREQUENCY AND MOTOR PARAMETERS

Because the SLIM of low-speed maglev has quite different structure with that of RIM [12], the control strategy is also quite different. Considering the unique phenomenon of normal force, constant slip frequency control strategy is chosen to minimize the influence on suspending control [17]. But the reference slip frequency must be confirmed before using constant slip frequency control.

Set slip frequency as the independent variable and normal force as the dependent variable, the relation curve is show in Fig. 3. The figure shows that the normal force is very close to zero when slip frequency equals to 12 Hz. Hence, 12 Hz is selected as the reference slip frequency in performance calculation.

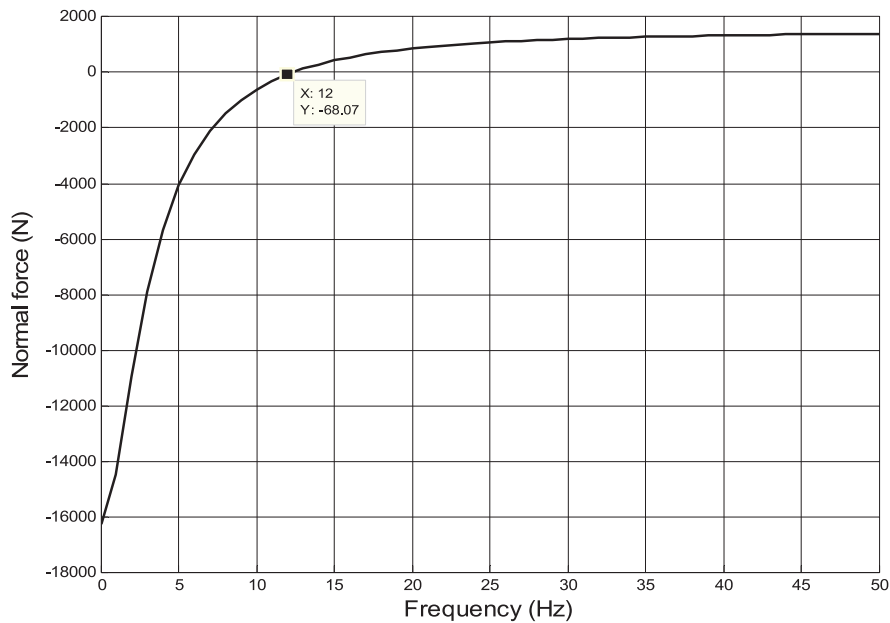


Fig. 3. Normal force curve at different slip frequency

After confirming the slip frequency, all parameter could finally be substituted into T-model equations. The main parameters of the SLIM in this paper are listed in Table 1, and the vehicle configurations are listed in Table 2.

Table 1. Main parameter of the SLIM

Items	Unit	Value
Width of primary iron core	mm	190
Pole pairs		9/2
Silicon steel sheet length	mm	1783
Gap flux	T	0.1467
Rated frequency	Hz	42.5
Pole pitch	mm	202.5
Secondary sheet thickness	mm	4
Width of secondary sheet	mm	200
Mechanical air gap	mm	10
Primary slots number		79
Slot width	mm	16.1
Tooth width	mm	6.4
Series turns per phase		96

Table 2. Vehicle configuration

Motor number per section	10
Section number	3
Full loaded mass per section (kg)	30 000
Motors in series	5
Paralleling motor branches	2
Maximum inverter current(A)	300



## RESULTS AND DISCUSSION

This paper focus on speed increasing of low-speed maglev, so the most important performance index is maximum running speed. T-model circuit is used to calculate the propulsion thrust force at each  $v_2$  of primary side, which is the running speed of maglev vehicle too. It's easy to find that the cross point of thrust force curve and resistance force curve is the ultimate running speed.

In order to indicate the variation trend of running performance when adopting different over voltage mode, we set the highest voltage 2 times to the current rated voltage, that's 2.0 pu. Then set another 5 uniform distributed voltage grades with 0.2 pu step, from 1.0 to 2.0 pu. Calculation results are illustrated in Fig. 4.

From the results we can draw some preliminary findings,

- Maximum running speed at 1.0 pu condition is about 108 km/h, the turning point of thrust force curve is around 40 km/h and the start acceleration is about  $1.15 \text{ m/s}^2$ , all these results accord with the design index and the actual testing results. The fact proved that the calculation model built in this article is accuracy and could be used to verify the over voltage performance.
- Voltage has great influence on the maximum speed, when the highest input voltage of the SLIM doubled, maximum speed increased over 50 %. Taken 3 sections formation as example, the maximum speed increased from 108 km/h to 166 km/h.

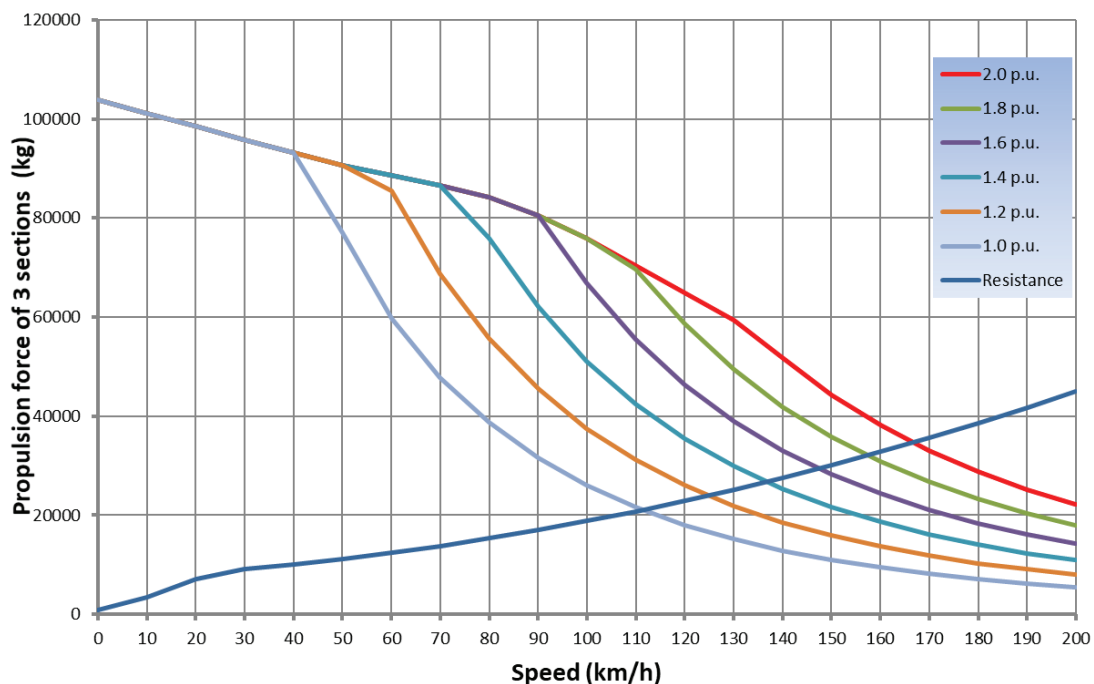


Fig. 4. Thrust force versus resistance force

- The appearance of constant power area of the SLIM is significantly delayed with voltage increased, the higher voltage increased, the later SLIM comes into constant power area;
- With voltage doubled, the curve of propulsion force drops slightly, and there is almost no turning point on the curve. From this we can see that the end-effect, especially longitudinal end-effect significantly affects the performance of the SLIM when high speed running.

Acceleration ability is also an important performance index. To indicate the acceleration ability, we assumed that vehicle running at a straight line without any turning curves and slopes, then record the distances and times when vehicle get the maximum speed, the results are listed in Table 3. When taking the look at 2.0 pu condition column, although the goal speed of 160 km/h is achieved, the acceleration distance is about 2.5 km, it's too long if the station spacing is less than 5 km. Furthermore, there must be some speed limitations when applied to actual running line with smaller radius curves and slopes, the acceleration distance would surely be much longer than figures in Table 3.

Table 3. Performance of the 3 sections formation vehicle

Index	2.0/pu	1.8/pu	1.6/pu	1.4/pu	1.2/pu	1.0/pu
Maximum speed (km/h)	166	157	146	135	122	108
Acceleration time (s)	298	288	272	265	252	245
Acceleration distance (m)	2520	2337	2058	1879	1623	1404
Average acceleration (m/s <sup>2</sup> )	0.56	0.54	0.54	0.51	0.48	0.44

In Fig. 5, the power factor and motor efficiency curve on condition of 2.0 pu are drew. Efficiency rises from 0.4 to near 0.8 with speed increasing, and power

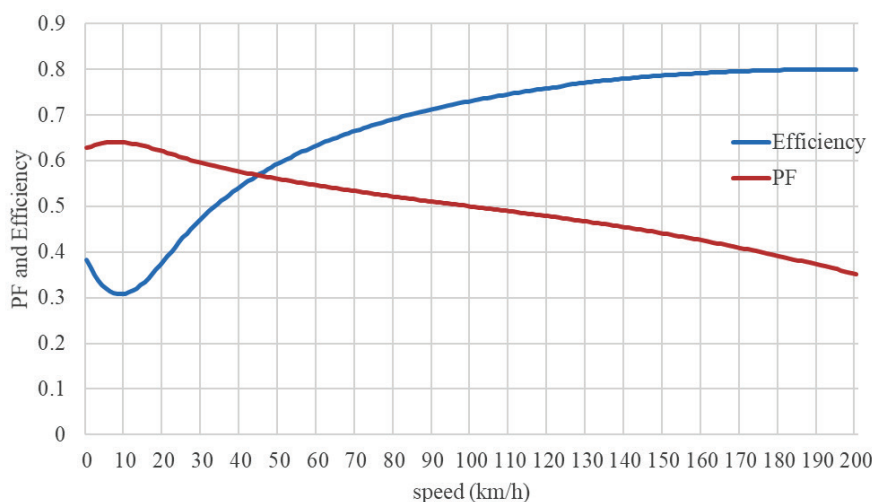


Fig. 5. Efficiency and PF of the SLIM at 2.0 pu

factor drops slightly from about 0.6 to under 0.4. Both index is relatively a bit lower than that of RIM, mainly because of characteristic of induction motor. Besides, big air-gap and more field excitation loss at over voltage mode deteriorate the power factor.

## CONCLUSION

This paper presented a speed increasing scheme for low-speed maglev by adopting 3000 V DC power supply. After building a T-model circuit in consideration of end-effect, analysis of the SLIM performance is made. Results show that increasing the input voltage of the SLIM is an efficient way to increase the maximum speed of low-speed maglev. Calculation of thrust force curve indicates a 3 sections formation vehicle can get the highest speed over 165 km/h on condition of 2.0 pu voltage.

This voltage increasing way rarely needs adjustment or redesign to the SLIM, the mechanical interface of the SLIM could remain unchanged, so do the structure of vehicle. It's an economical way to increase running speed largely. However, the SLIM of low-speed maglev is originally designed to run at the maximum speed of 100~110 km/h, the performance is far from perfect when running at over voltage mode, for example, the acceleration ability is fairly weak when speed exceeds 100 km/h, and acceleration distance is too long to meet the demands of actual line. Therefore, further research is necessary to optimize the performance of the SLIM and take full advantage of the potentiality of increased terminal voltage.

## References

1. Yasuda Y, Fujino M, Tanaka M, et al. The first HSST Maglev Commercial Train in Japan. Proceedings of the 18th international conference on magnetically levitated systems and linear drives; 2004 Oct. 26–28, Shanghai, China.
2. Shin BC, Park DY, Han HS. Korea's First Urban Maglev System. Proceedings of the 22<sup>th</sup> International conference on magnetically levitated systems and linear drives; 2014 Sep.28–Oct.2, Rio de Janeiro, Brazil.
3. Duncan J. Linear Induction Motor-equivalent-circuit Model, IEE Proceedings B (Electric Power Applications). 1983;130(1):51-57. doi: 10.1049/ip-b.1983.0008
4. Kang G, Nam K. Field-oriented Control Scheme for Linear Induction Motor with the End Effect. IEE Proceedings-Electric Power Applications. 2005;152(6):1565-1572. doi: 10.1049/ip-epa:20045185
5. Lipa TA, Nondahl TA. Pole by Pole d-q Model of a Linear Induction Machine. IEEE Transactions on Power doi: <https://doi.org/10.1109/tpas.1979.319448>
6. Apparatus and Systems. 1979;PAS-98(2):629-642. doi: 10.1109/tpas.1979.319448

7. Lu CA. A New Coupled-circuit Model of a Linear Induction Motor and Its Application to Steady-state Transient Dynamic and Control Studies [dissertation]. Kingston, Ontario: Queen's University; 1993.
8. Idir K, Dawson GE, Eastham AR. Modeling and Performance of Linear Induction Motor With Saturable Primary. Conference Record of the 1991 IEEE Industry Applications Society Annual Meeting; 1991 28 Sept. 4 Oct., Dearborn, MI, USA. New York: IEEE, New York, 1993. doi: 10.1109/ias.1991.178147
9. Higuchi T, Nonaka S, Ando M. On the Design of High Efficiency Linear Induction Motors for Linear Metro. *Electrical Engineering in Japan*. 2001;137(2):36-43. doi: 10.1002/ej.1086
10. Xu W. Research On the Performance of Single-sided Linear Induction Motor. IEEE International Electric Machines and Drives Conference; 2007 3–5 May; Antalya, Turkey. Piscataway: IEEE, 2007.
11. Nonaka S. Investigation of equations for calculation of secondary resistance and secondary leakage reactance of single sided linear induction motors. *Electrical Engineering in Japan*. 1997;117(5):616-621.
12. Poloujadoff M. The Theory of Linear Induction Machinery. 1st ed. Clarendon: Oxford University Press; 1980, 273 p.
13. Wang K, Shi LM, He JW, Li YH. A Decoupling Control of Normal-and-thrust Forces in Single-sided Linear Induction Motor. *Proceedings of the CSEE*. 2009;29(06):100-104.
14. Yan JP, Wang DW. Prospect Analysis of Application the Low-speed Maglev System in Changsha. *Underground Engineering and Tunnels*. 2016;4:29-31.
15. Deng JM, Liu YM, Chen TF. Discussion on Facing Higher Speed Engineering Applications of Short-primary Linear Induction Motor. *Electric Locomotives & Mass Transit Vehicles*. 2017;40(4):1-5.
16. Long XL. *Theory and Electromagnetic Design Method of Linear Induction Motor*. 1<sup>st</sup> ed. Beijing: Science Press; 2006.
17. Rotating electrical machines-Part 18-1: Functional evaluation of insulation systems – General guidelines. IEC 60034-18-1. Edition 2.0 2010-03.
18. Zhang LL. Study on Premature Failure Mechanism of PWM Inverter-Fed Traction Motor [dissertation]. Chengdu (Sichuan): Southwest Transportation University; 2004.
19. Deng JM, Chen TF, Tang JX, Tong LS. Optimum Slip Frequency Control of Maglev Single-sided Linear Induction Motors to Maximum Dynamic Thrust. *Proceedings of the CSEE*. 2013;12:123-130.

**Information about the authors:**

**Wang Xiaohua**, Master degree, assistant researcher; Tongji university, Caoan Road, Jiading district, Shanghai, China.

ORCID: 0000-0003-1061-6370;

E-mail: wangxiaohua@tongji.edu.cn

**Jin Yu**, Master degree, assistant researcher;

E-mail: jinyu@tongji.edu.cn

**Lin Ying**, Master degree, assistant researcher;  
ORCID: 0000-0002-2270-272X  
E-mail: carfieldlin@tongji.edu.cn

**Lu Diqiang**, Doctor degree, assistant researcher;  
E-mail: ludiqiang@tongji.edu.cn

**Qin Feng**, Doctor degree, assistant researcher;  
E-mail: qinfeng@tongji.edu.cn

**To cite this article:**

Wang XH, Yu J, Lin Y, et al. Speed Increasing Scheme by Using 3000 V DC Power Supply for Low-Speed Maglev. *Transportation Systems and Technology*. 2018;4(3):102-116. doi: 10.17816/transsyst201843102-116

DOI 10.17816/transsyst201843117-133

© A. L. Wolek

Senior Engineer, ATKINS – SNC Lavalin Group  
(Orlando, Florida, USA)

## MAGLEV FREIGHT – ONE POSSIBLE PATH FORWARD IN THE U.S.A.

**Background:** As high-speed rail and other transportation technologies are moving forward and gaining funding in the United States, the push for MagLev is not receiving the necessary support that would make it a viable alternative in the near future. Major changes in the approach to implementing MagLev could make a better case for it, specifically for carrying freight. One alternative that has been considered in the past is the modification of existing freight railways to support MagLev. For this to be economically feasible and practical, such a solution has to be able to support both conventional freight trains and MagLev freight.

**Aim:** The successful application of Partially Magnetically-Levitated Freight (PMLF) technology achieved by integrating superconducting MagLev technology with current railroad design and operations.

**Methods:** A MagLev freight system that is envisioned to use existing rail routes must be designed to be compatible with the existing railway infrastructure. To accomplish this, every component utilized by the railroads must be examined in detail to determine if and how it could be affected by the proposed PMLF. In addition, components that will need to be modified for PMLF operation must undergo a retrofit design and testing process. The design scope must also include an examination of all existing tasks and activities that are being performed by the railroads such as track maintenance and repair. Any procedures that affect or are affected by the addition of PMLF will need to be modified. Finally, superconducting MagLev technology must be optimized and advanced for application to PMLF.

**Opinions and Discussions:** The dual use of railway lines has substantial cost advantages when compared to building new dedicated MagLev freight corridors. In fact it could make the entire proposition very appealing if proven to be technically feasible. However, there are certain limitations and concerns that would cause policy makers to reject such a proposal unless such obstacles can be shown to be temporary and non-critical. Essential rail installations such as switches are presently difficult to modify in a way that would ensure reliable functionality for both MagLev and conventional freight trains, and grade crossings pose safety risks. It is difficult to envision the tremendous leap forward of merging MagLev with existing freight rail lines when much more basic technologies such as positive train control are not even fully implemented. Consequently, it is a challenge to advance MagLev in the United States where new dedicated freight corridors are considered to be cost-prohibitive and dual use railway lines pose uncertainties that railroad companies simply do not want to solve. However, there is one more solution has not been considered that would allow a MagLev freight train to navigate on existing railway infrastructure without disrupting traditional rail utilization. This solution is a partially magnetically-levitated freight train.

**Results:** After reviewing the fundamental components, systems and operations of the railways in the United States, it will be feasible and practical to introduce magnetic levitation

technology to assist in moving freight on existing rail routes. PMLF trains will be able to take advantage of magnetic levitation on sections where the track has been upgraded to allow its use and much higher speed while still being able to travel on unmodified sections with the same speed as traditional trains.

**Conclusion:** Modifying existing freight rail with magnetic “quasi-lift” technology is a much lower cost alternative to building an entirely new MagLev infrastructure. This alternative will provide very important benefits including enhancing safety in the rail industry. In its first phase of implementation, the proposed PMLF system will levitate a significant portion of the weight of the train but still utilize the existing steel rails for traction and guidance. The most evident advantages of this approach include reduced wear on rail and other supporting elements, and a significant reduction in friction and energy use. Locomotives, freight cars and all other components could be made lighter and travel speeds will increase dramatically due to less impact and other effects. Later phases of implementation will focus on magnetic traction and guidance. The acceptance and success of this partially levitated system will eventually lead to fully levitated freight transport technology. Sometimes it is necessary to take smaller steps to achieve the desired future.

**Keywords:** MagLev Freight, MagLev Cargo, Partially Magnetically-Levitated Freight, Positive Train Control

## INTRODUCTION

This is the first of what is hoped will be a series of papers that focuses on partial magnetic levitation as the most viable way forward to the transport of goods using MagLev freight in the United States. The basic concept of the system is presented in this paper. The key design parameter that will be maintained throughout the development of this system is compatibility with existing track infrastructure. This is a crucial aspect that this introductory paper focuses on. Using existing rail lines will allow the advancement of MagLev technology for the purpose of carrying cargo more efficiently and in greater quantities than would be possible with the current generation of freight trains. This advancement will also have a relatively low cost. Furthermore, partial magnetic levitation will help to optimize and to maximize the system safety components. Safety features already in place for existing rail infrastructure will be utilized and married to additional safety mechanisms that magnetic levitation can provide, enhancing the overall redundancy in safety. This is critical since freight trains using partial magnetic levitation will need to eventually travel many times faster than their traditional steel-on-steel counterparts in order to justify the investment. Accidents in emerging technologies are scrutinized to a greater extent than in established technologies which will ultimately affect funding and progress.

This is not the first attempt at proposing to modify existing rail lines for the purpose of MagLev freight but it may be the first that bases this approach on partial

magnetic levitation. In fact there have been several different proposed solutions presented by various research organizations and private institutions in numerous countries that sought to utilize existing rail lines for MagLev. In the United States, the proposed MAGLEV 2000 system was based on superconducting magnetic quadrupoles that would allow the MagLev vehicle to travel on a planar surface such as existing railroad tracks with added aluminum loop panels. This solution and others represented almost a quantum leap from existing railway technology. A quantum leap can be very expensive and also easy to derail if problems abound during development and implementation.

Partial magnetic levitation provides a more gradual and practical approach rather than a revolutionary paradigm shift. Positive aspects of partial magnetic levitation in freight transport such as lower track maintenance and repair costs will help reduce the overall operating cost of freight trains assisted with magnetic levitation. Energy costs will be much lower as well. The major negative aspect of this gradual approach is that the greatest advantages of using MagLev such as high speeds will take longer to realize. A very important positive aspect of this gradual approach is that the three main components of MagLev technology – levitation, guidance, and propulsion – can be safely tested independently of each other and without the need for any expensive test tracks. Everything can be evaluated using existing railroad tracks with small and inexpensive modifications. Although the initial phase of the research and testing will focus on magnetic levitation, later phases will integrate magnetic guidance and magnetic propulsion into this proposed system and all three components will be continuously tested and improved until one day the technology will demonstrate that it can safely and effectively be used in full MagLev mode to transport cargo on existing rail corridors at tremendous speeds and efficiencies.

### **PARTIALLY MAGNETICALLY-LEVITATED FREIGHT TRAIN CONCEPT**

The success of using a partially magnetically-levitated freight (PMLF) system on existing rail corridors in the United States will depend on the ability of this system to be integrated into the existing rail infrastructure without impeding on the operation of this infrastructure.

In determining the most effective and practical adaptation of magnetic levitation technologies for implementation of PLMF on existing rail corridors, it is important to consider not only the components of the existing rail infrastructure but also the operational maintenance and repair activities that are constantly being performed on this infrastructure. Geometric constraints also need to be



considered. A brief synopsis of componentry and activities that are essential to the existing rail infrastructure is presented in below in the EXISTING RAILWAY INFRASTRUCTURE section of this paper. Major North American freight railroads are shown in Fig. 1.

The first question that must be considered is which MagLev technology is the most capable of fulfilling its function in the PLMF system while satisfying the constraints established by the existing railway infrastructure or if this is even reasonably possible.

The “parts bin” for MagLev currently includes four different systems [2]. The first system uses electromagnets on the MagLev vehicle that are attracted to metal rails on the guideway. The second system consists of permanent magnets on the MagLev vehicle and on the guideway and uses repelling forces between these permanent magnets for levitation. The third system uses permanent magnets on the MagLev vehicle and aluminum loops on the guideway and generates repelling forces by inducing currents in the aluminum loops. The fourth system

#### Ownership of Major North American Rail Lines, 2017



Source: Bureau of Transportation Statistics

Dr. Jean-Paul Rodrigue, Dept. of Global Studies & Geography, Hofstra University

Fig. 1. Ownership of Major North American Rail Lines, 2017 [1]

uses superconducting magnets on the MagLev vehicle that induce currents in the aluminum loops that are embedded in the guideway to generate repelling forces.

Clearly PMLF must utilize repelling magnetic forces for partial levitation since the rail track is a horizontal surface. The first system uses attractive magnetism and is not applicable. The second system that places magnets on the track is not very promising because it would be prohibitively expensive to implement. The intent is to have many thousands of miles of rail corridors available for PMLF so that placing metal loops on the track will be orders of magnitude less expensive than placing magnets on the track if such a quantity of permanent magnets can be even produced. In addition, track maintenance and repair operations will be much more complex if the magnets will have to be removed and replaced before and after such operations. The third system will not be practical because the gap between the permanent magnets on PMLF vehicles and the metal loops installed on the track will need to be on the order of about 0.13 m (½ inch.) The same limitation applies to the first and second system. In addition, the lifting power of permanent magnets is limited and could not generate the 80 % to 99 % levitation that is required to make PMLF advantageous. Superconducting magnets have this capability of lifting very heavy loads and with larger separation distances between magnets and coils. Thus, the fourth system is the only existing MagLev technology that is suitable for this application.

In addition to being very powerful with low energy requirements, superconducting magnets will allow system operation with gaps between magnets and coils as large as 0.1 m (4 inches) or more. Bare aluminum coils or coils with thin protective cover would not last very long after being attached to the railroad tracks and will likely be stolen due to the cost of aluminum. Aluminum coils that will have currents induced by superconducting magnets may be embedded in concrete panels with an inch or more of protective cover, leaving 0.76 m (3 inches) for the gap between the superconducting magnets under the PMLF vehicles and the concrete panels that are attached to the track ties. This should provide sufficient tolerance for the variability in the track's vertical alignment. It is also important to note that the track ties are not rigidly supported and could deflect 0.03 m (1/8 inch) or more vertically due to actions of concentrated wheel loads from traditional freight trains. The concrete panels must be able to accommodate differential motion and settlement between adjacent ties. The concrete panels with embedded aluminum coils must also be durable and capable of withstanding various track maintenance activities such as rail grinding. It is recommended that the concrete panels use steel pre-stressing strands in both horizontal directions to enhance durability and flexibility. Certain maintenance activities such as ballast tamping may require the panels to be temporarily removed. The ample construction tolerance due to the

large 0.1 m (4 inch) gap that is allowed means that track maintenance and repair crews can remove and re-attach the concrete panels containing the coils without the need for expensive surveys and vertical adjustments. The next question becomes where should the panels with aluminum loops be positioned on the track – inside the rails or outside the rails or both?

The least expensive solution for positioning concrete panels with aluminum loops would be to place a single strip of panels between the rails. However, this configuration will not be as stable as placing the panels on the outside of the rails when the PMLF train is in a state of nearly full levitation. The most effective and robust solution would be to position the panels both on the inside and outside of the rails but this would be a very expensive solution. It seems that the optimal solution in terms of cost and function is to place the concrete panels with aluminum coils on the outside of the rails. Placing the coil panels used for magnetic levitation on the outside of the rails will also allow plenty of space between the rails for testing future equipment such as traction and guidance panels if it is determined that the coil panels outside the rails will not be adequate for fulfilling these functions. It is also important to note that failure of the coil panels on the track or failure of the superconducting magnets on the PMLF train will not result in damage to the PMLF train or track since the PLMF train will be able to carry its weight on wheels.

This fact that the PMLF system uses flanged wheels in addition to magnetic levitation is a tremendous advantage in terms of adapting the PMLF system to the various railway track devices and components such as turnouts, crossovers and crossings. Guidance of the PMLF train at these locations will be identical to the mechanical guidance used by traditional freight trains. It may also be very difficult to install loop panels at these locations, making mechanical guidance essential. As a result, the PMLF train will need to rely on its wheels to carry its full load at these locations. Rather than trying to solve the problem of installing loop panels at these challenging and discrete locations, relying on flanged wheels will allow the focus of PMLF development to be placed on preparing the remaining 99 % of the rail route for effective PMLF operation.

Eliminating 90 % or more of the normal contact force between the PMLF trains wheels and the supporting steel track will result in a very significant drop in friction. Moreover, PMLF cars will be significantly lighter than traditional freight rolling stock because magnetic levitation will support over 90 % of the PMLF cars' weight during 99 % of the travel time, allowing the various mechanical and structural components to be designed and manufactured to a much lighter duty service than traditional freight rolling stock, including wheels and bearings. In addition, PMLF trains are intended to transport cargo at high speeds so it is unlikely that PMLF will be initially used for transporting heavy bulk items such as

coal, stone, cement, wood and other materials that do not require rapid transport. Energy efficiency for transporting items that require refrigeration and insulation will benefit significantly from PMLF, especially cryogenic liquids and liquefied natural gas (LNG).

The PMLF project will implement partial magnetic levitation first before integrating magnetic guidance and magnetic propulsion into the system. As a result, the first phase of the PMLF project will require locomotives that can generate considerable traction forces. These locomotives may also take advantage of partial magnetic levitation on tangents and on descending grades. Reducing concentrated contact forces between the steel wheels and rails means that there will be less impact and wear on the tracks, allowing longer maintenance intervals which will result in less disruption of rail routes and much lower maintenance costs. Electricity for the superconducting magnets mounted to PMLF cars will be supplied by fuel cells and from any excess electricity generated by the locomotives. Solar panels on top of PMLF rail cars may also be used to supplement the electricity supplied by the fuel cells. LNG has a greater energy density than rocket fuels such as kerosene and may be used to power both the fuel cells and the internal combustion engines (ICEs) on the locomotives if ICEs continue to be used on locomotives. Later phases of the project will transition completely to fuel cells (80 % + efficiency) and other energy sources. Emergency braking will be facilitated by diminishing the magnetic repulsive forces in order to increase friction between the wheels and rail. It may also be possible to have some magnets generate attractive forces to increase wheel to rail contact forces and enhance braking. Stopping distances will be much shorter than for traditional freight trains once magnetic propulsion is introduced into the system and wheel contact with rail will no longer be required for stopping. Finally, PMLF can transition to being fully magnetically levitated once both magnetic propulsion and magnetic guidance are fully implemented in later phases of this project, greatly increasing the maximum speed that the train can travel at in rural and unpopulated areas. As noted before, wheels will continue to be required unless the mechanisms for rail crossings, turnouts and crossovers are completely redesigned to include MagLev hardware to run continuously through these locations.

## SAFETY SYSTEMS

**Positive Train Control** – Railroad safety has improved dramatically over the past few decades thanks to enforcement and development of safety regulations as well as due to the implementation of advanced safety technologies. In the United States, railway accident rates have reduced by over 80 percent within the last

four decades. Many of the more recent accidents have been caused by human error. Positive Train Control is designed to prevent train accidents attributable to human error and to improve the operational safety of both freight and passenger railroads. PTC has the ability to slow or stop the train automatically and to safeguard against train-to-train collisions, derailments, unauthorized travel in work zones and movements of trains through faulty railroad switches [3]. The complete implementation of PTC in the United States would include about 113,000 route km (70 000 route miles) of the nearly 234,000 route km (145,000 route miles) that exist in the country. It is important to note that the United States has about 25 % of the world's rail routes which is the main reason why implementation of PTC has been slow and expensive in the United States. The original implementation deadline was December 31, 2015. The revised deadline is December 31, 2018 but the Federal Railroad Administration may approve an individual railroad's extension to an alternative deadline of December 31, 2020. What this means is that any proposed MagLev freight trains designed to share railways with other trains must be fully integrated within the PTC systems and networks if MagLev freight is not to have any restrictions on the type of cargo it carries or if it wants to use the primary rail routes. The basic system architecture for PTC is shown in Fig. 2.

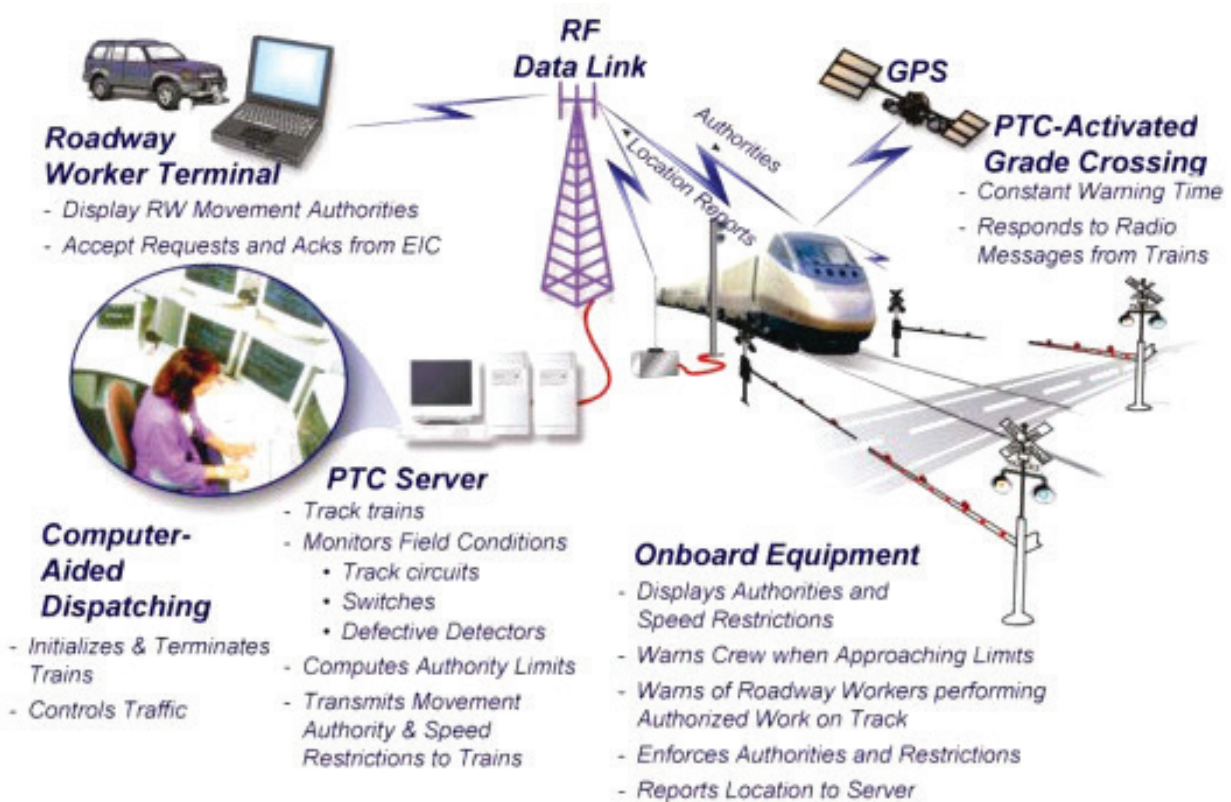


Fig. 2. Positive Train Control System Architecture [4]

Partially levitated MagLev freight is readily adaptable to the various types of PTC that have been developed for traditional trains. Although magnetically assisted freight trains are envisioned to operate at much higher speeds than other freight trains, the PTC system is already set up for high-speed operations including high-speed rail. Operating speeds for PMLF will not exceed maximum HSR speeds. The fact that PMLF physically uses the steel tracks, switches and signals means that it will be able to take full advantage of the safety mechanisms provided by PTC. Thus, from the onset, PMLF will be able to achieve at a minimum the level of safety offered by traditional train operations. It must be emphasized that because PMLF also uses magnetic systems in addition to existing rail hardware, its safety capabilities will exceed those of its conventional counterparts. A simple example of this is a misaligned or broken rail that could be catastrophic for a traditional train but not so for PMLF that relies to a great extent on repelling magnetic for stability.

**Scout Rail Vehicle** – As reliable as PTC may become, there will always be some risk of error or malfunction. One of the greatest safety concerns for railroads in the United States are railroad grade crossings. This is especially true for higher speed operations. PTC is intended to eliminate human error in controlling the movement of trains but PTC has little control over human error when it comes to cars, trucks and other roadway vehicles that use railroad grade crossings. Although PTC does interface with signals and gates that are used to control vehicle entry at railroad crossings, these measures may not always prevent roadway vehicles from attempting to cross or being stopped directly over a crossing when a train is approaching. There are over 200,000 railroad grade crossings in the United States.

Suppose a small un-manned rail vehicle travels a short distance ahead of the PMLF train to scout the tracks ahead and forewarn the train of any approaching hazards. Not only could it detect damage or obstacles on the tracks and signal this information to the PTC system (this could be very useful for traditional trains in seismic zones such as California) but it could also be used as an additional safety measure at railroad grade crossings. This scout rail vehicle could physically stop at a rail crossing as the PMLF train approaches, assuring that nothing else gets on the tracks. Its light weight and small size will allow it to accelerate rapidly ahead of the PMLF train once the train is nearly at the grade crossing. Its performance could also be enhanced through partial magnetic levitation, magnetic guidance and magnetic propulsion.

**Magnetic Forces** – Magnetic technology can be used to enhance traction, reduce stopping distance and to supplement guidance. As a result, PMLF has the inherent safety attributes of a freight train guided by steel rails complemented by

the additional performance benefits that can be obtained using magnetic fields. In addition, PMLF will exert much smaller concentrated forces on the tracks and other supporting elements, reducing fatigue and prolonging the service life of rail infrastructure.

## EXISTING RAILWAY INFRASTRUCTURE

Unlike previously proposed MagLev concepts that were intended to partially share railway routes with traditional trains, the PMLF train concept is envisioned to be completely compatible with existing railway infrastructure and requires no additional routes or track. Furthermore, changes to the existing track components necessary to accommodate the PLMF will be initially limited to modifications or additions and will not require complete replacement. Any such alterations or additions will not affect the operation of traditional trains that PLMF trains will share the rail routes with. It is important to identify and consider the function of each prime component used in a railway track in order to determine how it will affect or be affected by the addition of PMLF.

### **Track Components [5].**

The majority of railway infrastructure consists of track. PMLF can become a reality because the track itself is relatively simple to modify for use by PMLF trains. There is ample space to the outside of the rails to install panels housing metal loops and the loads from PMLF trains will be lighter and more evenly distributed to the ties, ballast and underlying layers.

*Rail:* The most expensive material in the track is the steel rail. The rail's primary function is to transfer the train's weight to the cross ties and to guide the train's wheel flanges. It also provides a smooth riding surface. Rail may vary in shape and weight. Heavy rail uses a 0.1525 m (6 inch) wide base and the preferred section weighs 70 kg/m (141 pounds per yard) of length. Light rail uses a 0.14 m (5 ½ inch) wide base and typically weighs 50 kg/m (100 pounds per yard).

*Ties:* Ties are typically made of timber, concrete, steel or alternative materials. Ties cushion the load of the train and distribute it from the steel rail to the ballast. Ties also maintain the gage (spacing) of the rail. Ties made from concrete require impact absorbing pads between the rail and the tie in order to achieve the desired level of cushioning. Wood ties provide impact absorption through the depth of the tie itself. Steel ties are very expensive and are used in areas not favorable to the use of timber or concrete ties including track sections with extreme curvature where the gage is prone to widening. Alternative material ties are typically made from recycled materials and are currently being tested for light rail applications. The two main types of ties are Track Ties and Switch Ties. Track Ties are typically

2.6 m (8 feet 6 inches) long but may be 2.75 m (9 feet) long on curved sections. Switch Ties vary in length from 2.75 m to 7 m (9 feet to 23 feet.) Heavy rail timber ties are 0.178 m by 0.229 m (7 inches by 9 inches) nominal in section. Typical tie spacing is 0.495 m (19 ½ inches) for heavy rail and 0.54 m (21 ¼ inches) for medium tonnage.

*Ballast Section:* The ballast section anchors the ties and stabilizes the track in lateral, longitudinal and vertical directions. It also serves to rapidly and properly drain any water from the track, to facilitate track maintenance and to distribute the load from the ties to the underlying subgrade. The preferred materials used for ballast are granite, hard limestone, open hearth and blast furnace slags. Important characteristics of the ballast particles include size and shape, degree of sharpness, angularity and roughness. Typical depth of the ballast section is 0.46 m to 0.61 m (18 to 24 inches) and extends 0.254 m to 0.305 m (10 to 12 inches) past tie ends.

*Rail Joints:* Rail joints are used at rail discontinuity points to hold in place and align two ends of rail. They consist of two joint bars that prevent lateral and vertical movement of the rail ends while allowing longitudinal movement of the rails due to thermal expansion or contraction. Standard rail joint bars connect two identical sections of rail. Compromise rail joint bars connect two rails that have different sections (weights). Insulated rail joints are used when track circuits are present in order to prevent the track circuit's electrical current from flowing between the ends of the joined rail.

*Tie Plates:* Tie plates provide a uniform bearing surface between the rail and the tie so that the rail does not damage the tie.

*Rail Anchors:* Rail anchors attach to the base of the rail and control longitudinal and transverse movement of the rail due to thermal effects, braking, grades and train traffic patterns.

*Fasteners:* Fasteners can be spikes, bolts and screws that are used to connect rail or track components together including fastening rails to ties.

*Derails:* Derails prevent unauthorized or unsecured rolling stock from entering specific tracks by guiding its wheels off the track.

*Wheel Stops and Bumping Posts:* Wheel stops prevent rail cars from rolling off the ends of tracks or into structures. Bumping posts are rail car stops that consist of braced blocks that are at the elevation of rail car couplers. These are heavy duty stops that are placed on track to prevent rail cars and other equipment from running off the track.

*Gage Rods:* Gage rods supplement ties in maintaining the gage of the track. They are also used to temporarily retrofit a defective tie until it can be replaced. Gage rods are either insulated where track circuits are used or non-insulated.

*Sliding Joints:* Also called Conley joints, these are used instead of rail anchors to allow longitudinal expansion and contraction of the rail on open decked



bridges. Sliding joints have beveled rail ends that move but still provide continuity and support.

*Mitre Rail:* Mitre rails allow track to be opened and closed at frequent intervals. These are most often used on draw bridges and swing span bridges.

*Guard Rails:* These are derailment rails typically used on bridges, in tunnels and for overpasses. These prevent derailed equipment from falling off a bridge or an overpass or from impacting the sides of a tunnel or structure. Inner guard rails are placed between the running rails and typically use a T-rail section. Outside guard rails may use timber members.

### **Turnouts.**

Turnouts allow trains to pass from one track to another track. They consist of a switch, a frog, rails connecting the switch and the frog, guard rails, and a switch stand for operating the switch. The three basic types of turnouts are Lateral, Equilateral and Lap. Lateral right hand turnouts have the diverging track running to the right. Lateral left hand turnouts have the diverging track running to the left. Equilateral turnouts have both tracks diverging and are often used in regions of higher operating speeds since the curvatures of the Equilateral turnouts are half of those required for Lateral turnouts. Lap turnouts are typically used in rail yards where maximum track lengths are required and contain two sets of switch points and three different frogs.

Designing turnouts to accommodate metal loops used by PMLF will require significant research and testing due to all the existing components that are present at these locations. Again, PMLF trains will initially cross these locations without relying on magnetic forces. Turnouts have a limited service life and a good opportunity to upgrade these to provide full PMLF functionality is during replacement.

*Switch:* A switch deflects the wheels of a train from the track upon which the train is running. The most common switch is the split switch in which two point rails are connected by switch rods and are supported on metal plates fastened to ties. The switch (point) rails taper to 64 mm (1/4 inch) or 32 mm (1/8 inch) point at the end which is appropriately called the point of the switch. The other ends of the switch rails are called the heel where the switch rails connect to the lead rails using joint bars about which the switch pivots. The switch stand controls the movement of the switch rails which is about 0.127 m (5 inches.) Switch rails are typically from 3.4 m to 11.9 m (11 feet to 39 feet) in length, but can be longer for high turnout numbers. Switches may be hand operated, power operated or both.

*Turnout Rails:* Turnouts are made from several special rails. Stock rails are the outside rails in a switch that the point rails bear against. Closure rails connect

the heel of the switch points and the toe of the frog. Knuckle rails are the rails that the movable point in a frog bears against.

*Frog:* A frog is used at an intersection of two running rails and it allows the flange of a wheel moving on one rail to cross onto the other rail. Frogs are classified as either rigid, spring rail or movable point frogs. Spring frogs provide continuous support for the wheel as it rolls over the frog flangeway. These frogs have a movable wing rail that is held closed by springs and a guardrail that pulls the wheel over, forcing the wing rail to open on the diverging side. Rigid frogs may use one piece castings as inserts or may be bolted together using machined rails. Movable point frogs are used where the angle between the two sets of crossing tracks is very acute and would result in an excessively long throat if conventional crossing diamond frogs were used. Movable point frogs use two movable center point rails to maintain the flangeway.

*Switch Ties:* Special standardized switch tie layouts are used for turnouts. Two head block ties are used under the switch mechanism. Heel block ties are used under the heel block assembly. Frog ties are used to support the frog.

*Stock Rails:* Stock rails have the same section shape as the switch point rails. The stock rail on the diverging side of the switch point is bent to assure a proper fit so that there is no wheel impact on the point.

*Switch Points:* Switch points are moveable rails that allow a change of route direction to occur within the turnout. Switch points typically consist of a tip, heel, planed (machined) portion, reinforcing bar, switch clips and stop blocks. Switch points are comprised of machined rails that are snug fit against the stock rail. The change of direction is achieved when the point is moved away from the stock rail. Stop blocks are used for lateral support due to the wheel pushing outward on the planed rail.

*Turnout Plates:* Different types of turnouts use a specific set of supporting and bracing plates, including gage, switch, heel, hook and frog turnout plates.

*Guard Rails:* Turnout guard rails are used to prevent misrouting or derailling at the frog. They also prevent the wheels from striking the frog point.

*Switch Stands:* Switch stands are used for operating the switch. High stand switch stands are used on main line applications and ground throw stands are used in yards or at industrial locations. Main line switch stands have a target that is colored green when the switch line is set for the normal route and red if the switches are reversed. A power switch is operated by an electric machine that lines the switch and can be operated remotely or manually. A spring switch is a hand thrown switch that uses a spring mechanism instead of a rigid connecting rod.

### **Railway Crossings and Crossovers.**

A railway crossing is used at an intersection of two tracks. A crossing requires four frogs and connecting rails. Crossings may be straight, single curve or double

curve. When crossing angles are greater than 25 degrees, rails and manganese castings are cut to fit against each other and are secured using filling blocks and well-bolted straps. For crossing angles smaller than 25 degrees, regular frog point devices are used and these crossings are designated as frog crossings. The end frogs of a frog crossing are similar to a rigid frog. The middle frogs have two running points and are often described as double pointed frogs. Crossovers are simply two turnouts except that the track between the frogs follows the frog angle. Crossovers pose the same challenges as turnouts in terms of installing PMLF components.

### **Road Crossings.**

Road crossings occur where roads, streets or highways intersect the track at grade and are thus often called grade crossings. These locations have increased maintenance requirements and present a very important safety concern. Different types of materials are used for road crossings including timber, asphalt, concrete and pre-manufactured rubber. Some crossings may be unsurfaced. The type of material used at a crossing is dependent on the amount of vehicular traffic that uses the crossing. Road crossings will be easy to modify to include embedded metal loop panels for PMLF use.

*Crossing Warning Devices:* Warning signs, signals and pavement markings are important means of warning motor vehicles approaching the crossing. Automatic warning flashers and gates are used at road crossings with higher vehicular volume or where higher speed trains use the track. It is important to note that a large number of road crossings in the United States do not use gates.

### **Utility Crossings.**

Various utilities such as pipes, cables, conduits and wires cross the railways at many locations. Utilities often also run along the track right of way. Utilities may be overhead or underground. There are numerous general and safety standards for utility crossings. These are not expected to be impacted by converting the track to PMLF use.

### **Maintenance and Restoration Activities.**

Railways must be maintained and rehabilitated at regular cycles with minimal disturbance to the track. Maintenance and rehabilitation programs include spot replacement of ties, correction of gage deficiencies, smoothing, elimination of joints, adjustment of continuous welded rail (CWR), turnout maintenance, repair of battered rail ends, and grinding of rail.

Major restoration and track renewal activities are performed using specialized production gangs. These activities include rail replacement, tie replacement, undercutting/ballast replacement, surfacing, road crossing renewal and turnout renewal.

Each activity will need to be evaluated in terms of how it affects the addition of PMLF service and how it needs to be modified in the future to better optimize PMLF utilization. A good example is tamping which is an activity that vibrates the ballast surrounding the ties. Initially, the concrete panels with embedded metal loops used by PMLF to generate repelling forces will need to be removed from the rail ties so that the ballast tamper can perform its function. However, it will not be difficult to modify the tamping machine to tamp the ballast without having to remove these panels.

### **Affects on Passenger and Commuter Trains.**

It should be noted that one specific area of concern regarding MagLev vehicles is the stray magnetic fields produced by the magnets and electrical components and how these could affect passengers [6]. This will not need to be considered for PMLF since all the superconducting magnets will be mounted to a freight train that will not carry passengers. The metal loops embedded in the concrete panels that will be attached to the track will not have any magnetic effects on passengers in trains that will pass over these regardless if the track is electrified either by overhead catenary or third rail systems.

## **FUTURE RESEARCH DEVELOPMENT**

There are three principal areas of research and development that are critical to the effective future implementation of PMLF on existing rail corridors:

- Superconducting MagLev Technology;
- PMLF Impacts on Railway Operations;
- Integration with Communication and Safety Systems.

First, superconducting magnetic levitation technology utilizing dipole and quadrupole magnets must be evaluated in detail and adapted to the design of a new fleet of freight rail cars and locomotives. This also includes research on the modification of existing rail infrastructure to accommodate PMLF, such as the installation of inductive loops and other components. Later phases of the project will require comprehensive R&D of magnetic propulsion and guidance.

Second, the effects of PMLF on all existing railroad activities must be considered in detail to assure that there is no disruption of service, maintenance, repair and other operations. This research will also allow future improvements and modifications to be made to the railroad infrastructure and to the equipment used. This will benefit both traditional freight and PMLF operation. The successful development of high speed PMLF will also provide more funding to maintain the rail infrastructure due to additional revenue from cargo shipments that require rapid transport.

Third, PMLF must be fully integrated with all railway communication, signaling and safety systems. This complete integration must be in place when PMLF trains are first entered into service. Much research, development and testing needs to be performed to meet this requirement, including incorporation of PMLF into the Positive Train Control network. However, the general approach for integrating PMLF with these systems will be based on the approach that is being used for traditional trains, making the process more efficient.

Finally, many MagLev researchers and contributors do not feel that it is feasible for any form of MagLev to share existing railway infrastructure and that MagLev systems must be designed as completely independent transportation systems [7]. However, the United States has such an extensive rail network that the possibility of sharing it with MagLev should be considered. In fact, other researchers have already considered this as being feasible but with a different approach than PMLF. The MAGLEV 2000 system proposed vehicles that could function on planar surfaces and modified railroad tracks by using quadrupole superconducting magnets.

## CONCLUSION

The United States has the largest rail network in the world. The successful application of Partially Magnetically-Levitated Freight (PMLF) technology in the United States would allow MagLev technology to be tested and used on nearly a quarter of the world's rail routes that exist in the United States without having to build a single kilometer of a test track. It is essential that any MagLev freight system that is designed to utilize existing rail routes be fully compatible with the existing railway infrastructure. PMLF makes this possible by combining superconducting MagLev technology with traditional wheels-on-steel-rail locomotion. PMLF will be able to take advantage of near full magnetic levitation and high speed on long stretches of rail routes while being able to rely on mechanical means used by traditional trains to navigate congested urban and industrialized areas with numerous turnouts and rail crossings. This backward-compatibility will assure that PMLF can be integrated into the Positive Train Control network and other safety systems used and required by railroads.

PMLF will allow goods to be transported by rail more efficiently than ever before and it will also allow freight operation on rail routes to achieve speeds many times higher than were ever achieved before in the USA. Similar systems could be adopted in other countries. Continued research and development of PMLF, including magnetic propulsion and guidance, will eventually allow fully magnetic operation of freight trains on rail routes that have been updated with MagLev equipment.

## References

1. Rodrigue J-P. The Geography of Transport Systems, Available at: [https://transportgeography.org/?page\\_id=1999](https://transportgeography.org/?page_id=1999).
2. Dona S, Singh A. *The Workings of Maglev: a New Way to Travel*, 2017. Research Report UHM/CE/2017-01.
3. Zhang Z, Liu X, Holt K. Positive Train Control (PTC) for railway safety in the United States: Policy developments and critical issues. *Journal of Utilities Policy, Elsevier*. 2018;51:33-40. doi: 10.1016/j.jup.2018.03.002
4. Federal Railroad Administration, *North American Joint Positive Train Control Project*, Washington, D.C., April 2009.
5. American Railway Engineering & Maintenance of Way Association. *Practical Guide to Railway Engineering* 2<sup>nd</sup> Ed. Lanham, Maryland: AREMA. 2013.
6. Han H-S, Kim D-S. *Magnetic Levitation – Maglev Technology and Applications*. Dordrecht: Springer, 2016.
7. Liu Z, Long Z, Li X. *Maglev Trains – Key Underlying Technologies*. Heidelberg: Springer, 2015.

### Information about the author:

**Arthur Lester Wolek**, MS Engineering; ATKINS – SNC Lavalin Group, 482 South Keller Road, Orlando, Florida 32810-6101 USA  
ORCID: 0000-0002-5211-3491;  
E-mail: [arthur.wolek@atkinsglobal.com](mailto:arthur.wolek@atkinsglobal.com)

### To cite this article:

Wolek AL. MagLev Freight – One Possible Path Forward in the USA. *Transportation Systems and Technology*. 2018;4(3):117-133. doi: 10.17816/transsyst201843117-133

DOI 10.17816/transsyst201843134-142

© **M. Kirchner**  
University of Applied Sciences  
(Deggendorf, Germany)

## EMPIRICAL INVESTIGATION OF POSSIBLE CONCERNS REGARDING THE USE OF MAGNETIC LEVITATION ELEVATORS

**Aim:** This study focused on an issue regarding an innovation of magnetic levitation elevators which was by different media coverage indicated as being unresolved: Are potential users of magnetic levitation elevators concerned about the safe use of these elevators and, if so, what kind of concerns exist?

**Methods:** To contribute a first scientifically sound assessment to this, a three-day face-to-face survey at the elevator test tower in Rottweil (Baden-Wuerttemberg), where aforesaid elevator technology is tested, has been conducted. (Touristic) visitors of the tower and the observation platform on it have been surveyed a standardized questionnaire.

**Results:** The results have shown that the average tendency of prospective conceivable users tends to be free of concerns. In addition, a share of about one-sixth has both expressed and concretized concerns. Those relate mainly to new characteristics of this elevator technology – absence of ropes, magnetic levitation, magnetic field presence – partially associated with known aspects such as power loss.

**Conclusion:** The study provides an explorative contribution to the topic described. Thusly it seems to be particularly interesting for both researchers willing to look further at this or similar areas and manufacturers or future clients of the technology in the context of, for instance, communicating its prospective implementations.

**Keywords:** Maglev Elevators, Concerns of Use, Multi, Prospective Use, Safety

## INTRODUCTION

A levitation system based on magnetic levitation technology, which is intended to enable vertical as well as horizontal movement of cable-free elevator cars, has lately been attracting attention in industry, mobility sector and public. Based on the principle of the paternoster, the elevator system should allow several cabins to circulate independently of each other in a shaft circuit. According to its German developer the innovation can be an important factor influencing future mobility in cities in the context of advancing urbanization and rising skyscraper construction [1].

At the time of this study (November/December 2017) tests were carried out in a company-owned elevator test tower in Rottweil (Baden-Wuerttemberg) [2]. Yet,

no persons were allowed to ride in tested prototypes, since qualifying certifications were still outstanding [3, 4].

Safety aspects are generally considered to be one of the main challenges in the realization of the technology as new systems and interaction “beyond known concepts [5]” are necessary. Accordingly, when promoting the magnetic levitation elevator phrases like „Fokus auf Sicherheit“ [6] („focus on safety”) or safety as „Schlüsselbegriff [7]“ („key term”) are used.

While the general public was dominated by enthusiasm for the progress made possible through this elevator innovation, aspects of safety regarding the potential use occasionally sparked concerns in editorial reports. Accordingly, the following question appeared to be in need of an answer:

**Are potential users of magnetic levitation elevators concerned about the safe use of these elevators and, if so, what kind of concerns exist?**

In a scarcely considered scientific field this work – hereafter presented in highly compressed shape – should enable to formulate a first objective assessment regarding the existence of concerns and their possible manifestations.

## METHODOLOGY & THEORETICAL APPROACH

In order to handle the topic adequately, the survey was chosen as the central methodology. More specifically, a three-day quantitative empirical investigation – realized by a standardized face-to-face questionnaire – was carried out to visitors of above-mentioned elevator tower in Rottweil.

Basically – not excluding own researching resources as a cause – no scientifically founded state of research on explicitly considered subject matter seemed to exist. Hence, it was necessary to both gain orientation on the basis of helpful theoretical topics and, in particular, develop guidelines as well as circumstances for the survey itself. In Figure 1 presented key content for the questionnaire arose based on findings from known concerns regarding elevator use, of the value of safety in the exercise of mobility, of technology acceptance tendencies and of individual risk assessment for the use of (new) mobility technologies – combined with an analytical consideration of the central issue.

Results of the subconscious and intuitive assessment of the use by a semantic polarity profile as well as of the open and concrete questioning of possible concerns should enable an answering of the central issue.



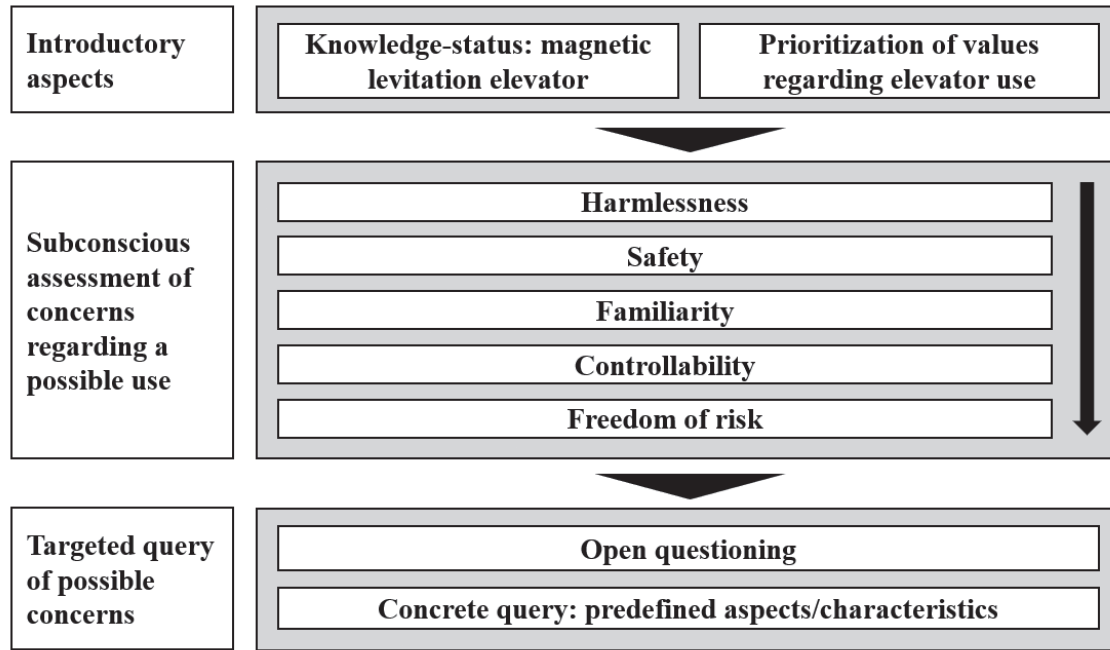


Fig. 1. Substantial-chronological structure of the questionnaire

## CONDENSED RESULTS

In total, 197 persons were questioned the complete questionnaire – almost two-thirds had already heard of the magnetic levitation elevator.

Central aspects of the survey revealed the following compressed discussion approaches and results, thematically depicted according to predefined guiding questions.

- How important is the personal value of safety regarding the use of elevators?

Among five predefined values, safety was rated as the most important value in elevator driving by 50.2 % of the sample size. Furthermore, for 24.4 % of the respondents it was the second most important value while another 25.4 % put at least two other values above safety.

Thusly, in the overall trend safety appeared to be the dominant feature by some margin followed by speed, availability, ride comfort and cabin design. The findings suggested that a large proportion of potential users of maglev elevators would prefer safety against effectiveness and/or efficiency. Above all, ‘being safe’ or ‘feeling safe’ combined with ‘moving quickly and ideally immediately’ seems to be important to many people in terms of elevator usage.

- How does the average potential user subconsciously assess a possible ride with the maglev elevator regarding personal concerns?
- Are there any differences regarding concerns among potential users and, if so, how do they share proportionally?
- Are there any connections between a subconscious assessment of concerns and their concrete questioning and, if so, which ones?

As Fig. 2 shows, respondents rated a potential ride with the magnetic levitation elevator as rather harmless with a slight tendency towards the middle. Furthermore, a possible trip was averagely considered fairly safe. Beyond that, interviewees estimated a potential usage between undecided and rather unfamiliar with a slight bias towards the former. Irresolution was dominating in terms of the ‘controllability’ while the sample average, slightly tending towards the middle, estimated a conceivable ride as rather risk-free.

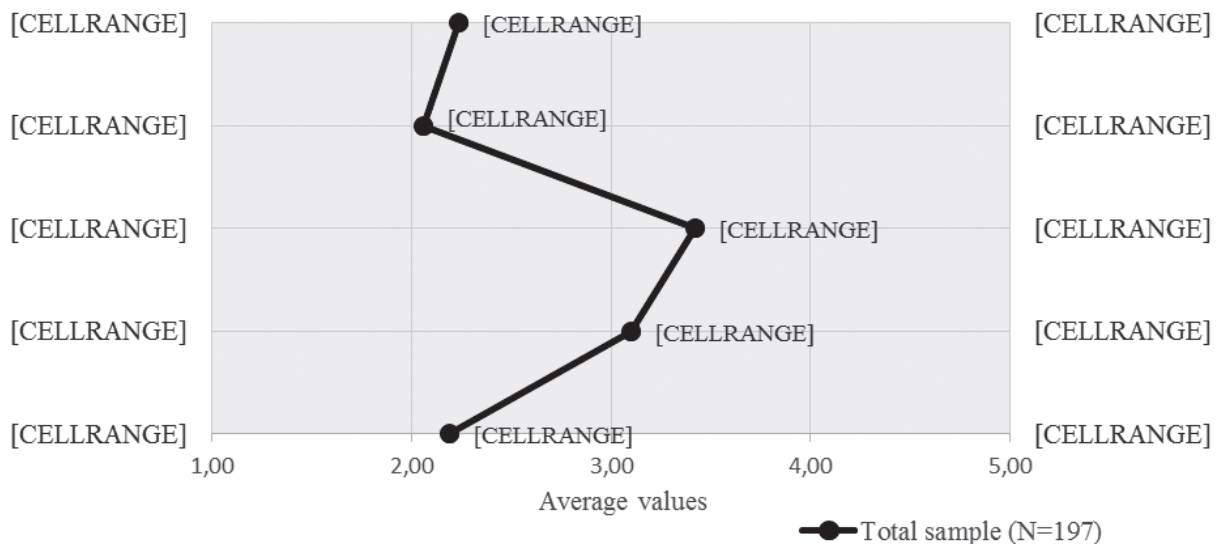


Fig. 2. Semantic profile of the total sample (N = 197)

Question: „Please assess from your perspective a possible ride with the magnetic levitation elevator by using the following contrastive pairs“

Further analysis showed that the personal assessment of the ‘harmlessness’, ‘safety’ and ‘freedom of risk’ are positively linked in terms of judging a potential trip with a magnetic levitation elevator. Therefore – with a moderately correlated interrelation ( $r = 0.586$ , significance level 0.01) – respondents appear to be more likely to assess a possible use as rather safe if they also consider it to be rather harmless (and contrariwise). Similar statements can be made regarding the other connections of this triumvirate of dimensions.

In addition to the consideration of these overall trends, possible categorical differences should be taken into account via an individual calculation methodology.

Relating to the polarity profile as in Table 1, the results of each questionnaire were determined using the following formula:

$$y_n = (x_{n1} + x_{n2}) * 1.0 + (x_{n3} + x_{n4} + x_{n5}) * 0.5$$

Table 1. Logic for the individual calculation methodology

	$x_n =$	2.0	1.0	0	-1.0	-2.0		Weighting
$x_{n1}$	harmless	<input type="checkbox"/>	<input type="checkbox"/>	<input type="checkbox"/>	<input type="checkbox"/>	<input type="checkbox"/>	worrying	*1.0
$x_{n2}$	safe	<input type="checkbox"/>	<input type="checkbox"/>	<input type="checkbox"/>	<input type="checkbox"/>	<input type="checkbox"/>	unsafe	*1.0
$x_{n3}$	familiar	<input type="checkbox"/>	<input type="checkbox"/>	<input type="checkbox"/>	<input type="checkbox"/>	<input type="checkbox"/>	unfamiliar	*0.5
$x_{n4}$	controllable	<input type="checkbox"/>	<input type="checkbox"/>	<input type="checkbox"/>	<input type="checkbox"/>	<input type="checkbox"/>	uncontrollable	*0.5
$x_{n5}$	riskless	<input type="checkbox"/>	<input type="checkbox"/>	<input type="checkbox"/>	<input type="checkbox"/>	<input type="checkbox"/>	risky	*0.5

Scores ranging from  $y_n = 7.0$  to  $y_n = -7.0$  were possible and every respondent could be assigned according to predefined categories of concerns. The outcome can be seen in Fig. 3.

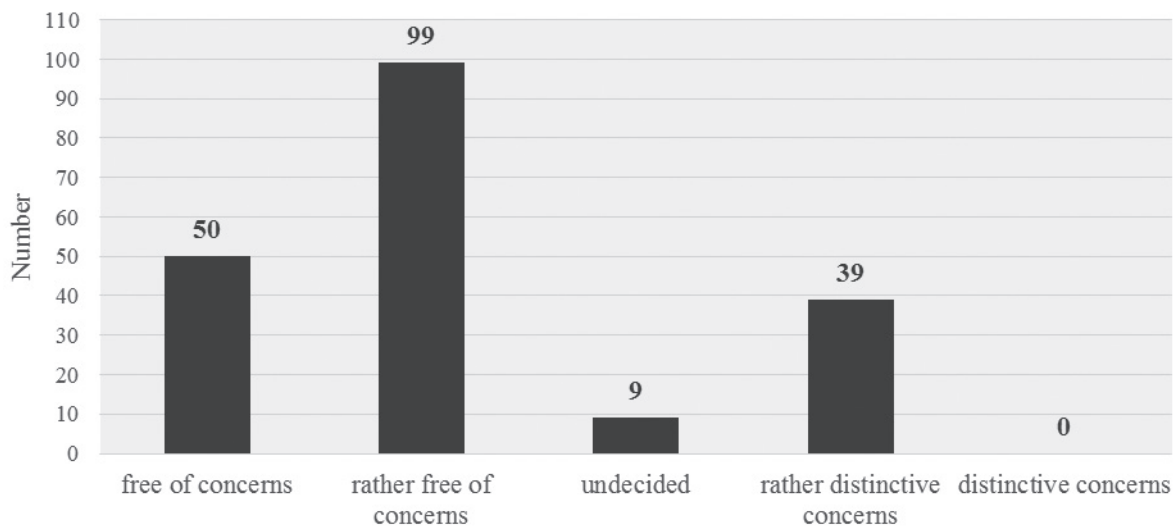


Fig. 3. Individual consideration of the total sample (N=197)

In total, 25.4 % could be classified as persons who seemed fundamentally free of concerns on the basis of their subconscious assessment. 50.2 % appeared to be rather free of concerns while nine persons fell into the category 'undecided'. Above that, 19.8 % of the sample appeared to have subconsciously expressed rather existing concerns by answering the polarity profile. Whereas apparently nobody

showed strong concerns the following needs to be noted: an application of the calculation to the total sample resulted in a categorization as ‘rather free of concerns’.

Deeper analyzes have shown that among people with quite pronounced concerns in about four out of five were able to express these in concrete, thus to substantiate them.

- Which quantitative and qualitative characteristics can be determined by an open questioning of concerns? Are concerns expressed and, if so, which ones?

The open questioning resulted in approximately one-third really concretizing aspects with more than half of them already being categorized as not free of misgivings. Below both causes for as well as manifestations of concerns are described.

Most frequently articulated were misgivings regarding suspected effects of power failure on the magnetic field stability (eleven times), followed by the absence of ropes (nine times) and doubts over the influence of magnetic fields on health (six times) of especially regular users and particularly on people with pacemakers (eight times). Furthermore, on a shared fourth place (six times each) felt uncertainty due to the innovation of the technology and therefore general risks associated with it as well as unspecified concerns relating to power loss would be expressed.

Followed by general doubt over the stability of such magnetic levitation (four times), concerns thanks to the pending cabins as well as felt uncertainty due to lacking knowledge about the technology itself and concerns relating to aspects of driving comfort came up as the divided eight place (three times each) of the most frequently mentioned aspects.

Eventually, with either two or less nominations followed: doubts about the technical/electrical functionality of the system; concerns over possible collisions or crashes of cabins; misgivings towards assumed possibilities of technical influence by “cyber-attacks”; reservations due to assumed negative leverage of magnetic field presence on electronic devices owned by users of the elevator.

- How are concrete and new aspects of magnetic levitation elevator technology assessed with regard to possible concerns?

Tangible aspects which seem to be novel to the user were – as Fig. 4 shows – all on average considered to be largely unobjectionable, especially the

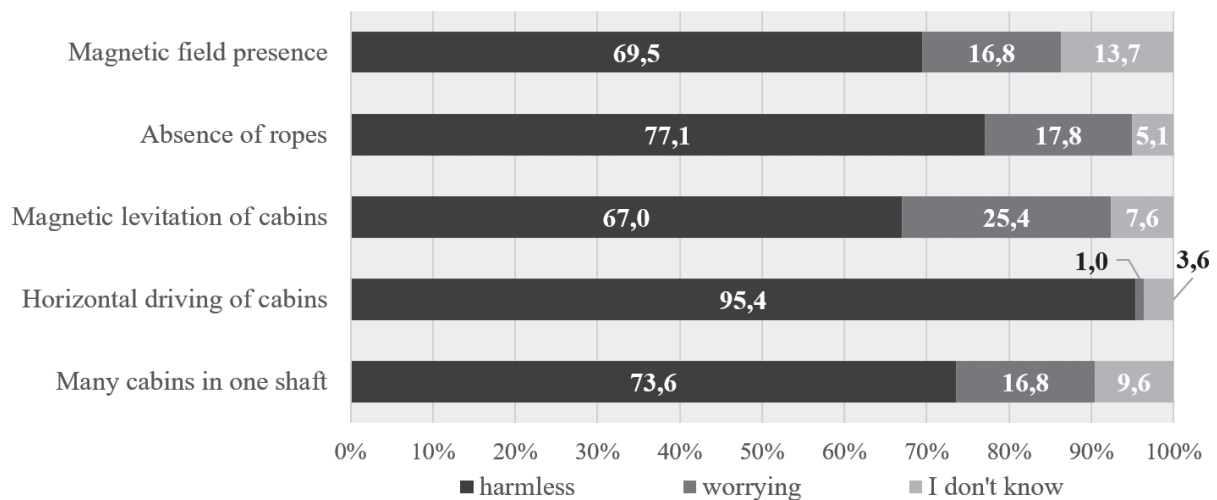


Fig. 4. Evaluation of predefined characteristics (N=197)

**Question:** How do you assess the following aspects of the magnetic levitation elevator?

locomotion of elevator cars in the horizontal. Nevertheless, there were proportionate differentiations. The presence of magnetic fields, a large number of circulating cabins in the elevator shaft and the absence of cables appeared to be of concern by averagely about one-sixth, while the levitation of the cabins by magnets was considered to be the comparatively most alarming aspect.

Specially, Magnetic levitation of cabins' as well as "Absence of Ropes" could be ranked and defined as significant and correlative content-related ( $r = 0.592$ ; level of significance 0.01) reasons for concerns. This relationship appears logical since both aspects are often highlighted in public reporting and appear to be related to one another: the lack of ropes results in a certain way from their replacement by the linear motor technology – ergo by 'magnetic levitation'.

## CONCLUSION

At the time of this study potential users in the overall trend appeared to be rather free of concerns about the safe use of magnetic levitation elevators. However, by an individual differentiation of this general bias, people with more pronounced concerns could be identified.

On closer inspection about a half of potential users could be categorized in said average trend, in about a quarter as completely free of misgivings and a small proportion as undetermined. As a result of subconsciously expressed reservations and clarification of concerns through naming, just under a sixth of potential users seem to have specific, significant concerns. After final compression of the data, those consist mainly of the following contentual nature:

- Health-related concerns due to suspected magnetic field presence
- Feelings of uncertainty due to mental perception of absence of ropes
- Concerns raised due to the magnetic levitation of the cabins, in particular with regard to doubted stability of the magnetic fields
- Uncertainty about possible effects of power outages in general and with regard to the stability of magnetic fields and cabin-maintenance

Using elevators has become part of everyday life for many people. Although there may be misgivings about conventional elevator systems, people have become accustomed to the use of elevators as a means of transportation – including potential disadvantages or perceived risks. This might be caused by the fact that characteristics and general conditions of the technology have changed little for a long time.

However, the magnetic levitation elevator technology will bring some new framework conditions whose actual perceptibility during the use itself remains to be seen but which are mentally both perceivable and conceivable for potential users.

While a large share of people in this respect seem to be free of thought, for some especially new characteristics and associated perceptions with it appear to lead to thoughts and assessments which primarily differ from traditional feelings related to elevators and partly eventuate in actual concerns.

## References

1. Thyssenkrupp Elevator AG. *MULTI: Der erste seillose Aufzug der Welt* [Internet]; n. d.; [cited 2017 Nov 29]. Available at: <https://multi.thyssenkrupp-elevator.com/de/>.
2. Arnegger P. *Applaus für ThyssenKrupps Multi: Die erste Fahrt des ersten seillosen und seitwärts fahrenden Aufzugssystems* [Internet]; *Neue Rottweiler Zeitung*. 2017 Jun 22; [cited 2017 Nov 27]. Available at: <https://www.nrwz.de/rottweil/applaus-fuer-thyssenkrupps-multi-aufzug/173172>.
3. Schwan B. *Turbolift wird Realität: Aufzug von ThyssenKrupp kann die Richtung wechseln* [Internet]; *Heise Online*. 2017 Jul 19; [cited 2017 Nov 27]. Available at: <https://www.heise.de/newsticker/meldung/Turbolift-wird-Realitaet-Aufzug-von-ThyssenKrupp-kann-die-Richtung-wechseln-3773967.html>.
4. Dierig C. *Der seillose Aufzug fährt sogar seitwärts* [Internet]. *Die Welt*. 2017 Jun 22; [cited 2017 Nov 27]. Available at: <https://www.welt.de/wirtschaft/article165845614/Der-seillose-Aufzug-faehrt-sogar-seitwaerts.html>.
5. Jetter M, Gerstenmeyer S. *A Next Generation Vertical Transportation System*. In: WOOD, A, GABEL, J. *The Future of Tall: A selection of Written Works on Current Skyscraper Innovations*. Chicago. 2015;104; [cited 2017 Nov 29]. Available at: <http://global.ctbuh.org/resources/papers/download/2408-a-next-generation-vertical-transportation-system.pdf>.
6. Thyssenkrupp Elevator AG. *MULTI: Der erste seillose Aufzug der Welt* [Internet]; n. d.; [cited 2017 Nov 29]. Available at: <https://multi.thyssenkrupp-elevator.com/de/>.
7. URBAN HUB. *Neue Ära der Aufzugstechnik revolutioniert die Gebäudekonstruktion* [Internet]; n. d.; [cited 2017 Nov 24]. Available at: <http://www.urban-hub.com/de/ideas/neue-ara-der-aufzugstechnik-revolutioniert-die-gebäudekonstruktion/>.

**Information about the author:**

**Kirchner Manuel**, Bachelor of Arts; Hubertusstraße 46, 83022 Rosenheim, Germany

ORCID: 0000-0001-6067-0936;

E-mail: Manukirchner@gmx.net

**To cite this article:**

Kirchner M. Empirical investigation of possible concerns regarding the use of magnetic levitation elevators. *Transportation Systems and Technology*. 2018;4(3):134-142. doi: 10.17816/transsyst201843134-142

UDC 629.439

DOI 10.17816/transsyst201843143-153

© V.A. Polyakov, N.M. Khachapuridze

Institute of Transport Systems and Technologies of Ukraine's National Academy of Sciences (Dnepr, Ukraine)

## MAGNETICALLY LEVITATED TRAIN'S LONGITUDINAL MOTION (SIMULATION RESULTS)

**Background:** The no-stationary regimes of the magnetically levitated train's (MLT) motion were the object of research.

**Aim:** The purpose of the study is to evaluate its dynamic qualities and loading in such regimes.

**Methods:** The work was carried out by conducting a series of experiments with a computer model of train's dynamics.

**Results:** The simulation results reflect its motion in the modes of acceleration, passage of the tunnel, as well as service and emergency braking.

**Conclusion:** An analysis of these results made it possible to evaluate the dynamic properties of a train in various non-stationary motion modes and its loading in their process.

**Keywords:** magnetically levitated train, non-stationary regimes of motion, dynamic qualities, dynamic loading, computer experiment.

© В. А. Поляков, Н. М. Хачапуридзе

Институт транспортных систем и технологий Национальной академии наук Украины, Днепр, Украина

## ПРОДОЛЬНОЕ ДВИЖЕНИЕ МАГНИТОЛЕВИТИРУЮЩЕГО ПОЕЗДА (РЕЗУЛЬТАТЫ МОДЕЛИРОВАНИЯ)

**Обоснование:** Объектом исследования были нестационарные режимы движения магнитолевитирующего поезда (MLT).

**Цель:** Целью исследования явилась оценка его динамические качества и нагруженности в таких режимах.

**Методы:** Работа была выполнена путем проведения серии экспериментов с компьютерной моделью динамики поезда.

**Результаты:** Результаты моделирования отражают его движение в режимах ускорения, прохождения туннеля, а также сервисного и экстренного торможения.



**Выводы:** Анализ этих результатов позволил оценить динамические свойства поезда в различных нестационарных режимах движения и его загруженность в их процессе.

**Ключевые слова:** магнитолевитирующий поезд, нестационарные режимы движения, динамические качества, динамическая нагруженность, компьютерный эксперимент.

## INTRODUCTION

The magnetically levitated train (MLP) is a large, complex system, the elements of which are very diverse. It's main purpose is to transport passengers and cargo. Quality of transportation is the key criterion for assessing the consumer properties of a train.

The dynamics of the electromechanical subsystem determines the specified quality. Particularly critical are the non-stationary modes of its motion. They are restrictive and subject to priority research. Carrying out such research is the main task of the work.

## THE MATERIAL AND RESULTS OF THE STUDY

The one-dimensional longitudinal motion of MLT is considered. The calculated scheme of its mechanical subsystem (MS) is adopted in the form of a solid body of mass  $m$ . It's motion is considered with respect to an inertial fixed Cartesian reference frame  $OXYZ$ . The Cartesian triadron  $Cxyz$ , axes of which are it's main central ones, is connected with this body. The change of body's position in time  $t$  is determined by Cartesian coordinate  $x(t)$  of it's center of mass. The analytical connections on the body are not imposed. The MS's of MLT's configuration is described by one generalized coordinate:

$$\eta^1 = x. \quad (1)$$

The motion is considered in an electrodynamic's levitation state – after separation from the direction-controlling structures. In the process of motion, the body's mass  $m$  center's deviations from a stationary trajectory parallel to the curve of the axis of the path and symmetrically disposed concerning it's structures are considered to be absent. The following forces acts on the body [1–3]:

$F_{Tx}$  – from the side of the linear synchronous motor (LSM) – the longitudinal component of the traction force;  $F_{ADx}$  – from the ambient air – longitudinal component of the aerodynamic force;  $F_{EDx}$  – on the side of the track suspension loops – component of electrodynamic's force;  $F_{Wx}$  – due to the presence of a longitudinal slope of the track – longitudinal component of train's weight.

The longitudinal translational motion of a MLT's MS is described by the equation of Newton's second law:

$$m \cdot \ddot{x} = F_{Tx} + F_{ADx} + F_{EDx} + F_{Wx}, \quad (2)$$

where  $\ddot{x}$  – is the longitudinal component of the C point's acceleration.

The values of the quantities  $F_{Tx}$ , in the case under consideration, are determined [4–6] by the relations:

$$\begin{aligned} F_{Tx} &= f_{x\lambda\chi} \cdot e^\lambda \cdot e^\chi; \quad e^\lambda = e^\chi = 1; \\ f_{\lambda\chi} &= l_{\lambda\chi} \cdot i^\lambda \cdot B_{\lambda\chi} \quad \forall \lambda \in [\overline{1, N}], \chi \in [\overline{1, 2}], \end{aligned} \quad (3)$$

where  $f_{\lambda\chi}$  – force of interaction of fields of currents of the  $\chi$ -it rectilinear element of the  $\lambda$ -mp loop of inductor of the motor and its armature;  $l_{\lambda\chi}, i^\lambda, B_{\lambda\chi}$  – the length of such an element, the current in it, and also the induction (conditionally homogeneous – within the element) of the magnetic field in which the element is located.

The values of the quantities  $F_{ADx}$  are estimated [7–9] in the following way:

$$F_{ADx} = -C_x \cdot q \cdot S; \quad q = 0.5 \cdot \rho \cdot \dot{x}^{(2)}, \quad (4)$$

where  $C_x$  – is the dimensionless aerodynamic coefficient in the direction of  $Cx$ ;  $S$  – characteristic cross-sectional area of the train in the same direction;  $\rho$  – ambient air density.

The values of the quantities  $F_{EDx}$  are approximated [10–12] by a polynomial of the form:

$$F_{EDx} = k_\rho \cdot \dot{x}^\rho \cdot e^\rho; \quad e^\rho = 1 \quad \forall \rho \in [\overline{1, n_r}], \quad (5)$$

in which  $k_\rho \quad \forall \rho \in [\overline{1, n_r}]$  – are obtained by regressing the experimental dependences  $F_{EDx}(t)$  with the selected degree of the approximation polynomial  $n_r$ .

Finally, the change of the force values  $F_{Wx}$  is described by the expression:

$$F_{Wx} = m \cdot g \cdot \sin \varphi_\kappa, \quad (6)$$

where  $g$  – is the gravitational constant;  $\varphi_\kappa$  – the angle of the gradient of the profile of the way section, along which the train moves.

The mathematical model (2) describes the longitudinal one-dimensional motion of the MLT's MS under the influence of external disturbances, as well

as control from its LSM. This model was adopted as an algorithmic basis for constructing a relevant computer model of the same process of motion, which is an instrument for its study. The elements of the computer model are programmatically fixed within the input language of the Mathematica computer mathematics system and are divided into the calculation and graphical parts. The first of these parts, functionally, solves the direct problem of the dynamics of the system under study, and the second of the parts – converts the results of calculations into a graphic form. The study was carried out by conducting a series of experiments with this computer model. Their results, in each of the considered modes of motion, were the graphs of the functional dependencies on time of various quantities characterizing and generating this motion. The motion was studied in the following non-stationary regimes: increasing the speed (from the moment of transition to the state of electrodynamics' levitation to the steady speed of motion); passage through the tunnel; service and emergency braking. Some of the results of this study are presented and analyzed further.

The frequency of the voltage, that feeds the LSM's armature winding, is always automatically maintained [1] by the proportional of the MLT's speed. In addition to frequency, system's control can have an additional component that provides an increase in the smoothness of electromagnetic processes in the LSM and a mechanical component in the MS. As such a component, amplitude or phase control can be used. In the first of these cases, in the process of increasing the MLT's speed, the smoothness of the LSM's power supply is provided by increasing the voltage amplitude, which is applied to its armature winding, for example, according to the law

$$U_a(t) = U_a^* \cdot th(t \cdot k_{vd}), \quad (7)$$

where  $U_a^*$  – is the limiting value of this amplitude;  $k_{vd}$  – coefficient, which determines the intensity of the voltage amplitude increasing.

In the case of the phase variant of controlling the train speed increase, the initial phase of the armature voltage can vary, for example, according to law

$$\theta_u(t) = \alpha_u \cdot [th(t \cdot k_{fd}) - 1], \quad (8)$$

where  $\alpha_u$  – is it's current phase;  $k_{fd}$  – coefficient, that determines the rate of initial phase changing.

Illustrative examples of the results of the investigation of the MLT's motion in the regime of increasing the speed are shown in Fig. 1–6. Fig. 1, 2 correspond to the control of only the frequency of the voltage; Fig. 3, 4 – amplitude-frequency

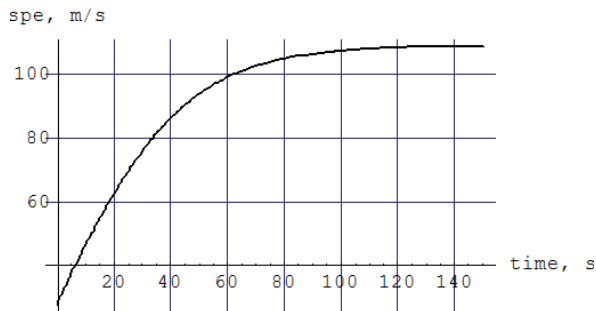


Fig. 1. The train's speed graph

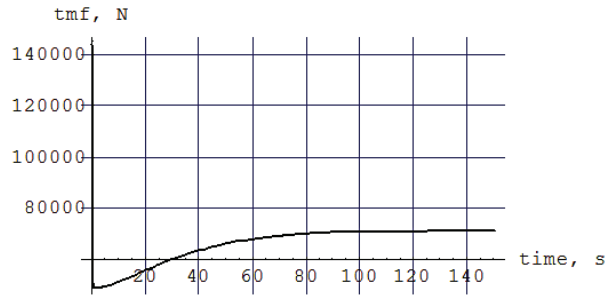


Fig. 2. The LSM's traction force graph

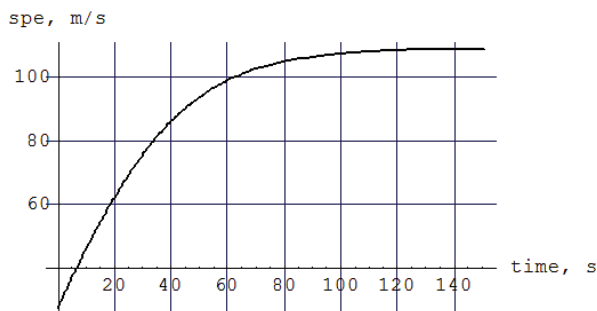


Fig. 3. The train's speed graph

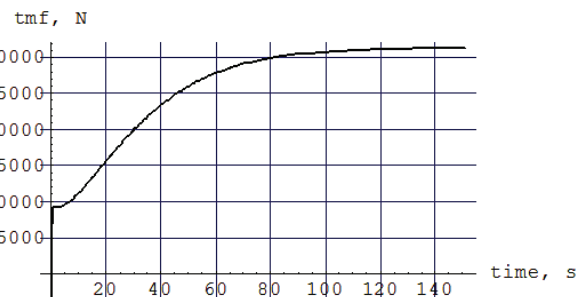


Fig. 4. The LSM's traction force graph

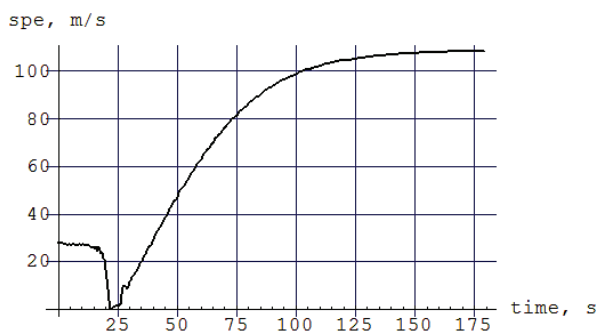


Fig. 5. The train's speed graph

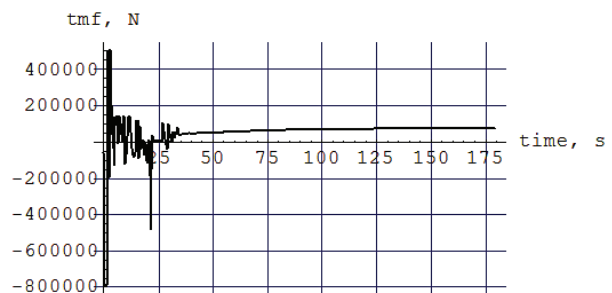


Fig. 6. The LSM's traction force graph

control; Fig. 5 and 6 – phase-frequency control; Fig. 1, 3, 5 show the train speed graphs; Fig. 2, 4, 6 – graphs of the LSD's traction force acting on it.

Analysis of the results of modeling the increase in train speed shows that it is unacceptable as an option to adjust only the frequency of the motor supply voltage – because of the high value of train acceleration, as well as the phase-frequency regulation of this voltage – because of the high-frequency oscillation of the MLT's speed. In addition, in the latter case, the LSM's armature's currents are unacceptably high. The most suitable is the amplitude-frequency version of the armature's voltage control.

Train's entrance into the tunnel and the exit from it lead to differences in the aerodynamic resistance to motion by about 30% [13–15], which can lead to

sudden fluctuations in acceleration and speed of this motion. This is unacceptable and makes it expedient to automate the control by it. At the entrance and exit from the tunnel, additional resistance to motion changes almost linearly. Therefore, when modeling this mode of motion, it was considered that the aerodynamic resistance is described by the relations:

$$F_{ADx}^* = F_{ADx} \cdot [1 + (1/0.7 - 1) \cdot \kappa];$$

$$\kappa = \begin{cases} 0 & \forall x < \xi_{ts} - 0.5 \cdot l_t \vee x > \xi_{tf} + 0.5 \cdot l_t; \\ (x + 0.5 \cdot l_t - \xi_{ts}) \cdot l_t^{(-1)} & \forall \xi_{ts} - 0.5 \cdot l_t \leq x \leq \xi_{ts} + 0.5 \cdot l_t; \\ 1 & \forall \xi_{ts} + 0.5 \cdot l_t < x < \xi_{tf} - 0.5 \cdot l_t; \\ (\xi_{tf} - x + 0.5 \cdot l_t) \cdot l_t^{(-1)} & \forall \xi_{tf} - 0.5 \cdot l_t \leq x \leq \xi_{tf} + 0.5 \cdot l_t, \end{cases} \quad (9)$$

where  $l_t$  – the length of the train;  $\xi_{ts}, \xi_{tf}$  – the distances from the starting point of the way to the beginning and end of the tunnel. The aim of motion control in the tunnel:

$$\ddot{x}(t) = \ddot{x}_{ts} = const, \quad (10)$$

where  $\ddot{x}_{ts}$  – acceleration of the train at the tunnel's entrance. Compliance with this condition is achieved by frequency, amplitude-frequency, or phase-frequency voltage  $U_a$  control. The required for this purpose laws of its change were found using the model (2) (in which  $F_{ADx}$  was replaced by a quantity  $F_{ADx}^*$ , that was calculated according to relations (9), and  $\ddot{x}$  was replaced by a quantity  $\ddot{x}_{ts}$ , that was calculated according to (10)), as well as the LSM's dynamics model [2].

Illustrative examples of the results of the investigation of the MLT's motion in a tunnel are shown in Fig. 7–12. Fig. 7 and 8 correspond to controlling only the frequency of the armature voltage, Fig. 9 and 10 – amplitude-frequency control of this voltage, and Fig. 11 and 12 – phase-frequency control. Fig. 7, 9 and 11 show the train speed graphs, and in Fig. 8, 10 and 12 – graphs of the LSD's traction force acting on it.

Analysis of the simulation results of these three options of controlling the motion of the train through the tunnel leads to the following conclusions. In the case of only frequency control by supply voltage, the jump of the MLT's speed is about 10%, which is definitely unacceptable. Other two methods of automatic voltage control are approximately equivalent, since in both of these cases there are no significant fluctuations of the MLT's speed and acceleration when passing the

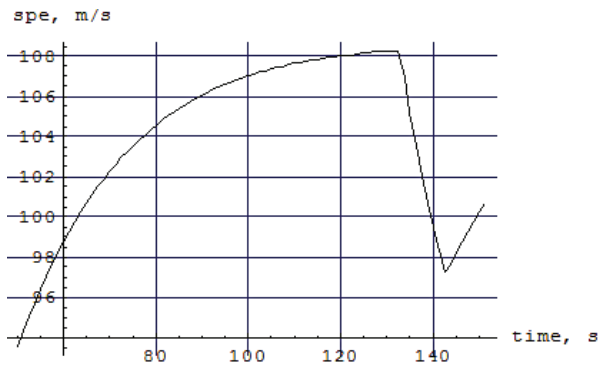


Fig. 7. The train's speed graph

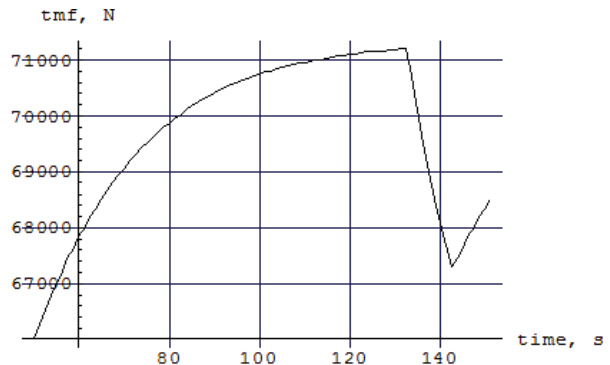


Fig. 8. The LSM's traction force graph

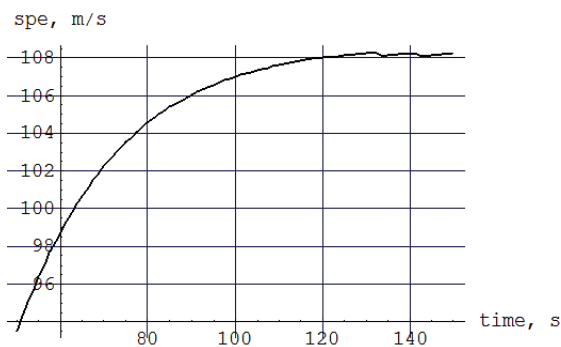


Fig. 9. The train's speed graph

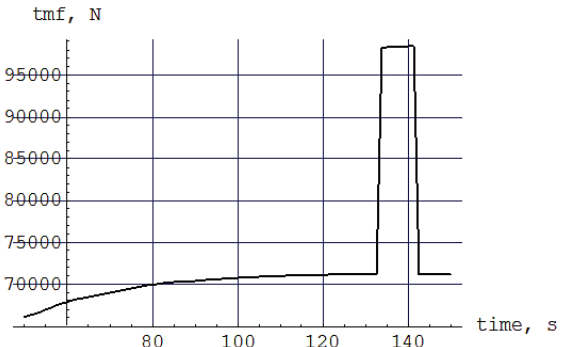


Fig. 10. The LSM's traction force graph

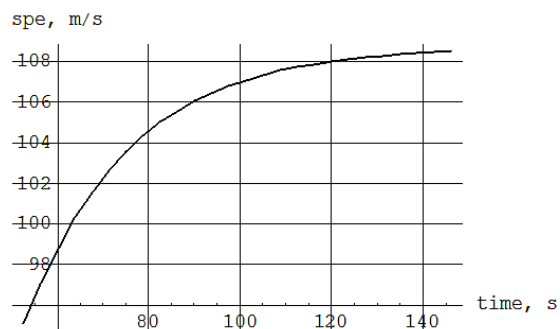


Fig. 11. The train's speed graph

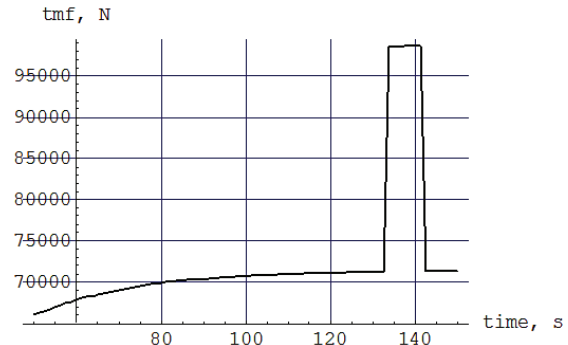


Fig. 12. The LSM's traction force graph

tunnel. At the same time, the phase-frequency control method is simpler (since there is no need to regulate high voltages). However, with amplitude-frequency control, the peak values of the phase currents are approximately one and a half times lower, which reduces the current load on the electrical equipment of the motor.

During the MLT's motion, the LSM's armature and inductor windings are reciprocally moved. In these windings, electromotive forces of mutual induction are induced, leading to the appearance of mechanical forces, which counteract the mutual displacement of the windings. The voltage feeding the armature winding of

the motor usually compensates of these electromotive forces and LSM operates in traction mode. But if the current value of the armature voltage decreases, the motor automatically goes into braking mode. As well as MLT's acceleration, its electrodynamic's braking should be smooth. Therefore, the two most appropriate ways to implement service braking of the train are the amplitude-frequency and phase-frequency control of the LSM's armature voltage. To implement these smooth control modes, the amplitude and the initial phase of the armature voltage can vary, for example, according to the laws.

$$U_a(t) = U_a^* \cdot [1 - th(t \cdot k_{vi})]; \quad (11)$$

$$\theta_u(t) = -\alpha_u \cdot th(t \cdot k_{fm}), \quad (12)$$

where  $k_{vi}$ ,  $k_{fm}$  – the coefficients determining the rate of amplitude and the initial phase of the armature voltage changing. These laws can be used for implementation of the train's service braking. For emergency braking, instantaneous removal of the supply voltage from the motor's armature winding is possible, but with the preservation of its circuits retained – by means of the double-breasted three-phase short circuit of this winding.

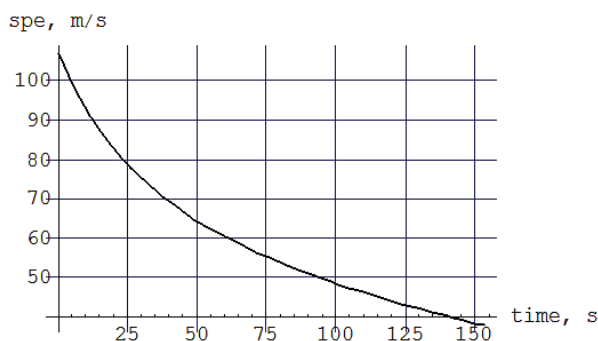


Fig. 13 The train's speed graph

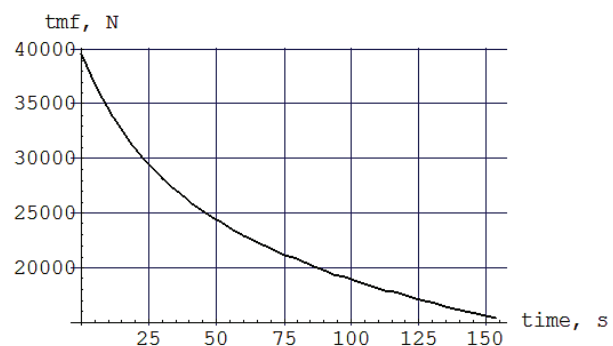


Fig. 14 The LSM's braking force graph

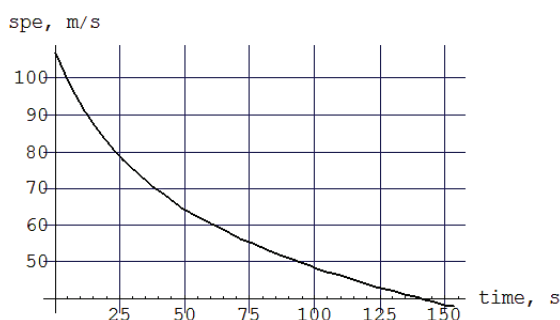


Fig. 15 The train's speed graph

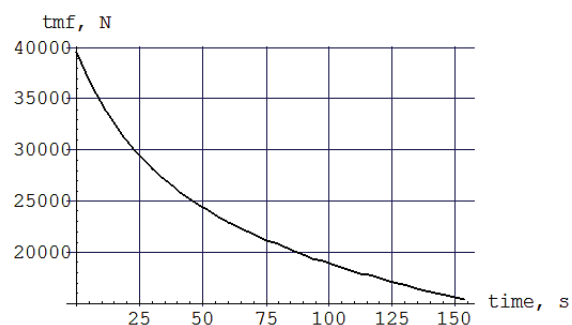


Fig. 16 The LSM's braking force graph

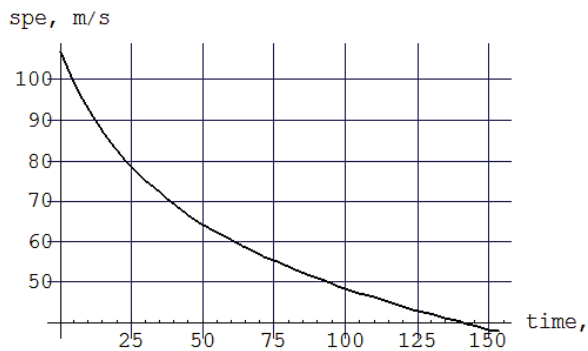


Fig. 17 The train's speed graph

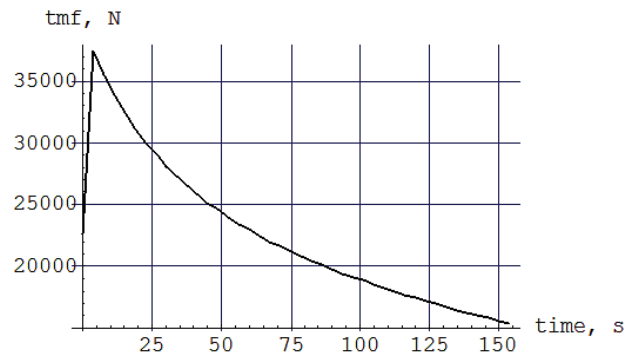


Fig. 18 The LSM's braking force graph

Illustrative examples of the investigation results of the MLT's motion in various braking regimes are shown in Fig. 13–18. Fig. 13, 14 correspond to the implementation of service braking with amplitude-frequency voltage control; Fig. 15, 16 – with phase-frequency control. Finally, Fig. 17, 18 correspond to emergency braking – by means of a double-breasted three-phase short circuit of the LSM's armature winding. Fig. 13, 15, 17 show graphs of train's speed; Fig. 14, 16, 18 – graphs of the LSM's braking force acting on it.

Analysis of the simulation results of the indicated MLT's motion brake regimes allows drawing the following conclusions. The considered modes of service braking (with amplitude-frequency and phase-frequency regulation of the motor's armature voltage) are approximately equivalent on the brake characteristics being realized. Both of them provide sufficient smoothness of the change in acceleration and speed of the train. The peak values of acceleration do not exceed  $0.15 \cdot g$ , which is quite acceptable. The implementation of emergency braking leads to significant peak acceleration – about  $0.22 \cdot g$ , which can't be eliminated. However, such a short-term increase in acceleration in extreme situations is justified.

## CONCLUSIONS

By way of computer simulation, the dynamics of a magnetically levitated train, subjected to natural disturbances, and controlled by a linear synchronous motor, in the modes of acceleration, passage of the tunnel, as well as service and emergency braking are studied. The analysis of the obtained results made it possible to evaluate the dynamic qualities of the train in the considered non-stationary modes of motion, as well as its loading in their process. This solves the problem of this part of the study.



**Библиографический список / References**

1. Дзензерский В. А., Омеляненко В. И., Васильев С. В. и др. Высокоскоростной магнитный транспорт с электродинамической левитацией. – Киев: Наукова думка, 2001. – 479 с. [Dzenzerskii VA, Omel'yanenko VI, Vasil'ev SV, et al. Vysokoskorostnoi magnitnyi transport s elektrodinamicheskoi levitatsiei. Kiev: Naukova dumka; 2001. 479 p. (In Russ.)].
2. Atherton DL, Eastham AR. High speed Maglev studies in Canada. In: *5-Th International Cryogenic Engineering Conference (ICEC-5)*. Kyoto; 1974:46-50.
3. Zhigang L, Long Z. *Maglev Trains. Key Underlying Technologies*. Berlin: Springer, 2015:215.
4. Поляков В. А., Хачапуридзе Н. М. Модель процесса реализации тяговой силы двигателя магнитолевитирующего поезда//Наука та прогрес транспорту. Вісник Дніпропетровського національного університету залізничного транспорту ім. акад. В. Лазаряна – 2016. – № 4 (64). – С. 55–62. [Polyakov VA, Khachapuridze NM. Implementation Model of Motor traction Force of Maglev Train. *Science and Transport Progress. Bulletin of Dnipropetrovsk national university of railway transport named after academician V. Lazaryan* 2016;4(64):55-62. (In Russ.)]. doi: 10.15802/stp2016/77909
5. Fujiwara S. Superconducting Maglev and its electromagnetic Characteristics *SAE Technical Paper Series*. 1995;SAE 95-1922:1-6.
6. Lee KB, Kim CA. Study on Energy Efficiency Analysis by Maglev Trains. *Electrical and Electronic Engineering. Advanced Science and Technology Letters*. 2015;118:48-53.
7. Лебедев А. А. Динамика полёта беспилотных летательных аппаратов. – М.: Машиностроение, 1973. – 616 с. [Lebedev AA. *Dynamics of Flight of Unmanned Aerial Vehicles*. Moscow: Mashinodstroenie; 1973. 616 p. (In Russ.)].
8. Wairagade AKR, Balapure MBH, Ganer P. Magnetic Levitation Train. *Journal for Research*. 2015;01(08):1-5.
9. Chong Y, Kane W. Maglev train's development prospects in China *Maglev Train in China Journal*. 2016;2:75-90.
10. Дзензерский В. А., Зевин А. А., Филоненко Л. А. Устойчивость вертикальных колебаний в системе электродинамического подвеса с дискретной путевой структурой // Прикладная механика. – 1995 – Т. XXXI. – № 7. – С. 88–93. [Dzenzerskij VA, Zevin AA, Filonenko LA. Stability of vertical oscillations in a system of electrodynamic suspension with a discrete track structure *Applied Mechanics*. 1995; XXI(7):88-93. (In Russ.)].
11. Russell J, Cohn R. *List of Maglev Train*. Johannesburg: Book on demand; 2015. 135 p.
12. Antlauf W, Coates KC. Fast Tracks: Building the Shanghai Maglev *Civil Engineering*. 2004;11:59-66.
13. Fuji J. Ground transportation on suspension on superconducting magnets. II. Suspension system on superconducting magnets. *Dengakushi*. 1991;3:457-459. (In Japan).
14. Zhigang L, Zhiqiang L, Xiaolong L. *Maglev Trains*. Berlin: Springer; 2015. 250 p.
15. Tandan GK, Sen PK, Sahu G, et al. Review on Development and Analysis of Maglev Train *International Journal of Research in Advent Technology*. 2015;3(12):14-17.

**Information about the authors:**

**Vladislav Polyakov**, Ph.D. of Engineering Sciences;  
eLibrary SPIN: 5744-2789; ORCID 0000-0002-4957-8028;  
E-mail: p\_v\_a\_725@mail.ru

**Nikolai Khachapuridze**, Ph. D. of Engineering Sciences;  
eLibrary SPIN: 2115-4942; ORCID 0000-0003-0682-6068;  
E-mail: itst@westa-inter.com

**Сведения об авторах:**

**Поляков Владислав Александрович**, кандидат технических наук, старший научный сотрудник;  
eLibrary SPIN: 5744-2789; ORCID 0000-0002-4957-8028;  
E-mail: p\_v\_a\_725@mail.ru

**Хачпуридзе Николай Михайлович**, кандидат технических наук, старший научный сотрудник;  
eLibrary SPIN: 2115-4942; ORCID 0000-0003-0682-6068;  
E-mail: itst@westa-inter.com

**To cite this article:**

Polyakov VA, Khachapuridze NM. Magnetically levitated train's longitudinal motion (simulation results). *Transportation Systems and Technology*. 2018;4(3):143–153. doi: 10.17816/transsyst201843143-153

**Цитировать:**

Поляков В. А., Хачапуридзе Н. М. Продольное движение магнитолевитирующего поезда (результаты моделирования) // Транспортные системы и технологии. – 2018. – Т. 4. – № 3. – С. 143–153. doi: 10.17816/transsyst201843143-153

DOI 10.17816/transsyst201843154-163

© P. Sun<sup>1,2</sup>, Q. Ge<sup>1</sup>, Y. Li<sup>1</sup>, X. Wang<sup>1</sup>

<sup>1</sup>Key Laboratory of Power Electronics and Electric Drive, Institute of Electrical Engineering, Chinese Academy of Sciences

<sup>2</sup>University of Chinese Academy of Sciences  
(Beijing, China)

## RESEARCH ON SPEED SENSORLESS CONTROL OF MAGLEV TRAIN WITH DOUBLE-END POWER SUPPLY

**Background:** The core technology of the stable operation of the maglev train is how to accurately obtain the train speed, position and motor angle information.

**Aim:** Using speed sensorless control method to estimate the speed and position of the maglev train.

**Methods:** In the double-end power supply mode of the maglev train, the principle of the extended back electromotive force (EEMF) of the AC motor is extended to the control of the long stator permanent magnet synchronous linear motor.

**Results:** The mathematical model for the power supply system of long-stator permanent magnet linear synchronous motor is established; based on the principle of EEMF of rotating motor, the EEMF observer is designed. The speed of the maglev train and the rotor angle are obtained by the method of phase locked loop (PLL).

**Conclusion:** Through the semi-physical simulation experiment, the speed sensorless control method is verified to be effective.

**Keywords:** Maglev train, long stator permanent magnet synchronous linear motor, speed sensorless control, extended electromotive force, double-end power supply

## INTRODUCTION

The maglev train overcomes the friction of the vehicle with the rail, resulting in a significant increase in the speed of the rail train. The Germany TR system uses electromagnetic suspension technology (EMS). The Japanese MLX system uses electrodynamic suspension technology (EDS). The maglev of people transfer system in Shanghai is driven by the long-stator linear synchronous motor. The research content is also based on PMLSM mathematic model.

The core technology of the stable operation of the maglev train is how to accurately obtain the train speed, position and motor angle information. Usually at low speed, the speed and angle information can be determined by the sensor detecting the stator tooth and the positioning mark plate on the track and sent to the control system via the wireless transmission system. However, when the train is running at high speed, the long position information acquisition period cannot guarantee the control system to obtain accurate rotor field orientation angle and

train speed, resulting in poor control performance. Therefore, the effective solution is to use speed sensorless control algorithm. Real-time calculation of train speed and motor angle could ensure the stability control of the maglev train.

The speed sensorless technology of AC motor mainly includes direct calculation method, estimation method based on inductance change, back electromotive force integral method, extended back electromotive force method, extended Kalman filter method [1], model reference adaptive method [2], adaptive control, sliding mode observer [3], high frequency injection method [4, 5] and so on. These methods are for situations which single converter drives AC motor. The speed sensorless control method for long-stator linear synchronous motors in double-end power supply mode has not been reported in the works of literature.

The motor structure of the long-stator linear synchronous motor is quite different from the conventional rotary synchronous motor. The stator segments of the maglev train are laid along the track and the track parameters of the different stator are different. The inductance of the motor stator windings consists of multiple parts. The stator parameters of the stator windings in the area covered by the train differ from the uncovered portion. EEMF method is the use of motor armature current and voltage to calculate the flux and angle information. Compared with other methods, the method is simple and easy to implement, and has the strong robustness to the change of line parameters. Therefore, it is suitable for the control of the long-stator linear synchronous motor.

Compared with the single-end power supply, the mathematical model of maglev train with double-end power supply is more complicated. The input and output variables increase. If you want to directly calculate the EEMF, you need to design two observers. In this paper, the mathematic model of the converter and the long-stator linear synchronous motor is established. Then, combined with the EEMF theory proposed in [6], the EEMF principle of the AC motor is extended to the control of the long-stator linear synchronous motor. The observer of EEMF is designed. Finally, the semi-physical simulation experiments verify the effectiveness of the algorithm.

## **MATHEMATICAL MODEL OF LONG-STATOR LINEAR SYNCHRONOUS MOTOR WITH PARALLEL POWER SUPPLY**

Maglev train in the high-speed operation uses double-end parallel power supply. Parallel power supply can provide greater drive current to meet the needs of high-speed operation; at the same time, it can reduce the output capacity of a single converter and ensure the reliability of power supply. The equivalent circuit of PMLSM with double-end power supply is shown in Fig. 1.

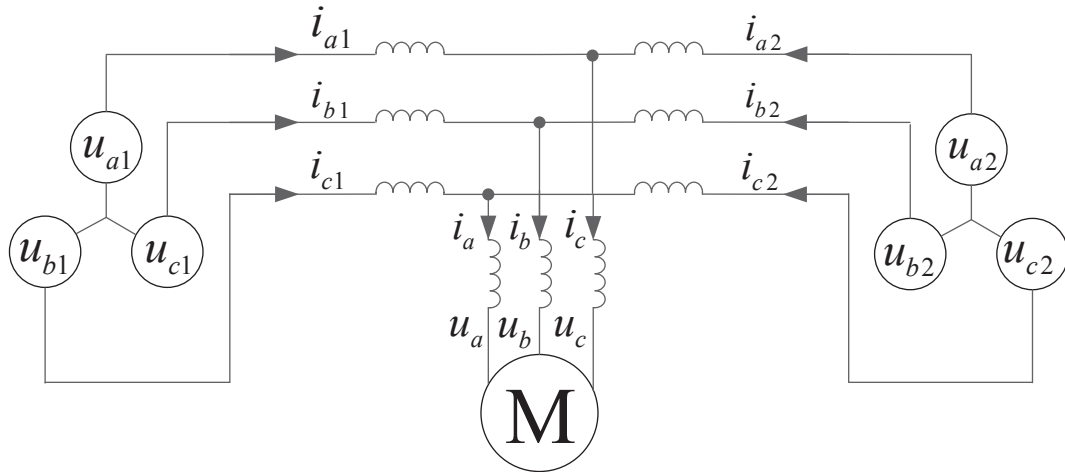


Fig. 1. Equivalent circuit of Long-Stator Linear Synchronous Motor with Double-End Power Supply

where  $u_{a1}, u_{b1}, u_{c1}, u_{a2}, u_{b2}, u_{c2}$  represent the output voltage of two converters;  $i_{a1}, i_{b1}, i_{c1}, i_{a2}, i_{b2}, i_{c2}$  represent the output current of two converters;  $u_a, u_b, u_c$  represent the voltage of stator windings;  $i_a, i_b, i_c$  represent the current of stator windings;  $M$  represent the long-stator linear synchronous motor.

Select the output current of each inverter as the state variables, the inverter output voltage as the input variables. The voltage equation of two converters and long-stator linear synchronous motor in the coordinate system is expressed as

$$(L_{k1}p + R_{k1}) \begin{bmatrix} i_{\alpha 1} \\ i_{\beta 1} \end{bmatrix} = \begin{bmatrix} u_{\alpha 1} \\ u_{\beta 1} \end{bmatrix} - \begin{bmatrix} u_{\alpha} \\ u_{\beta} \end{bmatrix} \quad (1)$$

$$(L_{k1}p + R_{k1}) \begin{bmatrix} i_{\alpha 1} \\ i_{\beta 1} \end{bmatrix} = \begin{bmatrix} u_{\alpha 1} \\ u_{\beta 1} \end{bmatrix} - \begin{bmatrix} u_{\alpha} \\ u_{\beta} \end{bmatrix}, \quad (2)$$

where  $L_{k1}, L_{k2}$  are the inductances of the feed cable;  $R_{k1}, R_{k2}$  are the resistances of the feed cable;  $u_{\alpha 1}, u_{\beta 1}$  are the output voltage of the first converter;  $i_{\alpha 1}, i_{\beta 1}$  are the output current of the first converter;  $u_{\alpha 2}, u_{\beta 2}$  are the output voltage of the second converter;  $i_{\alpha 2}, i_{\beta 2}$  are the output current of the second converter;  $u_{\alpha}, u_{\beta}$  are the voltage of the linear motor;  $p$  is the differential operator. The equation of the long stator linear synchronous motor is shown in (3).

$$\begin{bmatrix} u_{\alpha} \\ u_{\beta} \end{bmatrix} = R \begin{bmatrix} i_{\alpha} \\ i_{\beta} \end{bmatrix} + \begin{bmatrix} pL_d & \omega_{re}(L_d - L_q) \\ -\omega_{re}(L_d - L_q) & pL_d \end{bmatrix} \begin{bmatrix} i_{\alpha} \\ i_{\beta} \end{bmatrix} + \quad (3)$$

$$\begin{aligned}
& + \{(L_d - L_q)(\omega_{re} i_d - i_q) + \omega_{re} K_E\} \begin{bmatrix} -\sin \theta_{re} \\ \cos \theta_{re} \end{bmatrix} \\
= R \begin{bmatrix} i_\alpha \\ i_\beta \end{bmatrix} & + \begin{bmatrix} pL_d & \omega_{re}(L_d - L_q) \\ -\omega_{re}(L_d - L_q) & pL_d \end{bmatrix} \begin{bmatrix} i_\alpha \\ i_\beta \end{bmatrix} + Ex \begin{bmatrix} -\sin \theta_{re} \\ \cos \theta_{re} \end{bmatrix},
\end{aligned}$$

where  $L_d, L_q$  are the inductances of the direct-axis and quadrature-axis;  $R$  is the resistance of stator per-phase winding;  $\omega_{re}$  is the electrical angular velocity;  $K_E$  is the coefficient of the EMF;  $\theta_{re}$  is the rotor angle. The last term of (3) is the EEMF.

Substituting (3) into (1) and (2), the voltage equation as shown in (4) can be obtained. The equation describes the mathematical relationship between the first converter and the long-stator linear synchronous motor.

$$\begin{bmatrix} u_{\alpha 1} \\ u_{\beta 1} \\ u_{\alpha 2} \\ u_{\beta 2} \end{bmatrix} = \begin{bmatrix} L_{k1} + R_{k1} + L_d p & (L_d - L_q)\omega_{re} & L_d p & (L_d - L_q)\omega_{re} \\ -(L_d - L_q)\omega_{re} & L_{k1} + R_{k1} + L_d p & -(L_d - L_q)\omega_{re} & L_d p \\ L_d p & (L_d - L_q)\omega_{re} & L_{k2} + R_{k2} + L_d p & (L_d - L_q)\omega_{re} \\ -(L_d - L_q)\omega_{re} & L_d p & -(L_d - L_q)\omega_{re} & L_{k2} + R_{k2} + L_d p \end{bmatrix} \times \\
\times \begin{bmatrix} i_{\alpha 1} \\ i_{\beta 1} \\ i_{\alpha 2} \\ i_{\beta 2} \end{bmatrix} + Ex \begin{bmatrix} -\sin \theta \\ \cos \theta \\ -\sin \theta \\ \cos \theta \end{bmatrix} \quad (4)$$

## DESIGN THE OBSERVER OF EEMF

The current of the long-stator linear synchronous motor with double-end power supply is equal to the sum of the current of the two converters. The relationship between them is shown as follows

$$\begin{bmatrix} i_\alpha \\ i_\beta \end{bmatrix} = \begin{bmatrix} i_{\alpha 1} \\ i_{\beta 1} \end{bmatrix} + \begin{bmatrix} i_{\alpha 2} \\ i_{\beta 2} \end{bmatrix}, \quad (5)$$

where  $i_\alpha, i_\beta$  are the current of the motor.

The first two equations in (4) are symmetrical with the latter two equations, and both include the EEMF terms. Substituting (5) into (4) could obtain a new voltage equation.

$$\begin{aligned} & \begin{bmatrix} (L_{k1} + L_d)pi_{\alpha1} + L_d pi_{\alpha2} \\ (L_{k1} + L_d)pi_{\beta1} + L_d pi_{\beta2} \end{bmatrix} = \\ & = \begin{bmatrix} u_{\alpha1} \\ u_{\beta1} \end{bmatrix} - \begin{bmatrix} R_{k1}i_{\alpha1} \\ R_{k1}i_{\beta1} \end{bmatrix} - \begin{bmatrix} Ri_{\alpha} \\ Ri_{\beta} \end{bmatrix} - \begin{bmatrix} (L_d - L_q)\omega i_{\beta} \\ -(L_d - L_q)\omega i_{\alpha} \end{bmatrix} + \begin{bmatrix} Ex \sin \theta \\ -Ex \cos \theta \end{bmatrix} \end{aligned} \quad (6)$$

In (6), both the current differential terms of the first and second converter are included. The complex formula adds difficulty to designing the observer. Therefore, it is necessary to eliminate the current differential term of one converter.

According to the voltage equations (1) and (2), the relationship between the voltage and current of the two converters can be obtained as shown in (7).

$$\begin{bmatrix} pi_{\alpha2} \\ pi_{\beta2} \end{bmatrix} = \begin{bmatrix} (u_{\alpha2} - u_{\alpha1} + R_{k1}i_{\alpha1} - R_{k2}i_{\alpha2} + L_{k1}pi_{\alpha1}) / L_{k2} \\ (u_{\beta2} - u_{\beta1} + R_{k1}i_{\beta1} - R_{k2}i_{\beta2} + L_{k1}pi_{\beta1}) / L_{k2} \end{bmatrix} \quad (7)$$

According to (6) and (7), the estimated value of the EEMF can be obtained by the action of the PI regulator by the difference between the current calculated value and the current measured value. The mathematical expression of the extended back EMF observer can be obtained.

$$\begin{aligned} & [(L_{k1}L_{k2} + L_{k2}L_d + L_{k1}L_d)p + (L_dR_{k1} + L_{k2}R_{k1} + L_{k2}R)]\hat{i}_{\alpha1} \\ & = (L_{k2} + L_d)u_{\alpha1} - L_d u_{\alpha2} + (L_dR_{k2} - L_{k2}R)i_{\alpha2} - \\ & - L_{k2}(L_d - L_q)\hat{\omega}(i_{\beta1} + i_{\beta2}) + L_{k2} \frac{K_p s + K_I}{s} (i_{\alpha1} - \hat{i}_{\alpha1}) \end{aligned} \quad (8)$$

$$\begin{aligned} & [(L_{k1}L_{k2} + L_{k2}L_d + L_{k1}L_d)p + (L_dR_{k1} + L_{k2}R_{k1} + L_{k2}R)]\hat{i}_{\beta1} \\ & = (L_{k2} + L_d)u_{\beta1} - L_d u_{\beta2} + (L_dR_{k2} - L_{k2}R)i_{\beta2} + \\ & + L_{k2}(L_d - L_q)\hat{\omega}(i_{\alpha1} + i_{\alpha2}) - L_{k2} \frac{K_p s + K_I}{s} (i_{\beta1} - \hat{i}_{\beta1}), \end{aligned} \quad (9)$$

where  $\hat{i}_{\alpha1}$ ,  $\hat{i}_{\beta1}$  are the measured values of the first converter current.

According to the mathematical expression of the EEMF observer, the EEMF observer shown in Fig. 2 can be designed.

Among them,

$$\begin{aligned} A &= L_{k1}L_{k2} + L_{k2}L_d + L_{k1}L_d \\ B &= L_dR_{k1} + L_{k2}R_{k1} + L_{k2}R \end{aligned}$$

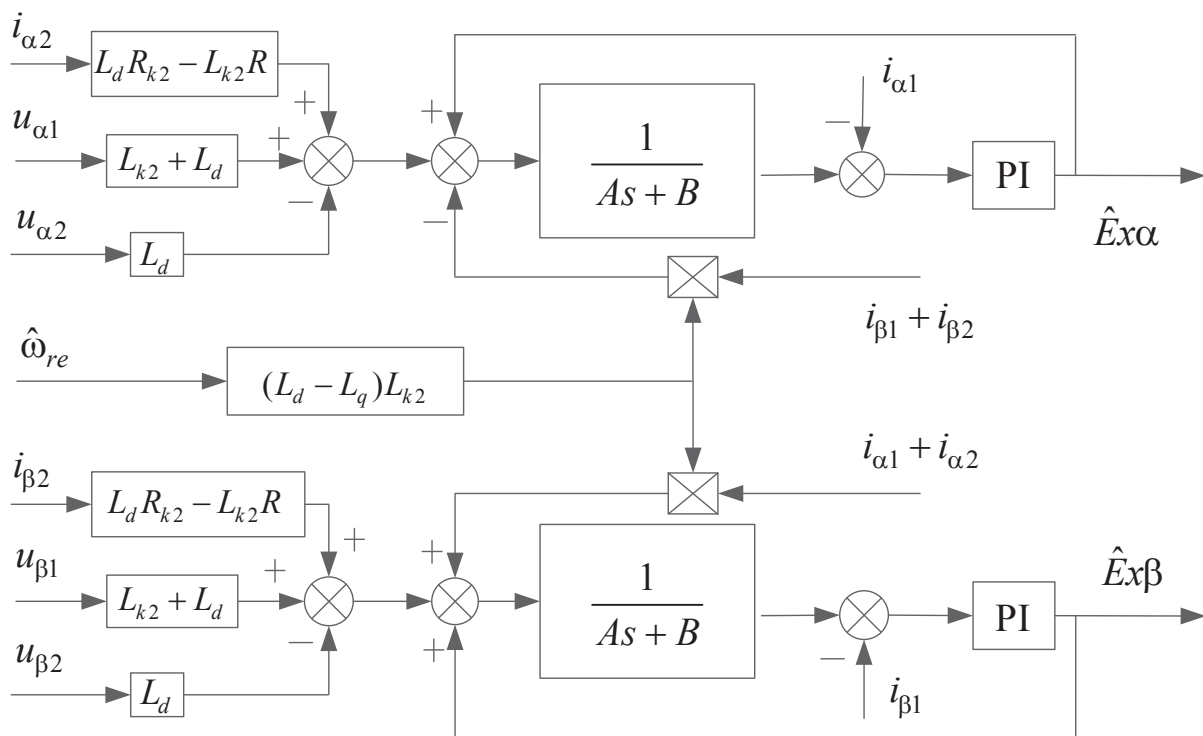


Fig. 2. Diagram of EEMF Observer

## PHASE LOCKED LOOP TECHNOLOGY

The two quadrature components of the EEMF have been obtained in the previous section. According to the second section, it can be seen that the EEMF contains the rotor position information. In this paper, the principle of the phase locked loop is used to extract the rotor angle information of the long-stator linear synchronous motor. The principle of PLL is expressed as

$$\ddot{\Delta}\theta = Ex(-\sin\theta)\cos\hat{\theta} + Ex\cos\theta * \sin\hat{\theta} = Ex\sin(\hat{\theta} - \theta) \quad (10)$$

Among them,  $\Delta\theta$  is the angle difference;  $\hat{\theta}$  is the estimated angle of linear motor;  $\theta$  is the actual angle of the linear motor.

Equation (10) is defined as the tracking error function. When the tracking error is equal to zero, the actual angle  $\theta$  and the estimated angle are approximately equal.

The angle difference after the PI regulator processing can be treated as the rotor electrical angular velocity; the rotor is obtained by the integration of the angular velocity. The principle of PLL is shown in Fig. 3.



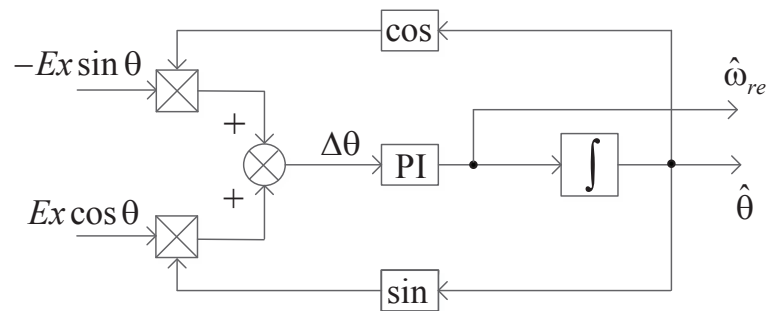


Fig. 3. Diagram of Phase-lock Loop

## SEMI-PHYSICAL SIMULATION RESULTS

In order to verify the feasibility and effectiveness of the speed sensorless control algorithm proposed in this paper, the experimental study was carried out on the high-speed maglev semi-physical simulation platform. The simulation platform is shown in Fig. 4.



Fig. 4. Experimental platform of maglev train semi-physical simulation

The goal of the experiment is to make the train with five groups achieve the maximum speed of 430 km/h acceleration and deceleration process.

Fig. 5 is the experimental comparison of the estimated speed and actual speed. The whole running process lasted 380 seconds, the maximum speed of maglev train reached 430km/h. It can be seen from the velocity curve that the estimated speed of the speed sensorless algorithm is basically consistent with the actual speed.

Fig. 6 is the experimental curve of the EEMF. When the train is running at low speed, the EEMF is affected by the current, so it has some chattering. When

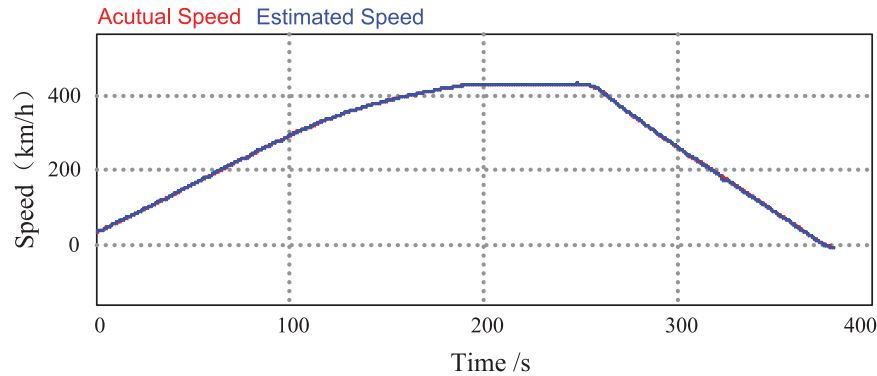


Fig. 5. Comparison of actual speed and estimated speed

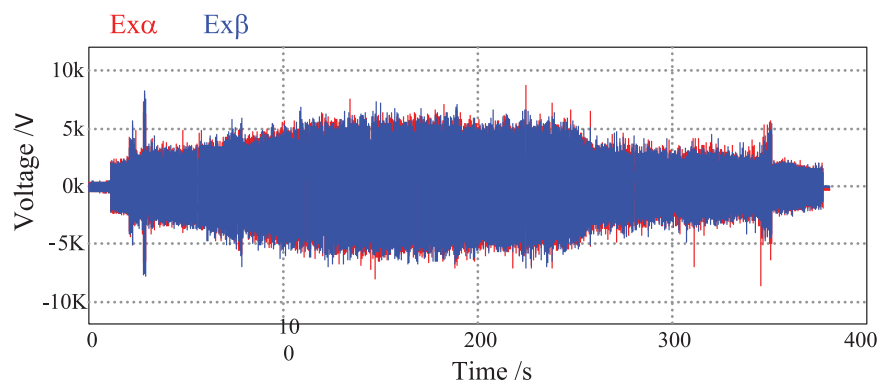


Fig. 6. Experimental results of EEMF

the train is running at high speed, the EEMF is stabilized. It can be seen from the figure that the EEMF is consistent with the train speed variation.

According to the comparison between the actual angle and the estimated angle in Fig. 7 and the partial magnification, it can be seen that the angle calculated by the speed sensorless is substantially coincident with the true angle.

The switching of the stator segments in the train operation is achieved by a two-step method. When the stator segment is switching, the stator voltage and current on one side are reduced, resulting in a decrease of the EEMF, so the calculated angle is not accurate. As shown in the first picture in Fig. 8. But the stator current and voltage on the other side do not change. The result of the calculation using the converter parameters of the other side is still accurate. As shown in the second picture in Fig. 8.

In order to obtain an accurate angle in the operation of the train, the angle calculated from the B-side converter data will be used when the A-side stator changing segment, and other times still using the A-side of the converter data to calculate the angle.

Through the use of the above method, the maglev train can be stably controlled in the two-step mode.

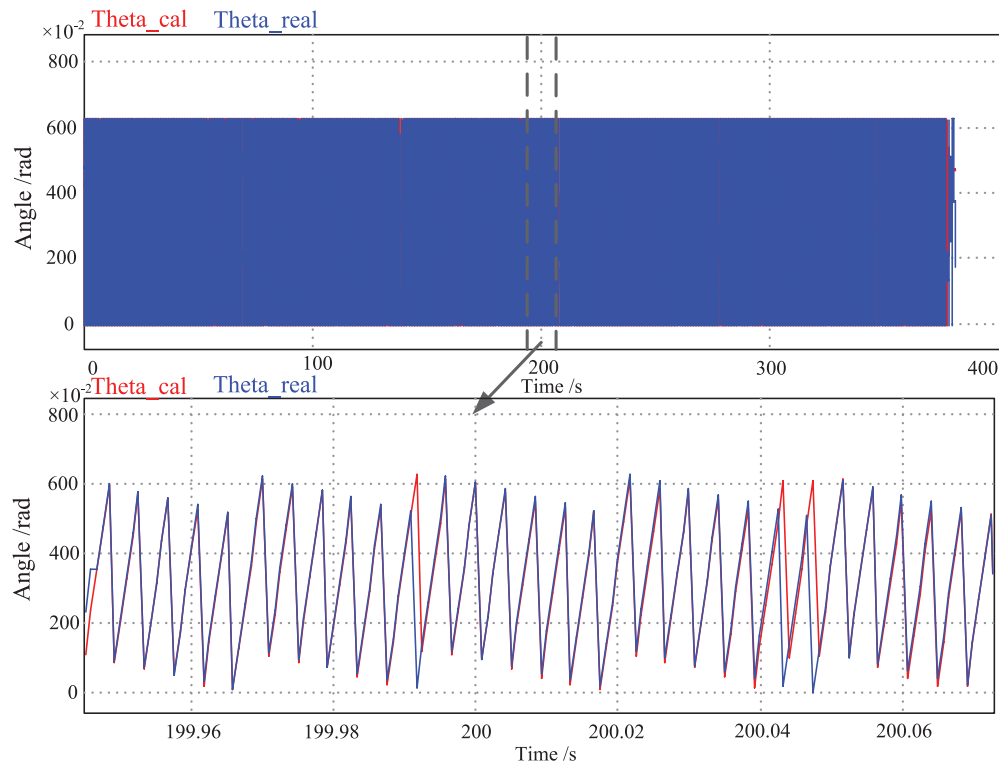


Fig. 7. Comparison of actual angle and estimated angle

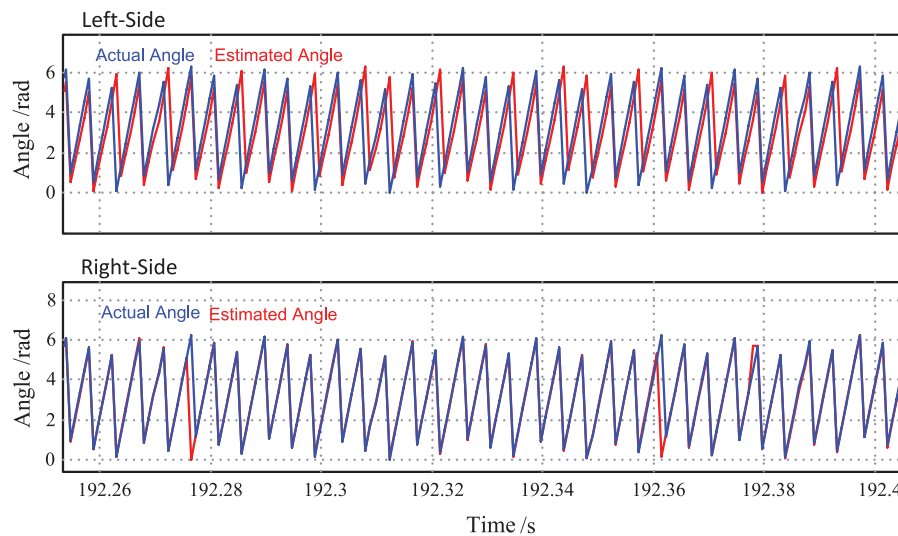


Fig. 8. The angle differences between both sides of the track when stator changing step

## CONCLUSION

In this paper, a mathematical model of the long-stator linear synchronous motor in double-end power supply mode is established. Based on the basic principle of extended back EMF, an observer of EEMF is established. In this paper, the design of the observer, involving only  $\alpha$ - $\beta$  coordinate system transformation, does

not involve the d-q coordinate system transformation, reduction the use of the estimated angle of the link, so that the entire control system is more stable. From the results of the semi-physical simulation, the design of the speed sensorless algorithm can realize the effective control of the high-speed operation of the maglev train, which is of great value to the practical application of the high-speed maglev train.

## References

1. Yin Z, Xiao L, Sun X, et al. A Speed Estimation Method of Fuzzy Extended Kalman Filter for Induction Motors Based on Particle Swarm Optimization. *Transactions of China Electrotechnical Society*. 2016;31:55-65.
2. Angelo A, Maurizio C, Marcello P, et al. Closed-Loop MRAS Speed Observer for Linear Induction Motor Drives. *IEEE Transactions on Industry Applications*. 2015;51(3):2279-2290. doi: 10.1109/tia.2014.2375377
3. Zhao L, Huang J, Liu H, et al. Second-Order Sliding Mode Observer with Online Parameter Identification for Sensorless Induction Motor Drives. *IEEE Transactions on Industrial Electronics*. 2014;61(10):5280-5289. doi: 10.1109/tie.2014.2301730
4. Li Y, Huang S, Xu Q, et al. Sensorless Control of Permanent Magnet Synchronous Motor Based on High Frequency Voltage Signal Injection. *Transactions of China Electrotechnical Society*, 2013;28:326-330.
5. Yoon TM, Sim HW, Lee JS, et al. A Simplified Method to Estimate the Rotor Position Using the High Frequency Voltage Signal Injection. *IEEE Applied Power Electronics Conference and Exposition (APEC 2014)*. 2014 March; p. 2453-2458. doi: 10.1109/apec.2014.6803647
6. Zhiqian C, Tomita M, Doki S, et al. An Extended Electromotive Force Model for Sensorless Control of Interior Permanent Magnet Synchronous Motors. *IEEE Transactions on Industrial Electronics*. 2003;50(2):288-295. doi: 10.1109/tie.2003.809391

### Information about the authors:

**Pengkun Sun**, graduate student; Address: No.6 Beiertiao, Zhongguancun, Beijing, China  
ORCID: 0000-0001-8958-2606;  
E-mail: sunpengkun@mail.iee.ac.cn

**Qiongxuan Ge**, Doctor of Philosophy  
E-mail: gqx@mail.iee.ac.cn

**Yaohua Li**, Doctor of Philosophy;  
E-mail: yhli@mail.iee.ac.cn

**Xiaoxin Wang**, Master Degree;  
E-mail: wxhit@mail.iee.ac.cn

### To cite this article:

Sun P, Ge Q, Li Y, Wang X. Research on Speed Sensorless Control of Maglev Train with Double-End Power Supply. *Transportation Systems and Technology*. 2018;4(3):154-163. doi: 10.17816/transsyst201843154-163